The Feasibility of Bio-Lubricants as Automotive Engine Oils

Julia Carrell

Supervisors: Dr T. Slatter &
Professor R. Lewis

Submitted to the Department of the University of Sheffield
in Partial Fulfilment of the Requirements for the Degree of

Doctor of Philosophy

January 2018

Abstract

The use of and demand for bio-lubricants is slowly increasing, primarily as a result of newly introduced legislation. Mineral oil based lubricants are now prohibited in certain areas, such as in lakes and forests, by several countries, including Belgium, Germany, Austria and Switzerland. The European Union's Registration, Evaluation, Authorisation and Restriction of Chemicals (REACH) is thought to be the most important legislation to aid the development of bio-lubricants. REACH has been implemented in an attempt to clean up the chemical industry and reduce the use of toxic substances. Additionally to the environmental reasons, the increase in cost of crude oil, along with concerns around the security of supply, gives a long term financial incentive to switch to bio-lubricants. It is critical therefore, that the performance of bio-lubricants can match mineral based lubricants.

The aim of this research was to assess the feasibility of using bio-lubricants with materials found in a typical oil circuit in four stroke internal combustion engine. This was done by assessing the tribological properties of bio-lubricants through the use of various experimental and analytical methods, including reciprocating wear, elastomer relaxation, advanced microscopy, and chemical analysis.

Current and novel automotive surface treatments were used in multi-layers. This was done to analyse the interaction of the bio-lubricants with these treatments and assess if any performance gains could be made if they were used in automotive contacts. The treatments used were: diamond like carbon (DLC), a calcium based chemical dip, shot blasting using a molybdenum disulphate doping media and nano fullerene.

The surface treatments used did not give any performance advantages in comparison to a super finished steel surface. A reduction in wear and coefficient of friction was found when bio-lubricants were used with DLC coatings, compared with mineral based lubricants. The calcium based chemical dip proved to be as effective, in terms of wear protection, as DLC and works well with bio-lubricants. There was no apparent tribological benefit to using multiple layers of surface treatments.

Wear and friction data was acquired to assess tribological performance. Potential bio-lubricant base stock candidates jojoba, soybean and palm kernel oil were used, with a mineral base stock for comparison. An assessment of lubricant performance was also made through calculations of spreading parameter and Hanson Solubility Parameters.

Stress relaxation tests with EPDM, nitrile rubber and fluorocarbon rubber, with the bio-base stock candidates revealed that soybean and palm kernel oil are compatible with EPDM, which is in disagreement with industry chemical resistance data that presents a cautious overview of compatibility. Jojoba and mineral oil cause relatively high levels of swell with EPDM. Tests with nitrile rubber found no difference in the compatibility of bio-base stocks compared with mineral base stock. All base stock candidates were found to be compatible with fluorocarbon rubber. The use of Hanson Solubility Parameters to predict material compatibility was found to work for EPDM.

Overall, this work has shown that there may be some performance benefits to using bio-lubricants over conventional mineral based lubricants, in internal combustion engines. Bio-lubricants can offer lower wear rates and coefficient of friction, particularly with the novel multi-layer surface treatments used in this work. Bio-lubricants are at least as compatible with elastomers as mineral based lubricants.

Acknowledgements

I wish to show appreciation to my supervisors, Dr T. Slatter and Professor R. Lewis for their invaluable support and guidance throughout my time at the University of Sheffield.

I would also like to extend my appreciation to the countless academic and technical staff and fellow PhD students, who have helped with many aspects of this research with technical advice and guidance, as well as my family, whose support was essential during my PhD.

I would like to acknowledge the contribution of the IMechE Whitworth Senior Scholarship Award in supporting this research. I would also like to thank The Douglas Bomford Trust for their financial support of research costs, and the Peter Jost Travel Fund for their financial support to attend a conference to disseminate my research.

Table of Contents

Table of Nomlecture

	Units	
h	m	Film Thickness
H_{min}		Dimensionless Film Thickness Parameter
W		Dimensionless Load Parameter
U		Dimensionless Speed Parameter
G		Dimensionless Material Parameter
k		Dimensionless Ellipticity Parameter
P	N	Load
η	Pa.S	Viscosity
u	m/s	speed
α	GPa^-1	Pressure Viscosity Coefficient
R_x	m	Reduced Radius in x Direction
R_y	m	Reduced Radius in y Direction
E^*	Pa	Reduced Modulus
E_1	Pa	Elastic modulus for contact surface 1
E_2	Pa	Elastic modulus for contact surface 2
λ		Dimensionless Lamda Ratio
σ_1^2	µm	Surface Roughness Value, R_a for Surface 1
σ_2^2	µm	Surface Roughness Value, R_a for Surface 2
γ_S^D	mJ/m^2	Dispersive Component of Surface Energy
γ_L^D	mN/m	Dispersive Component of Surface Tension
γ_S^P	mJ/m^2	Polar Component of the Surface Energy
γ_L^P	mN/m	Polar Component of the Surface Tension
γ_L	mN/m	Total Surface Tension
ΔG_1	kJ/mol	Gibbs Free Energy of Dilution
H	J	Enthalpy
T	˚C	Temperature
S	J/K	Entropy
U	J	Internal Energy
R	J/mol/K	Universal Gas Constant
V	m^3	Volume
p	Pa	Vapour Pressure
L	KJ/mol	Molar Latent Heat
E	KJ/mol	Cohesive Energy Density
δ_D	$MPa^{1/2}$	Dispersive Solubility Parameter
δ_P	$MPa^{1/2}$	Polar Solubility Parameter
δ_H	$MPa^{1/2}$	Hydrogen Solubility Parameter
δ	$MPa^{1/2}$	Total Solubility Parameter
H_v	KJ/Kg	Latent Heat of Vaporisation
Ra	$MPa^{1/2}$	Relationship Between two Substance in HSP Space
L_{C2}	N	Adhesive Critical Scratch Load
L_{rate}	$N\ min^{-1}$	Rate Of Application Of Force
L_N	mm	Distance From Start Of Scratch To Start Of Damage
X_{rate}	$mm\ min^{-1}$	Rate Of Horizontal Displacement
L_{start}	N	Pre Load At Start Of Test
k	m^3/Nm	Wear Coefficient (Archards Wear Equation)
L	m	Sliding Distance (Archards Wear Equation)
H	N/mm^3	Hardness
F	N	Force
F_0	N	Original Force

Table of Acronyms

a-C:H DLC	Amorphous Carbon Hydrogen containing DLC
AFM	Atomic Force Microscope
ASTM	American Society for Testing Materials
CaF_2	Calcium Fluoride
$CaSO_4$	Calcium Sulphate
CD	$CaSO_4$ Chemical Dip
CEC	Coordinating European Council
CR	Chloroprene Rubber
Cr-DLC	Chromium Containing DLC
CrAlN	Chromium Aluminium Nitride
CoF	Coefficient of Friction
DLC	Diamond like Carbon
DOC	Dissolved Organic Carbon
EDX	Energy Dispersive X-Ray Spectroscopy
EHL	Elasto-hydrodynamic Lubrication
EP	Extreme Pressure
EPDM	Ethylene Propylene Diene Monomer
FKM	Fluorocarbon Elastomer
FTIR	Fourier Transform Infrared Microscope
H-DLC	Hydrogen containing DLC
HSP	Hanson Solubility Parameter
HSPiP	Hanson Solubility Parameters in Practice Software
ICE	Internal Combustion Engine
JO	Jojoba Oil
MO	Mineral Oil
MoDTC	Molybdenum Dialkyldithiocarbamate
MoS_2	Molybdenum Disulfide
NBR	Nitrile Rubber
NF	Nano Fullerene
PAG	Polyalkylene Glycol
PAO	Polyalphaolefin
PO	Palm Oil
PTFE	Polytetrafluoroethylene
PVC	Pressure Viscosity Coefficient
PVD	Plasma Vapour deposition
RED	Relative Energy Difference
SAE	Society of Automotive Engineers
SB	Shot Blasting with MoS_2
SEM	Scanning Electron Microscope
Si-DLC	Silicon Containing DLC
SF	Superfinished
SG	Surface Ground
SO	Soybean Oil
SP	Spreading Parameter
SR	Silicone Rubber
ta-C DLC	Tetrahedral Amorphous Carbon DLC
TC	Traction Coefficient
VI	Viscosity Index
W-DLC	Tungsten Containing DLC
WS_2	Tungsten Disulphide
ZDDP	Zinc Dialkyldithiophosphate
ZnDTP	Zinc Dialkyldithiophosphate

1 Introduction

Lubrication is a vital part of many engineering systems, with the primary purpose of reducing wear and friction by separating contacting surfaces. Lubricants also dissipate heat, trap and move debris away from contact regions and prevent degradation of surfaces due to oxidation and/or corrosion. The properties of lubricants are determined by the base oil, the bulk oil used to make up the lubricant, and the type of additives used. Base oils can be mineral based, synthetically generated, such as polyalklene glycol, or bio-based from plant material, such as soybean. The majority of lubricants are made from mineral based oils from fossil sources and make up 98% of the lubricants market (1). Bio-lubricants are a small emerging market that could provide an alternative to mineral based oils if performance can be comparable.

1.1 The Need for an Alternative

Industry must reduce their dependency on fossil fuels. Reserves are diminishing, and although it is difficult to obtain reliable figures for the level of reserves of fossil fuels with predictions of peak oil production ranging from 2006 to beyond 2025 (2), it is widely thought that the era of cheap (i.e. easy to extract) oil is coming to an end. Oil commodity prices are over 300% higher than pre-2000 levels (3), but are also heavily dependent on world events, as can be seen in Figure 1-1.

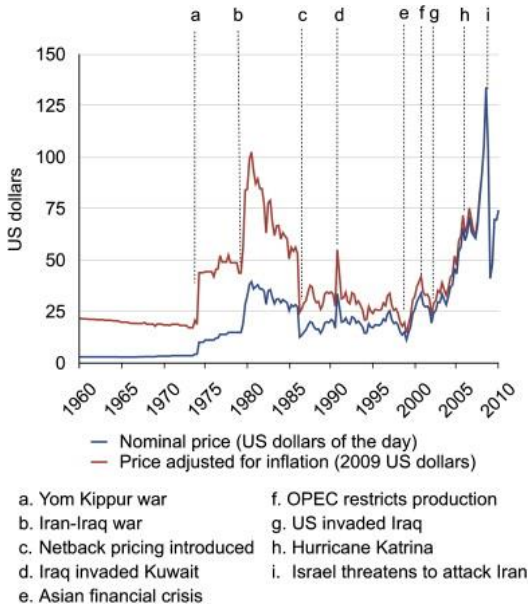

Figure 1-1, The Variation in the Price of Oil Linked with World Events (3)

The uncertainty in the impact of production and distribution of oil due to the world events shown in Figure 1-1 causes these fluctuations in price. Political instability or uncertainty and poor diplomatic relations between oil producing countries and countries that import large amounts oil is also a cause for reduced security in oil supply.

Figure 1-2 shows that there has not been a significant change in the countries that produce and export oil since 1992, but a small diversification in oil producing countries

has increased security (4). A move away from importing fossil fuels, along with developing domestic sources, such as shale oil in North America, significantly increases energy security.

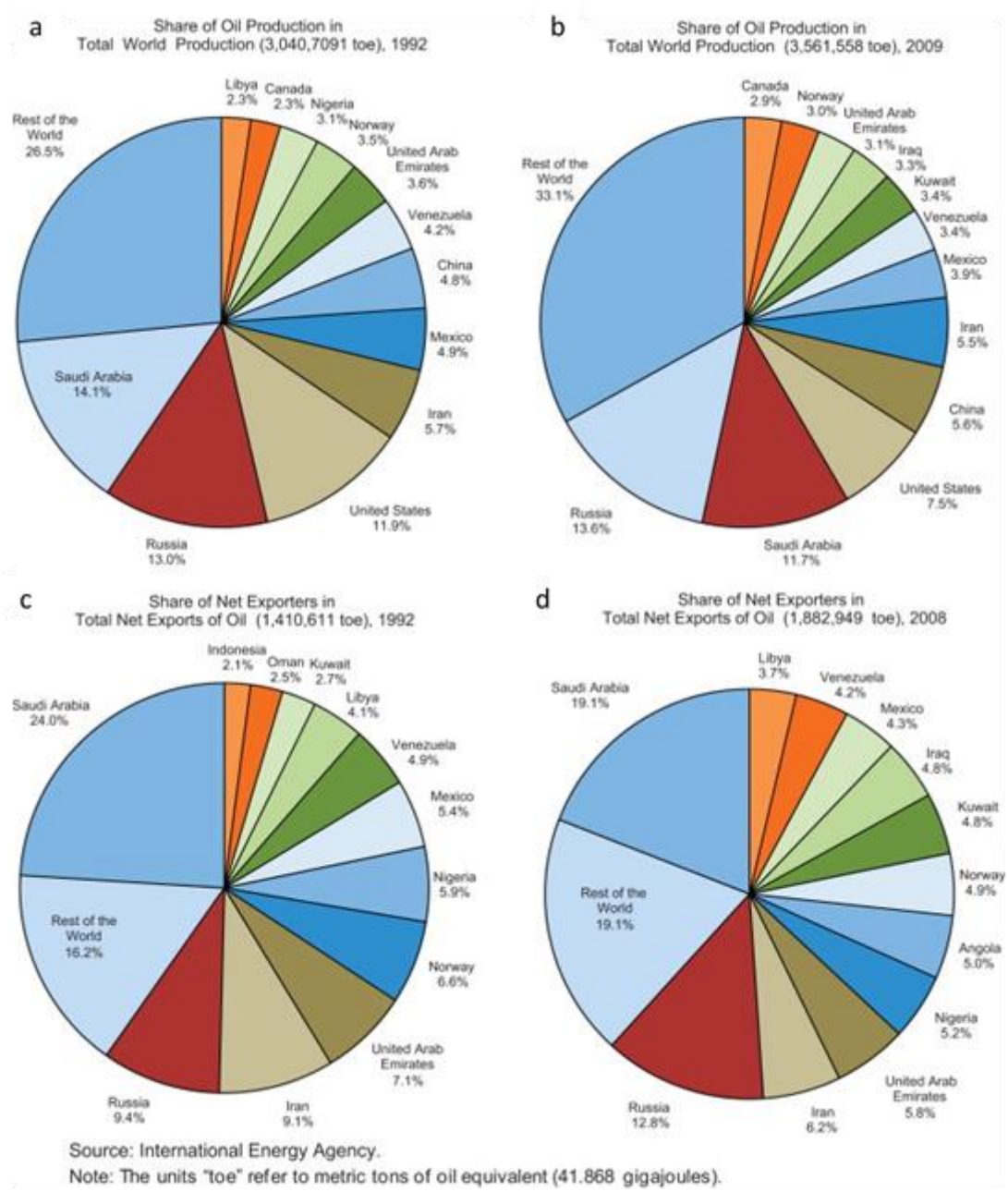

Figure 1-2, The Share in Production of Oil per Country from a. 1992, b. 2009, The Share of Net Exporters of oil in c. 1992 and d. 2008 (4)

The most important factor driving the need to reduce the use of fossil fuels, is the effect they have on the environment, both in terms of global climate change and the immediate impact of fossil fuels due to their toxicity and persistent polluting nature. Climate change is inevitable due to historic levels of greenhouse gas emissions, but there is still the potential to reduce the impact of climate change by ensuring global temperature increases do not increase by more than 2°C. In order to achieve this, 35%

of oil reserves must stay in the ground and be unburnt by 2050, and similarly 52% and 88% for gas and coal respectively (5). The Paris Agreement (6) is seen as the most important international convention that can provide a global response to tackling climate change through 'nationally determined contributions' to keep global temperature increases below 2°C. This should lead to a reduction in the use of fossil fuels and products based on fossil fuels.

The immediate negative effects of fossil fuels can occur at any point in their typical cycle of use; from extraction from oil wells, through their use in service, and to improper disposal at end of life. The "Gulf War Spillage" is cited as one of the worst oil spillage in history with around 460 million gallons of Kuwaiti oil intentionally released in to the Persian Gulf by the Iraqi armed forces (7). The spillage contaminated around 700 km of Saudi Arabian shoreline, it was estimated that between 50-90% of the fauna was killed by the oil. A drop in seawater temperatures was considered to be the most detrimental side effect of the spillage, killing fish and almost wiping out the prawn industry in the gulf. Three years after the spillage most fauna had recolonised the Saudi Arabian coastline, but after 10 years oil was still present on some beaches and underground (8).

The toxicity of mineral oil based products used in lubricants is a particularly important environmental issue because it is reported that 50% of all lubricants escape into the environment (9) due to spillages, improper disposal and total loss systems. This poses a significant environmental risk. One gallon of mineral based oil has the potential to contaminate one million gallons of drinking water, produce an eight acre oil slick on water and render four acres of land unusable (10). Petroleum products are cited as a significant issue in the loss of soil biodiversity in urban areas (11). Mineral based oils kill important microbes in soil, as well as making the soil toxic, while bio-based oils can stimulate microbe growth in soil as they degrade.

The cost of fossil fuels, the security of supply and the environmental issues mean that if there is a possibility for industries to reduce their dependency on fossil fuel derived products, significant advantages can be made in these three areas. It is also important that any fossil fuel replacement can match or improve current levels of performance. Therefore it is of significance to investigate the performance of fossil fuel alternative.

1.2 Scope of Work

This thesis aims to expand the current knowledge of bio-lubricants and assess the feasibility of their use in internal combustion engines. Clearly, this is a very large subject area, so the following constraints were made to the scope of the work:

- Legislative constraints are a considerable driver for the commercial development of bio-lubricants, therefore the relevant legislation was analysed and used to help form parameter requirements for the bio-lubricants tested in this work. Particular consideration was made to the international Lubricants Standardisation and Approval Committees standard for passenger car engine lubricants. GF-6 is the next standard to be introduced in April 2018.

- There are many potential lubricants that could be described as 'bio-lubricants' so these were selected early on in the project based on the outcomes of a series of learning experiments and previous work conducted by the author.

- Materials commonly found in automotive engines were used so areas of lubricant development can be linked with GF-6 to structure work clearly and make it relevant to an industry that could see significant environmental, cost and security benefits.

- Fundamental tribology studies were performed to simplify analysis of the performance of bio-lubricants, with an automotive application in mind. Test conditions were not aimed to replicate engine conditions exactly, but certain parameters, such as common loads and temperatures were used to make results relevant.

1.3 Aim and Objectives

The aim of work presented in this thesis is to assess the feasibility of using bio-lubricants in four stroke internal combustion engines (ICEs), through assessing the tribological properties of bio-lubricants with experimental methods.

To achieve this aim, the following objectives were identified.

Objective 1; to conduct learning experiments to set experimental parameters and to establish if an optimal blend of jojoba and mineral base stocks could be found for enhanced wear protection, as literature suggested performance benefits.

Literature suggest that blends of vegetable and mineral oils results in favourable levels of wear and that jojoba oil, with its unique chemical structure, may have superior wear protection characteristics compared with other vegetable oils. Section 6.1 gives further details of published literature on blending oils. The first objective therefore, aims to find the optimal blend ratio of jojoba and mineral oil that results in low levels of wear.

Objective 2; to assess the interaction of bio-lubricants with diamond like carbon and novel surface treatments of nano fullerene and calcium sulphate.

Research shows that surface treatments and coatings reduce friction and wear in a variety of tribological settings, yet little is known about the behaviour of bio-lubricants and coatings. DLC is one of the most common automotive coatings currently used. The current state of the art on surface coatings and bio-lubricants is discussed in

detail in Section 6.2 to 6.6. Therefore, the assessment of the interaction of bio-lubricants with diamond like carbon and novel surface treatments of nano fullerene and calcium sulphate is a key objective of this work.

Objective 3; to assess the compatibility of bio-lubricants with common automotive elastomer materials.

Based on this understanding of current literature no work has assessed the compatibility of bio-lubricants with elastomer materials using stress relaxation test methods, which can more closely represent in-service conditions. Only one piece of work looks at bio-lubricants and static immersion tests, further details of this can be found in Section 6.11. Elastomeric seals are important to the efficient operation of automotive engines, loss in sealing around the lubrication network of an engine may cause loss of lubrication, which can result in catastrophic damage.

1.4 Structure of Thesis

This thesis begins by summarising typical lubricant formulations currently available and describing their properties. Using material found in literature, comparisons are then made between conventional lubricants and bio-lubricants. Some current applications of bio-lubricants are included, with a focus on lubricants in internal combustion engines.

The current literature is also carefully reviewed to identify areas of research and development of bio-lubricants where knowledge is lacking. The subsequent theory section also focuses on these areas.

The work presented in these first sections forms the basis for selecting experimental methods and materials. From experimental methods, results are discussed and recommendations for further developing bio-lubricants are made. Experiments focus on the wear and friction properties of a blend of bio-lubricant and conventional lubricant to identify if a blend can be made with optimal performance and environmental benefits. Experimental work then looks at the performance of bio-lubricants with some common and novel automotive surface treatments. To continue with a material compatibility theme, the interaction of bio-lubricants and elastomers is experimentally assessed.

2 Laws and Guidelines for Lubricants

This chapter gives an outline of the legislation that is driving industry towards using less toxic chemicals. The legislation discussed in this chapter is an ideal opportunity to increase the development of bio-lubricants. An understanding of the legislative landscape is essential for developing a lubricant that will meet environmental and legal guidelines. The current and near future standards for automotive lubricants are also assessed. Standards, such as those set by the International Lubricants Standardisation and Approval Committee and SAE International, as well as automotive manufacturers. These standards set the performance requirements for lubricants and will help define the type of work that needs to be carried out to ensure any new bio-lubricant is suitable for its application. The background analysis for bio-lubricants finishes with a brief examination of the bio-lubricants market and projections for grow, showing that there is an appetite for the development of bio-lubricants. There is a small amount of growth in the market, meaning that it is an idea time to develop the technology.

2.1 Legislation

The move, by industry particularly, towards lower toxicity fluids for lubricants has predominantly been driven by legislation, and the European Union's Registration, Evaluation, Authorisation and Restriction of Chemicals (REACH) is one of many sets of regulations now in force aimed at reducing the impact of chemicals on the environment. Recent amendments to this legislation also now places the burden of proof on small and medium sized companies (as well as large) to show that chemicals are used safely, that they are correctly classified, and that the uses of chemicals must also be defined. Additionally, companies now need to apply to use chemicals classed as 'substances of very high concern' (SVHC), such as chromium, and this is only granted on the condition that as soon as safer alternatives are available they stop using SVHCs. This has encouraged industries to become innovative in finding alternatives to SVHC. As well as legislative pressure, The European Chemicals Agency state (established to manage REACH) that 'downstream users' of chemicals also act as a significant pressure in driving industries to safer alternatives. The European Chemicals Agency state (12);

> " *the operations of REACH and CLP have effectively steered companies towards manufacturing, formulating, importing and using industrial chemicals more safely. This constitutes significant progress towards meeting the aims of the Regulations, namely providing a high level of protection for human health and the environment*'.

REACH affects all components of lubricants manufactured and imported in to the EU, from additive manufacturers, lubricant formulators and users. Chemicals have been categorised, in one such category there are 78 different base oils that companies must now apply to use (13). Exposure scenarios must be defined under REACH and must cover the full life cycle of the lubricant. The technical association of the European lubricants industry (ATIEL) are aiding the lubricants industry to comply with REACH, they have identified over 200 lubricant uses and have also developed a database of generic exposure scenarios (14).

In the USA there has been a recent amendment to the Toxic Substance Control Act (TSCA), the Chemical Safety for the 21st Century Act (15), which is similar to the new regulations defined under REACH. Changes include improved identification and classification of risky chemicals and development of risk based safety standards. Other similar frameworks are also seen around the world, such as the Ministry for Environmental Protection in China, Canada's Domestic Substances list and the Korea Existing Chemicals Inventory (16).

REACH (and TSCA) offers an ideal opportunity to increase the market share of bio-lubricants as increased awareness of toxicity of chemicals and substances by 'downstream users' increases, this may influence the demand for lower toxicity lubricants. Through REACH some lubricant additives may be phased out, for example trixylyl phosphate, used in the formulation of lubricant additives is now classed as a SVHC due to its reproductive toxicity (17), as are mixed alkyl diesters (18). Short chain chlorinated paraffins (SCCPs) have also been classed as SVHC under REACH (19) due to being a persistent organic pollutant, very bio accumulative and toxic to aquatic organisms. They are used in lubricants and coolants, particularly in cutting and machining fluids. The intersessional working group on SCCPs (working under The Persistent Organic Pollutants Review Committee of the Stockholm Convention) gave extensive recommendations for alternative to SCCPs including multiple recommendations for using bio-lubricants for metal working fluids based on oils including soybean, rapeseed and coconut oil (20).

There are many other standards and regulations that promote the use of bio-lubricants. In France an amendment to the Farming Bill, (Section 44, Act 2006-11) bans the use of mineral oil based lubricants in natural areas classified as 'sensitive' if the application can easily use bio-lubricants. Under the same amendment, a general tax has been added for lubricants in total loss systems, such as two-stroke engines and chainsaws, with only EU eco labelled bio-lubricants exempt. Both Italy and The Netherlands also place a tax on mineral based lubricants. In Belgium bio-lubricants must be used in and around non-navigable waters. Germany, Austria and Switzerland have banned mineral oil based lubricants in inland waterways and forest areas (21). Germany also ran a Market Introduction Program from 2001 to 2008, the program gave financial grants and technical advice to companies and users who switched from mineral based lubricants to bio-based versions that had at least 50% renewable content. A list of 250 approved products was compiled under the program, which saw 25,000 pieces of equipment switched to bio-lubricants, 95% of the equipment converted were mobile hydraulic equipment used in agriculture and forestry. A post program evaluation found that 94% of those that converted to bio-lubricants were satisfied with the change (22).

The USA is stated to be around 10 years behind Europe in terms of legislation that promotes the use of bio-lubricants (16). In conjunction with its Market Introduction Program, Germany has developed comprehensive legislation to promote bio-lubricants, particularly the Water Management Act and the Soil Protection Law, with water and soil contamination a significant issue with mineral based oils, as discussed in Section 1.1. The Water Management Act classifies chemicals in relation to their harm to water based on oral, fish and bacterial toxicity as well as biodegradability. Bio-lubricants are classed as 'not water hazardous', mineral base oils (no additives) are classed as 'slightly water polluting', with the remainder classed as either 'water

polluting' or 'very water polluting' depending on the design of their additive packages. The act aims to ensure;

"*…installations for handling substances hazardous to water must be designed, constructed, maintained, operated and decommissioned in such a way that no adverse changes in the properties of waters are to be feared. This is deemed to be fulfilled if measures for primary and secondary safety have been taken and the operator meets specific obligations, including monitoring.*"

The Soil Protection Law aims to protect again harmful effects of chemical contamination or misuse, the act states that negative effects on soils must be avoided and if they do occur, soil must be 'rehabilitated'. Legislation in the USA on the protection of soil and water varies from state to state, the Great Lakes Water Quality Initiative bans all zinc compounds, zinc can be found in some lubricant additives. The USA government does promote the use of bio-based products particularly in government departments through the Federal Bio-based Product Preferred Procurement Program, which comes under the Food, Conservation and Energy Act 2008, section 9002 (23). A wide range of lubricants are recommended under the Act, including engine oils, hydraulic fluids and machine oils, and this has aided the development and promotion of bio-derived products.

2.2 Labels

Labelling programs have been developed in order to help with the classification of bio-lubricants, as well as many other products. The EU Eco label is considered the first major international label that has contributed to creating a single standard. Established in 2005, lubricants with this label are assessed in areas such as their biodegradability, their aquatic toxicity, and bioaccumulation, as well as having a renewable content of at least 50%. Nordic Swan is another international label that covers the Nordic countries and certifies lubricants based on biodegradability, aquatic toxicity, technical performance and renewability. Germany and Sweden have national labelling programs called Blue Angel and the Swedish Standard respectively. Blue Angel is the only label that requires complete biodegradability but interestingly has no renewable content requirements. It does have requirements under aquatic toxicity and bioaccumulation, however. Figure 2-1 gives examples of these labels.

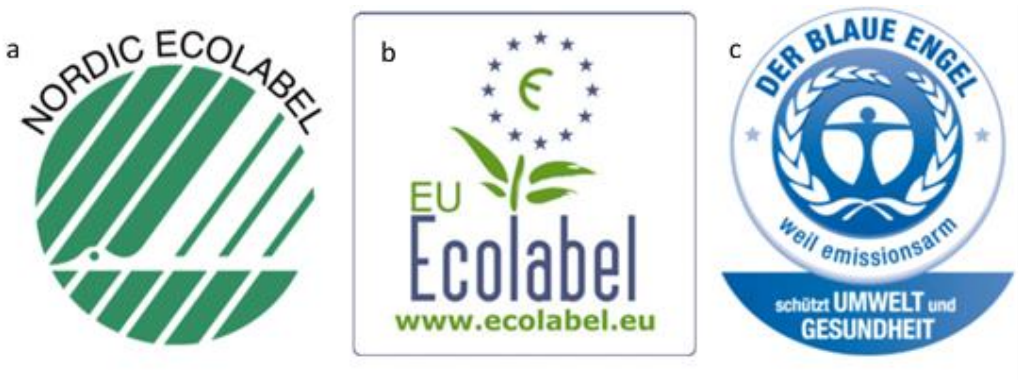

Figure 2-1, An Example of the Some Eco Labels Used for Environmentally Friendly Fluids, a. Nordic Swan, b. The EU Ecolabel, c. Blue Angel

2.3 Standards

The International Lubricants Standardisation and Approval Committee set a standard for passenger car engine lubricants, it is developed and approved by a consortium of automotive manufacturers, General Motors, Ford and Daimler Chrysler and the Japan Automotive Manufacturers Association. The standards developed set the minimum performance requirements of lubricants for the satisfactory performance of equipment and it also defines the chemical and physical properties car engine lubricants should possess.

The current standard in place for spark ignition internal combustion engines is known as GF-5 and has been in place since October 2010, with GF-6 is set to supersede GF-5 in April 2018. There are similar standards in place for diesel internal combustion engines and motorcycle engines (24, 25, 26), with the main aim of increasing fuel efficiency and reducing greenhouse gases. The new GF-6 specification is representative of the trends in lubricant formulations, particularly for internal combustion engines lubricants. All specifications are demanding lower viscosities, maintained compatibility with emissions systems, increased durability of the lubricants and longer drain intervals, all in order to meet wider environmental legislation.

Lubricants have a significant impact on fuel efficiency due to their ability to reduce friction (direct frictional losses account for 28% of fuel consumption (24)) and manage wear so that components work in an optimal manner, therefore the current emissions legislation is an important consideration when these standards are developed, the average fuel efficiency target for the USA is 54 mpg by 2025 (25), the EU's current target is 57.4 mpg by 2021 (26), this equates to 163 and 153 g CO_2 per mile respectively.

Figure 2-2 compares the current GF-5 standard to GF-6, and shows how lubricant properties need to be improved for durability, specifically in sludge formation, piston cleanliness and oxidative stability. Engine sludge control is a new area not previously specified, as is ensuring lubricant formulations do not cause low speed pre-ignition (27).

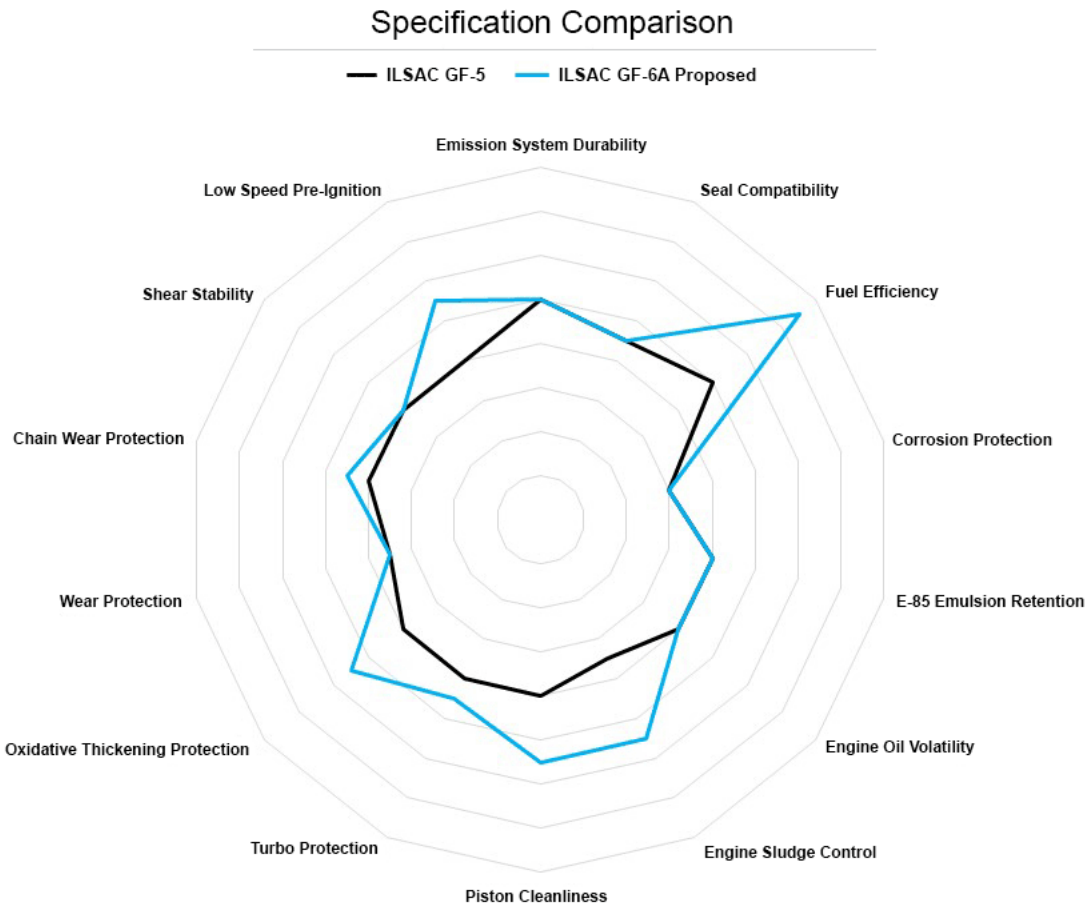

Figure 2-2, A Comparison of the Current Passenger Car Standard, GF-5 and the Proposed New Standard, GF-6 (30)

Table 2-1 shows some of the relevant proposed requirements for the new GF-6A standard as an example of the comprehensive nature of the standard and the performance demands the new low viscosity lubricants are under.

SAE International standards also play a role in lubricant development. The international recognised standards define product requirements, such as the viscosity requirements stated in Table 2-1 as well as test methods that enable results to be compared and confidence to be had in experimental methods. The American Petroleum offer a voluntary certification programme for automotive lubricants to give consumers confidence that the lubricants meet certain quality standards. All automotive manufacturers also have their own internal standards for lubricants, such as Volkswagen's 504.00 for petrol engines. These benchmark performance requirements, lubricant and automotive manufacturers work together to develop these.

1. Fresh Oil Requirements		
Standard		**Test Output Limits**
1.a SAE J300	Viscosity grades should be limited to SAE 0W-20, 5W-20, 0W-30, 5W-30 and 10W-30 multigrade oils and meet all SAE j300 requirements.	
2. Engine Test Requirements		
2.a Wear and Oil thickening	ASTM Sequence IIIG ASTM D7320	Kinematic Viscosity Increase @ 40˚C max. 100% Average Weighted Piston Deposits, max. 5 merits Hot Stuck Rings – None
2.c Valve train Wear	Sequence IVA ASTM D6891	Average Cam Wear, max. 90µm
2.e Fuel Efficiency	Sequence VIE ASTM D7589	Varies dependant on viscosity grade FEI SUM min. 2.5-3.6% FEI 2 min. 1.1-1.7% after 125 hours aging
2.f Chain wear	TBC	TBC
3. Bench Test Requirements		
3.a Catalyst Compatibility	ASTM D4951 ASTM D7320 ASTM D4951 ASTM D2622	Phosphorus Content max. 0.08% by mass Phosphorus Volatility min. 79% Sulphur Content max. 0.5-0.6% mass dependant on viscosity
3.b Wear	ASTM D4951	Phosphorus Content min. 0.06% by mass
3.n Elastomer compatibility	SAE J2643 ASTM D7216 ASTM D471 ASTM D2240 D412	Five reference elastomers used to test compatibility. Limits for change in property are; Volume change -5 – 40% Tensile strength -65 – 40 % Hardness -30 – 10 pts with durometer

Table 2-1, Some of the Relevant Requirements for Lubricants Proposed for GF-6 (30)

2.4 The Bio-lubricants Market

The bio-lubricants market is growing mainly due to stricter regulations on chemicals and 'downstream users' demanding more environmentally sustainable products, as discussed in 2.1. Possibly one of the most comprehensive reports on the bio-lubricants market, by Grand View Research, was released in September 2016 (1). In 2015 the bio-lubricants market was estimated to have produced 630,000 tons of lubricants (2% of lubricant market) and is projected to grow to 1.12 million tons by 2024, representing a 6.9% growth. 88.1% of bio-lubricants were derived from vegetable oils in 2015 and this source is predicted to grow the most at 7.6%, while animal product derived oils make up the majority of the rest of the market with no significant growth predicted.

Hydraulic fluids were the main application for bio-lubricants in 2015 with application in lifts, forklift trucks, hydraulic equipment near waterways and chain saws and other forestry equipment, this is linked to the legislation in force discussed in 2.1. The report stated that 20-30% of hydraulic fluids end up in the environment due to leakages and hose ruptures. The automotive industry demand for bio-lubricants was estimated at 200,000 tons in 2015.

The bio-lubricants market is the most mature in Europe and the USA, with both regions combined accounting for 84% of the global bio-lubricants market. Europe currently has a larger share than the USA, but the USA is predicted to grow faster up to 2021 when it is likely to overtake Europe. This growth is mainly attributed to pieces of legislation such as the bio preferred program mention in 2.1 and the fact that the USA is a major producer of bio-lubricant feedstocks, such as rapeseed and soybean oil. Emerging markets such as India, Brazil and China are also predicted to have high growth in the bio-lubricants market, based on the predicted increase in passenger vehicle use and manufacture in those economies, also in addition to being major producers of bio-lubricant feedstocks.

There is some (legitimate) concern that production of non-food products based on vegetable oils could impact the amount of land available to produce food, particularly with bio-fuels (28), this debate could also be associated with the increase in use of bio-lubricants. Developing economies, such as Malaysia, are susceptible to this, where the draw from economic stimulation from exporting crops to produce bio-lubricants could take propriety over low cost food for citizens. In 2015 global bio-fuel production was 80 million tonnes (29) and global lubricants production was 39 million tonnes (30). The bio-fuels market growth predictions have been downgraded, particularly in Europe due to taxes on carbon dioxide emissions and import tariffs on USA-sourced bio-diesel. Major car manufacturers are also focusing more on developing electric vehicles rather than bio-fuel compatible internal combustion engines. This could provide an opportunity for the lubricants industry to replace bio-fuel production with bio-lubricant production. As global lubricant demand (volume) is significantly smaller then bio-fuel demand, the risk to food supplies is reduced.

2.5 Conclusions

To summarise, background research shows that the current legislative environment is a significant driver for industry, and somewhat for downstream users, to seek lower toxicity chemicals. The European Union's REACH legislation being the most comprehensive and stringent set of legislation aimed at cleaning up the chemical industry. Similar legislation in other parts of the world also legislate for lower toxicity chemicals, such as the USA's Toxic Substance Control Act. Some individual countries, particularly in Europe, also have legislation aimed to protect water and soil. This type of legislation class's mineral oil derived products, such as lubricants, as a contamination risk. Eco labels offer an ideal framework within to develop bio-lubricants, but legislation is a more significant motivator.

Automotive lubricant standards, such as GF-6, are a vital set of guidelines to consider in developing a bio-lubricant for the automotive sector. The performance parameters, such as viscosity, durability and wear protection requirement, act as a useful guide for developing a set of experiments for testing the suitability of a bio-lubricant for this market. Additionally, due to variations in engine designs and materials used, it is important to consider internal standards set by individual automotive manufacturers.

Market research predicts that the bio-lubricants market will grow by 6.9% by 2024. The European and USA markets are currently the largest, but emerging markets, such as India, Brazil and China are predicted to grow faster due to the increase in

passenger car use and the availability of crops to produce bio-lubricants. There is an opportunity to take advantage of the legislative restrictions being imposed on bio-fuels and switch some bio-fuel production to bio-lubricant production to avoid some of the issues with using land that could produce food to produce none food products. Before this can be done, an improvement in the tribological understanding of bio-lubricants is required and therefore acts as a bio-lubricant development driver.

3 Lubricant Tribology

This chapter discusses some of the key tribological aspects of lubrication. A general overview of the types of base stock used to formulate lubricants is given and their environmental impact in terms of biodegradability and toxicity. The important properties of lubricant should possess is detailed, as are the types of additives used to improve lubricant performance. The chapter goes on to look at lubrication regimes and the mechanisms for lubrication.

3.1 Lubricant base stocks

The tribological properties of a lubricant are dependent on the chemical composition of the lubricating fluid and the way in which it interacts with the contacting surfaces. The molecular structure directly effects the frictional behaviour of a lubricant. The easier molecules can shear over one another, the lower the friction of the system. Intermolecular interactions, particularly of functional groups, as well as the shape and size of molecules dictates how much a fluid will resistance shear. Functional groups are sites of enhanced reactivity and have the ability to form adhered films on surfaces, these properties are discussed in more detail in this chapter.

The bulk of a lubricating fluid is known as the base stock, of which there are many different types, and its selection is application dependant. Lubricant base stocks can be gas (compressed), liquid, semi-solid (greases) or solid (dry lubricants such as soft metals), this section will focus on liquid lubricants due to the physical state of the vast majority of bio-lubricants. Three main groups of base stocks are used in lubricant formulation; mineral oil based, synthetic and bio-based and within these groups there are many variations. Lubricants tend to be made up of two to three different base stocks in order to meet a variety of application demands.

3.1.1 *Mineral Base Stock*

Mineral oil base stocks can be defined by three sub-groups; paraffinic, naphthenic and aromatic oils. The difference in these three oils is in the molecular structure of their hydrocarbons, as shown in Figure 3-1.

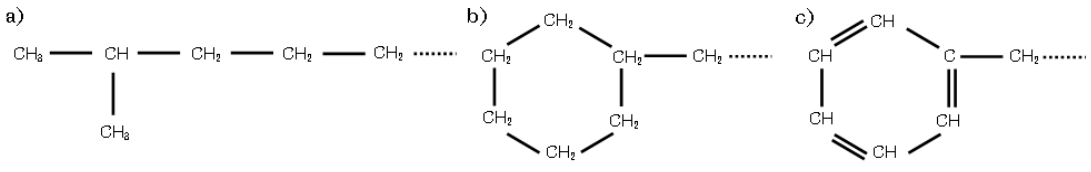

Figure 3-1, The Molecular Structure of a) Paraffinic, b) Naphthenic and c) Aromatic Mineral Oils

Paraffinic oils are the most commonly used base stock, particularly in engine oil formulations, as they are fully saturated and therefore chemically and thermally stable. They comprise of mainly (approx. 65%) long chained hydrocarbons with

branching, but no ring structures, as seen in Figure 3-1a. The viscosity of paraffinic oils is determined by chain length and processing temperature.

Naphthenic oils have a high cycloalkanes content and are classed as naphthenic oils when the paraffinic content is less the 60%. The oil consists of saturated hydrocarbons, of which some form rings, as shown in Figure 3-1b. An interesting property of naphthenic oils is that the products produced due to degradation are soluble in the oil and therefore degradation related sludge formation is much reduced.

Aromatics, shown in Figure 3-1c also have ring structures but unlike naphthenic oils, they are not fully saturated, with alternating single and double bonds. The double bonds make aromatics more reactive and prone to oxidation. Aromatics also tend to be at around 2% concentration in otherwise paraffinic and naphthenic oils (16, 31).

3.1.2 *Synthetic Base Stock*

Synthetic oils have been developed to meet the needs of more demanding applications and allows for the oil properties to be tailored to a given application. This means that they have performance advantages over mineral or bio-base stocks and can be tailored to a wide variety of applications. Synthetic oil can be separated into those from renewable and non-renewable sources. Synthetic oils are made by reacting different chemical compounds together, often mineral oil based, which are non-renewable, but can also be through the esterification of vegetable or animal based oils, which are renewable. This can create an oil formulation that has enhanced properties, particularly in its oxidative and temperature stability. Commonly used compounds include poly-α-olefins (PAOs) and polyalkylene glycols (PAGs), which are mineral oil derived, and synthetic esters, which derived from animal or vegetable oils. Even though PAOs and PAGs are mineral derived, they can still be highly biodegradable, particularly the water soluble versions (32). A synthetic lubricant will not necessarily be biodegradable; this will entirely depend on the synthesised structure of the finished lubricant.

The use of synthetic oils is limited to applications that require high performing lubricants or very specific needs as they are expensive in comparison to mineral oils due to their complex process route. Semi-synthetic oils, often a blend of mineral oil and PAOs are more widely available and cheaper than fully synthetic oils and commonly found in automotive applications. Synthetic oils also tend to have inferior elastomer compatibility compared with mineral oils, as they have lower polarity (16, 34). Synthetic lubricant is most commonly used in hydraulic and marine applications.

3.1.3 *Bio-based Base Stock*

Bio-based base stocks are mainly derived from vegetable oils, but can also come from animal fats or fish oils. Animal fats, such as tallow, are no longer common lubricants. Historically they were important and as an example, tallow was used in steam engines as it was resistant to being washed away by the steam and hot vapours. There are some more recent applications, such as in cold rolling mills (33) and a US lubricant manufacture has incorporated waste fat from the meat industry in to their bio-degradable lubricant (34).

Most vegetable oils have a triglyceride structure that consists of a glycerol backbone with three fatty acid chains attached. The fatty acids dictate the tribological

performance of the oils, fatty acids are hydrocarbon chains, most commonly between twelve and twenty-two carbons long.

Generally, longer fatty acid chains are better at protecting against wear and reducing friction, this is due to their ability to support shear stress more readily and that the molecules, if they possess a high degree of linearity relative to each other and their motion, are able to shear over one another easily. The degree of saturation of these fatty acids is also an important property; fatty acids with high levels of unsaturated double bonds have lower oxidative stability and lower melting points. Fatty acids with higher levels of saturation have higher oxidative stability, but higher melting points, which can mean oils, such as unrefined palm and coconut oil, are solid at room temperature (16, 35). Figure 3-2 shows four of the commonly occurring fatty acids, stearic, oleic, linoleic and linolenic acid, these are all eighteen carbons long, but have varying degrees of saturation, stearic acid is saturated, having no double bonds, while the other fatty acids have double bonds and therefore varying degrees of saturation.

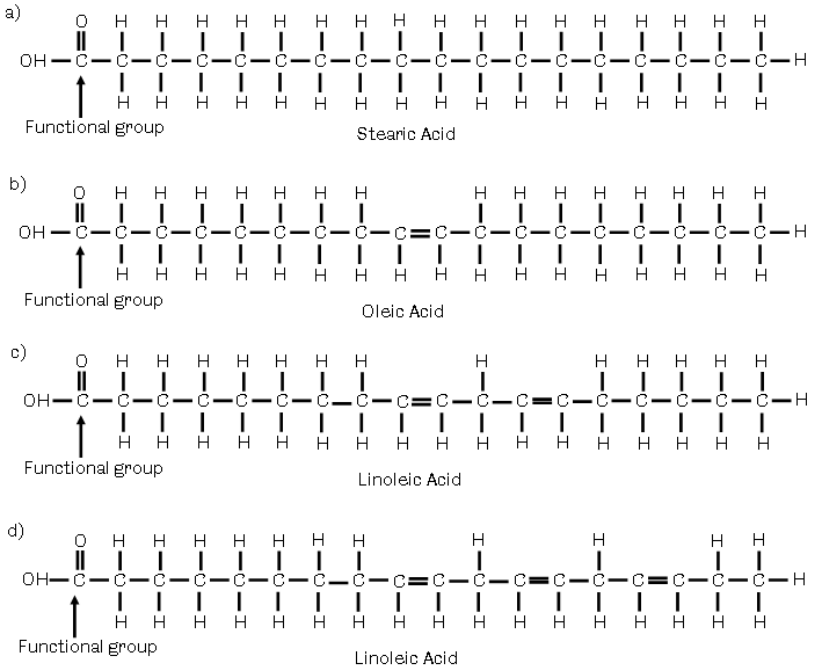

Figure 3-2, The Molecular Structure of Some Common Fatty Acids Found in Vegetable Oils, a) Stearic Acid, b) Oleic Acid, c) Linoleic Acid, d) Linoleic Acid

The highly polar functional groups situated at the ends of these chains (shown in Figure 3-2) also dictate the tribological performance of the oil. These function groups are attracted to and adsorbed onto the oppositely charged atoms on the metallic contacting surface. This means that the fatty acids adhere to the contacting surface and become aligned perpendicular to the surface, as shown in Figure 3-3. The hydrogen bonding forces between the molecules aids this formation and results in a molecular structure that is difficult to compress, but easy to shear (36). Oleic and stearic acid are particularly good at forming these bonds; stearic acid is a common lubricant additive used to protect surfaces that operate under very thin lubricating films. These acids are particularly effective at forming these layers due to their active function groups and the strong lateral intermolecular attraction between chains (31).

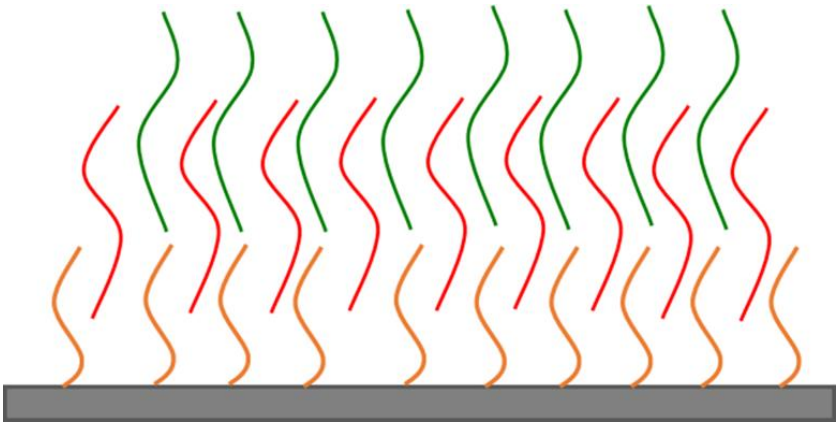

Figure 3-3, A Representation of Fatty Acid Chains Adhering to a Metallic Surface and Aligning with Each Other

3.1.4 *Comparing Base Stocks*

An important factor with bio-based base stocks is that they are readily biodegradable, this also causes their lack of stability in a number of tribological properties such as oxidative and thermal stability, as well as this vegetable oils can have poor low temperature properties and a narrow viscosity range. Table 3-1 shows a general comparison of the different base stocks discussed, as can be seen, mineral base stocks are low cost, relatively chemically stable and have reasonable tribological properties, but have poor biodegradability and toxicity. Synthetic base stocks can exhibit excellent chemical and tribological properties, have moderate biodegradability and toxicity (depending on the type used), but are the most expensive. Bio-based base stocks have reasonable tribological properties, poor chemical stability and are moderately expensive.

Property	**Paraffinic**	**Naphthenic**	**Aromatic**	**PAO**	**Bio (generalised view)**
Oxidative stability	High	Moderate	Low	High	Low
Pour Point	Moderate	Low	Very low	Very low	High
Viscosity Index	High	Moderate	Low	High	High
Flash Point	High	Low	Varied	High	High
Solvency	Poor	Excellent	Excellent	Moderate (poor for polar additives)	Good (but can be oil dependant)
Biodegradability	15 - 35%			5 - 30%	70 - 100%
Cost	Low			High	Medium
Polarity	Low	Low	High	Low	High

Table 3-1, A General Comparison of Different Type of Lubricant Base Stock (16) (37)

3.2 Biodegradability and Toxicity

The main driver for replacing mineral oil based lubricants with bio-lubricants is that they can be considered 'environmentally acceptable', this means they leave minimal negative impact on the environment they are used in. Labelling programs discussed in 2.2 require that bio-lubricants have a certain level of biodegradability and toxicity.

Primary biodegradability is the most widely used measure, with the Coordinating European Council (CEC) L-33-A-93 test the industry preferred method of evaluation. This method looks at dissolved organic carbon (DOC), CO_2 production and oxygen uptake during a given test period, usually 28 days or at the point in which the values stated plateau (37). For a substance to be readily biodegradable it must reach 70% removal of DOCs, and 60% of both CO_2 production and oxygen uptake within a ten day period that begins once one of the stated values reaches 10%. As stated in Table 3-1, bio-based fluids are readily biodegradable, while mineral oil based and PAO are not. Not all synthetically derived products have poor degradation properties, synthetic esters have been shown to have degradation properties closer to vegetable based oils than mineral based oils (38). It is well documented that mineral based oil have poor degradation of on average 25% and are classed as inherently biodegradable (39, (39). . Interestingly, studies on biodegradability in soils have found that mineral oil based lubricants penetrate into soil twice as deep as bio-lubricants (39).

The toxicity of lubricants is another important measure for defining a bio-lubricant and labelling programs also have guidelines for toxicity levels. There are several different tests available to define toxicity and several different tests must be performed so that a complete understanding of a given substances toxicity on various organisms is gained. OCED 201 (40), 202 (41) and 203 (42) guidelines are commonly used, these are also other standards such as ASTM D6046. OCED 201 measures algae growth inhibition; exponentially growing algae is exposed to the test substance for 72 hours and the reduction in growth rate is measured. OCED 202 measures water flea immobilisation, similarly to 201; the fleas are exposed to the test substance for 48 hours and the concentration of the test substance required to immobilise 50% of the fleas is recorded. 203 guidelines cover fish toxicity, the concentration of the test substance to kill 50% of the fish is determined over a 96 hour exposure. ASTM D6046 (43) is also a fish toxicity standard. Other organisms such as Eruca sativa seeds (rocket leaves) (44) and Eisenia foetida (earthworms) (45) are also used to test toxicity. The toxicity of many different lubricating fluids is well defined and mineral oil based lubricants are toxic. 'Toxic' is defined as at least 40% mortality, immobilisation or inhibition, to be classed as 'non-toxic' these values must be less than 10% and signs of toxicity 10-40%. Tests carried out with used mineral based lubricants were found to have higher toxicity rates, attributed to polycyclic aromatic hydrocarbon concentrations (46). Polycyclic aromatic concentrations increase in used engine lubricants as they form during combustion (11). Bio-based lubricants have been found to be non-toxic to fish, even in very high concentrations of 10,000 mg/L, while mineral based counterparts were lethal at 380 mg/L. Similar results have been observed on toxicity tests with fleas. Synthetic lubricants tend to possess signs of toxicity (39).

3.3 Lubricant Properties

The most important property of a lubricant is their ability to reduce wear and friction. Lubricants do this by separating two contacting surfaces and as the lubricating fluid has a low resistance to shear, the contacting surfaces can move over one another with relative ease. The viscosity of the lubricant is a measure of a fluid's resistance to shear motion (35) and is cited as the most important rheological property.

Reducing wear and friction is the most important part of a lubricant's function, but in order to meet the demands of applications there are many other important properties a lubricant must possess. The demands on automotive lubricants discussed in Section 2.3 demonstrate the extent to which lubricant properties must be refined so that engine performance is not compromised. Some further key properties include;

3.3.1 *Oxidation*

The oxidation of lubricants is a form of chemical degradation that is caused by the reaction of the lubricant with oxygen from air or moisture, metallic wear debris can act as a catalyst for this process, as does increasing temperatures. Oxidation causes an increase in viscosity due to the initiation of polymerisation (47) as well as the formation of small chain fatty acids; these oxidation products can develop in to deposits (16). The process of oxidation is discussed in more detail in Section 3.7. As can be seen in Table 3-1 in Section 3.1, vegetable oils have poor oxidative stability due to their polar nature and level of unsaturation, unlike paraffinic and naphthenic based mineral oils.

3.3.2 *Pour Point*

The Pour Point of a lubricant is the lowest temperature at which it will still flow, and in practice when used in an application this value should be at least 10˚C lower than the lowest anticipated ambient temperature (16). The pour point of bio-based lubricants tend to be high, meaning that the oil can be solid at relatively high temperatures. In a triglyceride structured vegetable oil, there is a tendency to form microcrystalline structures at lower temperatures as the glycerol backbone can stack in a relatively uniform manner resulting in a loss in kinetic energy (48). Additionally, longer fatty acid chains have higher melting points and fatty acid chains with double bonds have lower melting point (47).

3.3.3 *Viscosity Index and Shear Stability*

Viscosity Index (VI) is a measure of the change in viscosity of a lubricant with a change in temperature. This value is derived by measuring the viscosity of the lubricant at 40˚C and 100˚C. The viscosity values are then compared with the VI of two reference oils (35). The higher the VI value the more stable the viscosity is with changing temperature. The VI is an important measure because lubricant applications often work over a wide temperature range. Bio-based lubricants have higher VI than mineral oil due to their long chained fatty acid structure and lack of aromatics (16). Shear stability is a measure of the lubricants ability to resist change in viscosity under mechanical stress.

3.3.4 *Flash Point*

The flash point is the lowest temperature at which the lubricant will ignite, but not continue to burn (16). Vegetable oils have higher flash points due to their longer carbon chains, this is a useful property particularly in combustion engines as lubricants are less likely to be lost through combustion.

3.3.5 *Solvency*

Solvency is the ability of a lubricant to react with other compounds, such as additives or wear debris. The polarity of the base stock is the main determining factor of this. It is an important to consider as the even distribution of additives is important so they can be effective. The ability of a base stock to transport wear debris away from a contact is also important to reduce further wear caused by the wear debris particles (16).

3.4 Additives

Additives are used in lubricants to improve important lubricating properties such as protecting lubricated surfaces and improving base stock performance. Fully formulated oils contain between five and fifteen different additives depending on the application demand. As part of some additive's functionality, they may be chemically changed during use or destroyed and any by-products neutralised by other additives. Most additives are considered to have low mammalian toxicity, but show persistence in terms of pollution and are harmful to aquatic organisms. Zinc dialkyldithiophosphate (ZDDP), one of the most common additives is, however, considered mutagenic due to the zinc content. Most additives have low biodegradability due to their low water solubility and high molecular weight, which means they are found with solid materials (such as soil), rather than water where the microbial degradation process occurs more readily. For this reason they are considered 'persistent' (11). Table 3-2 shows some of the common lubricant additives and their function. Some of these additives have dual functions such as ZDDP, which acts as an anti-wear, anti-oxidant and corrosion inhibiting additive (16).

Additive	Common chemical constituents	Function
Surface Protection		
Anti-Wear	Boron, sulphur, copper, zinc, lead , titanium	Binds to metal surface to form a stable layer, with low shear strength. For boundary lubrication. Reduces friction and wear. Most widely used additive.
Extreme pressure additives	Sulphur, phosphorus, chlorine, molybdenum, sulphurised jojoba oil and fatty acids such as oleic and erucic	As above, but higher film strength and load bearing capacity. High pressures can cause fluid film to rupture.
Friction modifiers	Molybdenum dithiophosphate, dialkyldithiocarbamate organic esters stearic acid	Reduce friction by postponing the onset of boundary lubrication by forming a film on the contacting surface.
Corrosion and rust inhibitors	Organic fatty acids, epoxidised 2-ethylhexyl talate.	Binds to metal surface to create protective layer, stops water or other chemicals from reaching the surface. Suppresses oxidation and the formation of acids.
Performance Enhancement		
Dispersants and Detergents	Sulphonates, phenates, succinimides, fatty acids, metal soaps, salicylates, thiophosphonates.	Polar, keep additives uniformly dispersed, prevent deposits of oxide products.
Viscosity Improver	Oil soluble organic polymers.	Aims to keep lubricant viscosity constant at varied temperatures. The polymers expand at increasing temperature to prevent excessive thinning of the lubricant.
Pour Point Depressants	Polymethacrylate or alkylated polystyrenes.	Reduces size and cohesiveness of crystal structure meaning lubricant still flows at lower temperatures.
Fluid Protection		
Antioxidants	Phosphites, tocopherol-disulphides.	Reduces oxidation of lubricant, and therefore increase in viscosity and corrosive deposits. Reacts with oxygen to form soluble inactive compounds, decomposes peroxides and stops free-radical reactions.
Anti-foaming	Poly-ethylene glycols, polyethers and polymethacrylates.	Prevents foaming caused by lubricant being mixed. Foaming causes reduction of oil circulating and lubricant ability. Works by reducing surface tension causing foam to collapse.

Table 3-2, Some of the Common Lubricant Additives and their Function (11, 16)

3.5 Lubrication Regimes - Stribeck Curve

There are four lubrication regimes lubricants may operate in: hydrodynamic, elasto-hydrodynamic (EHL), mixed and boundary lubrication. It is essential to understand which lubrication regimes a contact operates in, so that the correct lubricant is selected. The lubrication regimes are identified by the oil film thickness in the contact. Operating in boundary or mixed lubrication regimes means that some solid contact will occur between surfaces, but this can be acceptable if the contact has been designed to operate in this regime. Often bushes or plates will be inserted in contacts, such as in journal bearings, which are designed to wear during periods of solid contact, particularly during start-up and shut down of machines. In hydrodynamic lubrication, the surfaces are completely separated by the lubricant and no solid contact occurs.

The Stribeck curve plots the major factors that determine the oil film thickness, viscosity, speed and load against CoF and a typical curve is shown in Figure 3-4. The curve shows the level of friction from boundary lubrication, where CoF is high and solid contact occurs, to hydrodynamic lubrication, where a full oil film occurs in the contact and CoF is lower. The increase in CoF that occurs towards the end of the hydrodynamic regime is caused by viscous drag effects increasing, either due to a high oil film thickness or a high viscosity fluid. The minimum CoF occurs in the transition between the mixed regime and hydrodynamic lubrication; this is generally the ideal area of the curve for machines to operate in. The oil film thickness will be large enough to just separate most of the surface, although some asperity contact may still occur, causing local plastic deformation (35).

Contacts in ICEs often operate within all four sections of the Stribeck curve, boundary, mixed, elasto-hydrodynamic and hydrodynamic lubrication, as shown in (see Section 4.2.1, Figure 4-2). It is essential that contacts are able to operate with these types of lubrication in order to give effective wear protection and friction reduction, while not hindering the performance of the contact.

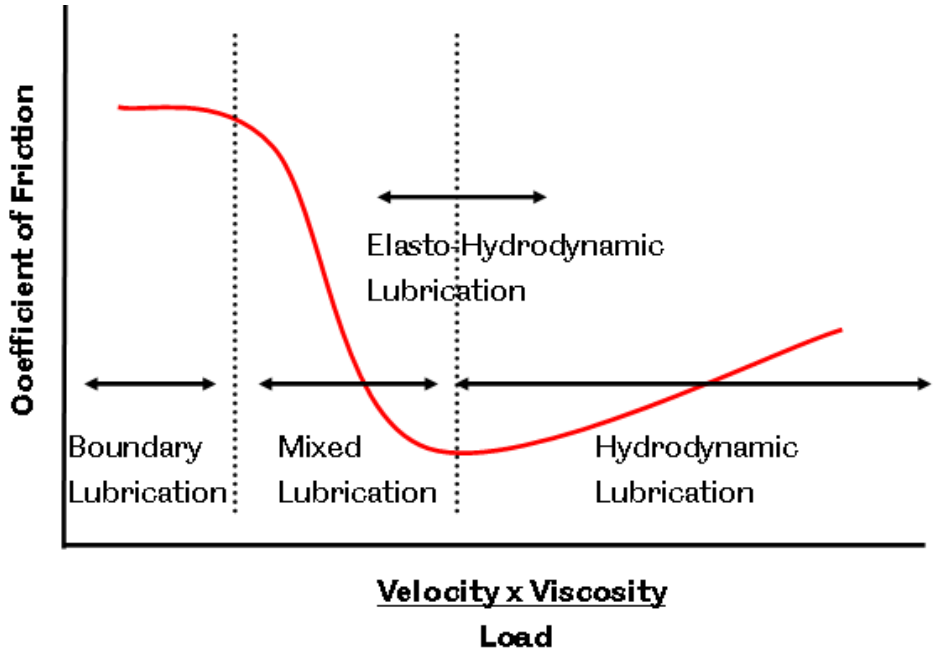

Figure 3-4, An Example of a Typical Stribeck Curve

In the mixed regime, solid contact can occur that causes elastic rather than plastic deformation. When this occurs with high contact pressures, it is known as elasto-hydrodynamic lubrication (EHL). It is an important phenomenon to consider as, in this region, lubricants can stop acting like Newtonian fluids and exhibit pseudo plastic behaviour (49). This behaviour causes a decrease in viscosity with an increase in shear rate. This occurs due to the molecular chains aligning themselves in the direction of increasing shear, so the fluid thins and viscosity decreases (50).

The Stribeck curve is a valuable tool for designing and optimising lubrication systems; through using a Stribeck curve or numerical solutions, the minimum film thickness that can be created by a contact can be obtained. The minimum film thickness occurs at the transition point on the Stribeck curve between mixed and hydrodynamic lubrication; this point is also known as the lift off speed, the speed at which full separation between surfaces occurs (51).

Viscosity has a pronounced effect on the Stribeck curve. In the mixed regime, as the temperature increases the coefficient of friction increases. This increase in CoF is caused by the reduction in viscosity, which means the lubricant is unable to provide adequate protection against the surfaces coming into contact (for the same relative velocity, applied load). In the hydrodynamic regime, an increase in temperature gives a reduction in CoF and this can be explained by the reduction in oil film thickness caused by the lower viscosity oil and lower viscous drag effects. Lubricants with lower viscosity cause the lift off speed to shift to increase (for the same load). It is advantageous to have the lift off speed towards the left of the Stribeck curve to minimise a component's time operating in boundary or mixed lubrication. Lift off speed is directly proportional to the load; in the mixed regime a lower load gave a smaller CoF while a high load gave a higher CoF (51).

In the hydrodynamic regime the reverse is true: the lower the load the higher the CoF and the higher the load the lower the CoF. In mixed lubrication, the load is supported by fluid pressure, as well as some asperity contact, and as the load increases, the solid contact increases; high fluid pressures can also cause an increase in CoF. With hydrodynamic lubrication, high loads are favourable, as this can give thinner films and lower CoF. The overriding factor in lubrication regimes is the relative speeds between contacting surfaces; they must be sufficient to allow oil entrainment and therefore a fluid film to be created (35).

Modern car engines often employ start-stop technology to reduce emissions (52). This means that ICEs operating in the boundary condition more often. As the engine stops, the oil pump stops pumping lubricant around the engine. The lubricant will begin to drain back in to the oil sump. Due to the polarity of bio-lubricants, they may be able to form stronger bonds to engine surfaces and therefore remain in crucial contacts, such as piston ring and liner interfaces, or cam follower, during the start stop period.

3.6 Film Thickness and Pressure Viscosity Coefficient

Most lubricants are piezoviscous, meaning that their viscosity increases significantly under high pressures. This effect is difficult to measure experimentally, as the increase in viscosity only occurs in the contact region and, as soon as the lubricant exits this region, the viscosity reduces again. The viscosity variation with pressure is an important variable to understand as it influences the thickness of the lubricant film in the contact and is required in order to calculate film thicknesses using elasto-hydrodynamic lubrication (EHL) equations (35). Equation 3-1 is one form that may be used to calculate film thickness; it comprises of dimensionless load, *W*, speed, *U*, and material parameters, *G*, as well as an elasticity parameter, *k*.

$$H_{\min} = 3.63U^{0.68}G^{0.49}W^{-0.073}(1 - e^{-0.68k})$$

Equation 3-1

where;

$$H = \frac{h}{R_x}$$

$$W = \frac{P}{2E^* R_x^2}$$

$$U = \frac{\eta_0 u}{2E^* R_x}$$

$$G = 2\alpha E^*$$

$$k = \frac{a}{b}$$

$$\left| \frac{1}{R_x} = \frac{1}{R_{1x}} + \frac{1}{R_{2x}} \right|$$

$$\left| \frac{1}{E^*} = \frac{1-\nu_1^2}{E_1} + \frac{1-\nu_2^2}{E_2} \right|$$

The Barus equation is one way that this effect can be modelled; it is an exponential equation that describes the increase in viscosity, η, by relating the base viscosity, η_0, pressure, *p*, and the pressure viscosity coefficient, α, as shown in Equation 3-2. The pressure viscosity coefficient is dependent on the molecular structure of oils; molecular properties such as interlocking, packing and rigidity, and viscosity temperature characteristics influence this value.

$$\eta = \eta_0 exp\ \alpha p$$

Equation 3-2

While the Barus equation is a common method for calculating pressure increases, experimentally it has been shown to overestimate the value for viscosity (35). Another relation to counter the overestimation of the viscosity increase is shown in Equation 3-3. This does not use an exponential term, it is a power law relationship and therefore the resulting viscosity values are lower. C and n are lubricant dependant constants (35).

$$\eta = \eta_0(1 + Cp)^n$$

Equation 3-3

The Roelands equation is thought to be the most suitable equation for mineral oil based lubricants. Equation 3-4 shows the Roeland equation (35).

$$\eta = \eta_0 \exp\left\{[9.67 + \ln\eta_0]\left[\left(1 + \frac{p}{p_0^*}\right)^{\beta} - 1\right]\right\}$$

Equation 3-4

ß is a lubricant dependant constant in the range of 0.5-0.7, p_0^* is also a constant with a value of approximately 2 x 10^8 Pa. For low pressures, this equation simplifies to the simple power law shown above in Equation 3-4. The Roeland equation is numerically complex, therefore requires computational methods to solve.

The Barus equation requires the pressure viscosity coefficient, which can be difficult to obtain. The PVC is usually well known for mineral based lubricants, but information is lacking for bio-lubricants. So and Klaus developed an expression for calculating the pressure viscosity coefficient based on the kinematic viscosity, ν_0, at the temperature of interest, the ASTM slope of the oil divided by 0.2, represented by *b* in the equation, and the atmospheric density at the temperature of interest, ρ (53), as shown in Equation 3-5.

$$\alpha = 1.216 + 4.143 * (log_{10}\nu_0)^{3.0627} + 2.848 * 10^{-4} * b^{5.1903}(log_{10}\nu_0)^{1.5976} - 3.999 * (log_{10}\nu_0)^{3.0975}\rho^{0.1162}$$

Equation 3-5

A true understanding of the importance of pressure viscosity coefficient and film thickness calculations is not clear. There are some suggestions that the ambient viscosity is the dominant factor for determining film thicknesses, even in elasto-hydrodynamic lubrication (54). Contrarily, other work has shown that PVC has a significant influence on film thickness values; as an example, Leeuwen compared 11 different methods for obtaining film thickness values and found that the PVC did have a noticeable effect on film thickness (55). Further work is required in this area to establish which parameters have a true impact on film thicknesses. Currently, the uncertainty in measurements of PVC and film thicknesses arises due to the complexity of performing experimental or numerical methods.

3.7 Oxidation and Degradation of Vegetable Oils

The degradation of lubricants comes from thermal and oxidative mechanisms. The oxygen containing function groups present in vegetable oils cause oxidation to take places; as degradation occurs, function groups of hydroperoxides, carboxylic acids, alcohols and aldehydes are formed (56).

The main issue with vegetable oils is their lack of oxidative stability, caused by bis-allylic protons; these are hydrogen atoms adjacent to double carbon bonds (known as the allylic position). The bis-allyic protons are areas of enhanced reactivity; due to their relatively weak bonds, this makes them more susceptible to radical attack. Molecules degrade and form polar oxy-compounds and this results in insoluble by products and an increase in viscosity and acidity of the oil. The increase in the acidity of the oil can lead to corrosion (57). Vegetable oils are also more prone to hydrolysis than mineral based oils, which can also lead to increased corrosion (58).

Three stages of degradation are thought to occur in vegetable oils: Initiation, Propagation and Termination. These stages can be described as shown below and represent a first order chain reaction of free radicals, reacting with other products, such as oxygen (59). These reactions are dependent on free radicals and products to react with these radicals. 'R' represents carbon chains. The O· notation represents a free electron.

Initiation

$$2RH + O_2 > 2R\cdot + H_2O_2$$

$$ROOH > RO\cdot + \cdot OH$$

Propagation

$$R\cdot + O_2 > ROO\cdot$$

$$ROO\cdot + RH > ROOH + R\cdot$$

Termination

$$2R\cdot > R\text{-}R$$

$$R\cdot + ROO\cdot > ROOR$$

$$2ROO\cdot > ROOR + O_2$$

The reactions shown above form peroxides and hydroperoxides (H_2O_2), the peroxy radicals (oxygen based compounds) attack the lipid molecules to remove the hydrogen atom, forming hydroperoxides, and this propagates the oxidation process; as they decompose this leads to an increase in the acidity of the oils. The hydroperoxides are not stable and decompose into volatile and non-volatile secondary oxidation compounds (60). The last stage of oxidation is a reaction of aldehyde and alcohol in an Aldol type reaction, forming carbon-carbon bonds, which is due to the carbonyl oxide product polymerising (61). The consequence of these reactions is the creation of high molecular weight compounds and deposits that are insoluble and 'sludgy', as well as increasing the acidity of the oil.

Metals also play a role in degradation; metal-alkylperoxide compounds can be formed at low concentrations of peroxides and high metal concentrations. Peroxide attack on fresh metal leads to the formation of metal oxides that react with acids to form salts. In the early stages of oxidation, the metals can act as a radical scavenger and reduce the amount of sludge formed, but as the peroxides accumulate, oxidation becomes more rapid (62).

Thermal stability of vegetable oils is dependent on the composition of the fatty acids; the first step is the decomposition of unsaturated fatty acids. Oxygen is absorbed through the fatty acid chains and peroxides will form. As this happens, there can be a slight increase in the mass of the sample, as two or more triglyceride chains link together. Thermal decomposition of mono-unsaturated fatty acids (such as oleic acid) happens at higher temperatures. The double bonds are broken and become saturated. Finally, the saturated acids decompose (palmitic). Endothermic reactions occur due to the decomposition of the saturated and unsaturated acids and exothermic reactions occur due to polymerisation of acids. (63).

Anti-oxidant additives can slow down the oxidation process, as can hydrogenation, where hydrogen reacts with unsaturated fatty acids to prevent the weak double bonds or the bis-allyic protons reacting with radicals. Fatty acids such as Stearic and oleic acid are more stable, as they have higher levels of saturation. Vegetable oils can be genetically modified so that they have higher levels of these fatty acids and therefore have high oxidative stability (16). Coconut and palm kernel oil have high levels of saturation and therefore higher levels of oxidative stability than oils such as sunflower and olive oil.

3.8 Lubrication Mechanisms

Many factors dictate the success of a lubricating film. The finish of the lubricated surfaces is important, for example rougher surfaces are able to retain lubricant more effectively, but if surfaces are too rough, asperities may protrude the lubricating film and cause abrasive or adhesive wear. The chemical interaction between the surface and the lubricant is a controlling factor for the effectiveness of a lubricant in boundary lubrication. This dictates whether a stable lubricating film can be formed and is heavily influenced by lubricant additives, as discussed in Section 3.4. If a lubricant base oil possesses the ability to form chemical bonds with surfaces, this reduces the demand for and on additives. The formation of these films is discussed in more detail in Section 3.8.3.

Other lubricant and system properties are also important in the generation of a lubricating film, these include viscosity, relative velocity of the two interacting surfaces and pressures, and these are discussed in Section 3.5.

3.8.1 *Lambda Ratio and Surface Roughness*

The lambda ratio, λ, as shown in Equation 3-6 compares the lubricant film thickness with the size of surface asperities (35).

$$\lambda = \frac{h}{\sqrt{\sigma_1^2 + \sigma_2^2}}$$

Equation 3-6

where;

h is the film thickness
σ_1^2 and σ_2^2 are the surface roughnesses of the interacting surfaces

There is no general consensus on which values of lambda correspond to the different lubrication regimes. As an example, lambda ratios in the range of 5 to 100 may indicate hydrodynamic lubrication, EHL may occur in the range of 3 to 10 and mixed lubrication between 1 and 5. There is consensus that boundary lubrication occurs with lambda

ratios of less than 1. As a general trend, larger values for lambda result in less contact between surfaces and lower friction. There is a trade-off between using a lubricant that generates a thicker film and losses due to the presence of a thicker fluid film (pumping and viscous).

3.8.2 *Wettability, Spreading and Surface energy*

The wettability of a fluid is defined by the contact angle between the surface and the outer edge of the fluid drop, the lower this is the better the wettability or spread of the fluid. The wettability of a lubricant is important in boundary lubrication regimes, however, in mixed to hydrodynamic lubrication, where thicker films form, the wettability is no longer an important parameter because viscous effects dominate. The wetting energy is the adhesion energy of the surface/fluid interface minus the fluids surface tension (64). The surface roughness will influence the wettability of a fluid, and friction and wear are influenced by this parameter, as it controls the coverage of the lubricant. Lower viscosity fluids exhibit better wettability as do fluids that have higher polarity. Bio-lubricants have a higher polarity than conventional mineral oil based lubricants, but tend to have a higher viscosity. For steel surfaces bio-lubricants tend to offer better wetting, as discussed in Section 6.7.1

Kalin & Polajnar (65) found that the important parameter to define wettability is spreading, as the contact angle of an oil on a surface does not correlate with the surface energy. A fluid's ability to 'spread' is based on the difference between cohesive forces. Intermolecular forces that resist a fluid fully separating and adhesive forces, which are attractive forces between dissimilar molecules, control cohesive forces (66). Kalin & Polajnar proposed a new model for calculating the spreading parameter, SP, that does not take in to account contact angle, shown in Equation 3-7;

$$SP = 2\left[\sqrt{\gamma_S^D \gamma_L^D} + \sqrt{\gamma_S^P \gamma_L^P} - \gamma_L\right]$$

Equation 3-7

Where,

γ_S^D *is the dispersive component of surface energy, mJ/m²*

γ_L^D *is the dispersive component of surface tension, mN/m*

γ_S^P *is the polar component of surface energy, mJ/m²*

γ_L^P *is the polar component of surface tension, mN/m*

γ_L *is the total surface tension, mN/m*

Polar forces create permanent electric dipoles between molecules and therefore are a strong force. Dispersive forces are much weaker, up to ten times smaller, as they only form instantaneous dipoles that are not permanent. Based on this theory, Kalin & Polajnar proposed a 'slip inducing interaction model based on surface forces' shown in Figure 3-5 this highlights the difference in dispersive and polar interactions.

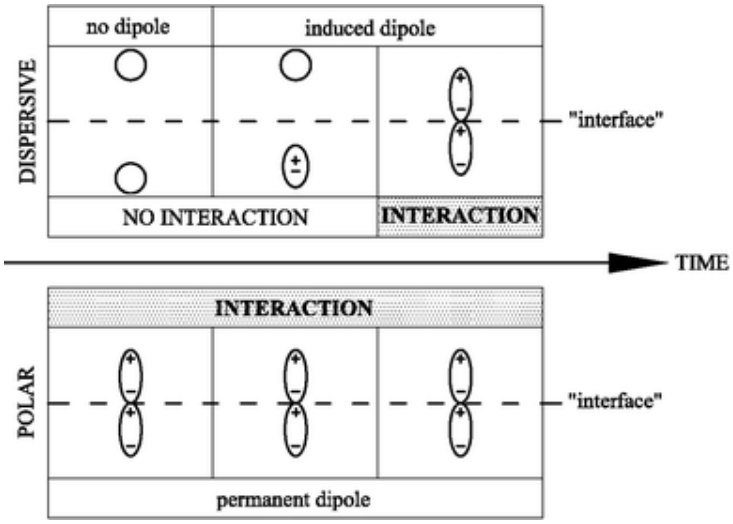

Figure 3-5, Slip-Inducing Interaction Model Based on Surface Forces, Describing the Difference Between Polar and Dispersive Interactions

3.8.3 *Film formation*

Lubricants react with contacting surfaces to form films, as represented in Figure 3-6. Physisorbed films are weak and easily removed, while chemically reacted films are strong and can withstand relatively high loads. Chemisorbed films are stronger than physisorbed films, but weaker than chemically reacted films. These films are formed by electron sharing or exchange between the lubricant and the contacting surface that form strong covalent bonds. This layer can be single or several molecules thick. Chemically reacted films are thicker than chemisorbed films and have the highest adhesion properties. Physisorbed films are the weakest class of film, where there is no exchange of electrons and van der Waal forces are dominant, and can be single or several molecules thick (67).

Chemisorbed films occur with bio-lubricants if the base stocks are highly polar; the formation of these films is well documented for vegetable oil base stocks such as soybean and jojoba oil (68) (67) (69) (70) and, second to biodegradability, is the most beneficial property of vegetable oils. In mineral oil base stock lubricant formulation, it is reported that additives with anti-wear functions can pass through all three stages of film formation, physisorbed, chemisorbed and chemically reacted. Physisorbed films break down when temperatures reach the melting point of the given additive and chemisorbed films can remain above the melting point of the additive, but will eventually fail (71)

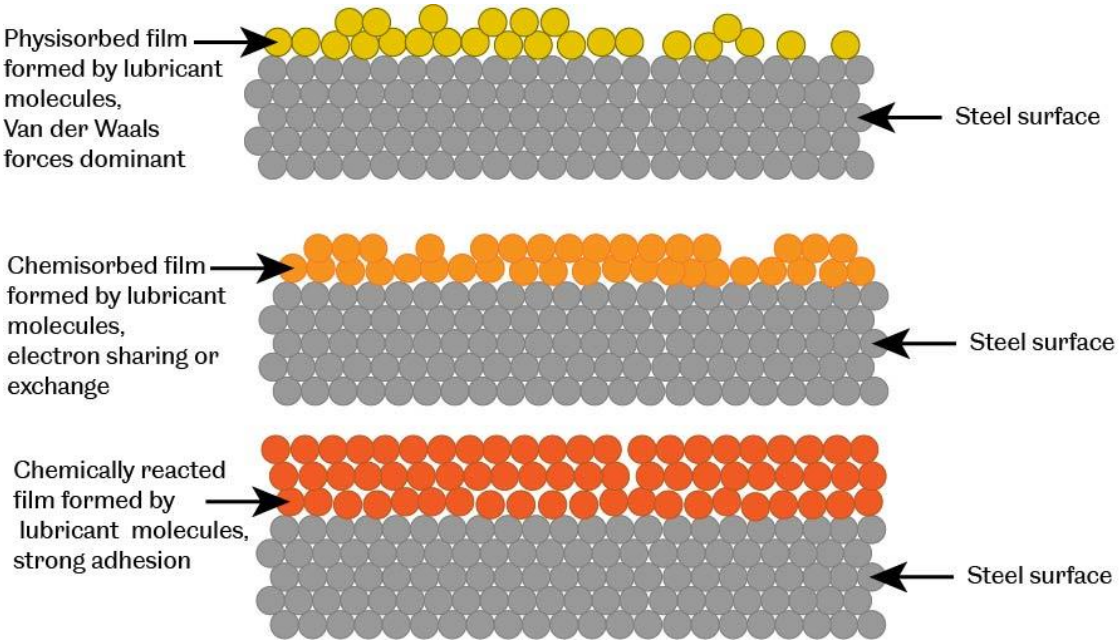

Figure 3-6, The Different Levels of Film Formation Between Lubricants and Steel Surfaces (colour strength represents strength of bond to surface)

3.9 Conclusions

This chapter summarises the importance of the molecular structure of base stocks and how they affect lubrication tribology. The molecular structure and intermolecular forces dictate how well molecules shear over one another, and therefore how well they lubricate. The three main types of base stock described were mineral, synthetic and bio-based. Mineral base stocks are cheap, their tribological properties are well understood, but they are toxic and not readily biodegradable. Synthetic base stocks can be tailored to meet almost any tribological performance requirements but are expensive and also toxic and not readily biodegradable. Bio-based base stocks are biodegradable and not toxic, but due to this do not possess good oxidative stability. They have the potential to have some favourable tribological properties, such as high VI and the ability to form films on contacting surfaces, without the need for additives. There are a wide range of additives that could be used to improve the performance of bio-based base stocks to compensate properties, such as poor oxidative and pour point.

The oxidative stability and degradation of vegetable oils, discussed in this chapter are one of the main barriers to wider implementations for their use in bio-lubricants. The process of oxidation has been detailed in this chapter and is useful to understand for any evaluation of changes in lubricants through use.

Of particular relevance to bio-lubricants is their ability to form physisorbed and chemisorbed films on surfaces. The literature review will assess how effective these films are at protecting surface compared with conventional lubricants. This chapter also discussed the theory of wetting and found that bio-lubricants may spread over a surface more readily then mineral based oils.

4 Uses for Bio- Lubricants

This chapter gives a brief historical of bio-lubricants, followed by an overview of the current uses of bio-lubricants available and the markets they are designed for. Some anecdotal performance information is provided, from the use of bio-lubricants in autorickshaws and scooters in India. Details of some engine and field tests are also given. An overview of lubricants in an internal combustion engine follows, which details the lubricants journey around the oil circuit.

4.1 Current Applications

The use of vegetable oils as lubricants dates back beyond the ancient Egyptians, who used animal fats to lubricate wooden chariot axles, and when metals began to replace wood for moving parts a wider range of sources, were used, such as tallow, olive oil and castor oil. Tallow, for example, was a common lubricant in steam engines as it is resistant to being washed away by steam (72). In the late 19th century mineral oils began to replace bio-lubricants. Early aircraft piston engines (and automotive engines) used castor oil as a lubricant (73). Castrol's first four stroke engine oil contained castor oil (74), but as engine performance increased so did the demands on the lubricant and mineral based lubricants offered a simpler solution.

Automotive lubricants account for approximately 70% of total lubricants sold, with industrial lubricants accounting for the remainder (75), and most major lubricant manufacturers now sell bio-based industrial fluids, particularly for hydraulic and metal working applications. Fully formulated bio-lubricants are also beginning to be increasingly available and in use, for example FUCHS Lubricants' PLANTO range of biodegradable lubricants, which includes chainsaw oils, hydraulic fluids and greases. These are mainly synthetic lubricants, with a few based on vegetable oils (76). John Deere have also developed an agricultural targeted hydraulic fluid based on canola oil called 'Bio HyGARD^{TM} II (77). The agricultural industry could see the most benefit from increased use of biodegradable lubricants, given the close proximity of machinery, such as tractors, to soil and the food chain.

In Southern India, abundantly available coconut oil is being used as a two-stroke engine lubricant in autorickshaws and scooters (78). Anecdotal evidence indicates that some experience more wear, but with increased fuel efficiency, acceleration, smoother operation and less smoke. Coconut oil has a high pour point and therefore could only be used in this manner in areas with high ambient temperatures.

Some small trials, with limited information on their success, have been carried out on fleet vehicles and bio-lubricants. The US Postal Service ran a trial with a soybean oil based bio-lubricants in 1999, in partnership with the United Soybean Board. The drive cycle of the postal vans is considered to place a significant demand on the engine lubricant to perform at boundary conditions, due to engines operating at low speeds and frequently idling, and therefore oil circulation rates were low. Effective boundary lubrication film formation is essential to protect components from wear. Figure 4-1 shows some of the results from engine oil analysis after the trial, mineral (petroleum) based lubricants had significantly higher levels of iron in them then their bio-based counterparts, indicating higher levels of wear (75). This shows that there is potential for bio-lubricants to offer benefits over conventional lubricants.

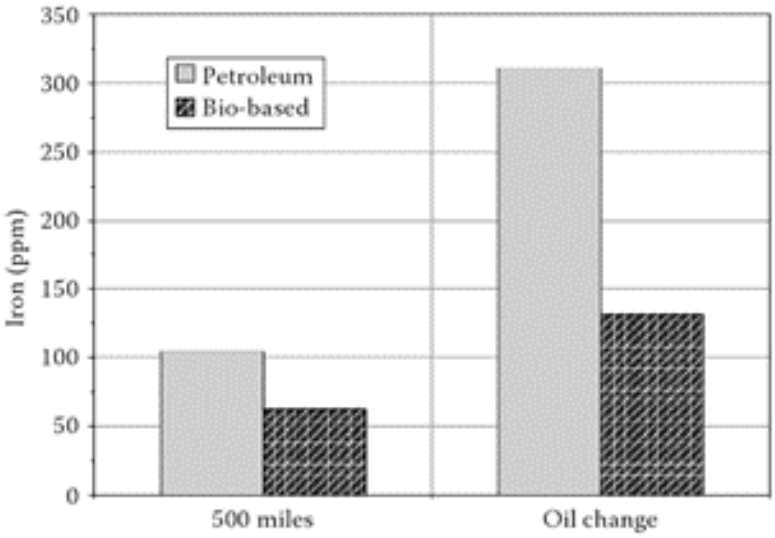

Figure 4-1, Results of Iron Levels in Lubricants from Field Trials Conducted with the US Postal Service (75)

Elsewhere in the USA, Colorado State University have variously used canola, sunflower, soybean and castor oil in a Ford Mustang engine running on a dyno, and Pennsylvania State University successfully trialled a corn based oil in fleet vehicles (75).

Hydraulic fluids are the fastest growing area of use for bio-lubricants, as discussed in Section 2.4, chemically modified vegetable oils are becoming popular due to their improved thermo-oxidative and low temperature performance, as well as some formulations being used in high pressure and temperature environments. Second to hydraulic applications, bio-lubricants are being favoured in two-stroke engine total loss lubricants, for applications such as motorcycles and chainsaws, due to their biodegradability, low toxicity and ability to adhere to metal surfaces readily due to their polar nature.

4.2 Lubricants in Internal Combustion Engines

The demand on the performance of internal combustion engine lubricants is increasing in line with the demand for increased fuel economy and reduced emissions. The GF-6 passenger car lubricant specification, discussed in Section 2.3, show the demand for lower viscosity fluids and increased performance. The lower viscosity means that viscous drag and coefficient of friction is reduced. The piston assembly, crankshaft bearing and valve train are seen as the three major areas for friction loss in an engine. As can be seen in Table 4-1, these areas all operate in different lubrication regimes.

The piston assembly accounts for 40-60% of friction in an internal combustion engine. Very thin lubricant films operate between the piston ring and liner interface. This interface is a significant contact as it plays a role in emissions and lubricant consumption, as well as fuel efficiency and engine performance through friction. In this region the lubricant is subjected to high loads and temperatures in excess of

200˚C, it is also exposed to unburnt oxygen and combustion by-products with can accelerate degradation (79).

Cam followers account for 20-30% of friction in an internal combustion engine. These non-conformal contacts are difficult to lubricate due to the high speeds, loads and temperatures they operate at. Nissan, along with many other automotive manufacturers, coat their cam followers in diamond-like-carbon (DLC) to reduce friction, and developed a lubricant based on poly-alpha-olefin oil to ensure effective lubrication with this type of coating (80).

Table 4-1 shows the main areas for lubrication in an internal combustion engine and based on knowledge presented in this chapter, bio-lubricant suitability to act as a lubricant in various engine contacts is hypothesised.

SYSTEM	TYPE OF LUBRICATION	BIO-LUBRICANT SUITABILITY
Crankshaft bearing	Hydrodynamic	Yes, loads and temperatures not extreme
Crank pin bearing	Elasto-hydrodynamic (mixed)	Potentially suitable due to ability to form tribofilms, a better understanding of bio-lubricants in EHL is however required.
Wrist pins	Elasto-hydrodynamic (mixed)	
Camshaft bearings	Hydrodynamic	Yes
Pushrod ends	Sliding Hydrodynamic	Yes
Rocker arms	Sliding Hydrodynamic	Yes
Rocker arm ends	Sliding Hydrodynamic	Yes
Oil pump gears	Sliding Hydrodynamic	Yes
Lifer bore	Hydrodynamic	Yes
Piston ring	Hydrodynamic, Boundary at TDC/BDC	Potentially, but high flash temperatures and long chains risk ingress in combustion chamber and increasing emissions
Skirt and valve stem	Hydrodynamic	Yes
Valve train	Boundary/mixed	Potentially, but difficult area to lubricate, effective tribofilm formation may aid this.

Table 4-1, The Types of Lubrication and Bio-Lubricant Suitability

4.2.1 *The Journey Around the Internal Combustion Engine Oil Circuit*

The internal combustion engine (ICE) is a harsh environment for lubricants and this is one reason why the development of biodegradable lubricants for internal combustion engines has been slow. As Table 4-1 highlights, ICE lubricants are exposed to many different environments and materials in one application. Figure 4-2 shows the areas in which a lubricant travels around the combustion engine.

The journey of the engine oil begins in the sump, it passes through the oil pump and filter, where the oil may also be exposed to elastomers, it travels on to the main crank bearing where the loads on the oil films begin to increase but the lubricant operates in hydrodynamic lubrication. The oil travels up the connecting rod to lubricate the

pins and the piston ring/liner interface and subjected to the highest loads and temperatures.

The engine block houses the main oil passageways and oil sump for an ICE. It is essential that the lubricant does not degrade this structure as it is essential for the safe effective operation of the ICE. The materials used for engine blocks have developed with the drive for weight reduction to optimise emissions and efficiency. The use of cast iron has reduced as the use of aluminium alloys has increased due to its low density and good thermal conductivity, and the ability to reduce the engine block weight by between 40-55% in comparison to a cast iron block (81). Magnesium alloy engine blocks are capable of reducing weight by 75% in comparison to those made from cast iron, and 25% compared with aluminium alloy they are also better able to cope with shocks and dents and dampen vibrations (82). BMW created the first magnesium-aluminium alloy engine block that went in to production in 2004, it required aluminium inserts for the cylinder liners due to corrosion concerns. Cast iron inserts are often used in areas where aluminium cannot offer acceptable wear protection, such as in the main bearings and to combat any thermal expansion issues that could arise with the use of aluminium. In order to improve strength in the cylinder bore and reduce friction, lining materials are often used, such as NikaSil (83) or chromium nitride plasma vapour deposition (PVD) coatings (84). Ceramics and DLC (85) are becoming more commonly used in many different engine contacts to reduce wear. Molybdenum is a popular facing material for rings due to its favourable wear resistance, as is graphite (86).

The valve train is one of the most difficult areas to effectively lubricate due to the small oil passage way, high loads and speeds, therefore works in the boundary/mixed regime. The materials used vary and can be grey cast iron or forged steel, and may have a coating, such as titanium nitride or DLC. The lubricant also acts as a hydraulic fluid in cam phasing devices, variable valve actuators and tensioners, which adds further demand on the lubricant as this can cause aeration, which the lubricant must be able to resist (16). The lubricant also acts as a coolant, transferring heat to the cooling system and transporting debris away from contacts to be removed by the oil filter to prevent further damage.

Phosphorus and sulphur in lubricant additives can effect catalyst performance if the lubricant makes it way in to the combustion chamber and therefore limits on the levels of these is set in specifications such as GF-6.

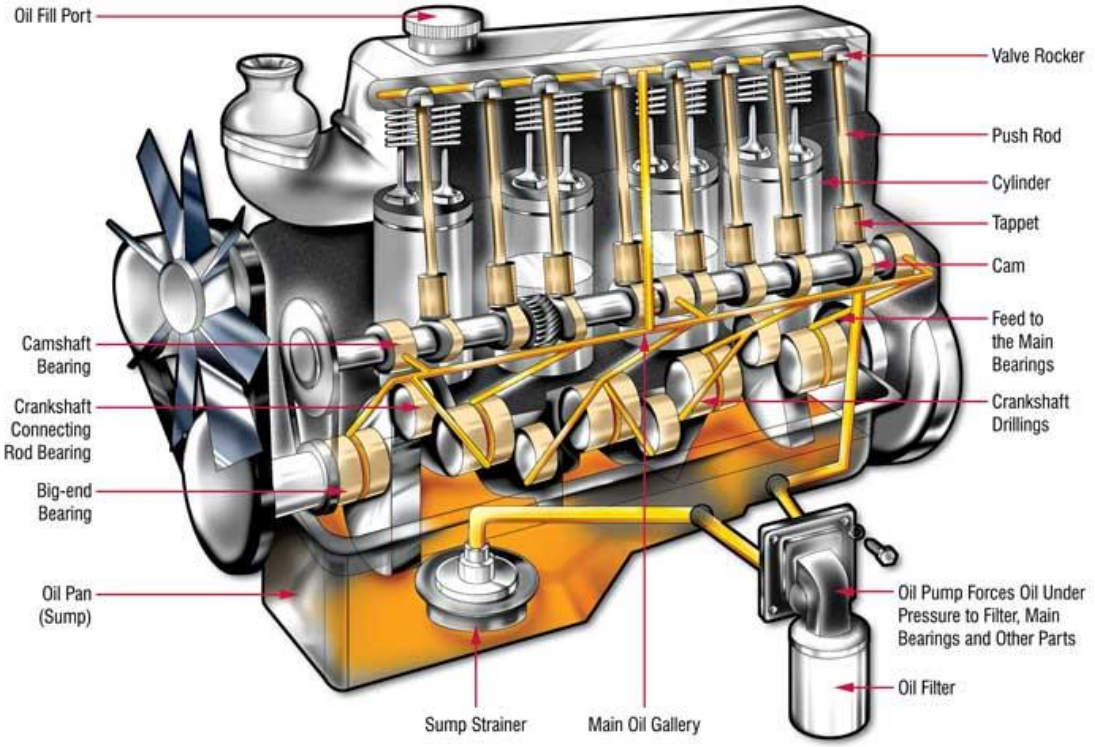

Figure 4-2, Areas in which a Lubricant Travels Around the Combustion Engine. (91)

4.3 Conclusions

Bio-lubricants have a long history of use in many applications, historically tallow, olive and castor oil were predominantly used. Bio-lubricants have been making a resurgence, becoming more common in hydraulic applications due to the high risk of spillages and the operating temperatures being less extreme.

Some trials have been conducted with two-stroke internal combustion engines. Anecdotal evidence showed improved fuel efficiency due to friction reductions, but higher wear when coconut oil was used.

There have been sporadic research trails with bio-lubricants and four stroke internal combustion engines. In boundary lubrication lower wear rates were observed with bio-lubricants then with mineral based lubricants. Internal combustion engines pose significant performance demands in reducing friction and wear, while not causing large viscous drag. Lubricant temperatures can reach 200˚C for short periods of time during its journey round the oil circuit, therefore thermal stability is important. Coatings are increasingly being used where lubricant technology struggles to improve wear and friction performance. Additionally to coatings, the lubricants come in to contact with many different materials in a combustion engine, from various grades of steel, aluminium alloys, cast iron, solid lubricants, elastomers and potentially magnesium. It is important that the compatibility between these material and bio-lubricants is well understood to ensure functionality.

The next chapter will focus on current research and knowledge of using vegetable oils as bio-lubricants, with thought to how they may be applied in an internal combustion engine. Literature will focus on the ability of bio-lubricants to reduce wear and

friction, a fundamental requirement of lubricants. As highlighted, automotive lubricants come in to contact with many different materials, and the development of new automotive coatings to reduce wear and friction is ongoing, therefore a review of current knowledge on the interaction of bio-lubricants and a variety of materials is explored.

5 Key Tribological Mechanisms and Material Interaction Related to Bio-Lubricants

This chapter explores current theories related to the performance of lubricants. It covers the fundamentals of wear and friction mechanisms, as well as lubricant and film formation mechanisms. Surface coatings are now commonly used in many engineering applications to reduce wear and friction. The effect of the type and finish of the substrate on coating performance is briefly discussed. The wear and friction mechanisms of a common automotive coating system, diamond-like-carbon (DLC), are explored, looking particularly at graphitisation, adhesion of the coating to the substrate and how lubricants interact with this coating. Shot-blasting is also a common surface treatment, so the effects of controlling surface roughness are examined, as well as benefits of the solid lubricant molybdenum disulphide as a doping medium. The use of calcium sulphate as a novel coating is also introduced; to date the use of such a coating in automotive applications is currently only known to have been used in motorsport. The use of multi-layer coatings to improve wear and friction is also discussed; there is currently little published work or theories covering this area. To follow on from the work on surface coatings, theory related to calculating film thicknesses and pressure viscosity coefficients are discussed.

One of the main disadvantages of using bio-lubricants in engineering applications is their lack of oxidative stability therefore it is necessary to present the theory and mechanisms that cause oxidation. Similarly, to complete this chapter, the mechanisms that are responsible for degrading elastomers are introduced. This includes the theory of stress relaxation of elastomers and Hanson Solubility Parameters. The parameter that has the potential to predict whether an elastomer will degrade when in contact with a given fluid is also discussed.

5.1 Wear, Friction and Lubrication Characteristics

There is no general theory governing the behaviour of interacting surfaces, this is due to so many influencing parameters. Friction and wear are the most important aspects, although there are many other parameters that influence the friction and wear of interacting surfaces, as listed in Table 5-1. By optimising the interacting surface and lubricant, significant reductions in friction and wear will occur, and the impact of the parameters listed in Table 5-1 will lessen.

Movement of components	Type of movement and distance Continuous or discontinuous
Shape of contact	Contact geometry
Type of material	Mechanical and physical properties, such as corrosion resistance, toughness, creep, fatigue, strength etc. Topography Surface stresses Surface energy (wetting and spreading of lubricant) Composition of both bodies in contact
Stresses	Contact pressure Sliding speeds Operating cycles Coefficient of Friction
Environment	Chemical reactivity Temperature Contamination
Lubrication	Viscosity Boundary lubrication properties Surface tension Additives

Table 5-1, Some Parameters that Influence Wear and Friction in Interacting Surfaces

5.1.1 *Primary Wear Mechanisms*

The main wear mechanisms in an internal combustion engine are abrasion, adhesion and corrosive wear. Frictional wear mechanisms include adhesion, ploughing and hysteresis, while wear mechanisms are adhesion, abrasion and fatigue combined with fracture mechanisms (64). Primary wear mechanisms are those wear mechanisms from which wear initiates.

5.1.1.1 Abrasion

Abrasive wear occurs when two surfaces are in relative motion. Hard surfaces (two body abrasion) or particles (three body abrasion) remove material from softer surfaces. For three body abrasion, particles only need to be approximately 20% harder than a contacting surface to become an issue (35). Rougher surfaces exhibit higher abrasive wear. Abrasive wear is characterised by parallel grooves in the direction of motion; material will not necessarily become detached from the surface but may be displaced plastically in a 'ploughing' action, with banks of material building up either side of the parallel grooves. 50% of wear in industrial machines is due to abrasion (35). This is the type of wear that can be seen in the piston ring/cylinder liner contact, where soot can act as a third body to cause abrasion. To reduce this type of wear, the role of the lubricant is to separate the two contacting surfaces. Ensuring the contacting surfaces have an appropriate surface hardness and low surface roughness will also act to reduce this type of wear.

5.1.1.2 Adhesion

Adhesive wear occurs when asperities of the two contacting surfaces adhere to each other in boundary lubrication conditions; the softer asperity will be removed and remain adhered to the harder asperity or detach to become wear debris. Adhesion can also be beneficial, for example, the ability of a lubricant to form a chemically bonded layer with the contacting surfaces can reduce material loss. Selecting dissimilar surface materials or materials that are chemically inert will reduce the likelihood of asperities adhering to one another.

5.1.1.3 Corrosion

Corrosion is likely to occur in piston ring cylinder liner contacts due to large temperature changes and acidic deposits from combustion by-products. Corrosion is the deterioration of a surface due to a reaction with a second substance, such as an acidic deposit or water. Corrosion of metallic surfaces is dependent on electron exchange and physical chemistry mechanisms, the type of metal, and thermodynamics (88). A chemically bonded lubricant layer will protect the surfaces, provided it is not acidic, as will selecting surface materials that are chemically inert.

5.1.1.4 Contact Fatigue

Fatigue is caused by cyclic loading. Subsurface plastic strain builds up over repeated loading and a crack is formed and propagates to form pitting on the surface. If cracks propagate and pits meet, larger sections of material may be removed, this is known as spalling. This type of wear is most likely to be seen in bearings and camshaft mechanisms in ICEs (89). Asperity fatigue can also occur; as the asperities are repeatedly loaded, fatigue takes place and the asperity tips will be removed. Rougher surfaces have more asperities to carry the load and therefore stress at individual asperities is reduced (64). The load carrying capacity of a lubricant, linked to its ability to remain in the contact zone, will contribute to reducing fatigue wear. The location and magnitude of stress in the contact zone, along with the type of material has a greater influence on fatigue wear. For a particular application, a material with an appropriate fatigue limit should be selected and the system optimised to keep the coefficient of friction as low as is feasible in order to design for reducing contact fatigue.

5.1.2 *Secondary Wear Mechanisms*

Secondary mechanism are those that result from primary wear mechanisms, those particularly relevant to ICEs are listed.

5.1.2.1 Scuffing

Scuffing is normally associated with adhesive wear and is caused by a breakdown in the lubricating film under high loads, which results in the contact being starved of lubricant. Scuffing occurs in the boundary lubrication regime at the very left-hand side at the top of the Stribeck curve, as seen in Section 3.5.

5.1.2.2 Delamination

Delamination can be described as a form of fatigue. Delamination is caused by cracks running parallel to the surface; these meet and cause large sections of surface material to be removed. Delamination can occur in surfaces with coatings, and can be formed due to flaws in the adhesion between the coating and the substrate, as well as cracks (90). As with contact fatigue, the reduction of this wear mechanism is achieved

through keeping coefficient of friction low, as well as ensuring an appropriate adhesion method is used for coatings.

5.1.3 *Friction Mechanisms*

Friction is a resistive force resulting from two surfaces interacting. Friction and wear are two distinct phenomena, but are intrinsically linked. Wear mechanisms contribute to the apparent level of friction, and friction can cause wear. Three main mechanisms govern friction; adhesion, deformation and hysteresis. These mechanisms do not always contribute to wear: in the case of adhesion, if there is shearing at the weld interfaces, then wear will not occur. Wear will only occur if deformation is plastic, not elastic. Hysteresis is a lag in response by the material due to internal damping during elastic or plastic deformation. This mechanism is dominant in visco-elastic materials, such as those discussed in Section 5.3, and would not result in wear over one cycle.

5.2 Surface Treatments and Coatings

Reducing friction in moving components is a major challenge, driven by the need to increase efficiency and longevity of components. Along with system design and lubrication, surfaces are a key area that can be developed to reduce friction. Surface engineering is now common practice in many different applications. Previously, engineering design focused on improving bulk material in combination with optimising lubricants. New coatings and treatments with properties and costs not achievable in the past have driven their increased use. That said, friction in a great many contacts can be adequately controlled through 'traditional' methods.

The surface is the most important part of a component and, in optimising this area of the component, significant performance improvements can be achieved. 95% of components fail due to surface related effects, through either wear, fatigue or corrosion (64). Surface coatings and treatments open the possibility of tailoring specific areas of a surface to specific properties. This can also mean that the substrate material can be altered, as there is less pressure on the bulk material to provide the component performance; for example, the substrate can be designed to be strong and tough, while the coating can act to reduce wear and resist corrosion.

Holmberg and Matthews (64) described four different zones of a coated component that all require optimisation to develop an efficient engineering surface. These zones are highlighted in Figure 5-1. The process of optimisation is a compromise between properties, for example it is difficult to engineer a coating that is both hard and has good adhesion to the substrate. Properties important to the substrate and coating alike are: thermal conductivity and expansion, hardness, elasticity and fracture toughness. While properties at the interface between the substrate and coating require good adhesion and shear strength, the surface of the coating requires good shear strength, optimised chemical reactivity and surface roughness. These properties are controlled by the type of coating used, the way the coating is applied to the substrate and how thick it is; they are dictated by the microstructure of the coating and substrate, such as the density, grain size, orientation and boundaries.

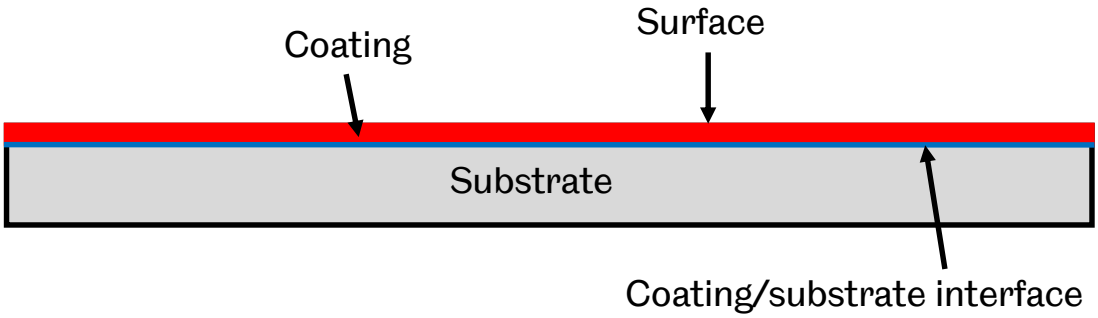

Figure 5-1, A Schematic of the Different Zones of Importance in a Coated Contact

Surface engineering includes the use of surface texturing to reduce wear, improve lubrication retention, remove or trap debris and reduce adhesive wear, with the size and orientation of such texturing important (91). Surface coatings are used to reduce wear and friction, alter surface properties, such as hardness and roughness, and improve conformity. The main types of surface treatments are:

1) Structural transformation; the surface properties are altered by transformation, hardening or mechanical treatments such as shot peening;

2) Diffusion treatments, which work by diffusing material in to the substrate, this material may or may not react with the substrate; metalloids and metals such as nitrogen or chromium can be used to form corrosion resistant or hard surfaces;

3) Conversion treatments, such as anodizing, which are used to reduce corrosion, either chemical or electrochemical reactions occur with the substrate material. Coatings can alter a wide variety of surface properties, they tend to sit on the substrate and very little diffusion or reaction takes place. Commonly used methods of applying coatings include physical or chemical vapour deposition, thermal spraying or electroplating.

There are many different types of material that can be used as coatings, soft metals such as silver, copper or lead are used due to their low shear properties and are known as solid lubricants. The thickness of a coating is an important parameter as this influences tribological properties. Thinner films can produce lower wear rates but, if the film is too thin, then asperities can break through and wear rates increase. If the coating is too thick, the contact area is increased and this can lead to increased friction. Micro cutting of the film is seen in thicker films, as asperities of the opposite surface cut through into the coating. In thin films, fatigue mechanisms are dominant. If the coating is too thick, delamination can occur, the delaminated coating can then act as a third body to propagate abrasive wear. For soft coatings on a steel substrate, generally the optimal film thickness is less than 1 μm. An increase in thickness with soft coatings is causes a decrease in load carrying capacity and an increase in ploughing wear.

5.2.1 *Diamond-Like-Carbon*

The use of DLC has become extensive due to its high mechanical strength, hardness, wear protection, low friction and because it is chemically inert (64). It is a well-studied coating and is capable of reducing wear and friction in boundary and unlubricated contacts. Amorphous DLC consists of sp^3 carbon structures (diamond) with sp^2 carbon structures (graphite) embedded in the sp^3 matrices, as shown in Figure 5-2. The ratio of sp^2 to sp^3 and the level of hydrogen in the coating are the most important factors for the resulting coating properties.

Up to 50% of DLC coatings with high levels of hydrogen exhibit higher CoF and lower wear resistance. Hydrogen DLC (H-DLC) has fewer cross links across the carbon structures. DLC with lower levels of hydrogen, less than 1%, has more cross links, higher wear resistance and lower CoF. H-DLC is a stable form of DLC, meaning it is less likely to become graphitic. Low hydrogen content DLC can have hardnesses of 40-80 GPa compared with 2-30 GPa for hydrogen containing DLC and Young's modulus of up to 900 GPa compared with 300 GPa (62).respectively. As an example, a tetrahedral amorphous carbon (a-C:H) has up to 50% hydrogen and is sp^2 dominant, a-C less than 1% hydrogen and sp^2 dominant and ta-CH and ta-C more sp^3 dominant.

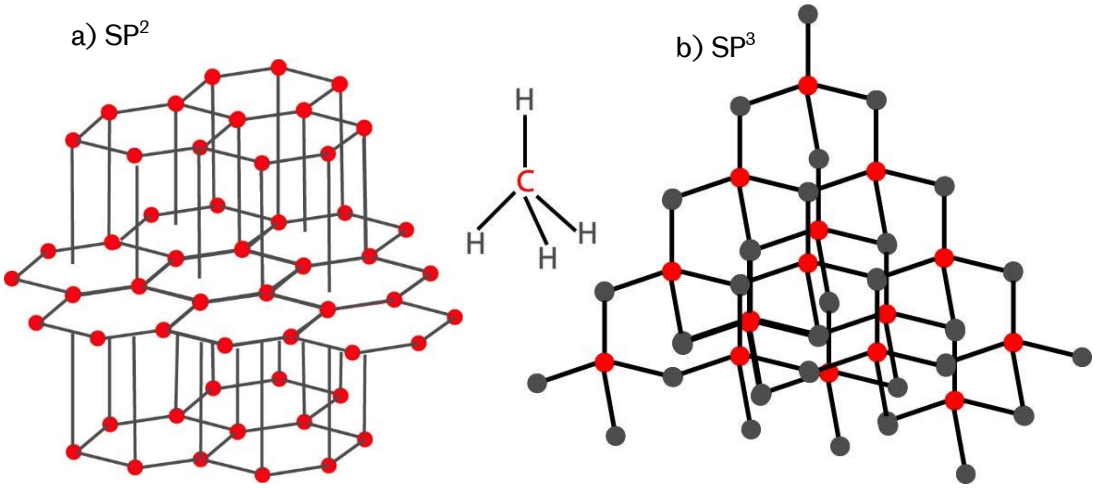

Figure 5-2, a) sp^2 Carbon Structures (graphite) and b) sp^3 Carbon Structures (diamond)

The tribological mechanisms of DLC can be separated into three scales; macro-, micro- and nano-; and different mechanisms are dominant in each scale. At the macro-scale, with a surface roughness of between 0.1 to 1 µm R_a, asperities, adhesion and abrasion are dominant. At a micro scale, with a surface roughness of 10 to 100 nm R_a, graphitisation is dominant and this process may also appear at a macro scale. At the nanoscale, with R_a values in the range of 1 to 30 nm, the dangling hydrogen weak van der Waals bonds are broken. The roughness of the coating is dependent on the roughness of the substrate. The superior wear protection of DLC coatings is attributed to the high hardness and the formation of transfer layers, as discussed in

5.2.1.1. The coating also has high elastic recovery, which means that higher loads are required to plastically deform the coating (92).

For steel and DLC coating on a soft substrate in contact, the dominant wear mechanisms are abrasion and ploughing. DLC has high in-plane compressive stresses; at thicknesses of over 2 µm, delamination is more likely as compressive stresses increase with increasing coating thickness (64).

The typical thicknesses of DLC coating are between 0.01-2 µm but they can be in the order of nano metres. Coatings thicker than 2 µm suffer very high intrinsic stresses and are at great risk of delamination (93). Adding Titanium or Silicon as a doping agent reduces the intrinsic stresses in thick coatings, as it reduces the number of connections in the carbon network. Alternatingly laying hard and soft DLC layers can also reduce the intrinsic stresses.

Doping can also be used to alter other properties, such as hardness, elastic modulus and substrate adhesion, as well as friction and wear. Dopants such as silicon, nitrogen and boron are most commonly used. Examples of metal dopants include Iron, chromium and molybdenum.

Along with intrinsic stress, moisture is considered the biggest issue with DLC coatings. This can also be improved with dopants such as nitrogen, flurine, silicon and titanium can reduce the sensitivity to friction increases due to humid conditions.

5.2.1.1 Graphitisation

DLC's ability to keep CoF low in contacts is attributed to the formation of a graphite layer. A low shear film may form during asperity contact, where temperatures may reach high enough values to transform carbon to graphite. The sp^2 graphite structures that are theorised work similarly to MoS_2, in that the hexagonal planes of covalently bonded carbon atoms lie in parallel. Weak van der Waals forces between these planes mean they slide over one another with relative ease (64). Fatigue wear within the contact is responsible for the formation of a graphite layer, due to interlayer bonds being broken and forming a transfer layer on the counter surface. Relatively high temperatures are required for graphitisation to occur, temperatures of 350 ˚C at asperity contacts have been calculated for high speed and load conditions (40 N, 3m/s). At this temperature, hydrogen diffuses out of the sp^3 matrix structure and can transform into the sp^2 graphite structure. At higher temperatures, graphitisation happens rapidly and the transformation may happen further than just at the surface of the coating and begin to affect the coating substrate interface.

5.2.1.2 Substrate hardness and roughness

Hard coatings, such as DLC (discussed in Section 5.2.1), on softer substrates are a widely used combination. A thin hard coating can protect the substrate from abrasion and ploughing as well as corrosion. Hard coatings can form a transfer layer on the counterface, resulting in low shear strength interactions between surfaces and very low friction. In this situation a lubricant can also act as a low shear interstitial layer. A limitation of hard coatings on soft substrates is the high stresses between the substrate and coating generated during the coating process. That said, stresses are generally compressive so can actually be beneficial for wear and fatigue. Homberg and Mathews stated that for hard thin coatings in unlubricated contacts;

'The increase in friction caused by the increased shear strength generally seems to be more dominant than the reduction in friction due to decreased ploughing.' (64)

The surface roughness of the substrate is also an important factor when considering the tribological performance of coatings. The wear rate of coated surface increases with increasing substrate roughness, this is due to with the increase in maximum contact pressure with increasing surface roughness. This also causes the dominant wear mechanisms to change from adhesion to chipping and delamination (94). The substrate roughness will influence the coated roughness. The deposition rate of a-C:H DLC has been shown to be faster at the tops of the peaks of the surface roughness, with lower growth rates in the valleys of the surface roughness (95). The smoother the coating finish, the lower the friction in the system and higher loads can be withstood without material transfer, due to lower adhesive wear.

Substrate roughness has been shown to influence the type of cracks that will develop in the coating. Singh et al. (95) found that for rougher substrates, radial cracks were dominant and occurred before ring cracks. Figure 5-3 shows this, R_a is equal to 38 nm for a & d, 81 nm for b & e and 627 nm for c & f. Images in c & f, show radial cracks and almost no ring cracks, while a & d show large ring cracks. This may be useful for understanding failure mechanisms linked to substrate roughness. Singh et al. proposed that for rougher substrates (and consequentially rougher coating finish), asperities on the coated surface plastically deform, which suppresses the formation of ring cracks and radial cracks are more likely to form.

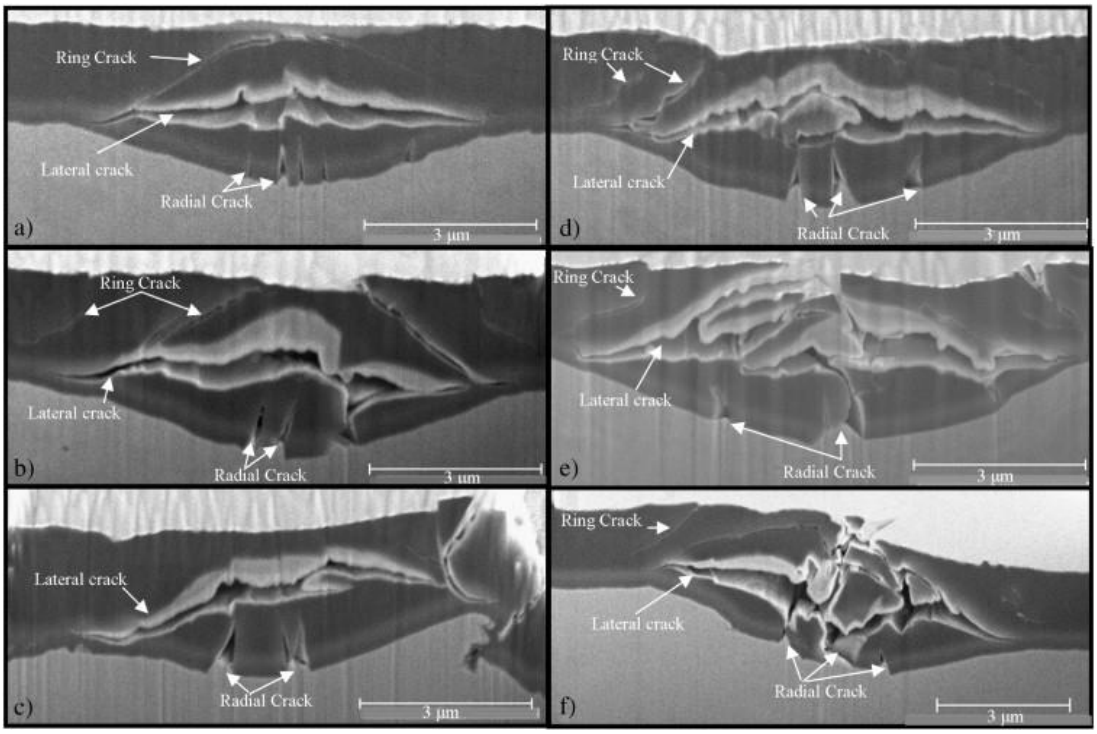

Figure 5-3, Different Crack Mechanisms After Spherical Indentation on a-C:H DLC Coatings with Varying Substrate Roughnesses, R_a= 38 nm for a & d, R_a= 81 nm for b & e, R_a= 627 nm for c & f (95)

The amount and type of wear is also dependant on the coating material (potentially different wear mechanisms dominant) (96) (97). Intentional surface texturing can be beneficial in aiding lubricant retention and acting as wear debris reservoirs, as discussed in Section 6.3.

The surface roughness can also influence the corrosion resistance of a PVD coated component. Due to shadowing effects during film growth, the rougher the surface will cause a less even coating finish (98). For thin coatings, the substrate hardness is important, as the coating will not support the load if the substrate deformation is high. This will contribute to an increase in friction due to a higher likelihood of ploughing and hysteresis. In a more severe case of deformation, fatigue cracks will appear and fracture the coating. A thicker hard coating can prevent this as it will then contribute to supporting the load and less substrate deformation will occur. If a substrate with a surface roughness is one order of magnitude lower than the thickness of the coating, frictional effects caused by the surface roughness will dominant. For coatings that are both thick and soft substrate surface roughness is not an issue.

5.2.1.3 Adhesion to the substrate

The adhesion between the substrate and coating is a determining factor in the coatings' tribological performance. If the adhesion layer of the coating fails, the coating will become delaminated. The application process, via deposition, affects the adhesion quality of the coating, as high internal stresses are induced. Poor adhesion and high internal stresses cause a higher likelihood of failure, particularly under rolling sliding under boundary conditions.

Interfacial layers, particularly carbides or nitrides, help with adhesion of DLC to the substrate. Under high static and dynamic loads and temperatures, these interfacial layers should yield locally and absorb compressive stresses to protect the coating from delamination. To reduce the risk of delamination, a lower coating thickness and interfacial layers are used, as well as reducing the ratio of stiffness between the substrate and coating (99). The strength of the bonds between the coating and substrate can be measured using a scratch tester.

The stress field in a hard coating on a soft substrate is dominated by four effects defined by Homberg et al. (100) for a sphere sliding on a flat surface, and are as follows;

1. Friction; resulting in compressive and tensile stresses in front and behind the sphere.
2. Geometric changes; as a result of the frictional forces deforming the surface elastically and plastically.
3. Bulk plastic concentration; Holmberg found that a sphere causes propagating circular stress fields of 45° from the coating plane, where the minimum tensile stress is at 0° and the maximum 90° (at the surface), as a result of elastic deformation in the coating and plastic in the substrate.
4. Residual stress; these are thermal or intrinsic compressive (and tensile) stresses can be in the order of 0.5-4 GPa from the coating deposition process and due to sliding.

The maximum compressive stress in directly under the contact, the depth of the maximum compressive stress is dependent on the load and friction in the contact. The higher the coefficient of friction the closer to the surface this is. The tensile and compressive effects on cracks in hard coatings was depicted by Holmberg et al. (100) and shown in Figure 5-4a. Figure 5-4b shows the more realistic geometry.

The Young's modulus and thickness of the coating are the main parameters that dictate the magnitude of the stresses in the subsurface. Holmberg et al. (101) state that having a thicker hard coating on a soft substrate gives better load carrying capacity then a thinner hard coating. They found that while this was true, at the interface between a hard thicker coating and the substrate, tensile stresses were present, while in a thinner coating compressive forces were still present. Tensile stresses in the interface region will increase the risk of crack growth and coating failure through delamination. A coating with a high hardness in comparison to the substrate will carry some load and therefore reduce the substrate stress. What may be the most important point made by Holmberg et al. is that optimising the elasticity of the coating may be more important than changing the thickness.

The ratio between the substrate and coating hardness is a useful parameter for understanding the likely failure mechanisms. Ho (102) developed an empirical plot for substrate and coating hardness ratio verses and defined likely scratch failure mechanisms for hard coatings, as can be seen in the scratch failure map for hard coatings in Figure 5-5.

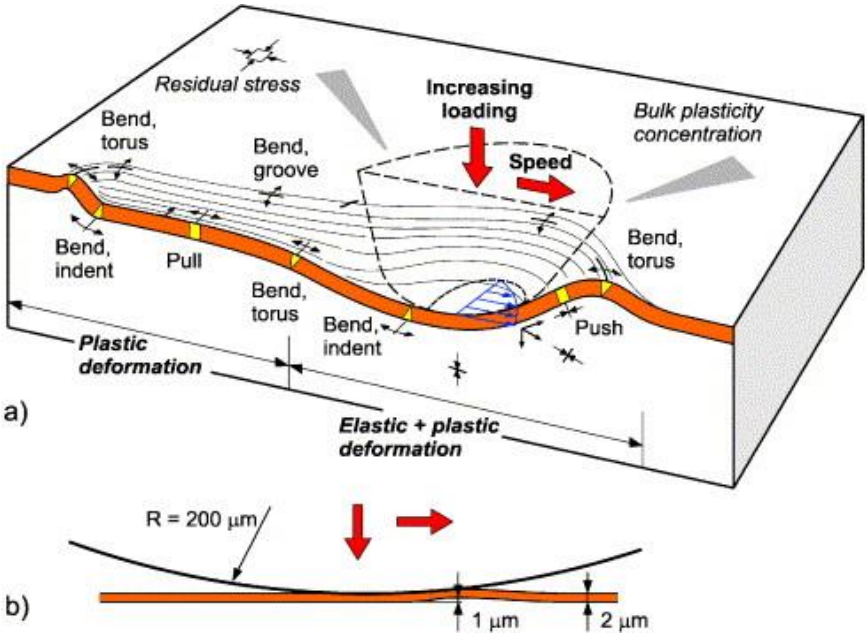

Figure 5-4a, The Stress Field Resulting from a Sphere Sliding on a Coated Surface, b) showing more realistic geometry, as Depicted by Holmberg et al. (100)

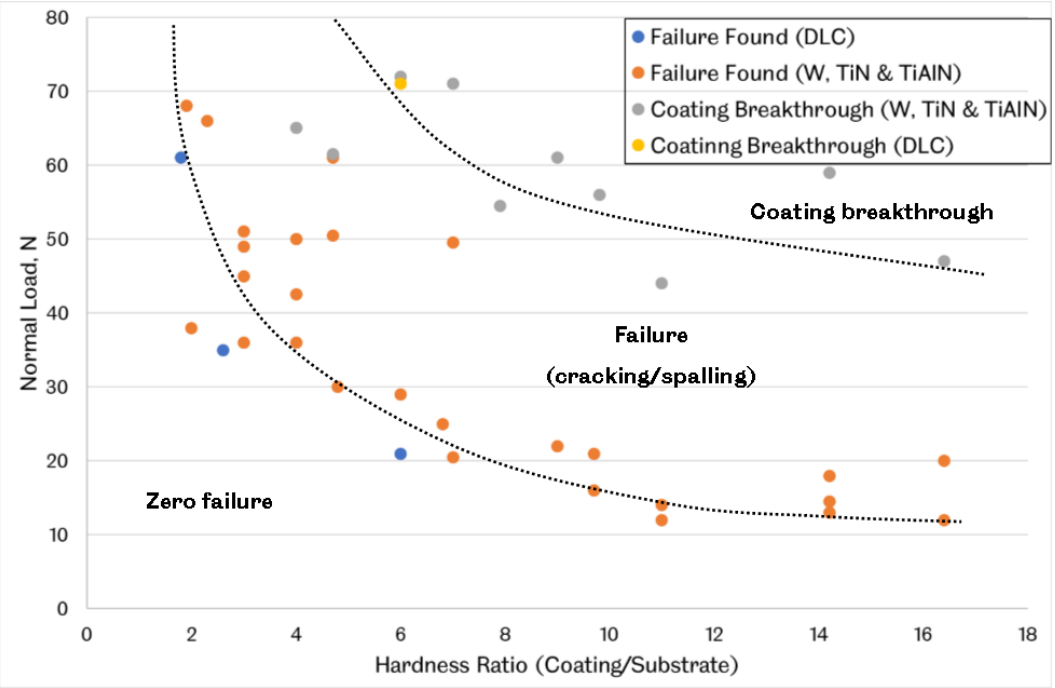

Figure 5-5, Scratch Failure Map for Hard Coatings, adapted from (102)

5.2.1.4 Lubricating DLC contacts

Currently, automotive lubricants are optimised for ferrous and aluminium alloy type materials, with well-studied additives that are known to reduce friction and wear in ferrous contacts. In contacts where one or more of the counterfaces also has been surface engineered, the same lubricating mechanisms are not necessarily present. Understanding the mechanisms between lubricants, additives and DLC is a growing body of research. Further details of current published work in this area is detailed in Section 6.2.

DLC is considered chemically inert, but is electrically conductive. Due to being chemically inert, the formation of protective films on steel with either anti-wear additives or polar carbon chains may not occur. There has been some hypothesis that the polar carbon chains found in vegetable oils can form bonds with the sp^2 structures in DLC (103) (104). There is also evidence that different types of DLC are offering varying success rates at reducing CoF in combination with oils. There is some evidence that highly polar ester type oils reduce CoF more than standard mineral based oils (80). At the surface of DLC coatings, there are dangling bonds of unsaturated carbon radicals. These get readily oxidised when the coating goes from the chamber it is produced in to atmospheric conditions. These bonds are weak and easily broken, therefore may offer a reaction site for polar function groups in lubricants and additives.

Graphitisation may be prevented by the presence of lubricants. There is however some evidence that highly unsaturated oils, such as canola oil, give lower friction values compared with conventional lubricants (105) (106). These oils have higher concentrations of oxygen, which absorbs into the DLC, displaces carbon in the coating, causing graphitisation and oxidation products that act as a low shear friction

reducing interface. This has however been shown to increases chemical wear long term. Additives, such as MoDTC, react with the hydrogenated surfaces to form a solid lubricant and reduce friction (86). Friction may also be reduced by the addition of metal doped in the coating, such as MoS_2. Some work has shown that in DLC/Steel contacts Mo increases wear. MoS_2 and MoO_3, which can be derived from MoDTC react with DLC, a transfer layer and hard Mo compounds are formed. These hard Mo particles cause abrasive wear. The steel counterface acts as a catalyst for the formation of Mo. Mo oxides also act as a catalyst for the oxidation and dehydrogenation of the DLC coating (107). Sulphur based additives have been shown to react with tungsten (W) to form WS_2, which acts similarly to MoS_2 in reducing friction (108). Particularly for lubricated contacts, a DLC-metal interface can give optimal performance, as the additives in the lubricant are effective on the metal surface. Recommendations given by Holmberg & Matthews (64) for lubricated contacts are that the substrate of the coated sample should be harder than the uncoated counter face. The substrate should not be rougher than 1 µm Ra.

5.2.2 *Shot Peening*

Shot peening a metal surface with ultra-fine hard particles (generally less than 200 µm) is one of the most common surface modifications for improving properties of materials. This method works by inducing compressive residual stresses in the material. By doing this, the fatigue properties and hardness are improved. 95% of all failures are due to fatigue mechanisms and occur at or near the surface. By inducing a compressive stress, crack growth is inhibited. Figure 5-6 depicts the improvement in fatigue strength due to shot peening. Figure 5-6a shows, for an unpeened surface, that fatigue strength is consistent in the depth direction; the stringers, or material imperfections are prone to crack initiation as they are areas of stress concentrations. As the intensity of shot peening increases (Figure 5-6b & c), so does the fatigue strength just below the surface, resulting in shallower crack propagation (109).

Shot peening may be performed on a component before it is treated with another method. Shot peening before chrome or nickel plating and anodising is common, to counteract the reduction in fatigue strength these surface treatments cause, due to residual tensile stresses and embrittlement. In order to reduce residual stresses caused by plasma coating, shot peening is used before the coating process and typically after surface grinding as well (110).

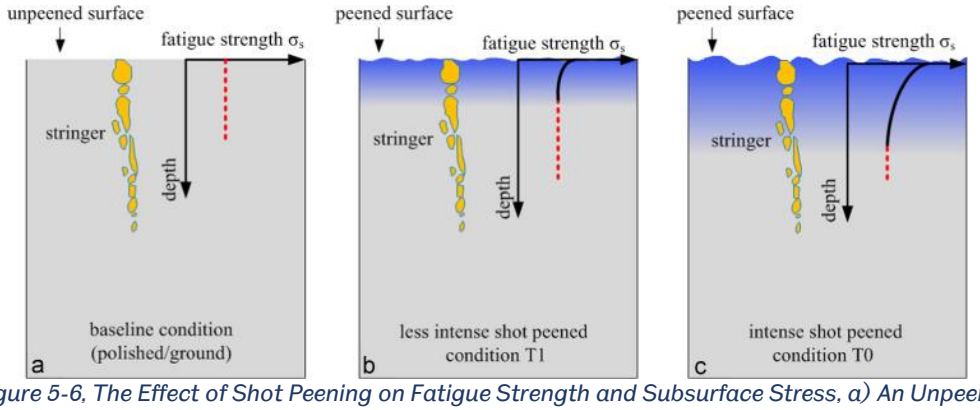

Figure 5-6, The Effect of Shot Peening on Fatigue Strength and Subsurface Stress, a) An Unpeened Surface, b) Less Intense Shot Peened Surface and c) An Intense Shot Peened Surface (109)

5.2.2.1 Molybdenum disulphide

Molybdenum disulphide (MoS_2) consists of layers of sheets of molybdenum and sulphur atoms. It has low shear strength due to its structure. MoS_2 has hexagonally packed planes of molybdenum sandwiched between two sulphur layer, the van der Waals forces between 'sandwiches' are very weak, therefore MoS_2 is strong in two planes but weak in the third. MoS_2 is stable at high temperatures (around 400˚C) and is used as a coating in piston rings, as previously mentioned, as well as space applications. Over 400˚C MoS_2 begins to oxidise, forming $MoO_3 + SO_3$. It can also be used as a lubricant additive and as a solid lubricant doping medium in shot peening (111). Transfer films are formed with MoS_2 coatings on the counterface. MoS_2 wear debris has been shown to collect together and form a reservoir in the contact zone and this enhances wear protection in the contact zone. The mechanism for the formation of these reservoirs is not understood and the formation of them is dependent on the coating (64). The transfer layer generates a low shear layer that reduces friction.

MoS_2 is relatively unreactive, unless it is physically or mechanically activated. The outer crystallites may oxidise to form MoO_3 at temperatures as low as 85˚C, this does not affect the lubricity of MoS_2. MoS_2 can react with steel to form 2FeS + Mo. This is more likely to occur at elevated temperatures above 700˚C, but the reactions have been observed at low temperatures as well. The coefficient of friction in systems using MoS_2 has been shown to reduce as temperatures increase; this is partly due to a reduction in water in the system at elevated temperatures but also due to weakening of bonds that allows the molybdenum planes to slide over one another more readily (111).

5.2.3 *Calcium Sulphate*

Calcium sulphate is a solid lubricant and effective at high temperatures (> 500 °C) while solid lubricants like MoS_2 discussed in Section 5.2.2.1 are more suited to lower temperatures (< 500 °C) (112). Sulphites are a well-known and effective lubricant anti-wear additive for surface containing iron, as can form chemisorbed films (113). Sulphate films have been shown to remain in a wear scar after tribological testing, even when the majority of the coating has worn away. They are also effective at reducing friction (114). Calcium fluoride (CaF_2), can form $CaSO_4$ under tribological conditions if sulphite is present, such as tungsten disulphate (114).

5.2.4 *Multi-Layer Coatings*

It is possible to use multiple types of surface engineering to improve performance of an engineering component. Table 5-2 shows some of the most common combinations of coating groups, as described by Holmberg & Matthews (64). These combined methods of surface engineering can have many different forms, often being able to exploit the best aspects of treatments, or counteracting negative aspects of surface treatments. A good example of this is described in Section 5.2.2; shot peening a surface to induce residual compressive stresses before applying a plasma coating, which generally reduces fatigue life.

	Transformation hardening	Mechanical treatments	Diffusion of metalloids	Sputtering	Conversion	Metallic coatings	Organic coatings	Physical or chemical vapour deposition
Transformation hardening								
Mechanical treatments								
Diffusion of metalloids								
Sputtering								
Conversion								
Metallic coatings								
Organic coatings								
Physical or chemical vapour deposition								

Table 5-2, Different Possible Combinations of Surface Treatments, recreated from (64)

Fatigue life may also be improved by using multi-layered coatings, as the stress concentrations in the surface region will be distributed in the many layers applied to the component, reducing the opportunity for cracks to form and grow between layers (115). This is particularly true if surface coatings with varying mechanical properties (elastic and plastic) are used. The benefit from having several coatings with varying mechanical properties may be extended to other aspects, such as corrosion protection, wear resistance, adhesion of the coatings to the substrate (see Section 5.2.1.3 for further details). Table 5-3 gives some examples of varying mechanical properties of different types of coating, partly reproduced from Holmberg & Matthews (64). Plasma vapour deposition processes are effective methods for producing multi-layer coatings, as a wide range of different materials can be used, both as substrate and coating material.

Mechanical Property	Type of coating	Coating material	Coating thickness, µm
Wear Resistance	Hard coatings	DLC, TiN, TiC	0.5 - 5
Low friction	Soft or layered coatings	DLC, MoS_2, PTFE	0.5 – 3
Lubricity	Liquid or soft coatings	PFPE, MoS_2	0.001 – 3
Corrosion resistance	Dense, inert coatings	Au, Zn, Cd	3 – 20

Table 5-3, Examples of Mechanical Properties for Different Types of Coating, partly reproduced from (64)

In combining different types of surface treatment, there are almost endless possibilities for resulting mechanical properties. Applying soft coatings with low friction properties, over harder coatings with good wear resistance, may result in low wear and low friction. Soft coating layers may act as a transfer layer, as described in Section 5.2.1.2, providing shearing at the interface, while the hard coating would protect the component from wear.

Multi-layer coatings may be beneficial in reducing the dependency on the performance of a lubricant. This type of coating may help the transition to more environmentally friendly bio-lubricants; they could offer surface protection to counteract the reduced performance or stability of bio-lubricants.

5.3 Elastomer Interaction with Vegetable Oils

Historically, elastomers came from natural sources, but due to advancements in synthetic versions, these are now predominant in the market. Elastomers formed from naturally occurring rubber are a hydrocarbon (C_5H_8), with a methyl side group (CH_3) on every fourth carbon atom. In its natural state, the rubber is susceptible to degradation due to the double bond, a site of enhanced reactivity. Synthetic rubbers were developed to improve performance. The structures of synthetic rubbers can vary considerably with varying chain component atoms and chain lengths; for example nitrile rubbers are CH chains with CN (carbon-nitrogen) side groups, while fluorocarbon rubbers will be made up of CF chains (carbon-fluoride) (116). Additionally, synthetic rubbers will contain various plasticisers, depending on the performance needs of the application for which they are used.

The main role of plasticisers is to improve flexibility and processability; this is done through the lowering of the second order transition temperature (point at which it becomes hard and brittle). These plasticisers are liquids of low molecular weight that form secondary bonds with the polymer chains, which reduces the amount of bonds possible between polymer chain (also known as cross-linking) and increases the distance between these chains (117). Cross-linking also improves the properties of the rubber. Carried out at high temperature, cross links are formed by short chained sulphur atoms linking polymer chains together. Cross-linked rubbers are stronger: the more cross-links present, the harder the material. Once cross-links are formed, the shape of the material cannot be changed, the material cannot be dissolved in solvents as the bonds formed are covalent. Without cross-linking, rubbers would behave more like liquids, as the individual polymer chains would be able to move independently of one another.

5.3.1 *Uses in Automotive Applications*

Seals are a fundamental part of an automotive engine and are made from elastomers. Seals act as barriers between materials, control the amount of oil in certain areas of the engine, such as valve stems, to prevent leakages, such as in the oil pump, or are there to help create a vacuum. Common seal materials include nitride rubber (NBR), ethylene propylene diene monomer (EPDM), polyacrylate, polychloroproprene fluoroelastomer (FKM), silicone, nylon and Teflon. There are several properties which seal materials need to possess in order to function correctly, as EPM seal manufacturers outline (118):

- Good chemical resistance
- Good resistance to heat, low temperature, ozone and weather aging
- Good elasticity
- High resistance to water
- Low compression set

O-ring seals work to prevent leakages, creating a seal when two mating surfaces come together. The O-rings are designed to be compressed and therefore fluid is not able to pass through. The more the O-ring is compressed, the less likely the seal is to leak. Static O-ring seals can be completely leak proof up to pressures of 35 MPa. Figure 5-7 shows an example of a static O-ring seal in a groove. The O-ring is shown in the groove after initial compression; the O-ring is slightly distorted in shape and is in contact with both mating surfaces; the change in shape of the O-ring is dependent on the size of the groove and O-ring (119).

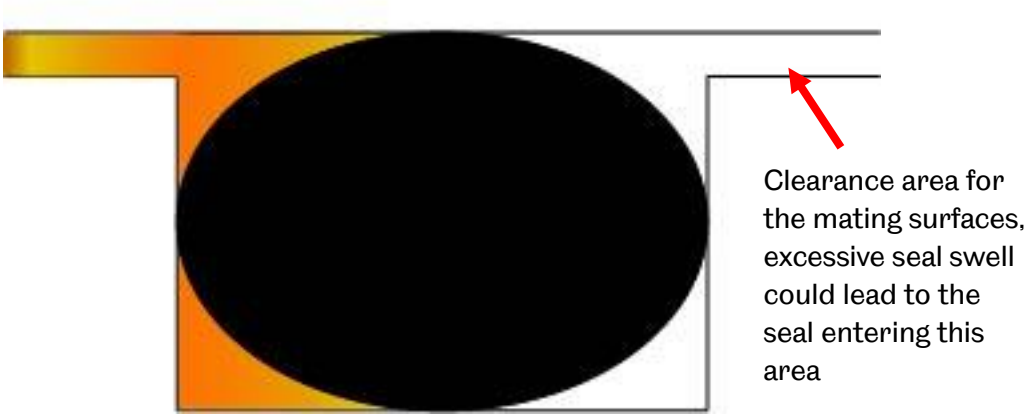

Figure 5-7, A Cross Sectional View of an O-ring Oil Seal in Compression

5.3.2 *The Theory of Stress Relaxation*

The seal manufacturer specification listed in Section 5.3.1 states that a low compression set is important, this test is considered to be less informative than stress relaxation tests (120). Compression set tests measure the amount of deformation at set time intervals, whereas stress relaxation tests measure the sealing force of the seal constantly throughout the test duration. In seal applications, stress relaxation has the potential to degrade performance (hardness, tensile strength, etc.). This stress relaxation is not necessarily caused by the seal itself, other factors that may contribute could be caused by thermal expansion differences in the surfaces containing the seal or from bolt stretch from joining these two surfaces together (119). Stress relaxation tests also give a clear indication as to how the seal will perform in application; the variation in force that the measurement system reads also demonstrates whether the seal has suffered swell or shrinkage.

5.3.3 *Seal Compatibility*

While seals cannot be dissolved by solvents, they can be significantly degraded. This degradation will be apparent in the form of the elastomer seal swelling or shrinking. Swell or shrinkage of seals in use is an important phenomenon to observe in the assessment of suitability for a given application. Seal swell is acceptable up to a certain level as this can aid sealing performance, increasing the sealing pressure, but high levels of swell may lead to the degradation or change of mechanical properties; reduction in hardness, tensile strength and tear strength may occur (121), as well as altering the dimensions. If the volume of the O-ring increases enough, it may move into the clearance area of the mating surfaces (see Figure 5-7); this could lead to bolt stretch if pressures are high enough.

In static applications, there are no defined acceptable levels of swell or shrinkage, it is application dependant. Some state that up to 50% swell is acceptable (119), others state 25-30% can be tolerated (120). Shrinkage of greater than 3-4% can cause leakages, as the O-ring may no longer be in contact with both mating surfaces, as well as increasing hardness and reducing the flexibility of the O-ring material.

The applied stress on an elastomer is also an important factor in the swelling behaviour. If the elastomer is subject to extension, swelling will increase, if the elastomer is subject to compression, the amount of swelling that occurs will decrease. The hydrostatic pressure component is the cause of this; for elastomer in extension the hydrostatic component is negative, and for compression it is positive.

As stated in Section 6.11 there is only one set of published work that focused on the effect of bio-lubricants on the degradation of elastomers, but a reasonable amount of work has been carried out with respect to biodiesel. The different processing techniques used in their production could potentially mean that bio-lubricants behave differently to biodiesel. The removal of the glycerides, which are made up of hydroxyl function groups could mean the two bio substances behave differently. The hydroxyl function groups are sites of enhanced reactivity, which is beneficial in terms of lubrication, as they help form strong bonds to the metal surfaces; but these could react with elastomers to dissolve them. Hydroxyl groups are contained within carboxylic groups and are also highly polar. In terms of lubrication, the hydroxyl and carboxyl groups aid the strong absorption of the oil molecules on to metal surfaces, creating stable lubricating films.

Base oils used in lubricants have a dramatic effect on the amount of hardening that occurs (122), but additives will also play a role. The additive package applied to the base oil, however, can also have a marked effect on the seal performance; some additives may actually aid seal performance, others will degrade. The effect of the additive will vary depending on the type of seal materials. As an example, the amine compounds in zinc dialkyldithiophosphates (ZDDPs) can create cross-links in standard NBR and FKM; while cross-linking is advantageous to a point, too many cross-links will reduce flexibility (123), and fully saturated monomers are required in order to prevent this.

5.3.4 *Diffusion*

Physically, diffusion controls the volume change of the elastomeric material. Swell is caused by the absorption of a medium (generally fluid or gas) into the seal, while shrinkage is caused by the extraction of seal material by a medium, particularly plasticisers, which causes them to harden.

Diffusion of chemicals with elastomers is a complex mechanism; it is highly dependent on kinetics, while thermodynamic theory can help to explain the principles and will define whether diffusion occurs. Treloar (116) explains that swelling behaviour can be approximated to a simple statistical thermodynamic model, considering two phases, one that is elastomer and liquid (mixed) and the other liquid (pure). The equilibrium between these phases is important, and determined by the condition that the free energy is minimal with respect to changes in the composition of the mixed phase. The change in free energy, resulting from the transfer of a small quantity of liquid from the pure phase to the mixed phase, is equal to zero. The change in the Gibbs free energy of dilution (ΔG_1) due to the transfer of a unit of the pure phase to a large quantity of the mixed phase, can be used to quantify this and is equal to zero for a constant pressure, relating this to the enthalpy, ΔH_1 and entropy ΔS_1 gives;

$$\Delta G_1 = \Delta H_1 - T\Delta S_1$$

Equation 5-1

The heat of dilution and entropy relate to the change of enthalpy, H, and entropy, S; for the transfer of a mole from the pure to the mixed phase, the heat content is defined by;

$$H = U + pV$$

Equation 5-2

Where U is the internal energy, p atmospheric pressure and V the volume. As the pV can be neglected, $H = U$. Considering the case where only the pure phase has an appreciable vapour pressure,

$$\Delta G_1 = RT \ln p/p_0$$

Equation 5-3

p is the vapour pressure of the pure phase in equilibrium with the mixed phase (p_0 is the saturation vapour pressure). Therefore;

$$\Delta H_1 = \frac{\partial(\Delta G_1/T)}{\partial(1/T)} = -RT^2 \frac{\partial \ln(p/p_0)}{\partial T}$$

Equation 5-4

This shows that, based on the relative magnitude of ΔG_1, ΔH_1 and $T\Delta S_1$, the latter is the most important term as it is significantly larger, as more clearly demonstrated in Figure 5-8. $T\Delta S_1$is significantly larger and always positive, while ΔH_1 acts to reduce ΔG_1 in absorbing heat on mixing; this reduction in ΔG_1 tends to oppose swelling. ΔH_1 can be negative, but the above is generally representative of most elastomers.

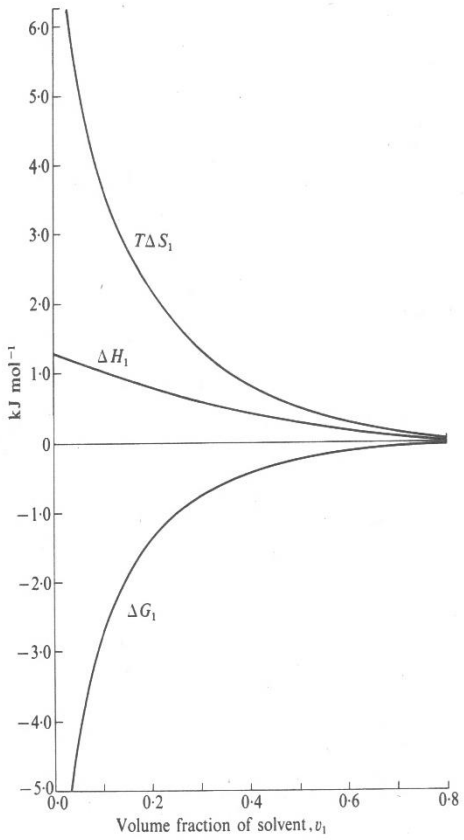

Figure 5-8, Magnitudes of Free Energy, Enthalpy and Entropy for an Elastome (116)

This theory indicates that a large increase in entropy is the driving force of diffusion, and therefore swelling. This would satisfy this theory, as they are associated with large increases in entropy. The relatively low ΔH_1 shows that no chemical or strong intermolecular forces are at play in this process.

Another interesting factor in this process is that values of ΔH_1 for liquid-liquid systems are in the same range as typical elastomer-liquid systems. This indicates that the length of the molecules does not have much impact in the process, i.e. intermolecular forces are not as significant. ΔS_1 is associated with the configuration of molecules and is affected, considerably, by length, showing that this value, unlike ΔH_1, would be considerably different in magnitude in liquid-liquid to liquid-elastomer systems. This proves that swelling is a purely physical mixing or inter-diffusion process, and the two phases are regarded as chemically neutral, in that there are no specific chemical attractions between liquid and elastomer phases.

Thermodynamically, there is a similarity between the swelling phenomenon and elasticity of rubber; they are both directly related to the configuration of long chain molecules (configurational entropy). For both elasticity of rubbers and swelling, the change in internal energy from the intermolecular forces are irrelevant and both cause an increase in elasticity. The increase in entropy arises from the greater probability of a mixed state in comparison to unmixed/pure. This is calculated by the number of configurations available at any given composition of mixed phase. To calculate this, Flory (124) defined a relatively simple method for calculating configurational entropy of mixing based on a three dimensional lattice; each site of

the lattice must be filled with either a segment of elastomer or a liquid molecule. Huggins (125) built on this assessment, looking in more detail at the number of available sites for elastomer segments. This gives an insight into the fundamentals, however, Flory-Huggins is not sufficient for cross-linked elastomers. The molecular weight of polymer network chains and degree of cross-linking also affects swelling: the more cross-links and higher molecular weight, the less swelling will occur in the system (molecular weight is also directly related to elastic modulus).

The interactions between elastomers and liquids are not specifically related to the polymeric nature of the polymer chains. The interactions are heavily dependent on the local forces between atoms. In an attempt to understand these intermolecular interactions quantitatively the cohesive energy density can be linked to swelling. The cohesive energy density is the amount of energy required to separate all the molecules, in a given material, from one another, it is equal to:

$$per\ mole = (L - RT)/V$$

Equation 5-5

L is the molar latent heat vaporisation, *V* the molar volume. Huggins (125) proposed that ΔH is at minimum when swelling is at maximum, i.e. for liquid and polymers with equal cohesive energy densities ΔH will be minimum as shown,

$$\Delta H_1 = \mathrm{k}V_1(E_1^{1/2} - E_2^{1/2})^2 v_2^2$$

Equation 5-6

Cohesive energy density is represented by E.

The square root of the cohesive energy density is related to the square root of the solubility parameter; the liquid-elastomers that have the closest solubility parameter are most likely to swell; this relates to Hanson Solubility Parameter.

5.3.5 *Hanson Solubility Parameters*

The Hanson Solubility Parameter is a way of predicting and defining the solubility of substances. Three parameters, dispersive forces, δ_D^2, dipolar forces, δ_P^2, and hydrogen bonding, δ_H^2, make up the Hanson Solubility Parameter, as shown in Equation 5-7. These values are based purely on thermodynamics (not accounting for kinetics). The values come from cohesive energy density, *E*, shown in Equation 5-7.

$$\delta^2 = \delta_D^2 + \delta_P^2 + \delta_H^2$$

Equation 5-7

$$\text{Where, } \delta^2 = {}^{E}/_{V} \quad \text{and} \quad E = H_v - RT$$

$$H_v = latent\ heat\ of\ vapourisation$$

These values can then be used to define a relationship between two substances, in terms of Hanson Solubility 'space', a three dimensional representation of how the given substances may interact. The 'distance' between the two substances in this space is defined by Equation 5-8;

$$(Ra)^2 = 4(\delta_{D2-}\delta_{D1})^2 + (\delta_{P2} - \delta_{P1})^2 + (\delta_{H2} - \delta_{H1})^2$$

Equation 5-8

$$RED = R_a/R_o$$

Equation 5-9

The Relative Energy Difference (RED) shown in Equation 5-9, is a useful parameter that can give an indication of how the substance will react. Is RED <1, then the two substances are likely to dissolve in each other, if RED>1, it is likely there will be little effect. Ro is the radius of interaction of one of the substances (often the polymer), it is found experimentally. The most common method for obtaining HSP values is by experimentally determining the solubility or miscibility of a given substance against solvents with known HSPs. Between 40-85 solvents with known HSPs are mixed with the unknown substance, left for a given time period, then assessed based on a whether the 2 substances remain mixed or not. A large number of solvents are required to improve accuracy and to compensate for the effect of molar volume (as discussed previously), which HSP does not consider. A best-fit model is then used in order to determine the HSP value. A quality-of-fit/best-fit model (e.g. GAMS or sp3D) is then used in order to determine the HSP value. Literature suggests that results obtained from this method were acceptable and compare well with other methods for assessing solubility of substances.

HSP is well documented to be successful in assessing the miscibility of paints (126) and effectiveness of rubber gloves for PPE (127). HSP is effective at describing the solubility of simple chemicals and polymers. Work is on-going to assess the suitability of using HSP for more complex substances; it is thought that, in its current state, it is only capable of giving an indication of the compatibility of materials, rather than being able to replace material compatibility testing.

5.4 Conclusions

This chapter has detailed the key tribological mechanisms and material interactions that are relevant to bio-lubricants. Wear and friction mechanisms have been discussed.

This chapter covered some of the key aspects of the surface treatments and coatings that will be used in experiments. The substrate hardness and roughness influences the type of wear mechanism on a hard coating, as does its adhesion to the substrate. Transfer films are one way in which DLC is able to reduce friction and wear. Shot peening is a useful surface treatment to use in combination with other surface treatments and coatings, particularly because it induces compressive stresses at the and near to the surface. Calcium sulphate is a useful surface coating for higher temperature applications. There benefits of using multi-layer coatings to optimise performance and counteract negative aspects one treatment may induce, such as reduced toughness.

Finally, this chapter covered the theory of stress relaxation and the process of degradation of elastomer. Hanson Solubility parameters were introduced and will be looked at in more detail in Chapter 6.

6 Literature Review

This chapter reviews the literature available on a variety of areas where the use of bio-lubricants has been explored, with particular focus on jojoba, palm and soybean oil. The aim of the review is to identify areas where the tribological understanding of bio-lubricants is well established and to highlight areas where further work is required to improve knowledge of the performance of bio-lubricants. The review looks at the interaction of bio-lubricants with materials commonly found in automotive engines. The literature review aims to identify common wear and lubrication mechanisms that occur with bio-lubricated contacts. Suitable tribological test methods that are effective at measuring the performance of bio-lubricants will also be identified.

The research topic of bio-lubricants is broad. There are a large number of performance parameters lubricants must fulfil, as highlighted Sections 2.3 and 4.2. There are also a vast number of plant sources for bio-lubricants; many plants have oils that can be extracted and potentially used as bio-lubricants. Therefore there is a considerable challenge to narrow the scope of the review in order to gain a meaning full understanding of the current state of bio-lubricants research.

The first section of this chapter focuses on the use of bio-lubricants to reduce wear, this includes blending vegetable oils for the purpose of further reducing wear and friction. Alternative methods for reducing wear and friction, used in combination with bio-lubricants, are explored by analysing literature that looks at using different surface treatments to enhance wear and friction performance; looking particularly at coatings that contain diamond-like carbon, calcium sulphate and fullerene, as well as the effects of surface texturing, as these surface treatments have been provided by academic partners to test the compatibility with bio-lubricants. Literature that explores some of the important tribological parameters such as measuring the film thickness of bio-lubricants is also considered and, to finalise, work carried out on the degradation of bio-lubricants and elastomers is explored.

6.1 Reduction of Wear and Friction Using Blends of Bio-Lubricants

A reasonable amount of research has been conducted investigating the ability of a bio-lubricants to reduce wear and friction. The most commonly researched bio-lubricants appear to be rapeseed, palm, soybean, castor and sunflower oil, (70) (69) (128) (129) although there are many other sources of bio-lubricants under investigation, such as avocado, peanut and olive oil (130). Materials most commonly tested with bio-lubricants are various grades and finishes of steel, some aluminium alloys and other metals such as copper (131) (132) (133). Some full-scale engine tests have been performed, to assess the ability of bio-lubricants, such as jojoba and palm oil to reduce wear and friction, and consequently performance and emissions, but research at this experimental level is limited (134) (69) (128). Literature has limited focus on wear and friction properties of jojoba oil. The review also highlighted a lack of research in to the use of bio-lubricants with common or novel automotive coatings.

Previous work carried out by the author (135), using reciprocating wear tests, using blends of jojoba oil with mineral oil, showed that when the oils were blended together in a 50:50 ratio, as shown in Figure 6-1. Resulting volume loss in the wear scar was 51% lower than when jojoba oil was tested on its own. Jojoba oil outperformed all other vegetable oils tested in terms of wear protection, producing volume loss of 3.75 mm^3 (0.04%). The next best performing oil, coconut oil, gave volume losses of 4.01 mm^3 (0.05%) on average.

Jojoba oil was also found to perform well when blended with the other oils to improve wear protection, as shown in Figure 6-2. When blended with castor and coconut oil, jojoba oil reduced wear scars by 35 and 15% respectively. Jojoba oil demonstrated no wear reduction when blended with palm oil, with volume losses increasing by 5%. Along with jojoba oil's highly polar nature, the long chained carbons are thought to be responsible for the wax's wear prevention attributes. These long chains offer a greater surface area through which stronger intermolecular forces act to anchor these chains to the lubricated metal surface and form a multi-molecular protective layer over the surface.

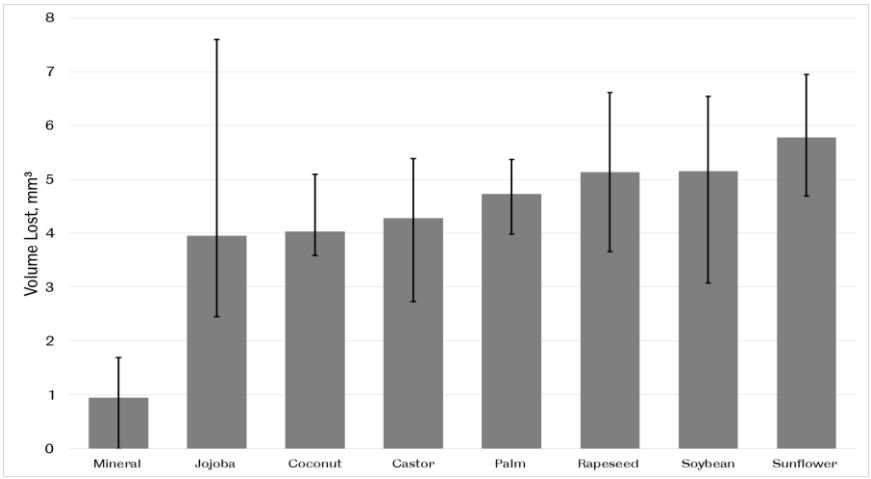

Figure 6-1, Volume Lost from Wear Tests with Various Vegetable Oils (57).

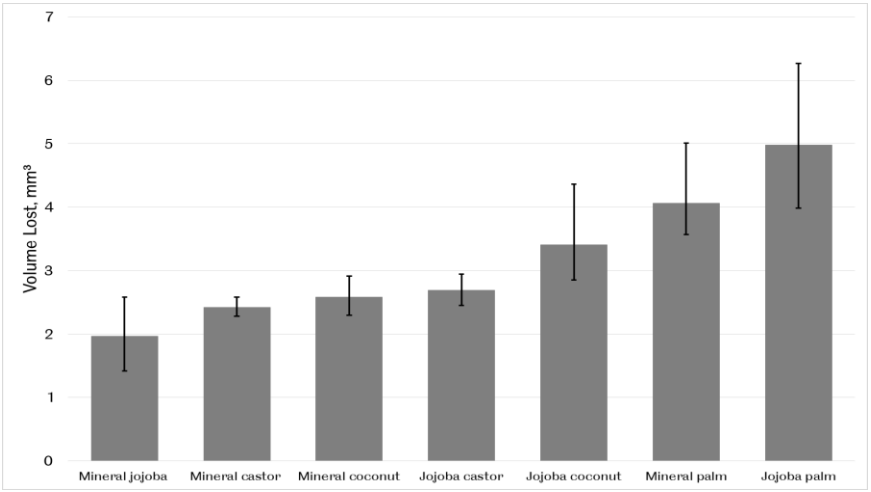

Figure 6-2, Results from Wear Test with Varying Blends of Vegetable Oils with Mineral or Jojoba Oil (57).

Kalhapure et al. (136) studied the wear characteristics of cottonseed and soybean oil in varying blends ratios with a fully formulated mineral oil (SAE 20W40), with a 0.5% by weight graphite additive. They found that a 10:90 volume ratio of either cottonseed or soybean oil to mineral oil reduced wear slightly. Higher ratios of the vegetable oils resulted in larger wear scars in comparison to tests with only mineral oil. No scientific explanation was provided for the cause of this reduction of wear protection for increased levels of vegetable oils.

A similar trend of an optimal blend ratio was observed by Bahari et al. (137), who assessed the effectiveness of a bio-lubricant blend of palm and a 15W40 mineral oil, as well as soybean and mineral oil. They found that blending at a 50:50 ratio of vegetable oil to mineral oil reduced wear and coefficient of friction (CoF) in comparison to tests with vegetable oils alone. The 15W40 mineral oil was fully formulated, which can explain the considerable difference in wear when comparing an unformulated vegetable oil to a fully formulated mineral oil. The mass loss, shown in Figure 6-3a, with mineral oil was 0.65mg, while with pure palm oil it was 45.76mg and with the mineral palm oil blend 34.02mg. The difference in CoF values was less extreme, as seen in Figure 6-3b, with CoF for PO 0.105, for the PO:MO blend 0.104 and for the MO alone 0.093. The SO:MO blend and SO was slightly higher than PO and its blends, at 0.109 and 0.112 respectively.

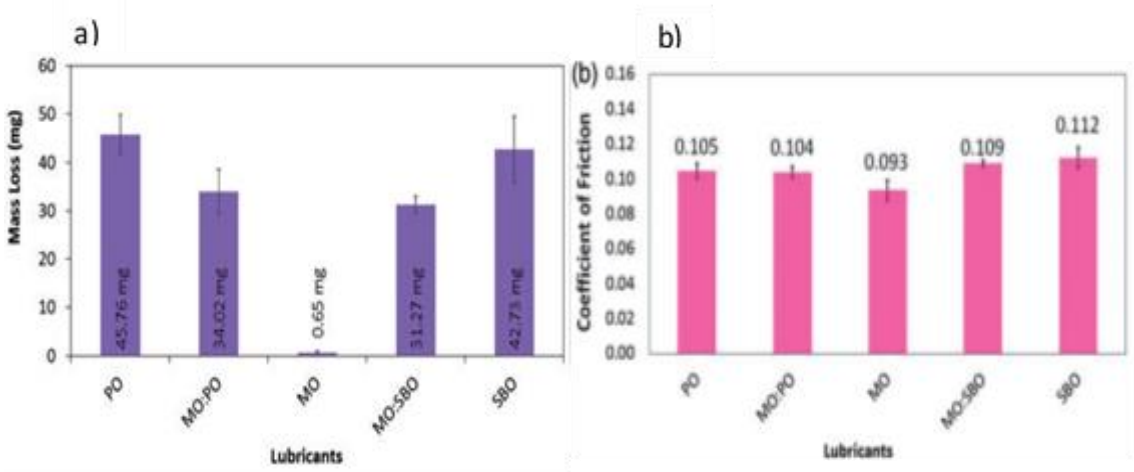

Figure 6-3a, Mass Loss and 3b, CoF Results Reciprocating Wear Tests Carried Out by Bahari et al. (137)

The difference in performance between PO and SO is attributed to the fatty acids that make up the oils and their level of saturation. PO has considerably higher levels of saturation than SO, and it is well documented that CoF increases with level of unsaturation, as saturated fatty acids can align themselves in straight chains perpendicular to the surface; unsaturated fatty acids are bent carbon chains, which cause higher motion resistance and therefore increased CoF. The authors also propose that, in blends, the fatty acids disrupt the additives layers' ability to form a protective layer on the surface, and that the carboxyl acids situated at the end of fatty acid chains that bond to the surface, are more easily removed during severe sliding conditions.

Much of the research with jojoba oil as a bio-lubricant is based around the oxidative stability of the oil, which can be improved with the use of additives. Jojoba oil has also been used as an extreme pressure additive (16). Bisht et al. (67) assessed the additive

properties of jojoba oil. They found that jojoba oil worked better as a viscosity improver than the commercial viscosity improver. Jojoba oil also showed good rust prevention properties in neat form and up to 30% concentration in base stock, attributed to its ability to create adsorbed films on the friction surface. In ball-on-flat reciprocating wear tests, jojoba oil developed smaller wear scars from a 10-100% concentration in comparison to the base stock, this is in disagreement with previous work carried out by the author (128). There are many factors that could have influenced this result. The author states that the variation of the base stock is thought to be key, as well as any potential natural variations in the jojoba oil due to the way it is cultivated and stored. Test methods for achieving this result are not documented so it is difficult to offer a comparison of results. Bisht et al. (67) also compared the friction properties of jojoba oil and various blends in base stock. There results showed that jojoba oil had considerably lower CoF, 0.0445, compared with 0.08 for the base stock tested, Bisht et al. also showed that with increasing proportions of jojoba oil added to the base stock CoF values reduced. As Bahari et al. (137) also suggested, the mechanism attributed to reducing friction is the ability of the bio-lubricant to form an adsorbed layer on to the surface it is in contact with.

Gupta et al. (134) studied the suitability of jojoba oil as a two stroke engine lubricant. When testing pure jojoba oil at a concentration of 2% in the fuel, they found significant levels of piston stick, power loss and exhaust port blocking. Using a blend of additives of 0.5% antioxidants, 0.75% viscosity improver and 8.5% detergent was adequate to give no piston stick, power loss or exhaust port blocking, with results comparable to a standard mineral oil based lubricant. Sivasankaran et al. (69) also studied the effectiveness of jojoba oil in two stroke engines, carrying out tests with a four ball wear tester beforehand. In the wear tests they found that jojoba oil demonstrated better anti-wear properties than the mineral based oil used as a comparison. Carbon residue values were also determined, as it is thought that this is an adequate way of predicting deposit forming tendencies. Jojoba oil exhibited very low carbon residue values, 0.03 when using the Conradson carbon residue method, while the mineral based oil value was 0.22. Castor oil was also tested and gave a value of 0.42.

Engine tests were also performed with unknown blends of additives with jojoba oil (blend TR-41). Figure 6-4 shows images of pistons after engine tests show that blends of jojoba oil were comparable to standard mineral oil based lubricants in terms of tendency to leave deposits around the pistons. These results are in agreement with Gupta et al. (134) in that jojoba oil has comparable operational performance to commercial mineral oil based lubricants for ring sticking, plug fouling and port blockage (nil) as well as ring wear.

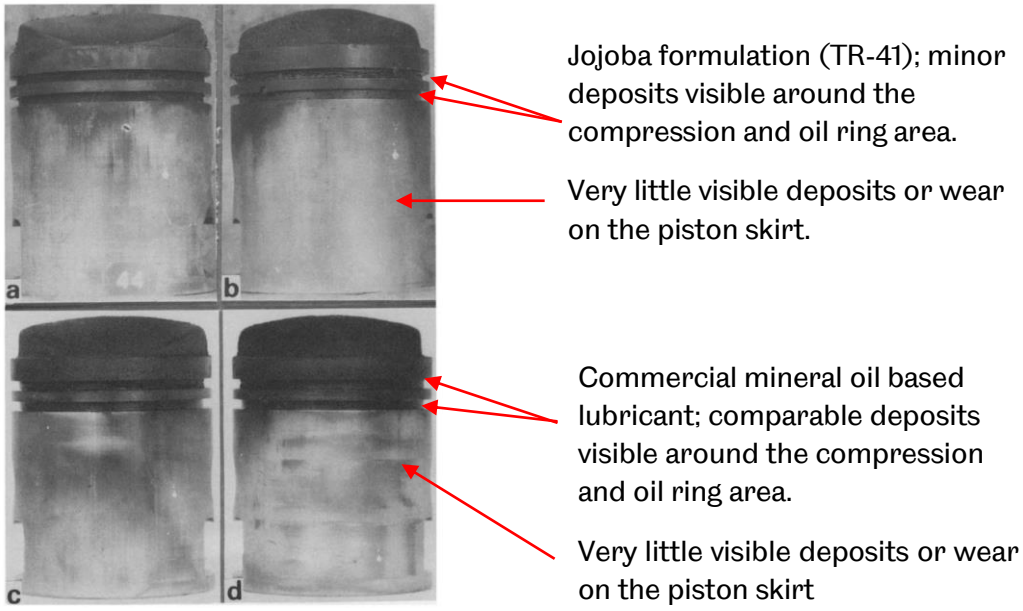

Figure 6-4, Condition of the Piston After 22 h Test: (a) Formulation TR-41, Thrust Side; (b) Formulation TR-41, Anti-Thrust Side; (c) Commercial Two-Stroke Engine Oil, Thrust Side; (d) Commercial Two-Stroke Engine Oil, Anti-Thrust Side (248)

Cheenkarchorn and Fungtammasan (128) performed engine tests with a four stroke motorbike engine. They produced a bio-lubricant blend of 50.6:41.6 palm to mineral oil with a 7.8% additive package to meet SAE 40 grade specification for viscosity, similar to the blend developed by Bahari et al (137). Wear scars (method of testing not defined) between palm oil and the commercial oil (not defined but assumed to be a commercial fully formulated mineral oil based lubricant) were found to be comparable, while the bio-lubricant blend produced wear scars half the size. They also found that other characteristics, such as viscosity index, flash point and evaporation loss, were better for the bio-lubricant blend than commercial oil. However, foaming characteristics and sulphate ash production were worse for the blend. The change in tribological characteristics was attributed to the polar nature of palm oil, as well as the additive package. The engine tests showed no change in engine performance or fuel consumption when the bio-lubricant blend was used.

6.2 The Use of Surface Treatments to Reduce Wear and Friction

There is a significant amount of research into surface treatments and coatings that improve the tribological properties of the surface. Diamond-like-carbon coatings (DLCs) are one of the most common surface coatings, used in a wide variety of applications. The use of these coating in biomedical applications is becoming more common partly because it is bio-inert, and also because of its resistance to wear; its use in hip and knee joints, heart valves, stents and contact lenses has been explored (138). The use of DLC has also been seen in razor blades. In automotive applications, DLC is becoming more prevalent, being used in areas where types of wear such as; adhesion, abrasion or impact are common, in drive components, pumps, various camshaft components, pistons and rings (139).

Literature shows limited work has been carried out with surface treatments and bio-lubricants. Research with surface treatments and conventional lubricants is relevant as this can give indication to the wear and friction mechanisms that makes these coatings effective.

Bobzin et al. (140) assessed the suitability of two different multi-layer coatings for automotive applications. The first was a tungsten carbide coating layered alternately with hydrogenated diamond-like-carbon (H-DLC), to produce layers a few atoms thick, with an overall coating thickness of 2.8 µm, surface roughness of 0.5 µm and hardness of 13.1 GPa. The second coating used was a ternary of chromium, aluminium and nitrogen (CrAlN) with a coating thickness of 6.3µm, surface roughness of 0.4 µm and hardness of 9.6GPa. Pin-on-disc and twin-disc experiments were carried out using a variety of different lubricants and additives. They found that a combination of PAO and ZnDTP increased coefficient of friction with H-DLC significantly, also increased with CrAlN, while lubricating with PAO or a mineral base oil both with a 4% Anglamol additive gave the lowest CoF for both samples.

The main wear mechanism observed was abrasion and, overall, the H-DLC coating had the lower wear rates for these oil combinations. This was attributed to the adhesion energy and wettability between the coatings and the lubricants. Results of friction and wear tests contradicted the hypothesis that MoDTC reduces wear and friction, with increases in both, particularly compared with H-DLC. No scientific explanation was given for this difference.

De Barros Bouchet et al. (141) also explored the boundary lubrication behaviour of H-DLC, a titanium containing DLC and a hydrogen free DLC, with MoDTC and ZDDP additives. Wear rates of $1*10^{-18}$ m^3 Nm^{-1} were observed for PAO MoDTC lubricant formulations with H-DLC; this is contrary to Bobzin et al. (140) findings of wear rates of $4*10^{-16}$ m^3 Nm^{-1} with H-DLC and PAO MoDTC. Bobzin et al. (140) carried out tests in a pin-on-disc configuration, which may have caused higher contact pressures than for de Barros Bouchet et al. (141) who used a cylinder on flat configuration. De Barros Bouchet et al. (141) found that the primary role of ZDDP was to improve the formation of a MoS_2 layer, particularly on the H-DLC coating. The authors state that there is a clear relationship between the hydrogen content and improved wear and friction characteristics. They hypothesise that in the contact area, friction causes the hydrogen terminated surface of the H-DLC to be disrupted, allowing for species within the additives to react with the surface to form molybdenum sulphide (MoS_2),

which acts as a solid lubricant to reduce both friction and wear. Figure 6-5 depicts this chemical reaction process. The presence of ZDDP provides the sulphur atoms; if sufficient sulphur is present MoS_2 can diffuse into the phosphate matrix in H-DLC.

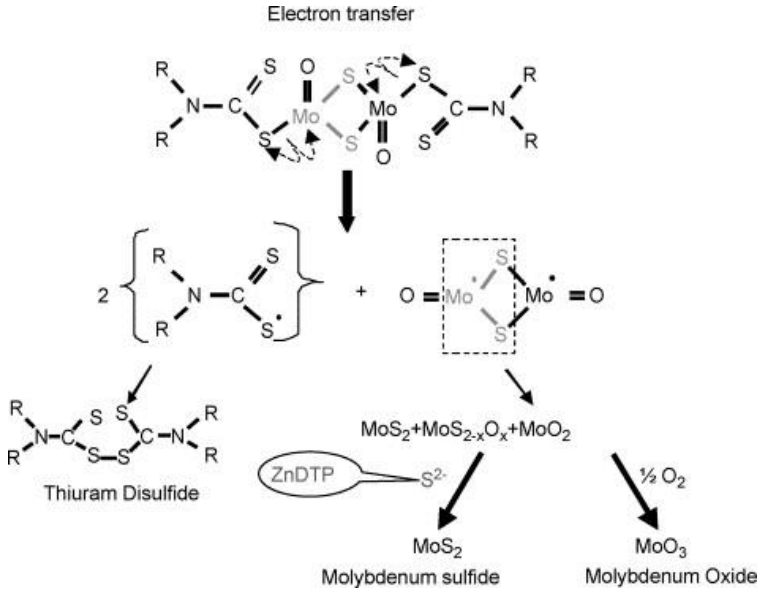

Figure 6-5, Chemical Process of the MoS2 Formation from MoDTC (141)

Haque et al. (95) considered the durability of H-DLC coatings under boundary lubrication, using a reciprocating pin-on-plate set up. The plates were coated in a 0.1 µm thick layer of chromium to promote adhesion; this was followed by a 0.5 µm layer of chromium carbide, and finally a 1 µm H-DLC coating was applied to the AISI 52100 steel plate. Five different oil blends were used; Poly-alpha-olefin (PAO) acted as the base oil with various combinations of a secondary ZDDP anti-wear additive, Moly Dimer and Moly Trimer.

Results showed that delamination of the coatings Figure 6-6a occurred in the wear track over the six hour test duration, most notably with oils that only had 1 additive. Figure 6-6a shows the extent of the delamination in the wear scar region, the authors proposed that this was preceded by polishing wear, Figure 6-6b shows irregular delamination with polishing wear. Less severe polishing wear is shown in Figure 6-6c. The test carried out with moly trimer/secondary ZDDP (Figure 6-6c) and moly dimer/secondary ZDDP exhibited less delamination and lower wear rates of the coating of $8.79x10^{-19}$ and $9.18x10^{-19}$ m^3 Nm^{-1} respectively, highlighting the need for a blend with both antiwear and friction modifying additives. Illustrated in Figure 6-6a and 5-6b are tests carried out with only one additive each, secondary ZDDP and Moly Dimer respectively. Haque et al. (95) theorised that the large scale delamination in the wear track was due to the presence of wear debris from the cast iron pin used; this accelerated wear through pressure induced graphitisation, causing the H-DLC coating to thin. They concluded that this was due to grooves in the direction of reciprocation caused by softer, less well adhered graphitic material being removed and entraining in the contact. Haque et al. (95) also stated that as a result of this

thinned H-DLC coating, the load bearing capacity reduced and caused plastic deformation and consequently delamination of the coating.

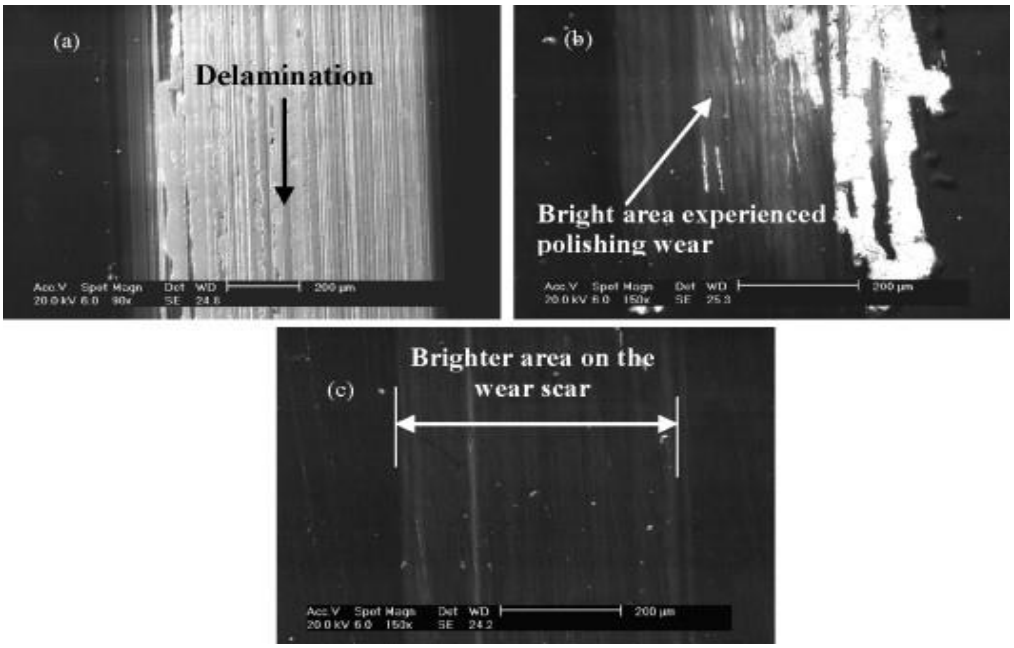

Figure 6-6, Mechanism of Wear of the H-DLC Coating: (a) Polishing Wear Followed by Continuous Delamination; (B) Polishing Wear Followed by Irregular Delamination; (C) Purely Polishing Wear (259).

Wang et al. (142) characterised the delamination mechanisms of chromium (Cr) and tungsten (W) containing DLC; these are deposited by magnetron sputtering with a 2-3 µm coating thickness. Figure 6-7a shows SEM analysis of a cross sectional view of the coatings and substrate, which revealed surface protuberances (spherical surface features) ranging from less than 0.1 µm in diameter to 3 µm for both Cr and W-DLC. Wang et al. state that these protuberances are solely due to the features of the substrate. They also observed parallel ridges on the coating surface and attributed these to the substrate surface features. A rotating steel cylinder in contact with the flat coated surface was used for tests, and lubricated with PAO. Figure 6-7b shows a significant amount of spalling was found at the exit of the contact region for Cr-DLC and extended laterally over the ridges, where large areas of delamination occur as some spalls reach the adhesion layer. Cracks within the DLC layer, near the adhesion layer were also observed, as shown in Figure 6-7c, these cracks extended in the direction of the ridges, the cracks formed under surface imperfections, such as the protuberances and ridges contributed to spalling. Spalling mechanisms were not found with the W-DLC coating, this was attributed to a superior adhesion classification in comparison with Cr-DLC.

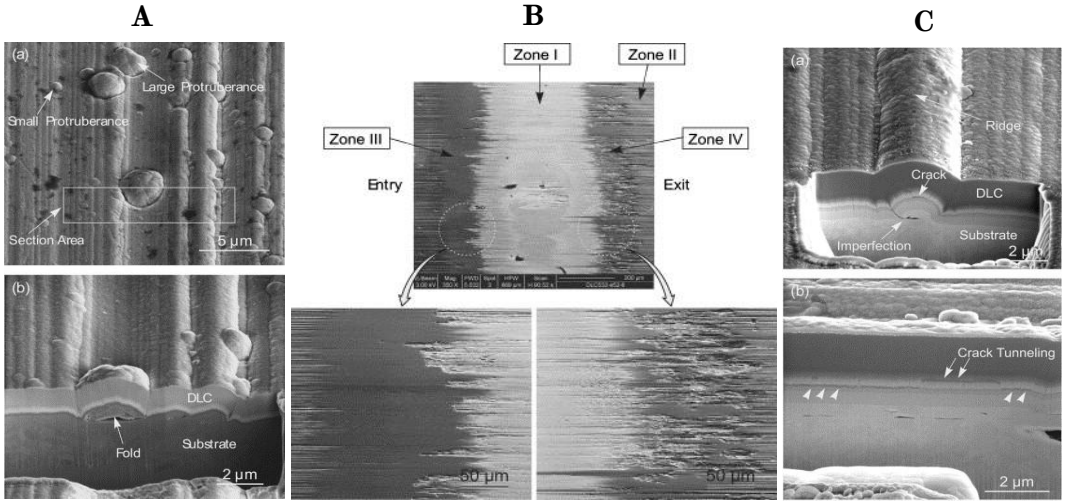

Figure 6-7 A. Plan Images of As-Deposited W-DLC Film. Parallel Grooves and Ridges as Well as Spheroidal Protuberances in a) FIB Cross-Section in b). Specimen Tilted At 52° T. B. SEM Wear Track Images of Cr-DLC. c) Cr-DLC-Coated Substrate With Longitudinal Cross-Section Revealing a Crack Tunnelling (142)

Research with DLC and bio-lubricants is less prevalent; although DLC coatings are generally considered inert, they are still electrochemically active. Vercammen et al. (103) studied the tribological behaviour of DLC with bio-lubricants. Five types of DLC were studied, two H-DLC, with different adhesion layers, a single layer titanium DLC (Ti-DLC), a multi-layer tungsten DLC (W-DLC) and a single layer silicon DLC (Si-DLC). An unsaturated ester, a saturated ester, sunflower oil and a mineral oil were tested either pure or with 1% AW or EP. In ball-on-disc tests, CoF was found to be lower with sunflower oil and unsaturated ester oil with all coated ball on a steel disc combinations. This is attributed to the polar COOH groups interacting with the steel disc to aid with boundary lubrication. The AW additive increased friction in all cases in comparison to the EP additive. The authors found that CoF was comparable for a lubricated DLC/steel contact and lubricated steel/steel contact.

The benefit of the coating comes from any lubrication starvation, as DLC/steel contacts were shown to have very low CoF in dry running. The main observed failure mechanism was delamination particularly with W-DLC and Si-DLC. The benefit of this low CoF is that there is the potential to reduce heat due to friction and reduce thermally induced biodegradation. In terms of wear, it was concluded that oils with conventional additives performed well for all DLC contacts under boundary lubrication and results were more dependent on the properties of the coating than the lubricants (wear was in the order of $0.1x10^{-18}m^2N^{-1}$).

Kano (80) found that using a poly-alpha-olefin oil (PAO) mixed with 1% by mass ester oil in combination with a tetrahedral amorphous carbon (ta-C) DLC coated (carburised steel substrate) disc in contact with a AISI52100 bearing steel pin gave super lubricity conditions. From speeds of 0.03 to 1 ms^{-1} minimum film thicknesses were calculated to be 0.0033 to 0.039 µm and lamba ratios of 0.14 to 1.58 respectively. Under contact pressures of 700 MPa CoF was a stable 0.006. The composite root mean square surface roughness went from 0.049 µm before testing to 0.024 µm after testing. When tests were performed with the same contact lubricated with SAE 5W30,

which had the same viscosity as the PAO at test temperature, produced CoF of 0.65 to 0.15 over speeds of 0. 03 to 1 ms^{-1}. No explanation for the reduction in CoF with the PAO ester oil was given, it is likely that the polar nature of the ester additive was able to form weak bonds with the ta-C DLC surface and offer a low shear interface. Kano also found that when ta-C DLC was replaced with a hydrogen DLC no large reductions in CoF were observed with either oil.

The most conclusive study performed by Simič & Kalin (104) used an atomic force microscope (AFM) to assess the adsorption properties of palmitic acid (16 carbon long straight chain hydrocarbon with a COOH tail) on H-DLC in static conditions. Tribological tests were also performed using a ball on flat configuration with palmitic acid mixed with PAO oil. Simič & Kalin (104) observed absorbed films of palmitic acid on the H-DLC surface and hypothesised that, while physisoption was dominant in the AFM tests, during tribological tests under boundary lubrication conditions, the fatty acids must have been chemisorbed due to a noticeable improvement in wear compared with steel surfaces. Coverage of the steel surface was greater than the H-DLC surface, due to the availability of more oxides on steel surfaces to react with the acids. The theorised mechanism of adsorption with H-DLC was that oxides on the surface enable hydrogen bonding. During tribological tests, the surface is disrupted, and hence bonds broken, allowing new bonds to form to sp2 structures. An increase in temperature caused an increase of surface coverage, as expected, as these surface reactions are driven by temperature, as well as frictional heat and rubbing.

Kalin et al. (143) found that, although with all DLC contacts CoF was reduced in ball on flat reciprocating tribological experiments, wear was higher with DLC/DLC contacts in comparison to steel/steel contacts; therefore they concluded that DLC surfaces are less suited to conventional lubricants and additives. Kalin et al. (143) also observed an increase in CoF when AW and/or EP additives were used in DLC contacts. The addition of AW and EP additives did have a positive effect in reducing wear for all oils tested, in agreement with Vercammen et al. (103). High oleic sunflower oil and unsaturated ester oil reduced wear more than the mineral oil or saturated ester oil, showing that polar and unsaturated fatty acids do react with DLC surfaces, as proved by Simič & Kalin (104).

A study by Mobarak & Chowdhury (144) conducted reciprocating ball-on-flat tests lubricated with canola oil. H-DLC was used and, as is well documented, the contact comprising of a steel ball and DLC coated flat surface demonstrated the lowest wear, as shown in Figure 6-8c, followed by a DLC/DLC contact shown in Figure 6-8d. Figure 6-8c, shows that a soft tribo-chemical layer was formed in the contact region and smoother worn surfaces when lubricated with canola oil and in comparison to other material combinations. A steel-on-steel contact, shown in Figure 6-8b, produced the largest wear loss, as well as CoF values double that of the other two contacts, whose CoF values were comparable.

Mobarak & Chowdhury (144) also produced SEM images that showed adhesive, abrasive, fatigue and corrosive wear. The corrosive wear is apparent in Figure 6-8b due to the darker appearance of the corroded surface. They hypothesised that the corrosive wear was caused by acidic by-products formed during the oxidation of the canola oil, due to its poor thermal stability. They also noted that the high levels of unsaturated and polar elements present in canola oil aid in the reduction of wear and

friction, but do not explain the mechanism with which saturation and polarity reduce wear and friction. This has, however, been discussed elsewhere (137).

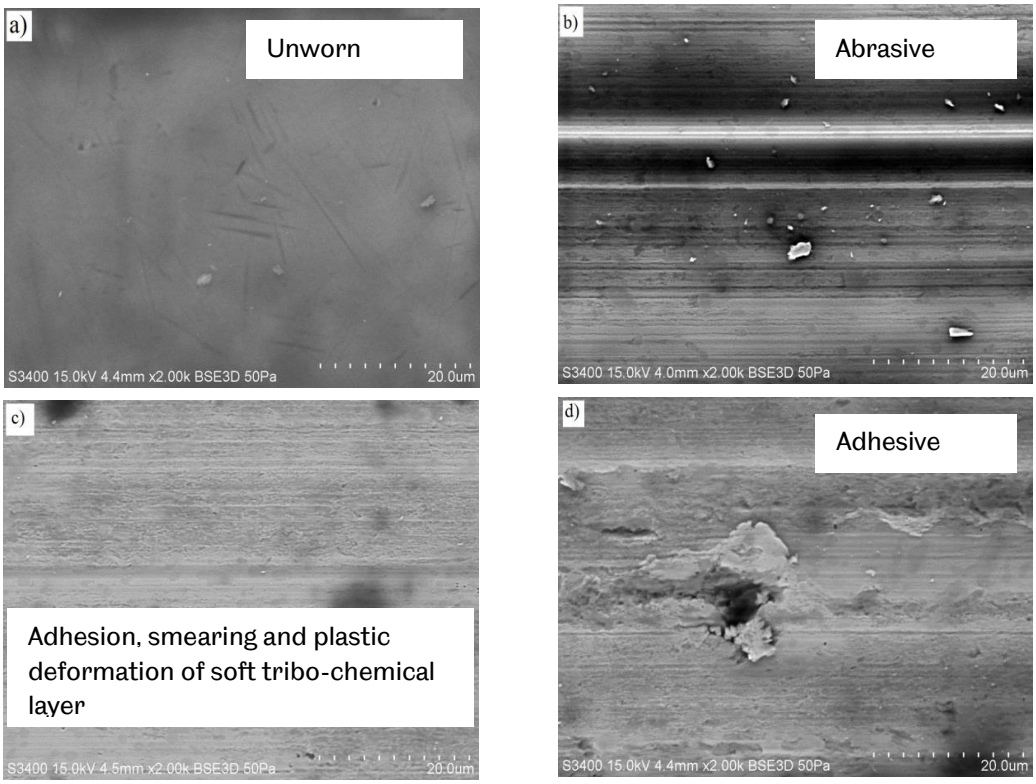

Figure 6-8, SEM Images of a) Deposited Surface of a-C:H DLC films; and Worn Surfaces when Lubricated with Canola Oil: b) Steel/Steel (WSD =416± 1.6 µm) c) Steel/a-C:H (WSD = 318± 1.3 µm) and d) a-C:H/a-C:H Combination (WSD = 355± 1.1 µm) (144).

Kalin & Vizintin's (145) work on coating combinations of H-DLC and steel agreed with that of Mobarak and Chowdhury (144). Kalin & Vizintin also observed a thin layer of wear debris generated on the steel ball in tests with a H-DLC counterface in tests with mineral oil. This layer adhered to the ball, and the authors hypothesised that;

'*This layer to a large extent accommodated the contact stresses, which resulted in relatively low wear*',

While tests carried out with sunflower oil did not show this layer of debris, indicating the formation of an effective tribofilm protecting the steel ball.

Mahmud et al. (146) also carried out work in this area and their findings were in agreement with both Mobarak & Chowdhury (144), and Kalin & Vizintin (145), in relation to the level of saturation of a vegetable oil influencing wear and friction. Mahmud et al. (146) compared three vegetable oils with increasing levels of unsaturation from coconut, palm and then sunflower oil. Tests with sunflower oil produced wear rates of around $35x10^{-6}$ mm^3 Nm^{-1}, while this was around $60x10^{-6}$ mm^3 Nm^{-1} for palm oil and $90x10^{-6}$ mm^3 Nm^{-1} for coconut oil. Interestingly, for tests carried out with a steel ball and coated flat surface, for both sunflower and palm oil the wear rate for the ball was lower, while for coconut oil the wear rate for the DLC coated

surface was lower. This re-enforces the theory Mobarak & Chowdhury (144) proposed in their research (144), that unsaturated fatty acids forming tribofilms readily on steel surfaces. In tests carried out with coconut oil, full delamination of the DLC coating occurred, accounting for the higher wear rate. Mahmud et al. (146) also observed through Raman analysis a graphitic transfer layer on the steel ball; its structure is highly disordered and the weak Van der Waals forces between the layers aid shearing at the interface and reduce friction.

6.3 Surface Texturing to Improve Tribological Performance

The use of surface texturing under DLC has been explored by Pattersson & Jacobson (147) in both dry and lubricated conditions. Uniform patterns of either parallel grooves or squares placed in quadratic arrays in widths of 5, 20 and 50 µm were used, and a 1 µm thick DLC coating was then deposited. In a ball-on-flat configuration, tribological characteristics were explored. Rather than carrying tests out in an oil bath, the balls were pressed onto filter paper saturated with PAO to leave a small oil film on the ball. This was done to demonstrate how the surface texture could retain oil effectively under boundary conditions. Pattersson & Jacobson (147) found that for textured surfaces, CoF was higher (0.12-0.22 compared with 0.07 for untextured) and more unstable, and there was no relationship between shape and size of the textures for unlubricated tests. Surface texturing in the turning point regions had greater accumulation of wear debris.

Analysis of the balls showed a thicker tribofilm on unlubricated tests with untextured DLC, the film contained wear debris from the coating. This tribofilm was not seen in lubricated tests, where the textured surfaces reduced wear and friction. The increase in CoF and wear in the unlubricated, textured tests is likely due to the lack of tribofilm formation as the 'sharp' edges of the texturing can act to scrap off any film formation. For lubricated tests, the surface texturing was important. Figure 6-9 shows the different surface textures tested and the resulting wear in the contact region. The 5 µm and 20 µm parallel grooves (20 µm parallel grooves shown in Figure 6-9b) and 5 µm squares exhibiting the low CoF of 0.05 (20 µm squares shown in Figure 6-9c). This research shows that in certain conditions, the combination of DLC and uniform surface texturing is beneficial, however in applications with a risk of lubricant starvation, surface texturing with DLC may cause excessive wear and higher levels of friction. For unlubricated DLC, surface texturing may not be advisable, due to the removal of an adequate tribofilm on the counter surface.

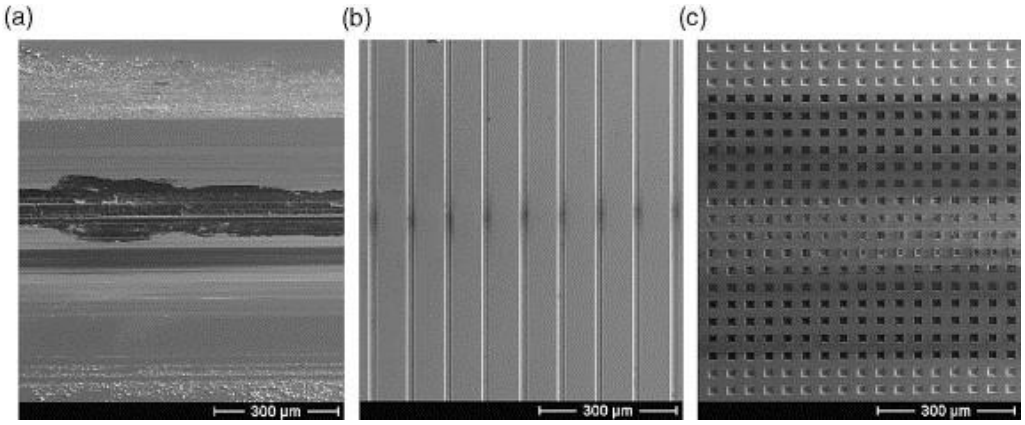

Figure 6-9, Wear Track Appearance of DLC Coated Surfaces After 20,000 Cycles Sliding Under Boundary Lubricated Conditions (SEM), a) Flat DLC Coated Surface, b) 20 mm Wide Groove Texture And c) 20 mm Wide Square Depression Texture 147 (147)).

Work has shown that for uncoated uniformly textured surfaces increase hydrodynamic pressure and allow contacts to operate in the hydrodynamic regime for a wider range of speeds and loads (148) (149) (150) (151).

Matsui & Kakishima (152) carried out cylinder on flat wear tests with three differently prepared samples, one was shot peened with ceramic balls, but no doping medium, another shot peened with ceramic balls and Molybdenum disulphide (MoS_2) and the third was just shot peened with MoS_2. Results showed significant reductions in CoF and wear rates with the samples shot peened with ceramic balls and MoS_2, resulting wear rates and CoF were 0.1 x 10^{-7} mm^3Nm^{-1} and 0.05. For the samples just shot peened with ceramic balls wear rates and CoF were 100 x 10^{-7} mm^3Nm^{-1} and 0.5. For samples only shot peened with MoS_2 wear rates were 60 x 10^{-7} mm^3Nm^{-1}, the CoF was initially as low, 0.05, but rose to 0.5 mid test. The authors stated the removal of MoS_2 for this increase in CoF. EDX analysis showed that MoS_2 remained on the surface when applied with shot peening and ceramic balls, due to the micro dimples created by the ceramic balls. EDX analysis also showed a transfer layer of MoS_2 on to the counter surface.

No work on the use of surface texturing specifically with vegetable oils was found.

Interestingly, shot peening has also been shown to increase the corrosion resistance of many materials including stainless steel, brass and titanium. Wang & Li (153) found that sand blasting 304 stainless steel using silica particles (50-70 mesh) and then annealing, altered the surface and substrate structure of the steel, giving a nano-crystalline structure of approximately 70 µm thick. The sand blasting was responsible for a heavily plastically deformed surface with high density dislocations; once annealed, Wan & Li found that the dislocation network or fine sub grains of approximately 20 nm resulted in a harder and more elastic material, compared with a regular grain structure. The increase in elasticity is attributed to an increase in the elastic limit and yield strength of the material with a finer grain structure.

Wang & Li (153) also assessed the corrosion resistance of samples using an electrochemical scratch technique. Samples were immersed in sodium chloride after being scratched with a diamond tip, variations in current represented the surfaces'

resistance to corrosion. They found that both cathodic and anodic currents had shifted to lower values. This is due to the increase in corrosion potential caused by the formation of a passive film. Wang & Li (153) speculated that high density grain boundaries (a result of the shoot peening process that induces nano crystallisation) may promote diffusion and form more compacted passive films. However, the authors state that further work is required, such as improving the understanding of the structure of these passive films, before conclusive theories can be established to explain the mechanisms of such passive films. Additionally, the work hardening of the substrate caused by the surface treatment could offer a stable support for the passive film. The increase in corrosion resistance of titanium by sandblasting and annealing was also found by Jiang et al. (154) and attributed to the same mechanisms. The change in corrosion potential of shot peened surfaces could be of particular interest in the application of bio-lubricants on metal surfaces, as there are some claims that the vegetable oils that form bio-lubricants increase corrosive wear.

6.4 Nano Fullerene

Nano fullerene is generally used as a lubricant additive rather than a surface coating (155); there are, however, a few examples of research into its potential as a surface coating, but none have explored the potential of these coatings lubricated with bio-lubricants. Alberdi et al. (156) considered the integration of fullerene-like material structures into conventional coating matrices to form nanocomposite coatings. Nano fullerene like materials can be made up of carbon atoms or a wide variety of inorganic compounds, such as transition metal chalcogenides like sulphides. The inorganic compounds particularly occur as large flat plates but can be synthesised in to nano-spheres, which have strong covalent interatomic bonds, Figure 6-10a shows the appearance and structure of these nano-spheres and Figure 6-10b show the close atomic planes of the fullerene nano-spheres.

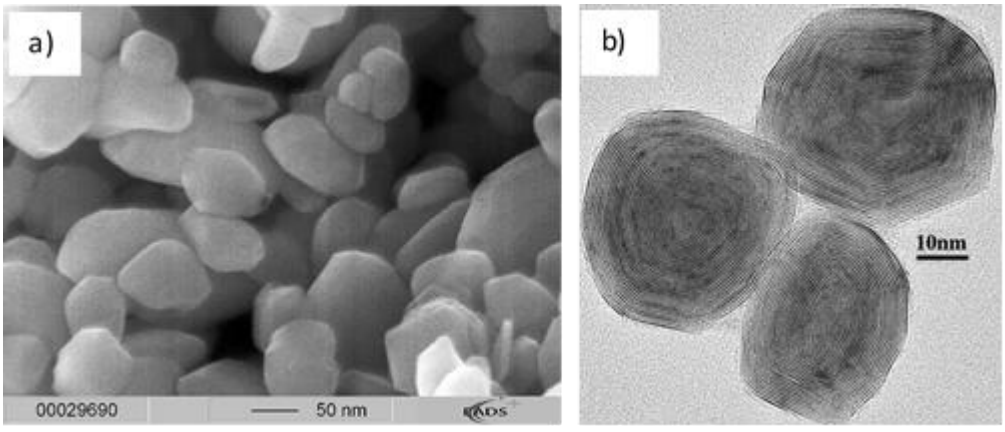

Figure 6-10a, Inorganic Nano-Fullerene, 5-10b. Closed Atomic Plane of Inorganic Nano-Fullerene (156)

Alberdi et al. (156) carried out a range of tribological tests including pure sliding, pure rolling, a combination of the two in pin-on-disc configuration, as well as fretting contacts. Tests were performed either unlubricated in controlled humidity or lubricated with white spirit and demonstrated considerable reductions in CoF values

and wear rates. DLC with fullerene incorporated into the coating for fretting tests gave CoF values of 0.17 and 0.06 for dry and lubricated tests respectively, for a commercial DLC coating tested these values were 0.3 and 0.08. The most significant reduction in wear rate was observed for dry conditions, with DLC coated wear rates of $9.02x10^{-16}$ m^3m^{-1} N^{-1} recorded and $2.99x10^{-16}$ m^3m^{-1} N^{-1} for the DLC with fullerene. In lubricated conditions, the reduction in wear rate for DLC fullerene coatings was less pronounced, but still just under half that for the pure DLC coating ($4.01x10^{-16}$ m^3m^{-1} N^{-1} for DLC and $1.96x10^{-16}$ m^3m^{-1} N^{-1} for DLC with fullerene). The authors attributed this improvement in wear to the formation of tribofilms, caused by the 'exfoliation' of the fullerene coatings under high contact pressures, as depicted in Figure 6-11, as well as the removed coating adhered to the surfaces (tribofilm) in the direction of sliding and oxidised to act as a lubricant. These coatings are claimed to be suited to very high load bearing capacity systems.

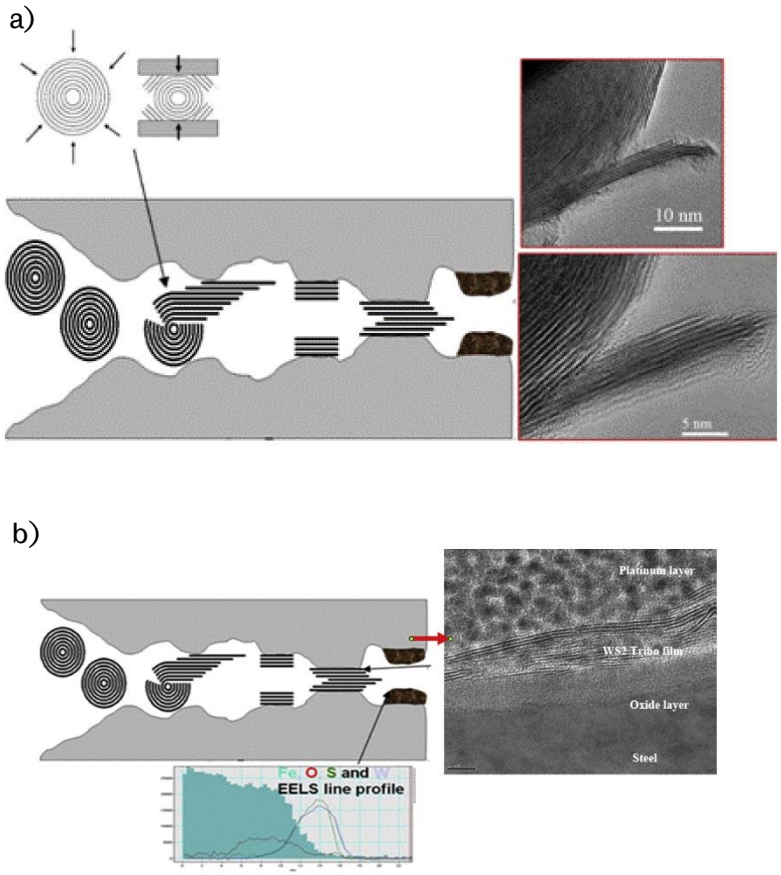

Figure 6-11, Scheme of Lubrication Mechanisms of IFLMs. (a) Pressure Induced Exfoliation of the IFLM particle. (b) WS2 Tribofilm and Oxidation (156)

Piazzoni et al. (157) assessed the friction and lifetime properties of fullerene like coatings based on molybdenum and tungsten disulphides (MoS_2 and WS_2). They found that MoS_2 fullerene like coatings performed well in comparison to WS_2 coatings, with MoS_2 demonstrating lower CoF values and a longer lifetime. Lifetime was defined by the time it took for the CoF in pin on disc tests to reach 0.3, indicating the coating had worn away leaving the steel substrate exposed. Piazzoni et al. (157) also found that increasing the film thickness of MoS_2 to increase lifetime, increased the CoF; this was

attributed to the fact that a thicker MoS_2 film had larger amounts of unreacted molybdenum and its oxides, which lowered the tribological performance.

Wu et al. (158) used ball-on-flat reciprocating tests to explore the tribological properties of fullerene-like hydrogenated carbon films compared with a H-DLC. CoF values were found to be comparable between the two coatings, 0.03 for H-DLC and 0.04 for fullerene. Wear tests were carried out for unlubricated and lubricated conditions for fullerene-like hydrogenated carbon films, with wear rates reduced by 37 times from unlubricated to lubricated.

6.5 Calcium in Tribological Systems

Calcium sulphate is known to be an effective solid lubricant, literature on its performance does appear to be limited however. John et al. (159) assessed the performance of composite layered coatings of calcium fluoride (CaF_2) and tungsten disulphide (WS_2). In wear tests they found that calcium sulphate ($CaSO_4$) was formed, aided by increased temperatures, pressures and force. This composite coating was found to have a CoF of between 0.2 to 0.3 in dry conditions and up to temperatures of 500 °C. They also assessed the performance of 1 µm thick $CaSO_4$ films and found these to outperform the CaF_2 WS_2 coating, with CoF values of 0.15. They did not propose a mechanism for $CaSO_4$ ability to reduce CoF. They observed that even in areas where the coating had worn significantly there was still a 'persistent' layer of $CaSO_4$. John et al.) (112) recommended that layering with $CaSO_4$ with other solid lubricants may assist the retention of the coating in the contact region.

Wang et al. (160) developed a blend of polyamide with and $CaSO_4$ whiskers and also found that the addition of $CaSO_4$ reduced CoF (0.41) in wear tests compared with just polyamide (0.53). There was also an improved wear resistance. Wang et al. attributed a transfer film on the steel counterface and adhered wear debris for reducing CoF and increasing wear resistance. The main wear mechanisms observed were adhesion and ploughing.

Calcium sulfonates can be found as detergents in lubricants, but as well as acting as detergents, have been found to act as anti-wear and friction reducing additives. Liu et al. (161) found, using XPS analysis that sulphur and calcium lubricant additives could form protective films on steel surfaces. Sulphur is a known and effective anti-wear additive, as discussed in 3.4. While Liu et al. did not detail the mechanism of these protective films, it is thought that they offer a stable low shear interface.

Hao et al. (162) used calcium borate nano particles as lubricant additives. They used blends of mineral oil, oleic acid and calcium borate. Through FT-IR analysis they found that oleic acid bonded to the surface of calcium borate nano particles. The stated that using lubricants with these nano particles '*extraordinarily improve the friction-reducing ability of base oil at the concentration ranging from 0.1 to 0.75 wr%'.* With CoF values stabilising at around 0.075 for calcium borate containing lubricants, they did not provide results for tests without calcium borate for comparison. Hao et al. (162) noted that in the lubricants without calcium borate, there were deeper scratches and furrows. They proposed that the calcium borate decomposed during testing to produce calcium oxides, borate oxides and iron borate.

The interaction with calcium and fatty acids has been utilised as a lubricant mechanism in medical applications. Yamamoto et al. (163) found that palmitoleic acid (C16:1), which is an anti-bacterial agent, reacted with calcium in tap water to form an enhance lubricity version of the fatty acid. They also looked at the interaction of lauric (C12:0), palmitic (C16:0) and oleic (C18:1) acid. They noted that the calcium fatty acid

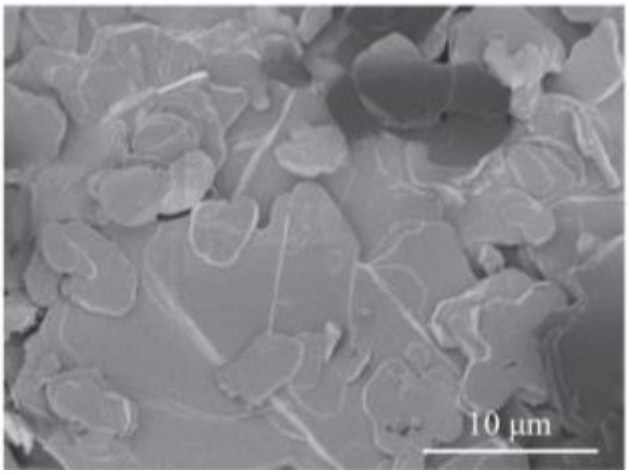

Figure 6-12, The Plate like Structure of Calcium Palmitoleic Acid (163)

salt produced, had a plate like structure as shown in Figure 6-12, and suggested this indicated particles had a lamellar crystalline structure. The performed friction tests with urethane rubber on a silicone rubber counterface and observed a CoF fifteen times lower then tests with no lubrication. Lauric, palmitic and oleic acid also gave friction reductions, the lowest CoF values were with palmitoleic and oleic acid, followed by palmitic then lauric acid. There is a trend that friction reduces as chain length increases. This work is of particular interest, as such finding could have significant implications for bio-lubricants derived from fatty acids and calcium, whether used as an additive or as a surface treatment, where the interaction could aid the formation of tribofilms. Yamamoto et al. (163) proposed that this research was the first of its kind.

6.6 Multi-Layer Coatings

Limited work has been carried out for hybridised or adaptive tribological coatings. Using nano structures, layers or multi-phase materials has become common practice, in hard coating applications particularly where ductile interlayers can be used to enhance the coatings properties (164) (165). There is little work on combining multiple bulk surface treatments. Multi-layer surface treatments offer a solution to the need to have hard and tough surfaces and retaining good levels of adhesion of coatings to substrates (166). These coatings are layers or composites of solid lubricants, adaptive coatings have the added benefit of having altered properties when subject to frictional forces (167). Sliney (168) looked at composite coatings with silver incorporated with barium fluoride or calcium fluoride. In both cases the addition of silver reduced low temperature (0-300˚C) CoF by half. Silver is a useful metal to use as a solid lubricant as it is soft and chemically stable, but plastically deforms easily under sliding and high loads. Combining it with fluorides, however, meant that ploughing, which would be seen in a pure silver coating, did not occur. These coatings had high surface roughness and dimensional tolerances, therefore

would not be practical for many applications as coatings were applied with an airbrush and then cured in a furnace.

Pauleau et al. (169) also tested multi-layer coatings of silver and calcium fluoride that were applied by sputtering. This gave high precision tolerances, unlike the coatings developed by Sliney (168). In dry aluminium ball on coated disc, the multi-layered coating performed well, giving CoF off between 0.3-0.35. A transfer layer of silver and calcium fluoride was found on the ball and SEM analysis of the wear track revealed that after 5000 cycles, both components of the coating still remained on the surface. There does not appear to be any published work that looks at lubricated multi-layer coatings containing calcium fluoride.

6.7 Surface Energy and Coating Lubricant Interaction

Prabhu et al. (170) assessed the wettability of coconut, sunflower and palm oil, with a mineral oil for comparison. They found that, due to lower viscosity, coconut and sunflower oil 'wetted' a larger area more quickly, or exhibited accelerated kinetics compared with palm and mineral oil. Figure 6-13 shows the spreading behaviour for mineral and palm oil with varying surface roughness from worked carried out by Prabhu et al. (170). They found that between a surface roughness of 0.25 to 0.5 µm there was a significant increase in wettability; after 0.5 µm there was not a significant change. For a system in equilibrium, wettability is dependent on interfacial energies at the surface liquid interface. The wettability is an important parameter to consider in the design of surface texturing in order to maximise lubricant coverage.

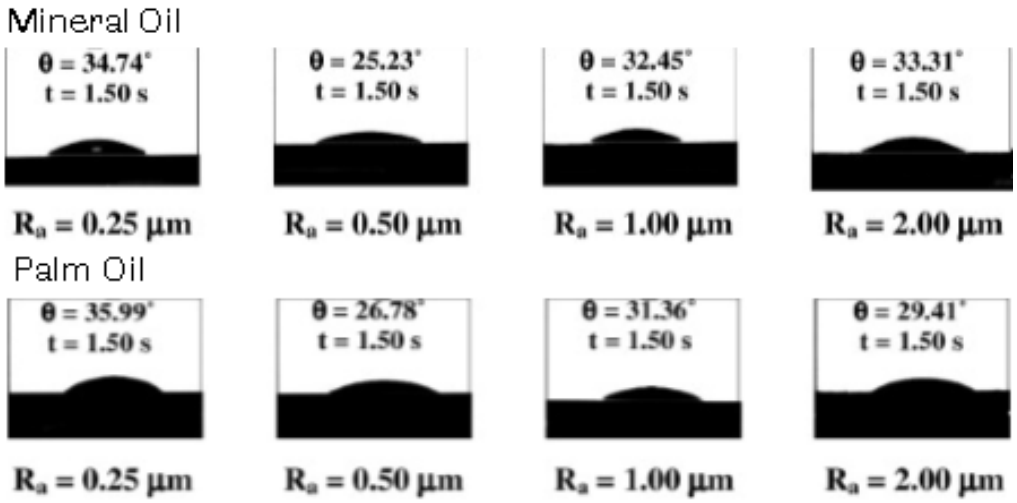

Figure 6-13, Final Drop Profile for Wetting Tests Carried Out by Prabhu et al. With Mineral and Palm Oil (170)

Podgornik et al. (171) investigated the role surface energy has on coatings and lubricant interactions. They used a-C:H DLC, WC-DLC and steel surfaces with base oils of sunflower oil and paraffinic mineral oil, as well as both these oils mixed with anti-wear and extreme pressure additives. Figure 6-14a shows the surface energy values for the specimens and liquids. The surface tension values for the liquids was calculated using the Wilhelmy plate method and the polar and dispersive components calculated using the Owens-Wendt-Rabel-Kaelble equation. The power contact angle

method was used to work out the surface energy of the coated surfaces and the Owens-Wendt-Rabel-Kaelble approximation used to work out the polar and dispersive components. The addition of anti-wear and extreme pressure additives increased the polar component values for the lubricants, as shown in Figure 6-14a, there was no polar component for the paraffinic mineral oil without additives. Figure 6-14b shows the polar and dispersive components for the solid phases tested.

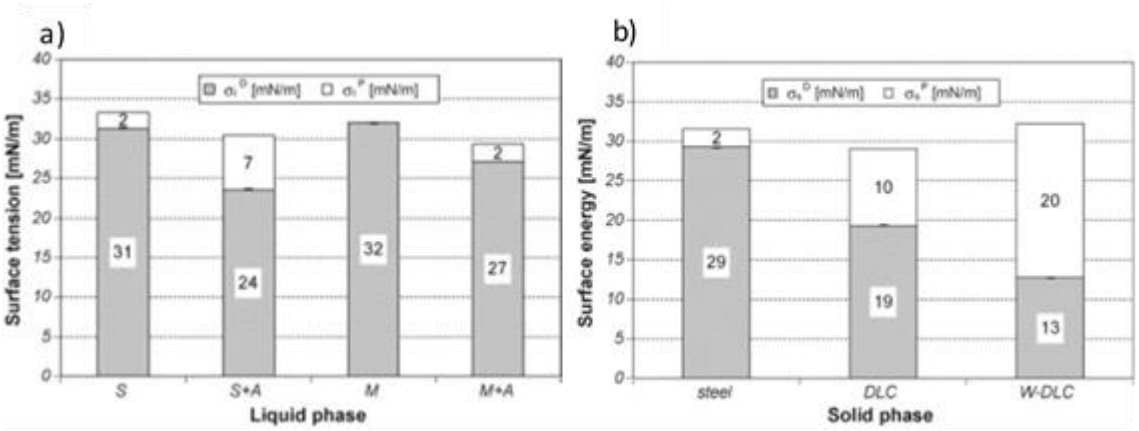

Figure 6-14 a) Surface Tension and its Polar and Disperse Share of Liquid Phases. b) Surface Energy and its Polar and Disperse Share of Solid Phases(171)

A steel and sunflower oil with additives combination gave the lowest contact angle. The lowest contact angle of all tested was sunflower oil and W-DLC. Neither sunflower oil nor W-DLC (see Figure 6-14a and Figure 6-14b) have the lowest surface tension or surface energy values, but they both have the largest polar components, which seems to be an important factor. Podgornik et al. (165) found no correlation between contact angle and CoF; the authors also proposed no clear correlation between surface energy, tension and CoF, citing that these are not the only factors influencing tribological performance. There is some correlation, in that mineral oil plus additive on DLC showed lowest CoF and surface tension and energy.

6.7.1 *Wettability, Spreading and Surface Energy*

Kalin & Polajnar (65) (172) developed an equation for calculating the spreading parameter, citing that this is a better parameter than contact angle for defining wettability. Esteban et al. (166) and Melo-Espinosa et al. (167) calculated surface tension values of various vegetable oils using density values and artificial neural networks respectively, with values in agreement with Kalin & Polajnar's work.

Experimentally, Kalin & Polajnar found poor correlation between contact angle and coefficient of friction. They found excellent correlation between spreading and surface energy, as shown in Figure 6-15a, and good correlation between coefficient of friction and spreading, seen in Figure 6-15b, for various types of DLC and steel surfaces.

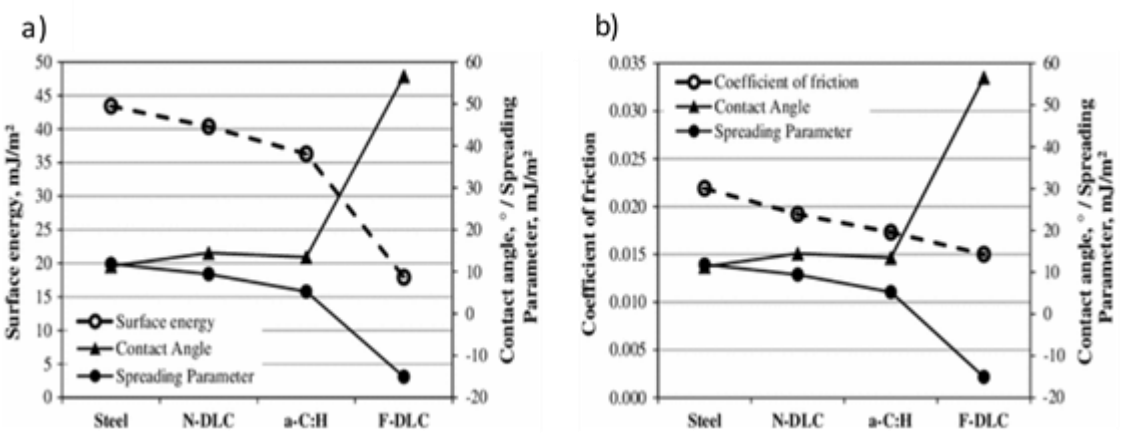

Figure 6-15 a) The Relationship Between Surface Energy, Contact Angle and Spreading Parameter for Steel and DLC, b) The Relationship Between Coefficient of Friction, Contact Angle and Spreading Parameter for Steel and DLC (65)

Kalin & Polajnar (65) (172) also stated that as steel has a higher surface energy then the DLC tested, there was higher viscous friction, due to stronger interactions with the lubricant. As Figure 6-15a shows, as surface energy (most importantly polar) reduces, so does coefficient of friction. Figure 6-16 shows the total surface energy for the material tested by Kalin & Polajnar and the dispersive and polar components.

As the DLC surface has lower surface energy the interaction at the surface with the lubricant will be weaker and be more inclined to 'slip' or move under shear, Figure 6-17 demonstrates the velocity profile difference between the slip and no slip conditions. This assumes that a fully no-slip condition can occur, but in reality, this may not be the case if the lubricant does not fully bond to the surface.

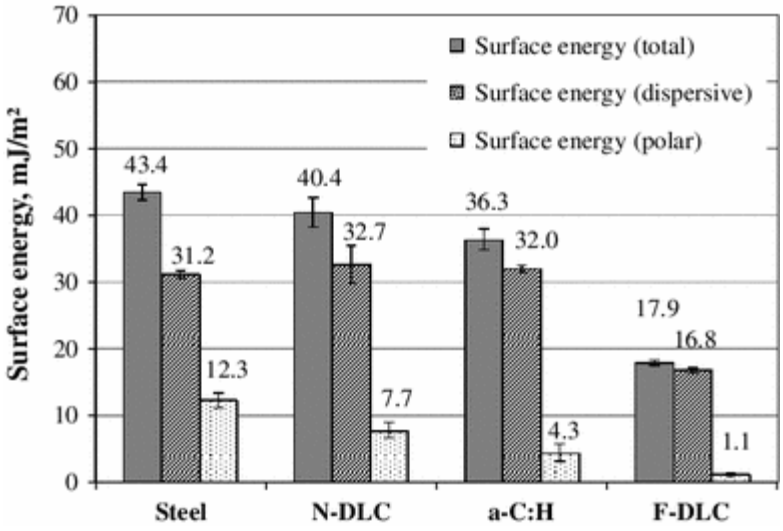

Figure 6-16, The Components of Surface Energy for Steel and Various DLC Coatings, as Calculated by Kalin & Polajnar (65)

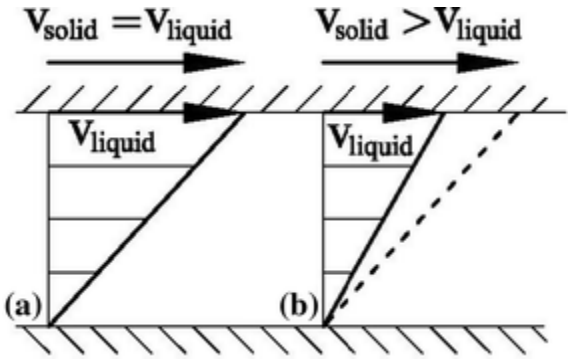

Figure 6-17, Velocity Profile of a Liquid Layer Adjacent to the Solid Surface for a) No-Slip and b) Slip Conditions (65)

6.8 The Performance of Bio-Lubricants in the Lubrication Regimes

As the molecular make up varies with mineral oils to vegetable oils, it is important to understand how vegetable oils behave in EHL contacts as well as boundary, mixed and hydrodynamic lubrication. Little work has been carried out to investigate the performance of bio-lubricants in hydrodynamic contacts and very little literature is available on creating Stribeck curves for bio-lubricants.

Durak et al. (175) studied the effects of sunflower oil as an additive to a mineral base oil in reducing CoF in journal bearings. Tests were conducted in a static journal bearing at various loads and speeds with concentrations of sunflower oil varying from 1-50%. Lubricant was pre-applied to the bearing contact to prevent the severe wear that can occur during start up and shut down. Tests were run at 25˚C and 100˚C. Results found that at 25˚C CoF decreased as the concentration of sunflower increased, this was partially attributed to sunflower oil being effective at boundary/mixed lubrication due to its ability to form chemisorbed films on metal surfaces. At 100˚C there was either no improvement in CoF or it was found to increase. Higher speeds gave the lowest CoF, as would be expected due to more effective entrainment of the lubricant in to the contact. The poor performance of sunflower oil at the elevated temperatures was due to the chemisorbed film becoming thinner and subsequently breaking down, as well as oxidation due to the elevated temperatures, which is a well-documented problem with vegetable oils.

Biresaw & Bantchev (176) investigated the traction properties of seed oils, including jojoba oil, in comparison with PAO and hexadecane using an EHL Ultra-Thin Film Measurement System from PCS Instruments. They carried out two types of tests, one to create a Stribeck curve, where entrainment speed was varied at a constant sliding to rolling ratio (SRR) of 50%. The other varied SRR and kept entrainment speed constant. In both cases the frictional torque and traction coefficient were measured at various loads and temperatures.

Their results showed that all the seed oils had lower traction coefficients (TC), the ratio of traction to normal force applied to the lubricant) the mineral oil based PAO and hexadecane. This gives the seed oils a functional advantage over the mineral oils as lower TC equates to less energy expenditure to overcome viscous drag. TC was

found to decrease dramatically from a temperature of 40°C to 100°C, which was attributed to the increased energy of the seed oil molecules due to the higher temperature, allowing them to overcome intermolecular attraction forces that oppose relative motion. SRR was also found to influence TC in an increasing trend, as with increasing load increasing TC. This trend did not occur in a uniform manner, the highest increase was seen between 0-20% SRR, and the increase then becomes more gradual after 20%. Jojoba oil exhibited the lowest TC of all the seed oils tested, a direct correlation between viscosity and TC was found, with lower viscosity came lower TC. This trend was not seen in the mineral oils.

Biresaw & Bantchev hypothesised that the seed oils had lower TC in comparison to the mineral oils due to their polar nature, this is in contradiction to the hypothesis of Durak et al, who thought that the polar nature and the ability of vegetable oils to create chemisorbed films hindered their performance in hydrodynamic lubrication, especially at elevated temperatures. Biresaw & Bantchev concluded that seed oils exhibited potential as alternatives to mineral oils as lubricants, with the potential of performing better.

6.9 Pressure Viscosity Coefficent and Film Thickness for Bio-Lubricants

Biresaw & Bantchev (177) have been responsible for the majority of the otherwise limited work published in this area. They have outlined various methods to calculate the pressure-viscosity coefficient (PVC) of ten different vegetable oils, including jojoba and soybean oil, in comparison to PAO and hexadecane. The work described several key relationships: PVC decreased with increasing temperature for both vegetable and mineral based oil, and increased with increasing viscosity. They found that PVC calculated from physical properties (i.e. using the So & Klaus method (53)) resulted in PVC values much higher than those derived from the EHL equations; this was attributed to the varying sensitivity to temperature which the different methods had. Lockwood et al. (178) proposed that this was due to the data used to generate the So & Klaus model being from a wide range of materials, including polymers, rather than a narrow set of commonly used lubricating oils.

Biresaw & Bantchev proposed that PVC is linked to the chemical structure of the oils and suggested they could be divided into 3 different categories, low, intermediate and high PVC oils, based on the varying molecular structure. Low PVC oils could potentially be categorised by their layered structure, with low interlayer interactions meaning they can slide over each other and shear easily, and are therefore not able to support much load. High PVC oils would have structures prone to entanglement, due to extensive branching and strong intermolecular interactions, meaning they offer good resistance to lateral motion and support high loads. Intermediate PVC, which both most mineral oils and vegetable oils could potentially be classed as, have structures that don't resemble either high or low PVC oils. They have little or no structure that causes layering or entanglement. While it is well understood that PVC is linked to the molecular structure of oils, this is the first work to use such categories. If these categories are verified, this could be useful for future classification and verification of results for PVC of oils.

Bantchev et al. (179) (180) compared experimental results to the theoretical model of Akei & Mizuhara and found that PVC as a function of composition showed little or no deviation from the model, but experimental values had a slight decrease with increased temperature, while the model predicted that the decrease would be a lot greater. They also stated that it would not be possible to directly correlate the results of EHL and boundary lubrication experiments they carried out, due to the use of different contacting surfaces, i.e. glass on steel rather than steel-on-steel.

Results of pressure viscosity coefficient (PVC) in literature show that the So & Klaus method (53) results in considerably higher oil film thickness values when compared with experimentally obtain values. Briesaw et al. (181) performed comparative analysis of the So & Klaus method and the Hamrock & Dowson method (182), which is an experimental method measuring film thickness to obtain pressure viscosity coefficient. They tested 3 of the same oils and found that the So & Klaus method gave results up to twice that of those found with the Hamrock & Dowson method; their results are shown in Table 6-1 with the calculated corresponding film thickness using both methods. Values obtained in Table 6-1 used the experimental set up given in Section 7.4.7.1, for load (40 N) and speed (0.13 m/s), the reference steel flat plate described in 7.3.2.2, a chrome steel ball described in 7.3.2.1 and viscosities stated in 7.3.1. This was done to show the inconsistencies in pressure viscosity coefficient values and how film thickness varies as a result. The test temperature used was 40˚C and, as pressure viscosity coefficient is highly temperature dependant, it can only give an indication of the magnitude of oil film thickness. Results show considerable variation in oil film thickness. It is clear that in order to obtain accurate results, measuring the oil film thickness using interferometry would be the best option, as there are so many varying parameters that comparisons of values in literature with experimental results is not possible.

Oil	PVC, GPa^{-1} @ 80˚C So & Klaus	Oil film thickness, µm	PVC, GPa^{-1} @ 40 ˚C So & Klaus from lit.	Oil film thickness, µm	PVC, GPa^{-1} @ 40 ˚C Hamrock & Dowson	Oil film thickness, µm
Jojoba	14.6	1.32	17.49	4.04	7.36	2.55
Soybean	14.7	1.10	18.79	3.10	8.33	2.15
Palm	14.2	1.17				
Mineral base	14.1	0.85				

Table 6-1, Pressure Viscosity Coefficient and Oil Film Thickness Values,

6.10 The Degradation and Oxidation of Bio-Lubricants

There is a significant body of research that demonstrates that the oxidative stability of vegetable oils can be improved with additives. Erhan et al. (183) examined ways in which oxidative stability and cold flow properties could be improved using a combination of chemical additives, diluent and high oleic versions of vegetable oils. With these alterations, they found that the vegetable oils offered comparable performance to mineral oil based lubricants. Although little work was found that looks at artificially aging oils to replicate used oil, a few different methods to achieve this have nevertheless been attempted.

The method developed by Dréau et al. (184) involved a device situated in an FTIR microscope, in which the oil could be heated and constant observation of the change in chemistry were possible. Only very small samples of oil, 0.05mg, can be used so it would not be a suitable method for aging large amounts of oil. They found that jojoba oil was very stable up to temperatures of 120˚C and, as the ageing temperature increased, the oil oxidised more quickly.

Another method for ageing involved tests done by Natarajan et al. (59), to assess the degradation of lubricants used in hot forging. Lubricants were placed in a furnace that was held at temperatures between 218 and 900˚C, samples were taken every 30 minutes and the changes in chemical structure assessed using gas chromatography.

Tenbohlen & Koch (185) artificially aged vegetable oils, including SO and PO among others, to assess their feasibility for use in power transformers. Various test parameters were used, with test durations between 164 hours to 1440 hours and either in the presence of air or without air, test temperature was held at 130 ˚C. The results showed that TAN increased when oils were aged, as did the rate of polymerisation. Viscosity increased considerably with tests in the presence of air, but no viscosity increases were observed in the tests without air.

Diaby et al. (62) studied the formation of deposits on the first piston ring groove of direct injection diesel engines, using a SAE 5W-30 weight oil. Tests showed that all the deposits occurred in the first ring groove, crown and top land, none were found on the second or third grooves or the piston skirt. Deposits were analysed using SEM/EDX, and found to be mainly carbonaceous with metallic elements, likely from engine wear. Further tests to analyse deposits were carried out using a tubular furnace; temperatures used were 150, 225 and 350˚C in order to simulate extreme engine and sump conditions. The duration of tests ranged from 2-10 hours, a mix of aluminium, iron and copper were also added from a concentration of 0-2%. From the tests in a controlled environment it was found that the most influential parameter during the oil degradation process was the temperature, the presence of the metallic compound caused the rate of degradation to increase when the test duration was increased. Although the tests were not carried out with vegetable oils, the experimental parameters are still significant and useful as a starting point for tests with vegetable oils.

In research carried out to assess the effects of ethanol fuel on deposit formation of aged mineral based lubricants, it was found that the origins of the deposits were partly from ZDDP and detergents when acetaldehyde was added to the oil (this is a common combustion by-product of ethanol). All of the constituent parts of ZDDP were found in deposits, phosphor, sulphur and zinc. When acetic acid was added in high concentrations, it produced a large amount of deposits, with the main ingredient in the deposits found to be calcium (found in detergents) at a 60% concentration (186). This work is of interest as ZDDP is a common lubricant additive and could be used in conjunction with vegetable oils to add wear protection.

6.11 The Degradation of Elastomers in Contact with Bio-Lubricants

Only one piece of published work has focused on the effect of bio-lubricants on the degradation of elastomers using stress relaxation methods, there is one piece of work that assessed the compatibility of elastomers and bio-lubricants. A reasonable amount of work has been carried out with respect to biodiesel. The different processing techniques could potentially mean that bio-lubricants behave differently to biodiesel. The removal of the glycerides, which are made up of hydroxyl function groups could mean the two bio-substances behave differently. The hydroxyl function groups are sites of enhanced reactivity, which is beneficial in terms of lubrication, as they help for strong bonds to the metal surfaces, but these could react with elastomers to dissolve them. Carboxylic groups are also prevalent in vegetable oils and give similar benefits, in terms of lubrication, as the hydroxyl groups, aiding the strong adsorption of the oil molecules on to metal surfaces creating stable lubricating films. Published work on the compatibility of elastomers and bio-diesel may still be of value to further understanding of the mechanisms involved in the degradation of elastomers and bio-lubricants.

Fafan-Cabrera et al. (187) published the only work found on the compatibility of bio-lubricants and elastomers. They used fluorocarbon (FKM), silicone (SR), neoprene (CR) and ethylene-diene monomer (EPDM) elastomers with jatropha oil in static immersion tests. Tests were conducted at 24 °C for 670 hours. Results showed that jatropha oil was highly compatible with all the elastomers experiencing less than 10 % volume change. After immersion in a standard engine oil EPDM and CR increased in volume by approximately 55 and 85 % respectively. Polar additives, such as those discussed in Section 3.4, in the engine oil were said to have caused these high levels of swell. High levels of swell with EPDM are seen across the literature discussed in this section. Fafan-Cabrera et al. (187) suggested that the 'like dissolves like' theory, discussed in 5.3.2, could not explain the interaction between the non-polar EPDM and the polar additives. The high level of swell was attributed to the high concentration of these polar additive in the oil. Less than 2 % volume change occurred with FKM and SR, this result is also seen across literature with a variety of different fluids, this is due partly to its extremely low permeability to a range of fluids (188). These results show that bio-lubricants have the potential to be more compatible with a range of elastomeric material.

Haseeb et al. (196, 197) carried out studies of the effects of palm biodiesel on various types of elastomers; this was done using static immersion testing at 25°C for 1000 hours and 25°C and 50°C for 500 hours. Elastomers tested were ethylene propylene diene monomer (EPDM), silicone rubber (SR), polychloroprene (CR), polytetrafluroethylene (PTFE) and nitrile rubber (NBR). In the tests at 25°C and 50°C NBR, CR and Fluorocarbon (FKM) were tested. Parameters measured during and at the end of the tests were change in weight, volume, hardness, tensile strength and elongation. The studies found that CR and NBR degraded considerably, swelling more in the biodiesel in comparison to mineral oil diesel. Trends in hardness and tensile strength were similar, decreasing more in CR, NBR and EPBM than in SR and PTFE, while FKM showed no change. FKM demonstrated very little weight or volume change, but did elongate slightly more than CR, NBR elongated greatest.

Degradation in elastomers is complex and the degradation of certain elastomers such as CR and NBR can be attributed to their polarity and the polarity of biodiesel. This causes the elastomers to dissolve more readily in the biodiesel as well as causing polymer chains to relax. High levels of carboxylic groups give the palm biodiesel its polarity. Another mechanism that causes the degradation of the elastomers is attributed to the crossing linking agents. The fillers in the elastomers react with the biodiesel to degrade the mechanical properties. These cross links are present in the elastomers as a result of curing agents and accelerators that produce links between the polymer chains and backbone, and these links determine the physical properties of the elastomer.

Alves et al. (189) used pressurised tests to study the effects of degradation on elastomers NBR and FKM in the presence of palm and soybean based biodiesel. Tests simulated a 200 bar pressurised fuel injection system with a normal load of 2500N placed on the NBR and FKM O-ring. Tests were run for 5 hours at 25°C. Mass, tensile strength and hardness were measured before and after the tests. Swelling tests in accordance with ASTM D3616 were also carried out, small samples of NBR and FKM were immersed in the biodiesel for 100 hours at 25°C. Results from the pressurised and swelling tests agreed with previous studies that were based on static immersion tests. NBR showed considerably larger weight changes in the biodiesels in comparison to FKM, as shown in Figure 6-18a, Figure 6-18b and Figure 6-18c show that there was little reduction in hardness in FKM, comparatively there was a larger reduction in the hardness of NBR.

A similar trend was observed for tensile strength; palm biodiesel showed a smaller loss in tensile strength than soybean biodiesel. It is thought that biodiesel's ability to attract and hold water, which then diffuses into the polymer matrix, also causes degradation of the elastomer. Small mass changes may be attributed to components such as plasticisers, stabilisers or additives dissolving in the biodiesel.

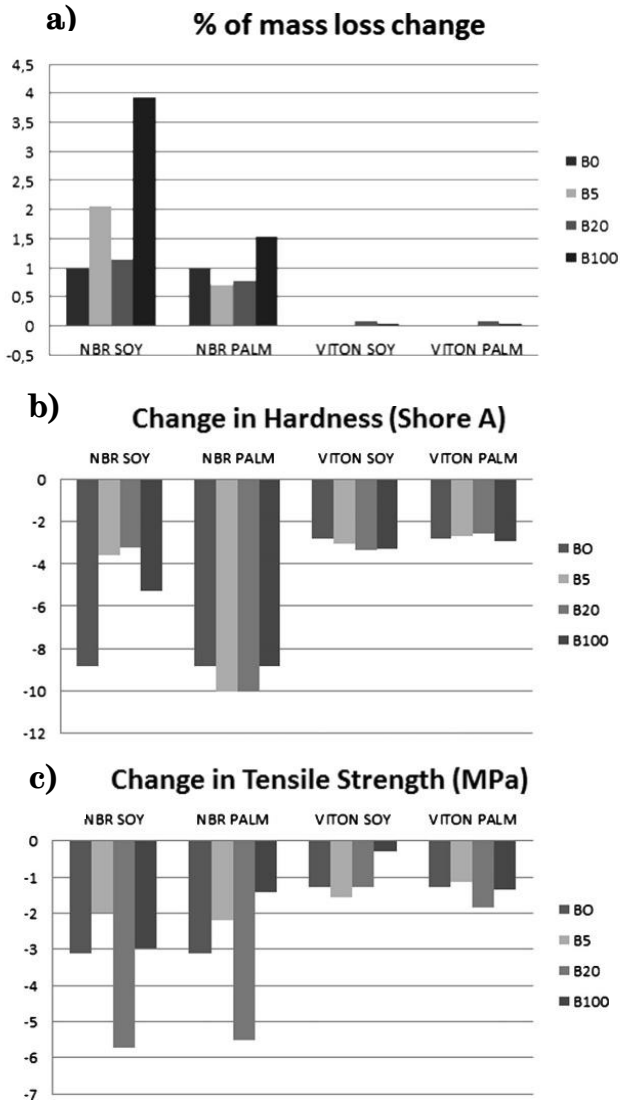

Figure 6-18, Changes in a) Mass, b) Hardness and c) Tensile Strength for Elastomers Tested with Vegetable Oils (189)

Chai et al. (190) investigated the effects of uniaxial compression on the swelling of NBR and CR as well as under cyclic loading, when immersed in palm biodiesel. Rubber samples had an applied compressive strain of 2, 10 and 20% and left under test conditions for 30 and 90 days. NBR and CR exhibited greater mass and volume change the longer the duration of the test. Mass and volume were used to calculate swelling. Swelling in rubber is the major cause of degradation and is caused by liquid penetrating the polymer network and sitting among the polymer molecules. As a consequence of this, the polymer chains are forced further apart by the liquid sitting between the molecules, and the stiffness of the material decreases. The study found that, as strain was increased, the amount of swelling in the rubber samples decreased; this is attributed to the area exposed to the biodiesel being reduced as compressive strain was increased. Lower stress was recorded for the swollen rubber. Under cyclic loading, both dry NBR and CR showed mechanical hysteresis and stress softening,

while swollen NBR and CR demonstrated less hysteresis and stress softening. There is no general consensus on the physical source of stress softening (Mullins effect).

Ch'ng et al. (191) developed a test machine to test elastomers under simple torsion, tension and combined torsion and tension in order to assess the diffusion of palm biodiesel in elastomers. Dumbbell shaped specimens were immersed in the biodiesel for 170 hours at room temperature. Varying axial extensions and twist angles were applied to the specimen and mass, and volume and swelling calculated before and after testing. Results from testing demonstrated that tensile strain had a greater effect on swelling than when torsion was applied to the specimen. This is thought to be due to the area available for diffusion to occur being increased, as well as a greater negative hydrostatic stress, which is also thought to be responsible for causing more diffusion. Two types of rubber were tested, CR and NBR; it was found that CR demonstrated consistently higher swelling levels than NBR. These results are in agreement with tests performed by Ch'ng et al. (190).

Barnes (192) provided an interesting insight into how elastomers interact differently to unused and used mineral oil based lubricants. Various tests were conducted, including immersion tests and compression set tests, with hydrogenated nitrile rubber (HNBR), two types of silicone (S2397 and S2541) and two types fluorocarbon (V2560 and V2097). The two silicone compounds where found to behave differently: The S2541 version suffered considerable degradation in used oil, with a 96% compression set after 1000 hours, as opposed to 30% in fresh oil in the same time duration, while the S2397 silicone has 'acid acceptors' which means there was little difference between the fresh and used oil during compression set testing; at its highest 50% compression set was observed. The V2097Viton performed poorly in fresh oil, this was attributed to HFP monomer. Little difference was seen with the V2560 or between HNBR in fresh and used oils. This work highlights the importance of understanding the effects aged oils can have on degradation of materials, and it appears to be a severely understudied area of research.

Heitzig et al. (193) compared data obtained from static immersion tests with NBR and FKM in a variety of biofuel candidates, with the relevant Hansen solubility parameters (HSP). The paper found that there was not sufficient agreement between experimental results and predictions with HSP. Three reasons for this lack of correlation between experiments and HSP were given; it is not clear if HSP can predict the extraction of plasticisers and fillers without doing specific checks with these compounds in HSP (rather than just the selected elastomer). The fact that NBR is a copolymer was also suggested as a potential problem, as it may be more informative to create an HSP sphere for each individual polymer; the copolymer is butadiene, with weak polar and dispersive forces ($\delta_{p,}\delta_H = 0,1\ MPa^{0.5}$) and acrylonitrile with strong polar forces ($\delta_p, \delta_H = 16.2, 6.8\ MPa^{0.5}$) (194). Lastly, HSP does not take account of molecular size, this is an important factor, particularly in interstitial diffusion.

Zhu et al. (195) linked with elastomer degradation with fatty acid carbon chain length. With increasing chain length in saturated fatty acids, swelling of NBR decreased. For unsaturated fatty acids higher swell occurred, the downward trend in volume change with increasing chain length can be seen in Figure 6-19 for C12:0, C16:0 and C18:0, the increase in swelling can be seen for C18:1.

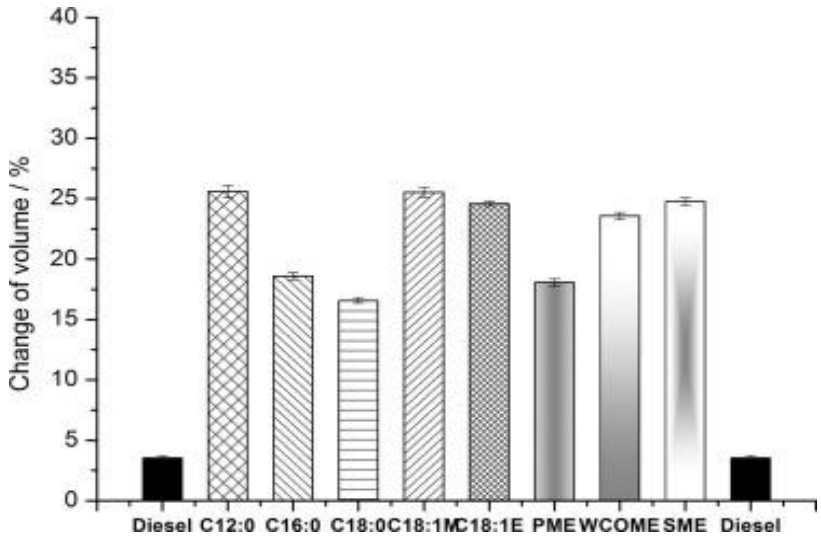

Figure 6-19, Change in Volume of Rubber Samples Immersed in Different Fuels (195)

NBR is a polar copolymer, therefore based on the HSP fundamental principle of 'like dissolves like', polar fluids will interact, and this results in dipole-dipole interactions that cause the swelling of the rubber or degradation. With the six fatty acids tested by Zhu et al., the HSP dispersive forces were very similar, while the polar and hydrogen values decreased with increasing carbon chain length. The polar and hydrogen values are noticeably higher for the C18:1 unsaturated fatty acid in comparison to the C18:0 saturated fatty acid. This relationship between chain length and chemical interaction with NBR extends to change in mechanical properties as well, for example change in tensile strength, elongation, tear strength and hardness, all decrease with increasing carbon chain length. While Zhu et al. (195) propose that the degradation in mechanical properties is caused by the destruction of cross links, this is only possible in unvulcanised elastomers. Based on this literature, and information obtained from an elastomer manufacturer, it seems likely that the mechanism involves parts of the elastomer becoming a mechanically weak gel like substance. It is highly unlikely that these substances would break a covalent cross link bond. Solvation is the likely cause, where weak covalent bonds are formed. The research goes on to comment on the likelihood that plasticisers and stabilisers will leach out during immersion in certain fluids. Low molecular weight esters are used as plasticizers in NBR, therefore due to fatty acids having a similar chemical make-up, it is to be expected that they will be extracted on exposure (196). This appears to be a plausible explanation of the slight change in mechanical properties and it is well known that this causes surface porosity that could lead to crack propagation and removal of additive materials and the creation of new function groups between the fluid and elastomer.

Zhu et al. (195) as well as Hansen & Just (197) explained that the Flory approach to solubility parameters cannot give a complete understanding of solvent elastomer interaction, as it does not explicitly take into account polar and hydrogen bonding. This would therefore suggest that HSP is a more accurate way of describing these interactions. The Flory-Huggins method takes greater account of molecular weight

than HSP, as the entropy value used in this method changes, dependant on the molecular weight of 'solvent' and elastomer (198).

Graham et al. (194) assessed the impact of various aromatics, found in aviation fuel, on the swelling behaviour of NBR, experimentally using static immersion methods, and using HSP. Like Zhu, Graham also commented on the link between increasing polar and hydrogen bonding values and increasing swell. Decreasing molecular volume and shape also contribute to increasing swell; this is well documented, e.g. (199). Graham employed volume additive rules in order to construct a mixture within HSP. It was, however, considered that this may underestimate the polar characteristic of the NBR copolymer. He found that there was on overall correlation between volume swell and solubility parameters. In particular, swell increased with increasing polar and hydrogen bonding values. The group contribution method is an alternative method to using volume additive rules to estimate solubility parameters of complex mixtures, this involves working out cohesive energies based on the different molecular groups. These can be combined to calculate solubility parameters (200).

Nielson & Hansen (201) found correlation with increasing RED and decreasing swelling with two types EPDM, the correlation for one of which is shown in Figure 6-20a. interestingly, two of the four types of EPDM tested had noticeably different molecular weights and branching, yet this had little effect on the resulting experimentally derived HSP values. The comparisons of FKM and RED highlighted no clear correlation between these values, particularly for REDs of less than 1.7, above this value only small amounts of swelling occurred, as shown in Figure 6-20b. The lack of correlation was attributed to the fact that FKM is a copolymer, as well as a curing agent that is thought to have contributed to swelling.

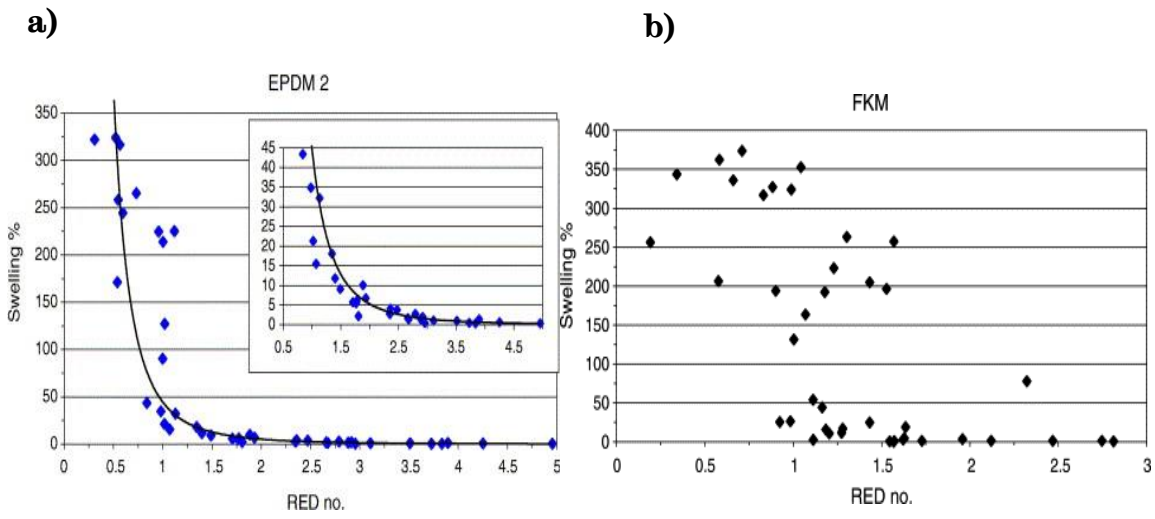

Figure 6-20, A Comparison of Swelling and RED for a) EPDM and b) FKM (201)

Seehra et al. (202) looked at the structural characteristics of 2 commercial elastomers with a variety of alcohol based fluids and aromatic fuels. They made the link that diffusion is not strictly Fickian, since the exponential differs from the 0.5 that is to be expected, being between 0.4-0.6. They assessed the relationship of swelling and HSP and came to the agreement with others that a trend of HSP likeness and

swelling was apparent. Of particular interest is that in static immersion tests the maximum mass increase was 90% (in toluene) in about 6 hours, and this decreased by 4% in the following 7 days, attributed to the removal of fillers, as mentioned by Graham et.al. (194).

Elastomers more often than not are made up of plasticisers, curing agents and stabilisers, which could contribute to the interaction of elastomers and solvents. Krauskopf (203) calculated HSP values for several plasticizers, using additive factors of molecular group functionality rather than experimental methods. Using this method could be useful if the plasticizers in the given elastomer are known. The issue is that often, elastomer manufacturers will not reveal which plasticizers and additives are used in their elastomer 'recipes', therefore only speculative conclusions can be formed.

6.12 Conclusion of Literature on Bio-Lubricants

The literature on bio-lubricants discussed in this chapter can be summarised in three tribological categories relating to wear, lubrication properties and electrochemical effects.

The polar nature of the vegetable oils is a fundamental characteristic in the oils' ability to protect a surface against wear, as described in more detail in Section 3.8. Limited work has shown that jojoba oil blended with mineral oil reduces wear when compared with jojoba oil alone. Jojoba oil's ability to reduce wear is attributed to its highly polar nature and long carbon chains. Blending palm and soybean oil with mineral oil has also been shown to reduce wear compared with the pure palm or soybean oils.

Little work has been done on the suitability of using a variety of surface coatings with bio-lubricants. DLC is an effective surface coating for reducing wear and friction, particularly in dry contacts. Many different wear mechanisms are observed in wear tests with DLC; delamination and spalling are predominant, with the substrate finish influencing these mechanisms. Abrasion, fatigue, adhesion and corrosion where also found in wear tests carried out with DLC/steel contacts. Although DLC is considered inert, chemical films are formed on the surface, and a pressure induced graphite transfer layer has been observed. Vegetable oils with high levels of unsaturation demonstrate better wear protection in DLC/steel contacts due to the formation of a tribofilm.

Calcium sulphate has been shown to be an effective solid lubricant and lubricant additive. Literature has revealed that calcium reacts with fatty acids and the resulting salt offers enhanced lubricity compared with fatty acids alone. This result is of particular interest, as this could lead to developing surfaces and lubricant additives that are optimised for fatty acid based lubricants.

Not all additives are suited to contacts containing DLC, there are mixed reports on the use of MoDTC, ZDDP on the other hand was shown to give good wear protection in DLC contacts. General findings are that both antiwear and friction modifiers are required. DLC used in combination with fullerene has the ability to reduce wear and friction. Surface texturing with DLC is only effective in lubricated contacts, in dry contacts the sharp edges of the surface texturing prevent any tribofilm being

produced. Surface texturing increases the load carrying capacity of the lubricant film. No research was found that explores the potential benefits of bio-lubricants and surface texturing. Shot peening increases the corrosion resistance of surface, a potentially useful property for use with bio-lubricants.

The surface energy of a coated (or uncoated) surface may give indication as to a how a lubricant interacts with a surface and how well it performs in reducing wear and friction. Literature shows that authors are conflicted in the role of parameters such as wettability, spreadability and contact angle. There is some evidence that lubricants with lower polarity will have lower CoF compared with higher polarity oils, this effect is attributed to viscous friction. However, the highly polar nature of vegetable oils has also been shown to be more effective in boundary or mixed lubrication, due to their ability to form effective chemisorbed films. At higher speeds these film may breakdown, due to increases in shear rate and temperatures, leading to oxidation. There is no conclusive work to explore the benefits of boundary lubrication performance compared with the lower performance in hydrodynamic lubrication. As work in this area is limited further work is required to improve understanding of these performance aspects have on the reduction of wear and friction.

There is work that shows jojoba oil has the ability to act as a viscosity improver, acts well at preventing rust and reduces wear in comparison to mineral oil. There is also some evidence that a blend of mineral, vegetable oil and an additive package results in a lubricant that is comparable to fully formulated lubricating oils in terms of wear and friction properties, but with the added benefit that less mineral oil is used. While there is no agreement on the optimal amount of vegetable oil to formulate an effective blend, there is agreement that beyond an optimal level, the polar nature of vegetable oils hinders the additive package forming a stable layer on a contacting surface.

Vegetable oils degrade more readily due to the bonding potential of fatty acid molecules; high oleic oils, with high levels of saturation, degrade more slowly. It is well documented that antioxidant additives prevent oxidation in vegetable oils. Temperature controls the rate of oxidation, with metallic compounds increasing the rate of oxidation and degradation. ZDDP has been found in large amounts in engine deposits in certain research, an important point due to widespread use of this additive.

No work has assessed the compatibility of bio-lubricants with elastomers in stress relaxation tests, only one piece of work with bio-lubricants and static immersion tests was found. There has been considerable work assessing the compatibility of elastomers with bio-fuels. The transesterification and removal of glycerides means that the two bio substances have the potential to behave differently. In terms of the compatibility of bio-fuels and elastomers, research shows that with certain elastomer materials, such as CR, NBR and EPDM, considerable degradation takes place. As the chain length of vegetable oils increases, the likelihood of swelling decreases. FKM is considered a stable elastomer with little degradation occurring. Hansen solubility parameters have the ability to predict interaction, but are unreliable in their current form.

This leads to the conclusion that research into the performance of vegetable oil as a bio-lubricant is inconsistent across most tribological areas and significant work is

required to improve the understanding of the performance of bio-lubricants as well as the mechanisms that explain their behaviour.

The experimental plan in Chapter 7 combined with theory and literature was developed to address some of the key areas in which significant contributions can be made to advancing knowledge on the suitability of bio-lubricants in a range of applications, with particular focus on their suitability as automotive lubricants.

The ability of vegetable oil to form chemisorbed films is well documented for ferrous surfaces, as the literature review has shown. It is not clear whether there are any significant benefit of using bio-lubricants and surface with treatments or coating applied, such as those discussed in Section 5.2.1, 5.2.2, 5.2.2.1 and 5.2.3. Experimental methods (detailed in Chapter 7) were used to assess the interaction of bio-lubricant base stocks with various surface treatments, results of which are detailed in Section 9.

The theory of wettability discussed in Section 3.8.2 was be used to assess the boundary lubrication performance and spreading ability of bio-lubricant base stocks, as this could be a useful tool for assessing and explaining the performance of lubricant and surface interactions. This is analysed further in Section 9.4.2.

The oxidation of vegetable oils is one of the main performance hindrances for bio-lubricants as discussed in Section 3.7. A comparison of the composition of unused and used bio-base stocks was made (see Section 9.4.1) to assess how the selected bio-base stock perform relative to one another.

A review of literature has found no work that directly looks at the interaction of bio-lubricants and elastomeric materials. An experimental plan to address this is detailed in Section 7.2.2. With the use of Hanson Solubility Parameters to help predict performance, detailed in Section 7.4.5.

7 Experimental Methods and Materials

This section describes in detail the experimental methods and test procedures used to assess the performance of bio-lubricants, the chosen bio-lubricant base stocks being, jojoba, soybean and palm oil. A Plint TE 77 reciprocating wear test machine was used for wear and friction tests and an Elastocon Relaxation Tester EB 02 for elastomer compatibility tests. Methods used to analyse samples are also described. Methods used were scanning electron microscope imaging, three dimensional optical scanning, coating adhesion measurements and viscometer.

Details of the experimental materials used to assess the performance of bio-lubricants under consideration in this work are given. It describes the properties of the bio-lubricant base stock candidates' jojoba, soybean and palm oil, as well as the mineral base stock used for comparison. Learning experiments were carried out using cast iron test specimens were used for wear tests with varying blends of jojoba and mineral oil are described. These set of tests were performed to help set the test parameters and confirm the type of bio-lubricants to be used. Test were then performed using multi-layer surface treatments consisting of varying combinations of diamond-like-carbon, ultra-fine shot blasting, a calcium based chemical dip and nano fullerene, which are detailed further in this chapter. For the assessment of elastomer compatibility with bio-lubricants, ethylene propylene diene, nitride and fluorocarbon elastomers were used, as described in this chapter.

7.1 Experimental Design

Quantitative research methods were used to assess the suitability of bio-lubricants as automotive lubricants. This approach was taken for two reasons; the industry standard route for assessing the suitability of new lubricants is assessed experimentally, as described in Section 2.3. Literature revealed inconsistent, or a lack of data, on bio-lubricants, as described in Chapter 6, therefore the most suitable method for improving understanding of the performance of bio-lubricants is through experimental methods. Qualitative methods were employed for the analysis of wear features.

Learning experiments for wear tests were conducted initially (detailed in Section 7.4.7.2). This was carried out in order to set the parameters for further tests using the novel multi-layer surface treatments (detailed in Section 7.3.2.3) in combination with bio-lubricant base stocks. Some variation in load and temperatures were trialled, to assess the variation in results. Blending oils was also trialled to see if this could improve tribological properties of the bio-lubricant base stocks.

For all experimental methods conducted, tests were repeated a minimum of three times for each base stock and material tested, unless otherwise indicated in Section 7.4. This level of repetition was felt to be reasonable in order to give data statistical significance and practical in the given time frame. The order in which tests were conducted was randomised to reduce any effect of time dependant systematic bias, such as instrumental drift, changes in raw materials, ambient temperature and humidity. Control or reference tests were performed were appropriate, details of which are given in test Section 7.4.

This work aimed to assess the suitability of bio-lubricants in automotive engines, therefore the test parameters, while not aiming to replicate exact engine conditions, are representative of some of the harsher environments an automotive lubricant may experience. The exact test parameters are detailed in test Section 7.4.

7.2 Test Equipment

This section details the equipment used to perform wear and friction tests for learning experiments and to assess the compatibility of bio-lubricants with multi-layer surface treatments. Test equipment used to assess the compatibility of elastomers with bio-lubricants is also detailed.

7.2.1 *Plint TE 77 Reciprocating Wear Tester*

The Plint TE77 reciprocating wear tester was used in a ball on flat contact arrangement for wear and friction measurements, as shown in Figure 7-1. The flat specimens, detailed in Section 7.3.2, were fixed in to an oil bath, which has heating cartridges situated underneath to heat the oil to the desired temperature. A thermocouple in the oil bath gives temperature readings. A load cell was attached to the oil bath and linked to a computer that gives the tangential load readings that enable coefficient of friction readings to be obtained. A normal load is placed on the reciprocating arm.

The Plint TE77 was chosen for its relative simplicity and easy to control test parameters, such as speed, load, temperature and test duration. Wear and friction measurements are relatively easily obtained, and tests under the same conditions are readily repeated. Reciprocating wear testers are a standard tribological method for assessing the wear and friction of material and lubricant pairings. It is an industry recognised test method for assessing wear and friction. Tests were conducted under the guidance of ASTM G133; *'Standard Test Method for Linearly Reciprocating Ball-on Flat Sliding Wear'* (204) and ASTM G181; *'Standard Test Method for Conducting Friction Tests of Piston Ring and Cylinder Liner Materials Under Lubricated Conditions'* (205)

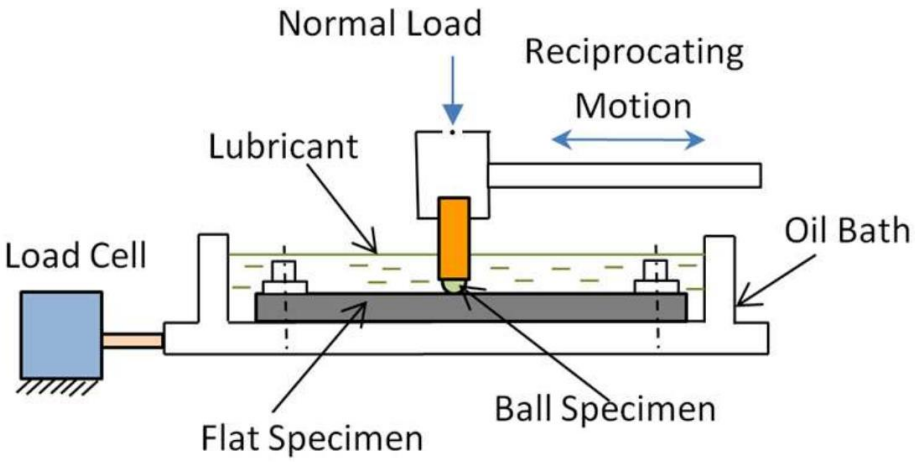

Figure 7-1, Schematic of the Plint TE77 (224)

7.2.2 *Elastocon Relaxation Tester EB02*

The Elastocon Relaxation Tester EB 02 was used to assess the compatibility of elastomers with bio-lubricants, in accordance with ISO 3384-1:2011, '*Rubber, vulcanized or thermoplastic – Determination of stress relaxation in compression – Part 1: Testing at constant temperature*' (206).

The test machine comprises of a compression rig that has compression plates attached to an adjustment screw, with a load cell and gauge attached. Figure 7-2 shows this. The load cell is able to measure and record the variation in force required to maintain the same compression. There is also a thermocouple probe situated next to the compression plates. An oil container can be attached to this compression rig so that the compression plates are immersed in oil. The compression rig can then be placed in the oven and held at a constant temperature for the desired test duration, as highlighted in Figure 7-3. An environment chamber is required in order to minimise the effect of the temperature difference between the sections of the compression rig sitting in the oven and above. If this is not minimised, cyclic force variations will occur as the temperature varies over the day.

The CombiLab software that is used with the Elastocon Relaxation Tester is able to record data for force and temperature every minute over the duration of the test.

For applications where a high level of accuracy is required, the spring effect in the load cell must be compensated for. The load cell will relax slightly as the elastomer sample relaxes under compression, this results in the sample being further compressed. To compensate for this, the adjustment screw can be used to bring the sample back to the original compression by noting the value on the dial gauge when first compressed and ensuring the rig is readjusted to this value periodically throughout the test. The results obtained from the tests detailed in this work are of a comparative nature, and the variation between different base oil candidates is of interest; it is felt that it is not necessary to perform the adjustment described above.

As the review of literature found in Section 6.11 testing seals under compression is an understudied area, particularly with experimental procedures that allow the seal force to be continuously measured without the need to stop testing, removing the seal and take static readings. It was therefore felt that using the stress relaxation method for assessing elastomer compatibility was an ideal opportunity to conduct tests that were more representative of in service conditions.

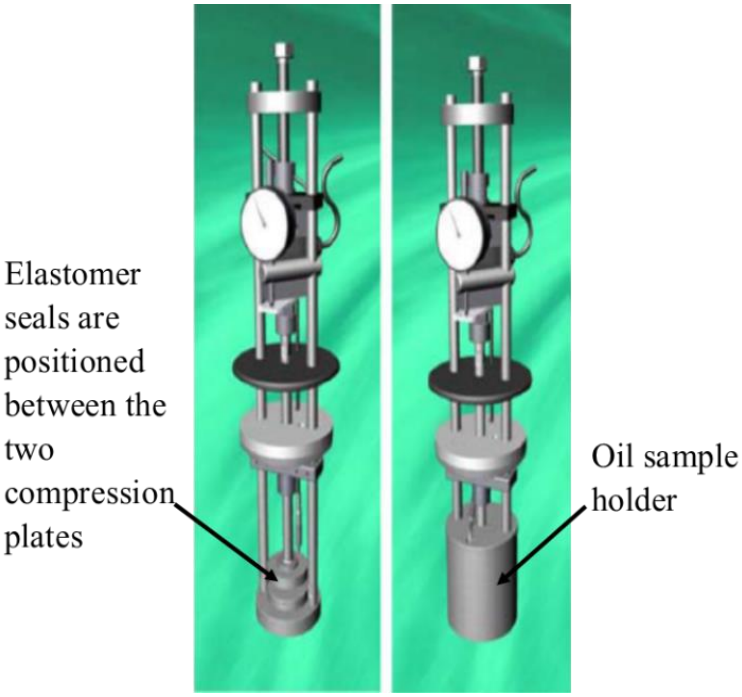

Figure 7-2, Example of the Compression Plates that Hold the Seal for Elastomer Compatibility Testing (257)

Figure 7-3, The Elastocon Relaxation Tester (257)

7.3 Test Materials

This section details all the materials used in testing with the equipment described in Section 7.2.

7.3.1 *Lubricant Base Stocks*

This section details the lubricant base stocks used with the test equipment detailed in Section 7.2.1 and 7.2.2. The bio-lubricant base stocks were selected based on knowledge gained from previous work, where wear tests were conducted on a larger selection of bio-lubricants (57). The selection was also made based on interesting properties of the oils described here, which could mean they are more suited to be used as a base stock for automotive applications. Further justification for the selection of the base stocks is given in Section 7.3.1.1 to 7.3.1.4.

7.3.1.1 Jojoba Oil

Jojoba oil (JO) is a unique vegetable oil, consisting of a mix of wax esters of long chain monohydric alcohols and carboxylic acids. The wax nature of this oil makes JO structurally different from typical triglyceride based vegetable oils. The oil used in experiments is shown in Figure 7-4, it is colourless, which is typical for a refined version of JO. The high molecular weight, of 610 $kgKmol^{-1}$ (207) and polar nature of the carboxylic acids means that the wax should have good tribofilm formation properties on metal surfaces. The main fatty acid composition of JO is paullinic acid (C20:1), shown in Figure 7-5, which makes up 72.2% of the wax. There is one double bond that causes a kink in the fatty acid chain. This is of importance as it can reduce the ability of molecules to shear over one another; this is discussed in more detail in Section 9.4. Erucic acid (C22:1) makes up 15.3% and oleic acid (C18:1 cis) makes up 8.4%. It contains predominantly monounsaturated fatty acids (93.5 g/100g). The viscosity of JO is 6.3cSt at 100̊C, with a VI of 220, as shown in Section 7.3.1.5. Full fatty acid composition given in Section 9.4.1.

Literature shows that there is some evidence that wax esters have higher oxidative stability than other vegetable oils and comparatively good resistance to hydrolysis. JO is less susceptible to oxidation because the antioxidants present in the wax are more potent than tocopherol, common in triglyceride based antioxidants in vegetable oils. The high linearity of the wax esters also means they exhibit higher viscosity indices, but low viscosity, which is in line with the latest demands for automotive lubricants. JO has a high flash point, does not exhibit foaming tendencies, and has low volatility and good thermal stability. As a wax ester, JO is potentially an excellent base stock for high temperature and high pressure applications. Sulphurised JO is already used as an extreme pressure additive, as sulphurisation improves the oxidative stability of the oil (67). JO is currently more commonly used in beauty products, such as moisturisers, than industrial applications.

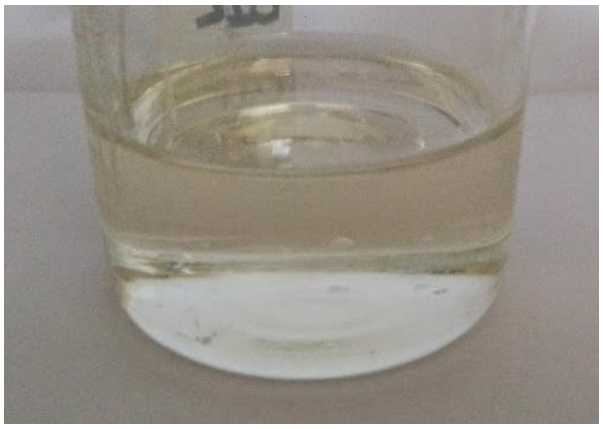

Figure 7-4, An Example of the Typical Appearance of Jojoba Oil

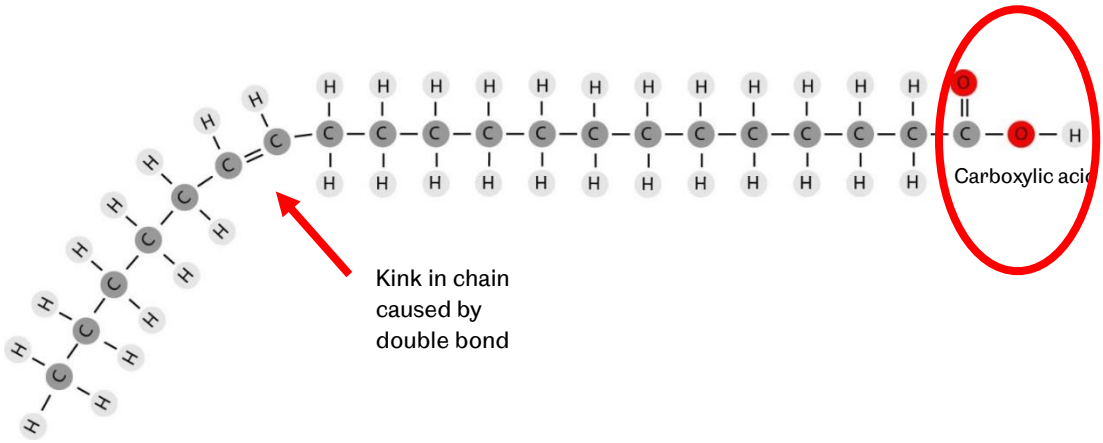

Figure 7-5, Paullinic Acid, the Main Constituent of Jojoba Oil

7.3.1.2 Soybean oil

Soybean oil (SO) is extracted from the seeds of soybeans; Figure 7-6 shows the typical appearance of SO. It is a triglyceride structured vegetable oil. Linoleic acid (C18:2) in the cis orientation, Figure 7-7, is the main fatty acid in SO, making up 52.9% of the composition. Oleic acid (C18:1 cis) makes up 23.9% and palmitic acid, at 10.7%, is the other major constituent of SO (Full composition given in Section 9.4.1). Mono- and poly-unsaturated fatty acids make up 23.4 and 56.3 g/100g respectively, while saturated fatty acids make up 15 g/100g. The molecular weight of soybean is 920 $kgKmol^{-1}$ (208). The viscosity of SO is 7.7 cSt at 100C, with a VI of 220, as shown in Section 7.3.1.5.

SO has polar carboxylic function groups situated at the end of the fatty acid chains, which mean it is effective at forming tribofilms on metallic surfaces, as discussed in Section 3.8.3. The double bonds, highlighted in Figure 7-7, have relatively low reactivity, but due to SO being rich in electrons, degradation compounds such as free radicals and cations, which are deficient in electrons, can degrade the oil readily. The double bonds, seen in Figure 7-5 and Figure 7-7 in the fatty acids, are close together, this increases the weakening effect of having double bonds in fatty acids (209).

Polymerisation has been observed in SO at relatively low temperatures (210). The double bond causes a kink, as discussed in Section 7.3.1.1, which may be of significance and is discussed more in Section 9.4.

As mentioned in Chapter 2, the intersessional working group on SCCPs gave extensive recommendations for alternatives to SCCPs for metal working fluids, one of which was SO. As discussed in Section 4.2, there have been some full scale engine tests with SO with the US postal service and Colorado University, with apparently encouraging results. The USA is a major producer of SO, therefore it has potential as a feasible source for bio-lubricant base stock. Pervious work carried out (57) and literature (discussed in Section 6.1) have shown inconsistent results with the wear and friction performance of SO. Literature has shown that bio-diesel versions of SO show good compatibility with elastomers, as discussed in Section 6.11. The most common use for SO is currently in food products.

Figure 7-6, An Example of the Appearance of Soybean Oil

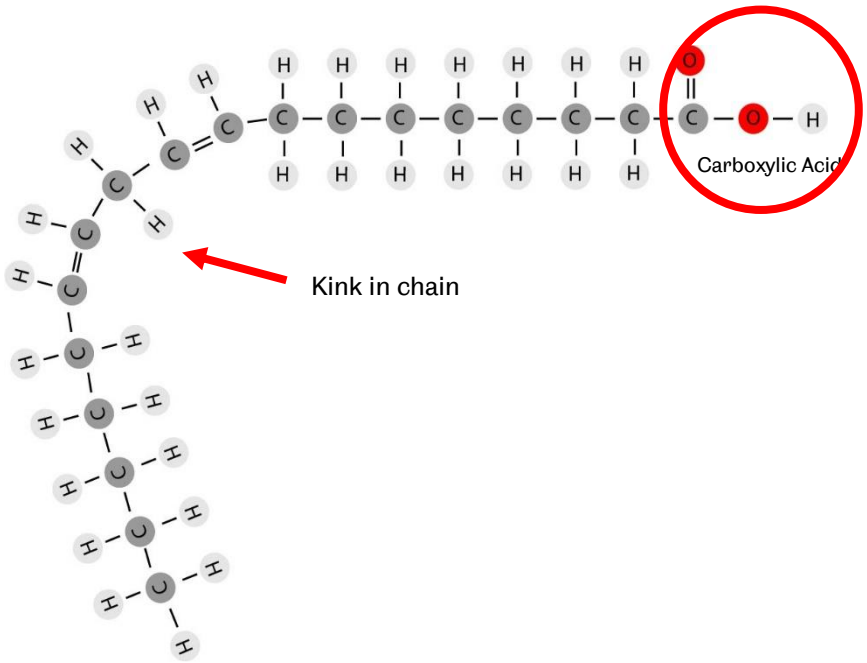

Figure 7-7, Linoleic acid, the Main Constituent of Soybean Oil

7.3.1.3 Palm Kernel Oil

Palm kernel oil originates from the kernel of the fruit of an oil palm. Palm kernel oil differs in composition and properties to palm oil, which is derived from the mesocarp (middle part) of the fruit (211). Palm oil is one of the most produced vegetable oils, with the largest production in Malaysia. It is solid at room temperature, as can be seen in Figure 7-8, which is the oil's main negative performance point. Palm kernel oil (PO) has high levels of alpha tocotrienols, a naturally occurring antioxidant; these are forty to sixty times more potent than tocopherols found in other vegetable oils. PO is the only natural source of tocotrienols (212). This should mean that the oil has superior oxidative performance compared with other vegetable oils. This is also discussed in Section 3.1.

PO has a slightly lower molecular weight than SO, at 846 $kgkmol^{-1}$ (213). PO is predominantly made up of saturated fatty acids, with 89.3g/100g. Mono and poly-unsaturated fatty acids make up 4.1 and 0.6 g/100g respectively. Lauric acid (C12:0) makes up 40.8% of PO, shown in Figure 7-9, while palmitic, stearic and myristic acid make up 12.4, 20.2 and 15.4% (Full composition given in Section 9.4.1). The viscosity of PO is 6.6cSt at 100̊C, with a VI of 250, as shown in Section 7.3.1.5.

A review of the literature, as discussed in Section 6.1, has shown that PO has good wear and friction properties in comparison to other vegetable oils, although results do appear inconsistent. Typical applications for palm kernel oil include soap and beauty products.

Figure 7-8, An Example of the Typical Appearance of Palm Kernel Oil

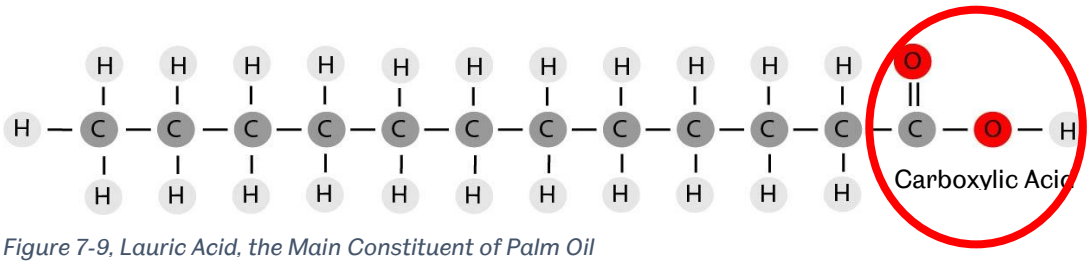

Figure 7-9, Lauric Acid, the Main Constituent of Palm Oil

7.3.1.4 Mineral Base Oil

Shell HVI 60 is a high viscosity index paraffinic group one base stock group, commonly used for automotive formulations. Group 1 base stocks have less than 90% saturates, more than 0.3% sulphur and a viscosity index of between 80 and 120 (34). The typical appearance of this oil is shown in Figure 7-10. This paraffinic base stock is commonly used because it is chemically and thermally stable, as discussed in Section 3.1. This oil was selected as it is a typical lubricant base stock, with no additives, which means it can be used as an effective comparator for assessing the performance of the bio-lubricant base stock candidates that also have no additives. The viscosity of MO is 64.4cSt at 100̊C, with a VI of 120, as shown in Section 7.3.1.5.

Figure 7-10, An Example of the Typical Appearance of the Mineral Base Oil used

7.3.1.5 Viscosity Results

The viscosity of the base stocks used for tests was measured using a Brookfield DV1 digital spindle viscometer, as described in Section 7.4.3. MO, PO and JO have very similar viscosity profiles, as seen in Figure 7-11 whereas SO has a higher viscosity than the other oils tested. Vegetable oils are often reported to have a high viscosity index (VI), and this is apparent from Figure 7-12. SO and JO have a VI of around 220, while PO's is 250. MO is considerably lower, with a VI of 120. A high VI is desirable as this indicates less viscosity change with temperature, meaning the oil has the potential to be an effective lubricant at a wider range of temperatures.

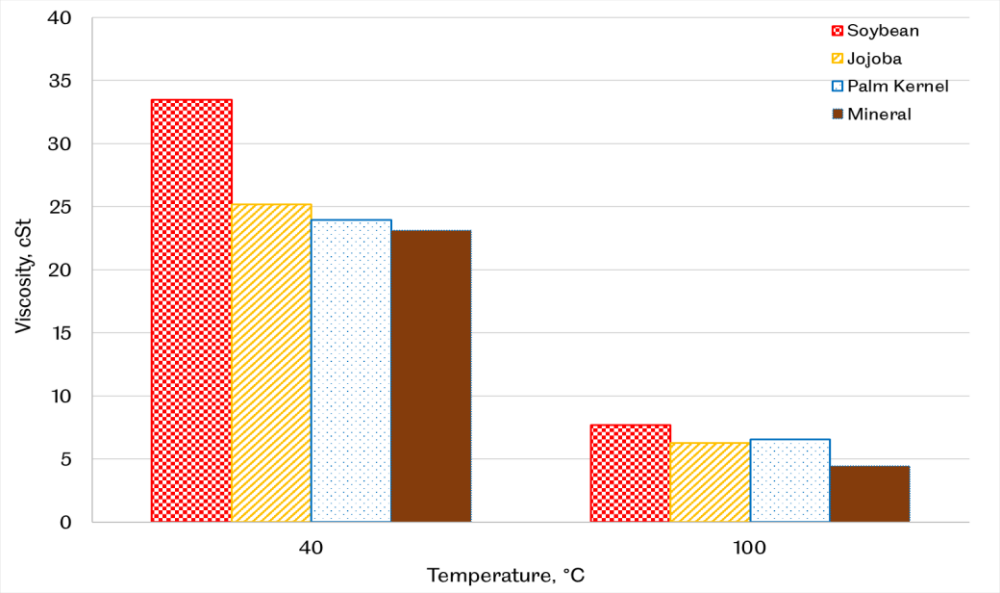

Figure 7-11, Averaged Viscosity Readings

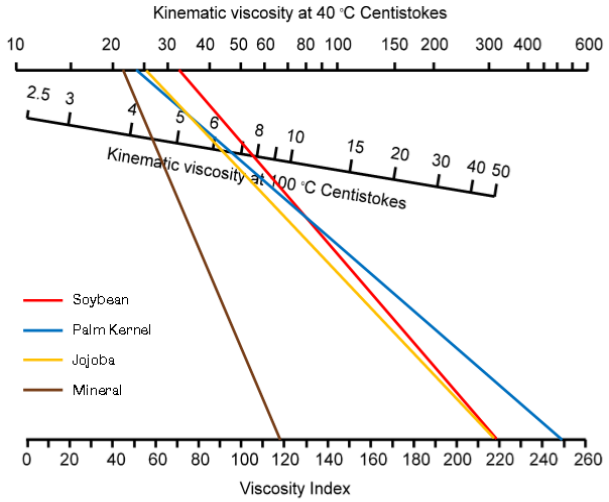

Figure 7-12, Viscosity Index of the Oils Tested

7.3.2 *Materials for Plint TE77 Reciprocating Wear Tester*

The materials used for the Plint TE77 reciprocating wear tester are detailed in this section. The steel balls described in Section 7.3.2.1 were used for all tests. Two groups of flat specimens were used, cast iron specimens for blend tests and multi-layer surface treatment specimens for tests to assess the interaction of coatings with bio-lubricants.

7.3.2.1 Steel Ball Counter Surface

Chrome steel balls were used as the counterface for all reciprocating wear tests. The chrome steel balls had a material designation equivalent to AISI 52100. The standard size 6 mm diameter ball for the Plint TE77 was used, it was not felt altering this would be of significance to the results. The balls were selected to be very hard and smooth

to ensure no significant wear would occur during wear tests. The specification states the surface roughness (R_a) was 0.038 µm and average hardness 800 Hv.

7.3.2.2 Cast Iron Specimens for Reciprocating Wear Tests

Cast iron specimens were used for learning experiments, as shown in Figure 7-13, were made with EN GJL 250 cast iron. The surface roughness (R_a) was 1µm and average hardness 200 Hv. A typical sample with a typical wear scar is shown in Figure 7-13.

Cast iron was selected as it is a common engineering material, particularly in the automotive industry. The use of cast iron has reduced as the use of aluminium alloys has increased, due to its low density and good thermal conductivity, and the ability to reduce the engine block weight by between 40-55% in comparison to a cast iron block (81). In smaller engines, cast iron is still the favoured material as it demonstrated better thermal conductivity, which is more important for efficient engine operation than weight saving. Cast iron inserts are often used in areas where aluminium cannot offer acceptable wear protection, such as in the main bearings and to combat any thermal expansion issues that could arise with the use of aluminium. Cylinder liners are often also made of cast iron.

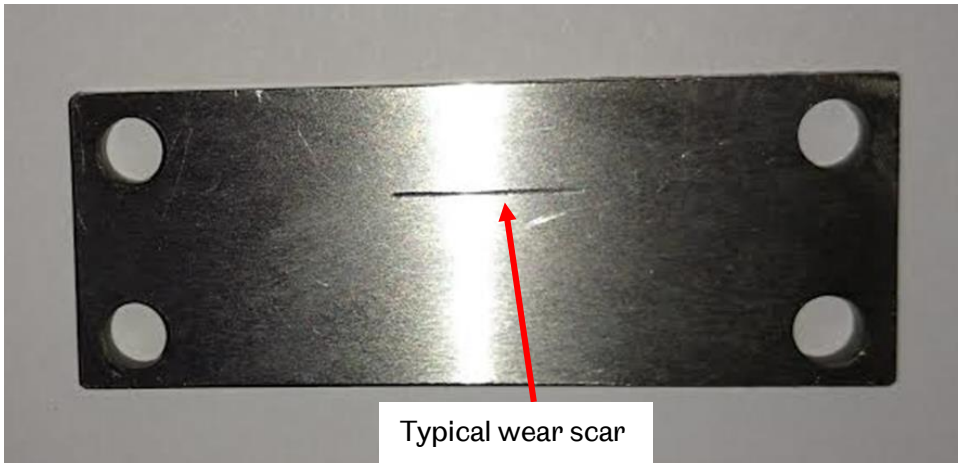

Figure 7-13, Typical Specimen for Wear Tests

7.3.2.3 Multi-Layer Surface Treatment Specimens

Wear tests with multi-layer surface treatments were carried out in conjunction with academic partners[1] who selected and supplied the specimens. All surface treatments were applied by external partners, mentioned individually in Sections 7.3.2.4 and 7.3.2.6. Surface treatments were selected for their relevance to internal combustion engines. Details of the surface treatments, and the combinations of surface treatments, are provided in the following sections. Varying combinations of these surface treatments were tested to explore the possibility of reducing wear and

[1]Expert in automotive coating technology and member of academic staff at South West College, N. Ireland

friction, Table 7-5 in Section 7.3.3 gives details of the order of the surface treatments. The substrate material for all coated samples was EN9 medium carbon steel.

7.3.2.4 Diamond-like-Carbon

The diamond-like-carbon specimens (DLC) were from the Teer Coatings Dymon-iC™ range. The exact construction of this coating is proprietary and commercially secret, but it is made of a chromium carbon build layer that can be up to 3 µm thick and a tetrahedral amorphous carbon of up to 1 µm on top. Teer Coatings state that their Dymon- iC™ coatings have high adhesion to substrates, low friction and high wear resistance. The deposition temperature is stated to be 250˚C (likely to be PVD application) and the maximum working temperature of the coating 350˚C (214). The surface roughness and hardness are dependent on the layering of surface treatments and are reported in Section 9.2.3 and 9.2.4. Teer Coatings report the hardness of this coating to be 1600 Hv (0.05).

7.3.2.5 Ultra-Fine Shot Blasting

The ultra-fine shot blasting was carried out with a molybdenum disulphide media, which acts as a solid lubricant. Shot blasting is carried out to increase the hardness and improve fatigue properties, as discussed in Section 6.3 and 5.2.2. The surface finish of specimens varies dependent on the combination of treatments and is reported in Section 9.2.3. This treatment has been used in the automotive industry, originating in Japan with Honda developing it for use in production engines (215).

This surface treatment is referred to as ‘SB’ in subsequent chapters.

7.3.2.6 Calcium Based Chemical Dip

These specimens were treated with a calcium sulphate (discussed in Sections 6.5 and 5.2.3) based chemical dip process, carried out by a company called TribUR, which is a novel surface treatment used in the motorsport industry. The exact composition of this proprietary treatment is not known, as it is commercially secret. Some elemental analysis reveals aluminum oxide particles contained in specimens with this treatment, as detailed in Section 9.2.5. This surface treatment is of interest as it does not change the dimensions of the piece. There is no published data available on this specific treatment. The coating layer was analysed using a low power SEM, as shown in Figure 7-14a, the chemical dip layer could not be seen. Using a higher power SEM, as seen in Figure 7-14b, a thin layer at the surface of the coating experienced charging; it is likely that this is the chemical dip layer. The layer appears to be less than 0.1 µm. Further images were not taken due to the charging issue.

This surface treatment is referred to as ‘CD’ in subsequent chapters.

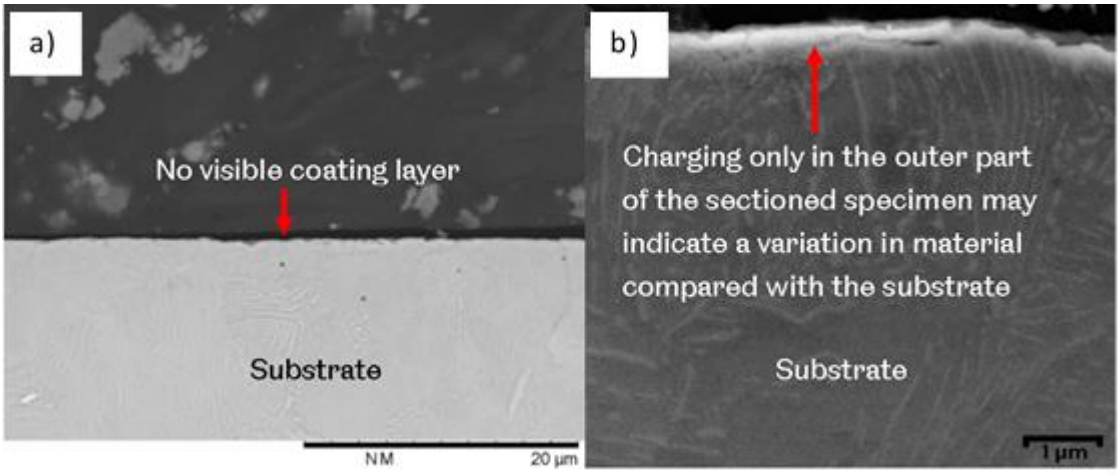

Figure 7-14 a), Cross Section SEM Image Of Specimen 6 Using A Low Power SEM, Highlighting No Visible Coating Layer, b) Using A High Power SEM, Showing The Possibility Of A Thin Coating Layer

7.3.2.7 Nano Fullerene

Nano fullerene is a carbon base coating consisting of spherical arrangements of carbon atoms, shown in Figure 7-15a. This coating was applied by academic partners by painting onto the substrate. The coating did not adhere to the substrate well; the resulting finish was flaky and did not cover the substrate evenly, as can be seen in Figure 7-15b.

This surface treatment is abbreviated to as 'NF'.

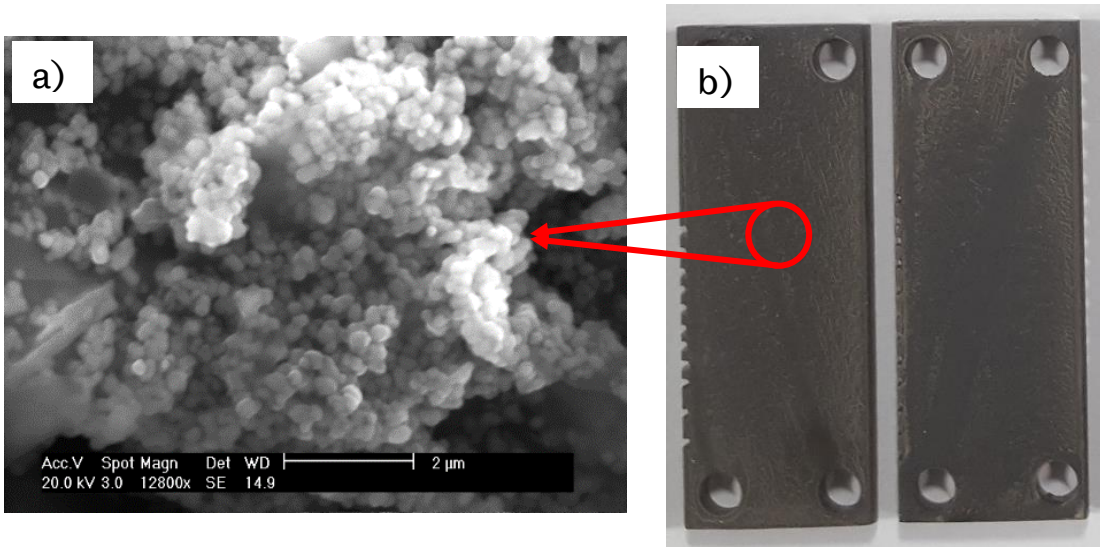

Figure 7-15 a) An Example of the Microstructure of the Nano Fullerene Coating and b) The Coated Specimen, Showing a Poor Surface Finish

7.3.3 *Combinations of Surface Treatments*

Table 7-1 shows the combinations of surface treatments that formed the multi-layers on test specimens. These surface treatments were applied over each other as distinct layers. The layers of treatment were applied in the alphabetical order stated in Table 7-1. As an example, for specimen 13 the first surface treatment was to give the substrate a superfinish, this was followed by the chemical dip process and to finish the specimen a layer of DLC was applied on top of the chemical dip layer. Super finished samples had a surface finish of 0.01 µm R_a. Surface ground samples had an average surface roughness of 0.4 µm (R_a).

Specimen Number	**Superfinished**	**DLC**	**Impact Technique**	**Chemical dip**	**Fullerene**	**Number of samples available**
0	Surface ground only					2
1		A				3
2	A	B				3
3			A			3
4	A		B			3
5	A	B		C		3
6	A			B		3
7		A		B		3
8	A		B	C		3
9				A		3
10			A	B		3
11			A		B	3
12					A	3
13	A	C		B		3
14		B		A		3
15		C	A	B		3
16		B	A			3
17	A	C	B			3
18	A					2

Table 7-1, Combinations of Surface Treatments and Layer Order in alphabetical order

7.3.4 *Elastocon Relaxation Test Materials*

Three elastomer materials were selected to be tested for compatibility with bio-lubricants. The elastomers were selected as they are commonly used in the automotive industry. All the elastomers selected conform to ASTM D2000, '*Standard Classification System for Rubber Products in Automotive Applications*' (216). This standard classifies elastomers based on their resistance to heat, aging and swell, as well as mechanical properties such as hardness, tensile strength and compression set. The seals were supplied by EDCO Seals. All seals tested were O-rings with an inner diameter of 15mm and 2mm thickness to ensure geometric and dimensional compatibility with the Elastocon Relaxation Tester EB 02 (Section 7.2.2). Typical examples of an untested sample, a sample that has suffered shrinkage and a sample that has suffered swelling during testing are shown in Figure 7-16.

Figure 7-16, An Example of an Untested Elastomer, One that has Suffered Shrinkage and One that has Suffered Swelling

7.3.4.1 Ethylene Propylene Diene Monomer

Ethylene Propylene Diene Monomer (EPDM) is a common automotive elastomer material for components such as hoses and weather seals. It is a saturated terpolymer of ethylene and propylene monomers with diene monomers used to saturate any unsaturated bonds after ethylene and propylene bonding (217). EPDM 70 was selected for testing; it is stable over a temperature range of -57 ˚C – 149 ˚C. Typical hardness quoted by the manufacturer is 70 Shore A and a tensile strength of 10 MPa.

7.3.4.2 Nitride Rubber

Nitride rubber (NBR) is one of the elastomer materials that must be used in GF-6 compatibility tests as discussed in Section 2.3. Nitrile 70 was used for testing. It is stable over a temperature range of -34 ˚C – 121 ˚C. Manufacturer stated hardness and tensile strength are 70 Shore A and 10 MPa respectively. NBR is an unsaturated copolymer of acrylonitrile and butadiene. It is one of the most commonly used elastomer materials in the automotive industry due to being relatively inexpensive with favourable material properties. It can be found in automotive fuel and lubricant hoses and seals (218).

7.3.4.3 Fluorocarbon Elastomer

Fluorocarbon (FKM) elastomers are polymers of fully saturated carbon and fluorine chains, with some hydrogen too. FKM is known for its excellent resistance to degradation and is therefore a common sealing material in automotive cooling, fuel

and lubricant systems. The higher the fluorine content the better its resistance to degradation by fluids (fluorine content unknown for these samples) (219). It remains elastic over a wide temperature range of between -26 - 205˚C. FKM 75 was selected for testing, the typical hardness and tensile strength quoted by the manufacturer are 75 Shore A and 10 MPa respectively. FKM is also an elastomeric material that must be used in GF-6 compatibility tests.

7.4 Test Methods

7.4.1 *Analysis Equipment*

The wear scars produced from tests carried out in the TE77 reciprocating wear tester were analysed using a scanning electron microscope to assess types of wear and any significant surface features. A 3D non-contact profilometer was used to measure the volume of material removed from wear tests, as well as to measure the surface roughness of the samples before testing. Hardness tests were also performed.

7.4.1.1 Scanning Electron Microscope

A Hitachi TM3030 Plus scanning electron microscope (SEM) was used to analyse wear test specimens and wear scar to identify wear mechanisms. Before specimens were placed in the SEM, they were cleaned with acetone and cotton wool to remove any base stock and loose wear debris. This was followed by a propanol rinse to remove any carbon residues from acetone.

7.4.1.2 3D Non-Contact Profilometer

An Alicona Infinite Focus SL was used to measure volume of material removed and surface roughness. This method was used for its ease of volume measurements, the results of which are discussed in more detail in Section 9.2. Surface roughness measurements were taken in the direction of the wear scar, measuring over a 5 mm length, to obtain average surface roughness values (R_a). Surface roughness values were also taken in the perpendicular to the wear scar direction, measuring over a 2 mm length. Results are reported in Section 9.2.

Profile measurements of the wear scars were also taken, as shown in Figure 7-17, a ‘Z’ is drawn over the wear scar; only the two lines that go perpendicular to the wear scar can give accurate width measurements. Figure 7-17 also shows two typical results from scanning wear scars. The coloured counter plot allows for ease of identification of ploughed ridges and variations in the depth the of wear scar.

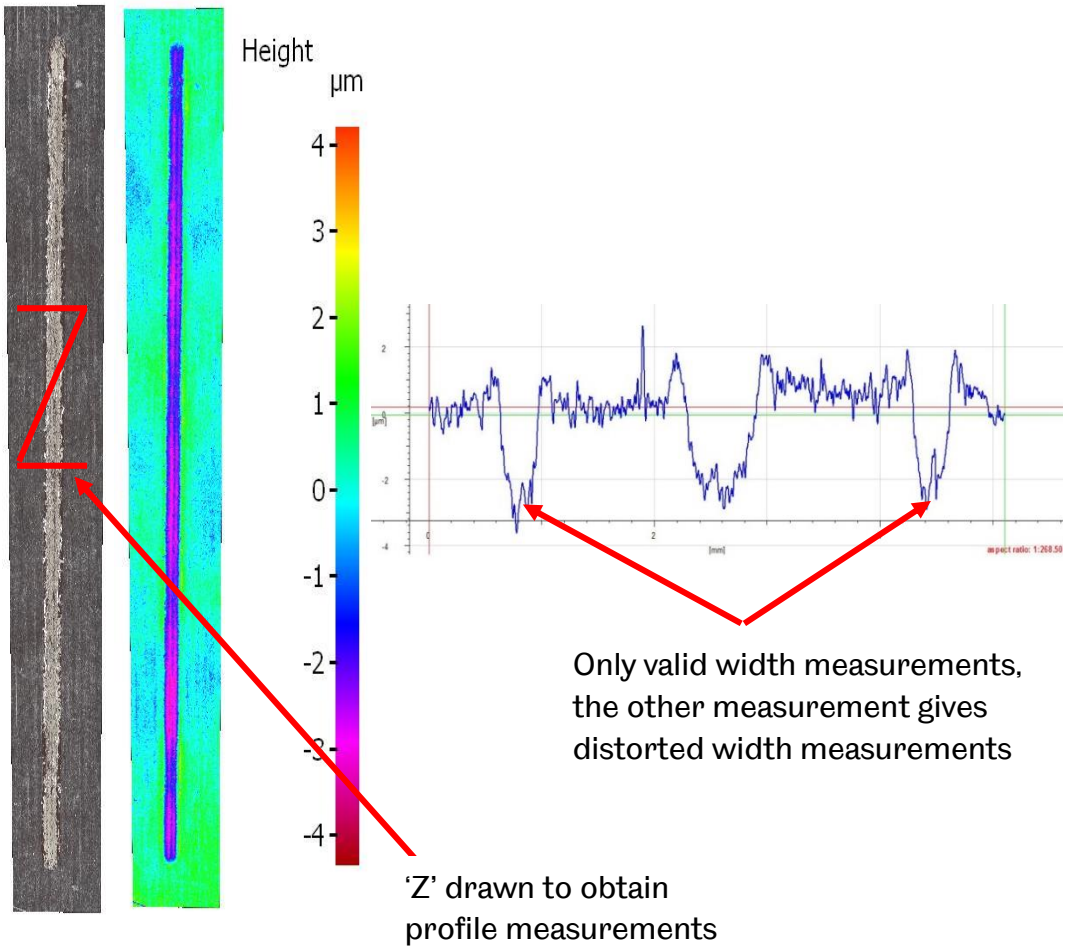

Figure 7-17, An Example of the Image Produced Using 3D Non-contact Profilometer and Method for Profile Measurements

7.4.1.3 Hardness Tests

Hardness tests were performed using a Vickers hardness tester for cast iron specimens using a load of 20 kg. Three measurements were taken at different locations on the specimens, averaged results are given in Section 9.2.4.

The hardness of specimens with the multi-layer surface treatments was analysed using a HM-122 Mitutoyo micro hardness tester (Hv 0.1). A minimum of five repeated measurements were taken at different locations on the specimen.

7.4.2 *Analysis of Coating Performance*

This section details how the coatings were analysed, in terms of the coating layers and the coating adhesion.

7.4.2.1 Analysis of Coating Layers

After the first round of wear scars were analysed, as detailed in Section 7.4.1.1, the samples were sectioned using a wire electrical discharge machining process to preserve the integrity of the coating so that an evaluation of the coating in the wear scar region could be made. Specimens were then prepared for SEM analysis. The locations of the wear scars were measured and recorded so that they could be identified once samples were mounted. Specimens were then mounted in a

Bakelite™ mounting material. Struers Metalog Method C was used to set parameters for grinding and polishing. This was carried out to remove any damage from machining and the oxide layer that had formed.

7.4.2.2 Coating Adhesion Assessment

An in house University of Sheffield scratch testing machine was used to assess the adhesion of the coatings. A diamond stylus is moved across the surface with an increasing load applied at a rate of 4.5 N mm^{-1}. The adhesion strength is calculated from the lowest load at which the coating fails. Cohesive failure, L_{C1}, begins with the coating cracking and chipping within the coating. As the stylus progresses, if the load is high enough, adhesive failure, L_{C2}, causes delamination of the coating from the substrate. During the test, the tangential load is recorded and any change in friction force is an indication of coating failure. Results are reported in Section 9.1.

Normal and tangential force readings were recorded, an example of the data is shown in Figure 7-19. A change in the tangential force corresponds to the adhesive failure of the coating; Figure 7-19 shows a small increase in the tangential force at around 5-6 mm. The scratches were analysed using the optical scanner and the distance from the start of scratch to the start of adhesive failure measured. Adhesive failure between the coating and substrate is characterised by arc tensile cracks and chipping failure, as defined by ASTM C1624-05 (220). Figure 7-18 is a schematic from ASTM C1624-05; this was used as a guide for identifying the start of adhesive failure. L_{C2} is the start of adhesive failure and L_{C1} is the start of cohesive failure. Cohesive failure of a coating means there is damage to the coating, with cracks forming, but no debonding of the coating from the substrate. Adhesive failure means there is debonding of the coating from the substrate. Figure 7-20 shows an example of a typical scratch (specimen 5, SF, DLC, CD), indicating the start of cohesive and adhesive failure.

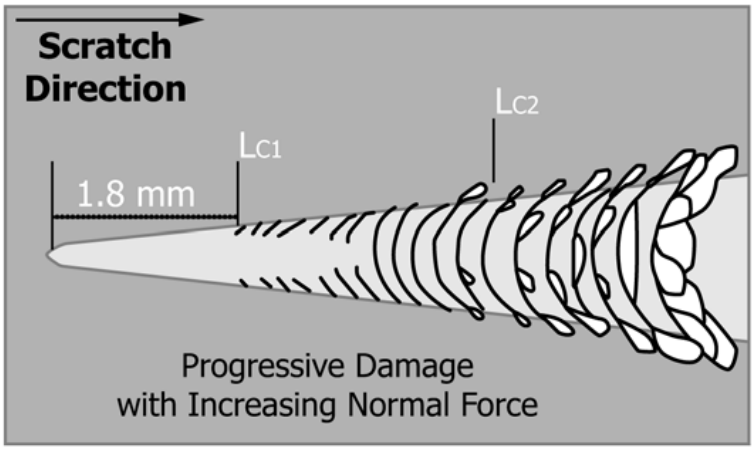

Figure 7-18, Schematic Example of Damage to Coating from Progressive Load Scratch Tests (220)

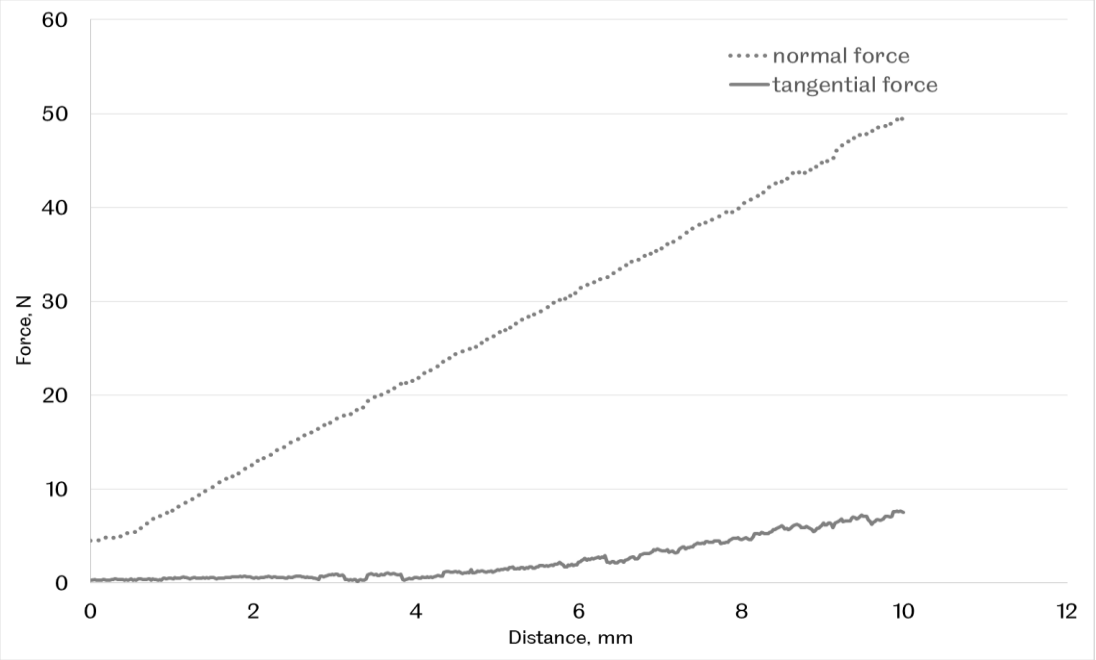

Figure 7-19, Force Data from a Scratch Test with Specimen 5 (SF, DLC, CD)

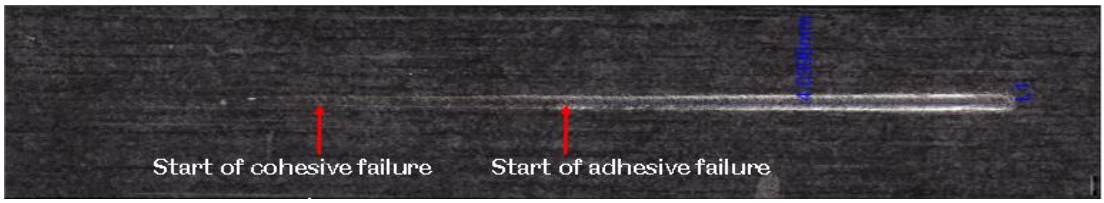

Figure 7-20, An Example of a Scratch from Specimen 5, Indicating the Point of Cohesive and Adhesive Failure

7.4.2.3 Test Procedure for Scratch Testing

The diamond stylus tip and specimen were thoroughly cleaned before testing. The specimen was placed in the specimen mount, as shown in Figure 7-21, and secured with location screws. The stylus was placed in the desired start position and lowered to 2 mm above the surface. The parameters were then set on software, a scratch distance of 10 mm was used with three scratches performed at 3 mm intervals. A pre-load of 5 N was used, with a final load up to 50 N. The adhesive critical scratch load was then calculated as per ASTM C1624-05 and described in Section 9.1.

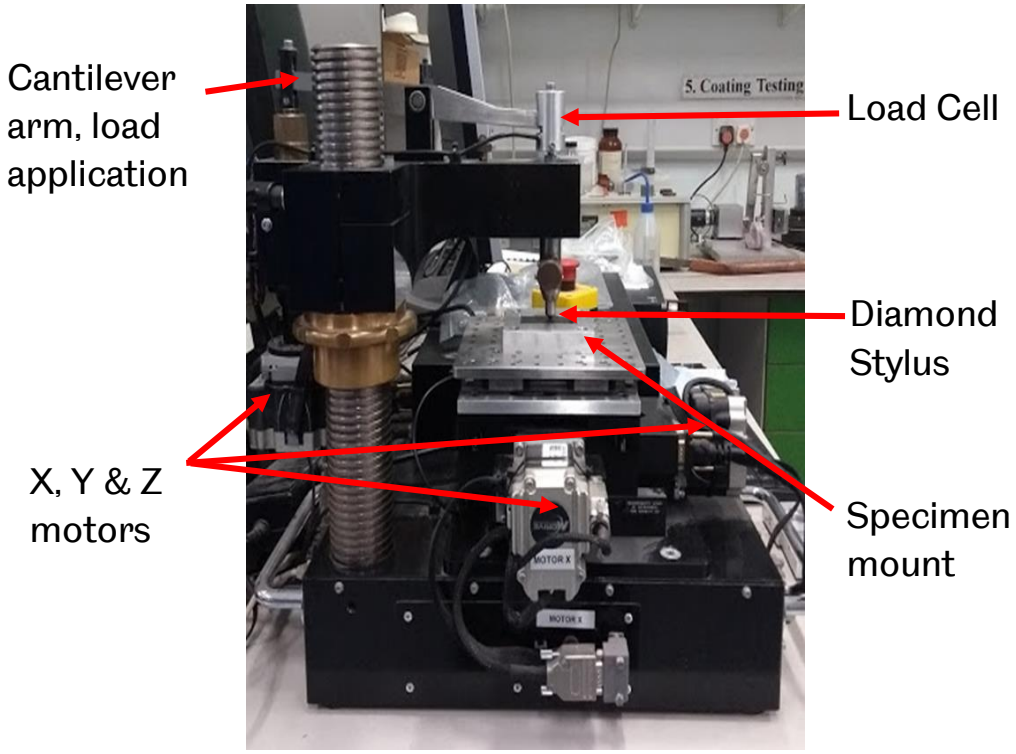

Figure 7-21, In House University of Sheffield Stylus Scratch Test Machine

7.4.3 *Viscosity Measurements*

Viscosity measurements were performed using a Brookfield DV1 digital spindle viscometer with a small sample adaptor. The small sample adaptor and spindle were cleaned with acetone before and after use. 7 ml of oil was placed in the sample adaptor and heated to 40˚C and 100˚C using a circulating silicone fluid based heater. Once samples reached the desired temperature required for each part of the analysis, they were held at that temperature for 5 minutes to ensure the samples were thermally stable. The spindle was turned on and speed selected based on manufacturer recommendations. Viscosity data was monitored to ensure a constant viscosity (no shear thinning or thickening) and taken after 2 minutes. This procedure was repeated three times for each oil and the results are given in Section 7.3.1.5.

7.4.4 *Fatty Acid Composition Measurements*

The fatty acid composition measurements of the vegetable oils tested were performed by an external laboratory[2] using a gas chromatography method. Unused and samples used in wear tests were sent for analysis and full results are reported in Section 9.4.1.

7.4.5 *Hanson Solubility Parameter Software*

The Hanson Solubility Parameters in Practice (HSPiP) software is a tool that allows interaction parameters to be visualised and solubility parameters to be calculated. Spheres of interaction are produced based on HSP data inputted, as discussed in Section 5.3.5. An example of a sphere of interaction generated by HSPiP is shown in

[2] Reading Scientific Services Ltd

Figure 7-22, for JO and EPDM. As the blue dot is inside the green sphere, it means that the elastomer and oil will interact, swell or shrink. Figure 7-22 outlines where the base stock HSP data is inputted and where the elastomer HSP data is shown.

HSP values were derived through volume additive rules using HSP values for the fatty acids that make up each bio-base stock, rather than experimentally determining them. This has shown to be a valid method for determining values (221). Graham et. al. (194) and Nielson et. al. (201) both hypothesised that this may underestimate the polar element of HSP.

HSP values for all fatty acids apart from stearic acid were available in the database. The HSP values for stearic acid were obtained using the DIY HSP function in the Y-MB solver. The Y-MB solver uses a combination of a Neural Network method and an automatic molecule breaking programme to fit data entered by the user to know data on HSP. The international chemical identifier for stearic acid was obtained via the Royal Society of Chemistry's chemical database (222). The values obtained from this method should be used with caution, on the advice of the software developers, who state an understanding of approximately what the HSP values are is important (221). The values obtained for stearic acid were in line with those for other fatty acids, therefore it was felt to be a fair approximation.

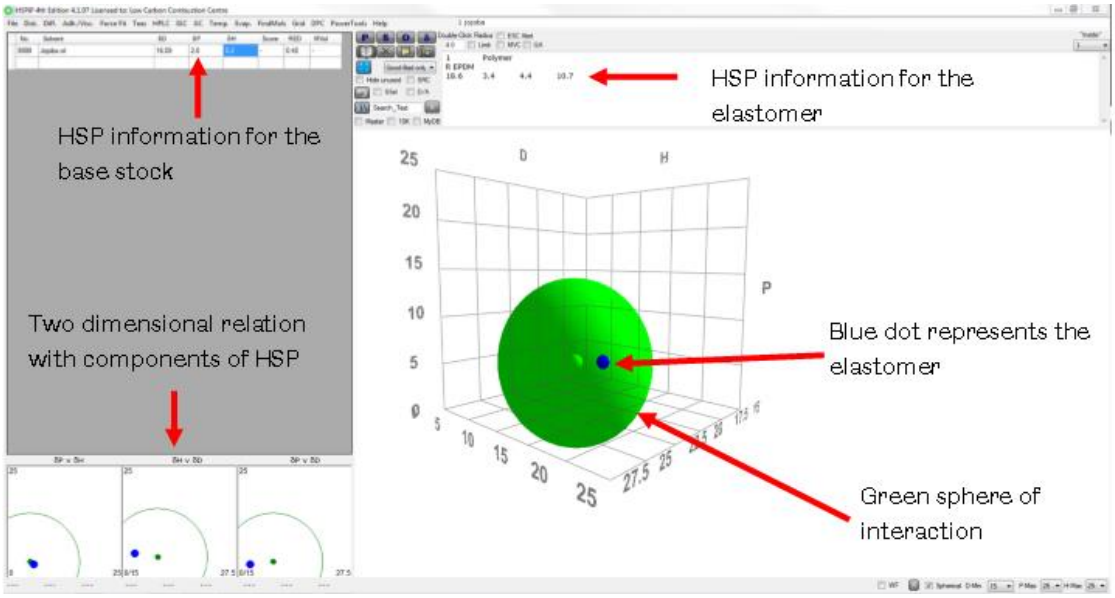

Figure 7-22, An Example of the HSPiP User Interface, Showing the Sphere of Interaction for JO and EPDM

7.4.6 *Plint TE77 Test Methods*

Wear and friction tests using the Plint TE77 reciprocating wear tester were performed, as described in Section 7.2.1. The methods used with this equipment are described in Section 7.4.7, variations from this method are described in Sections 7.4.7.2 and 7.4.7.4

7.4.7 *Test procedure for the Plint TE 77 Reciprocating Wear Tester*

All machine components were thoroughly cleaned using acetone before each test. For each test, a specimen was secured in the oil bath and 30 ml of base stock added (see Section 7.3.1 for details), ensuring the specimen was fully immersed. The oil bath was then heated to 100 °C; once this temperature was reached and the temperature was stable for 5 minutes, calibration could be performed. Calibration was performed to ensure the load cell gave accurate tangential force readings, which were used to calculate coefficient of friction. Using the Labview software, data acquisition was turned on, if the force reading was not zero, the calibration value was altered until a zero value was obtained. A known weight, (700 grams, equivalent to 6.86 N) was then applied to the load cell. The data acquisition software was then checked to ensure the force reading corresponded. If the values did not match, the calibration value was altered again. The weight was removed and the data acquisition software checked to ensure the value returned to zero. This method of calibration has its limitations, as only one known weight was used an assumption was made that the load cell gives a linear response when loaded. While this should be true, it cannot be said with certainty unless further weights were used.

Once calibration was performed, the ball was placed in the holder on the reciprocating arm. This was then placed in the oil bath and a normal load of 40 N applied. The speed was set to 260 rpm and the motor turned on for the 60 minute test duration. The tests were performed in boundary lubrication, which is apparent from the high maximum contact pressure of 1.08 GPa and the resulting wear on specimens. Film thickness measurements could not reliability be performed.

On completion of the test, the heaters were turned off and the system cooled down before specimens could be removed and a new test procedure started. The force data was collected so that coefficient of friction results could be analysed. The test specimen was thoroughly clean in preparation for analysis. The wear resulting from the main set of wear and friction experiments was measured using the 3D non-contact profilometer described in Section 7.4.1.2, which calculates the volume of material removed in the wear scar region. The wear volume calculation used for learning experiments were for a '*ball-on-flat surface linearly reciprocating sliding wear*' as described by Sharma et. al. (223), and is detailed fully in 0. The inaccuracy in using this method is also discussed in 0. Learning experiments were conducted prior to the 3D non-contact profilometer (described in Section 7.4.7.2) being available.

7.4.7.1 Test Parameters

As mentioned in Section 7.1, the test parameters, while not aiming to replicate exact engine conditions, are representative of some of the harsher environments an automotive lubricant may experience The experimental parameters were set after performing a set of learning experiments to assess the load and temperatures. These learning experiments were also used to test whether blending bio-lubricants with mineral oil would be beneficial (further details given in Section 8). The resulting

experimental parameters are shown in Table 7-2, they also align with wider work in the literature (137) (224). For both groups of wear tests the experimental parameters listed in were the same.

Experimental Parameters	
Speed, rpm/Hz	260/4.3
Sampling Frequency, Hz	10
Temperature, ˚C	100
Stroke, mm	15
Normal load, N	40
Chrome steel ball bearing, Surface roughness, µm	0.038
Ball Hardness, Hv	800
Volume of oil used, ml	30
Test duration, min	60

Table 7-2, Experimental Parameters for Reciprocating Wear Tests

7.4.7.2 Coefficient of Friction Data Acquisition

Coefficient of friction (CoF) values were obtained through tangential force readings, during wear tests on multi-layer surface treatments, carried out on the Plint TE77 reciprocating wear tester. The tangential force readings were divided by the normal force (40 N) to obtain CoF values. As the tests were reciprocating, the speed in the contact varied and was zero at the end of each stroke, as the direction of motion changed.

The sampling rate was set to 10 Hz and the reciprocating arm travelled at 4.3 Hertz. The sampling frequency was limited by the data acquisition capability of the computer recording data. The reciprocating arm moved 4.3 times while 10 data points were collected. This means that the full range of values (i.e. the minimum and maximum values) may not have been collected for each stroke. It is however thought that over the duration of the test a fair representation of the full range of values was obtained as 2-3 data points were still collected during 1 stroke of the TE77. Ideally the sampling frequency should have been increased by an order of magnitude above the frequency of the test.

The load cell suffered drift if the temperature in the oil bath changed by more than 2°C. When tests were started, the temperature dropped by up to 5°C before stabilising again. The force readings taken in the first 10 minutes for the test may not be a true representation of the tangential force, but may be due to drift in the load cell.

An example of the raw data obtained from wear and friction tests is shown in Figure 7-23. It was expected that the peak force readings at either end of the stroke would also be similar values. As shows, this was not always the case. There was significant variation in the distribution of results about zero, which also represents the middle of the stroke. The amplitude of the force readings should be correct as the response of the load cell to calibration was accurate.

The data was analysed by taking the absolute values of tangential force readings and dividing by the normal load to obtain CoF results for every data point. A moving average was then taken to get a trend in CoF values. An interval of 600 data points was

used; this represented one minute's worth of data. The final average CoF values were reported.

The moving average method for analysing CoF was not found in literature, it is however a known way to represent trends in data. ASTM G115-10 (2013), '*Standard Guide for Measuring and Reporting Coefficient of Friction Data*' (225), recommends that for reciprocating tests, the average, minimum and maximum CoF values should be reported. The standard also states it is common to calculate CoF values from average force data. Other methods for analysing CoF considered as guidance were those reported by Morina et al. (226) and Fam et al. (227), who averaged values based on the number of values in a cycle. Fam et al. also took average values every 200 and 400 data points to assess periodic CoF behaviour. An example of the data obtained through the moving average method is shown in Figure 7-24.

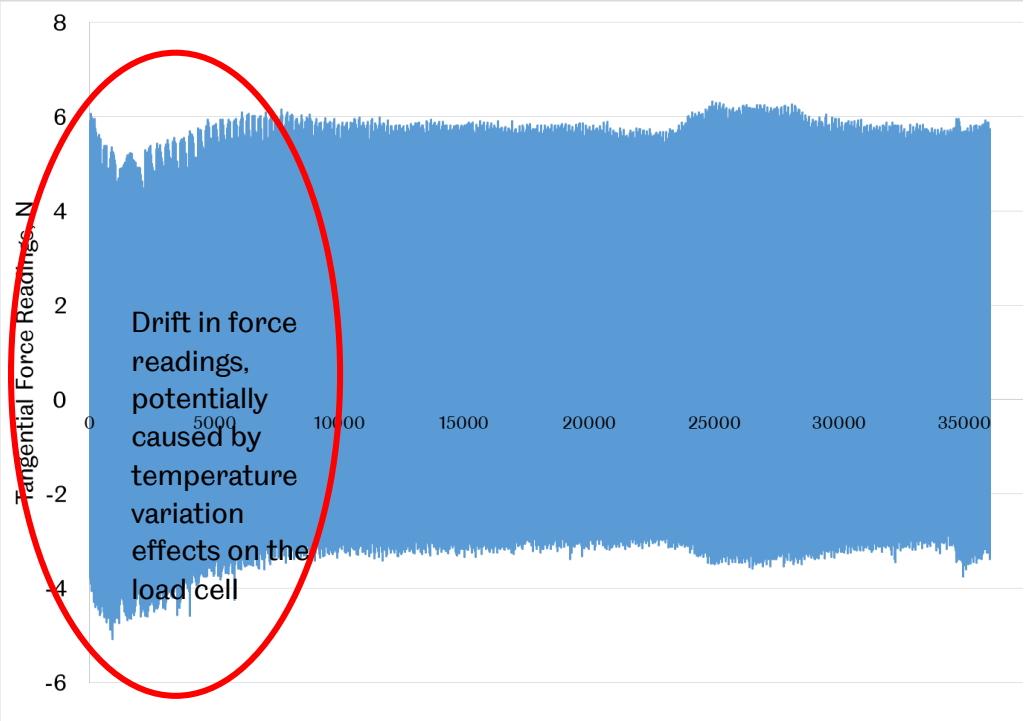

Figure 7-23, An Example of the Raw Data Obtained from Wear and Friction Tests

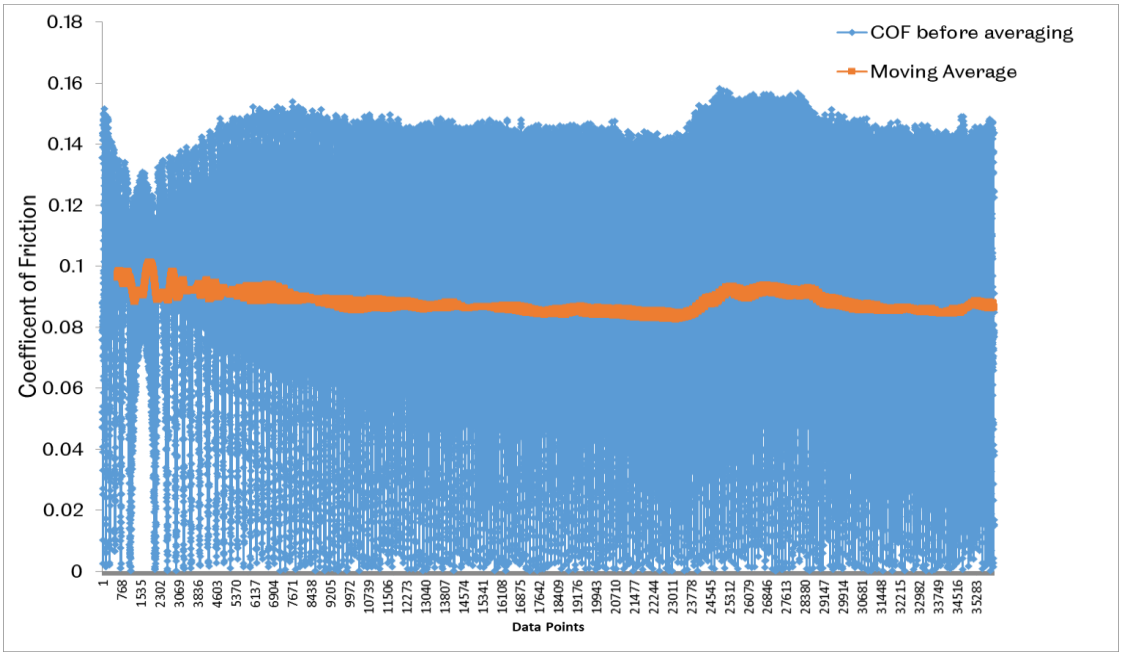

Figure 7-24, An Example of the Coefficient of Friction Data and Resulting Moving Average

7.4.7.3 Learning Experiments and Blending Oils

In order to set the test parameters for the tests detailed in 7.4.7.4 a set of learning experiments were performed. This involved setting the load, speed and temperature parameters (as listed in Table 7-2), as well as assessing the repeatability of wear tests. The value for load was used to a high contact pressure to ensure tests operated in boundary lubrication, loads and speeds used in similar work were also considered and informed the final values (137). The temperatures were selected to represent ambient oil operating conditions in an internal combustion engine. Additionally to setting the test parameters an assessment of whether blends of bio-lubricants with mineral oil should be used.

Learning experiments were conducted to compare results of wear tests with different loads and temperatures. The details of experimental parameters trailed in learning experiments are given in Table 7-3. All other parameters were as detailed in Table 7-2. Results are detailed in Section 8.

Experimental Parameters	**1**	**2**	**3**	**4**
Temperature, °C	80	80	80	100
Load, N	50	50	40	40
Duration, minutes	30	30	30	60
Lubricant	Jojoba Oil			

Table 7-3, Experimental Parameters for Learning Experiments

Previous work (57) indicated that blending bio-lubricants at a 50:50 blend ratio with jojoba or mineral base stock offered better wear protection compared with wear tests with single oils. Therefore a test programme was proposed to assess the optimal blend ratio for wear protection of jojoba with mineral base stock. Literature, as

discussed in Section 6.1, demonstrated a lack of consistent information on the ability of jojoba oil to reduce wear, particularly without additives. This test programme furthered understanding in this area.

Blends of between 0-50% mineral base stock and jojoba oil were tested, as shown in Table 7-4, Blend Ratios for Blend Tests to establish whether larger amounts of jojoba could be used without affecting wear results. The specimens used are detailed in Section 7.3.2 and oils used in Section 7.3.1. Single oil tests were carried out for comparison. Blends were created by stirring the samples using an agitator for 5 minutes to ensure uniform mixing. The blend was then placed straight into the Plint TE77 for testing. Tests were repeated a minimum of three times, more repeats were carried out if test results produced significant (greater than 30%) differences in wear scar measurements. The method for analysing wear scars is detailed in Section 7.4.1. The results from tests with blended oils are presented in Section 8.

Blend Number	Mineral base oil %	Jojoba oil %
1	100	0
2	0	100
3	50	50
4	10	90
5	20	80
6	30	70
7	40	60

Table 7-4, Blend Ratios for Blend Tests

7.4.7.4 Wear and Friction Tests with Multi-Layer Coatings

The specimens used are detailed in Section 7.3.2.3. Three repeats for each sample and each oil were performed on specimens 1 to 17, as detailed in Table 7-5. Two repeats were carried out with the surface ground reference specimens 0 and 18 as only two samples were available for testing.

Due to the poor adhesion properties of the nano fullerene coating (detailed in Section 7.3.2.7) and poor wear resistance in the first round of testing, specimens coated with this surface treatment were not taken forward for further assessment.

In the first round of testing, all specimens were tested with PO, SO, JO and MO base stocks, details of which can be found in Section 7.3.1. From initial data analysis it was clear that palm oil performed least well and therefore was discounted to reduce the complexity of analysing data (see Section 9.2.1.3 further details). Therefore round two and three were only carried out with SO, JO and MO base stocks.

Specimen	JO	SO	PO	MO
0	2	2	1	2
1	3	3	1	3
2	3	3	1	3
3	3	3	1	3
4	3	3	1	3
5	3	3	1	3
6	3	3	1	3
7	3	3	1	3
8	3	3	1	3
9	3	3	1	3
10	3	3	1	3
11	3	3	1	3
12	3	3	1	3
13	3	3	1	3
14	3	3	1	3
15	3	3	1	3
16	3	3	1	3
17	3	3	1	3
18	2	2	1	2

Table 7-5, Combination of Specimens and Base Stocks and Amount of Repeated Tests Carried Out

7.4.7.5 Comparing methods for obtaining volume lost data

Initially, wear scars were analysed using a method for calculating volume lost using the wear volume calculation for a '*ball-on-flat surface linearly reciprocating sliding wear*' as described by Sharma et. al. (223). Case one was used, this assumes that the ball does not wear. It is felt that this was a reasonable assumption as the ball was hard enough to resist wear, with no visible signs of wear present after tests. The width of wear scars was measured using the SEM and then calculations performed as per the method described by Sharma et al. using Equation 7-1Equation 7-2 Equation 7-3.

This method states that the wear scar generated can be represented as the schematic shown in Figure 7-25a. Figure 7-25b shows the top view, the middle section, Section A has cylindrical geometry, the two end sections, sections B have geometry similar to a truncated part of a sphere. The volume lost is calculated separately in each of Section A and B, as shown is Equation 7-1Equation 7-2Equation 7-3, where r is the radius of the ball, w is the width of the wear scar and L the length of the wear scar. Figure 7-25c represents the ball, the area outlined by P, Q and R corresponds to the cross section area of section A from Figure 7-25b.

$$V_A = L\left[r^2 sin^{-1}\left(\frac{w}{2r}\right) - \frac{w}{2}\left(r^2 - \frac{w^2}{4}\right)^{\frac{1}{2}}\right]$$

Equation 7-1

$$V_B = \frac{\pi}{3}\left[2r^3 - 2r^2\left(r^2 - \frac{w^2}{4}\right)^{1/2} - \frac{w^2}{4}\left(r^2 - \frac{w^2}{4}\right)^{1/2}\right]$$

Equation 7-2

$$V_{total=V_A+V_B}$$

Equation 7-3

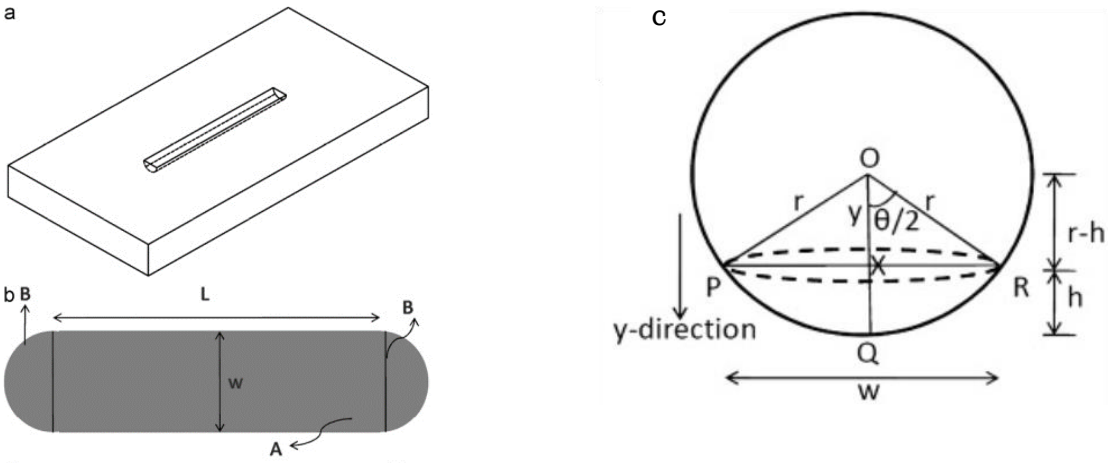

Figure 7-25 a and b, Wear Scar Volume Approximation Schematic, 8c, Geometry Related to the Ball and Cross Section of the Wear Scar (223)

This method has been shown to be effective by Green et al. (228) and Bahari et al. (224). Results from comparing are given in Section 9.2.1.3 in Figure 9-5 (MO, JO) and Figure 9-6 (SO, PO) show a comparison between the data obtained through the Sharma et al. method, and where possible, data obtained through the optical scanning method, for the first round of testing. There is no correlation between values obtained by calculating volume lost and values obtained using an optical scanner. It is hypothesised that the values from calculated volume lost are either an over- or underestimate, as it cannot take into account significant variation in the depth of the wear scar, which may be caused by three body abrasion from coating delamination. This calculation method also cannot take into account variations in wear scar width, which may occur due to imperfections in the substrate or coating, or collapse of the lubricant film. Therefore results using this method should be used with understanding of its limitation. Additionally to this, error from measuring wear scar widths using the SEM and then using Equation 7-1 Equation 7-3 would give a higher error in the resulting volume loss value compared with the uncertainty in measurement using a 3D non-contact profilometer (uncertainty 200 nm).

7.4.8 *Elastocon Relaxation Tester Method*

The first step in carrying out stress relaxation tests on the Elastocon was to allow the oven to heat up to 80 ˚C. Once the oven reached test temperature, the elastomer O-ring seals, detailed in Section 7.3.4, were placed between the compression plates and the thickness of the O-ring measured using the gauge on the compression rig. 150 ml of base stock (see Section 7.3.1 for further details) was poured into the oil container and attached to the compression rig. The compression rig was then placed in the oven, as shown in Figure 7-3. The oil was heated up to 80 ˚C and allowed to thermally stabilise for 5 minutes. Once the oil reached test temperature, the O-ring was compressed by 25% of its thickness. The environment chamber (shown in Figure 7-3)

was set to 18˚C. Data was logged for 168 hours in accordance with ISO 3384-1:2011, with variation in force reading continually measured for the duration of the test.

Additional tests were performed with SO and FKM as the weight of one seal could not be recorded due to contamination with acetone. Additional tests were performed with EPDM immersed in JO and MO, as the initial three repeats showed variation of more than 10% for force readings between repeats and the stress relaxation trend had noticeable variance over the test duration.

7.5 Conclusions

This chapter detailed the experimental plan developed to assess the feasibility of bio-lubricants for use as automotive engine oils. It is felt that given the review of literature that the understanding of the fundamental performance of bio-lubricants is still under developed. For it was felt that the level of testing should be at a laboratory level specimen test scale so that fundamental mechanisms that describe the performance bio-lubricants can be better understood. The next chapter gives the results of data obtained from the experimental plan.

8 Learning Experiments and Blended Oil Wear Tests

The chapter details the results from learning experiments carried out on the Plint TE77 reciprocating wear tester, to define the experimental parameters. These experiments were also conducted to assess whether there was any performance benefit to varying proportions of blends of jojoba and mineral base stocks in wear tests.

Results from initial learning experiments helped to define the experimental parameters used for all wear and friction tests described in this thesis. Results from initial learning experiments conducted with JO are shown in Figure 8-1. The wear rate was calculated based on the volume of material lost during the wear tests and the duration of the test. The volume loss was calculated based on measurements of wear scar width. The average from further tests with jojoba oil (JO) is given for comparison (data also in Figure 8-2).

The results in Figure 8-1 show that the majority of wear occurs at the start of a wear test as the shorter duration wear tests have higher wear rates. The variation in load makes little difference to calculated film thickness values and resulting wear. For this test set up, Table 8-1 shows the difference in film thickness for the different loads. The EHL equations (Equation 3-1) given in Section 3.6 and values for pressure viscosity coefficient (So & Klaus) at 80 °C, stated in Table 6-1 in Section 6.9 were used to calculate values. As discussed in Section 6.9, the validity of these results is questionable and results should be used as a comparative tool, rather than absolute values.

The results also show that the variation in temperature has more of an effect on film thickness calculations, as shown in Table 8-1, but this does not translate to a notable difference in wear rate. For this reason a load of 40 N was selected for all wear tests, this was done to ensure that coated specimens tested, as described in Section 5.2.1.2, would be less likely to fail due to excessive substrate deformation. If the scratch failure map for hard coating in Section 5.2.1 is considered, selecting a normal load of 40 N instead of 50 N may prevent complete failure of the coating. With a substrate to coating hardness ratio of approximately 5, this would mean the tests are conducted at the low end of the cracking and spalling failure zone, which may aid the assessment of coating failure mechanisms.

	Max contact pressure, GPa	SO	JO	PO	MO
100 °C		Film Thickness, µm			
40 N	2.1	4	3.3	3.8	2.6
50 N	2.25	3.9	3.3	3.7	2.5
80 °C		Film Thickness, µm			
40 N	2.1	6.6	5.4	5.3	4.5
50 N	2.25	6.5	5.3	5.2	4.4

Table 8-1, Maximum Contact Pressure and Film Thicknesses for Base Stocks in Learning Experiments

Figure 8-2 shows results from learning experiments with blended oil wear tests carried out on the Plint TE77 reciprocating wear tester. Tests were carried out as per the procedure outlined in Section 7.4.1. A minimum of three repeated tests for each base stock blend were performed. Wear results were inconsistent; further repeats were carried out in an attempt to identify a representative trend. Values for hardness are included on the secondary axis in Figure 8-2. Hardness measurements were taken to assess whether the variation in results for wear tests was linked to the hardness of the specimen. Results show that the variation in hardness did not correspond to the variation in wear performance.

Figure 8-3 shows results of averaged volume lost values with error bars representing spread of experimental results. Figure 8-2 clearly shows that results for specimen 2.1, 2.4, 3.6 and 4.4 (as described in 7.4.7.2, or Figure 8-3 links the blend ratios to specimen numbers) do not follow the trend of other results. This inconsistency and significant spread in some of the results cannot be explained. It is one of the major difference in the results of wear tests with blends of JO, compared with MO. Figure 8-3 shows the trend in wear performance when using varying proportions of JO oil in base stock blends. There is a general downward trend in values for volume lost from using 100% JO oil, to using 50%, showing that the addition of mineral base oil (MO) reduces wear. If however, the spread of results is considered, it is not possible to define a clear trend. The results for tests carried out with blends of JO and mineral base oil show that volume losses were significantly larger than for tests with just mineral base stock.

When comparing to other research, Bisht et al. (68) used up to 30% jojoba oil, with a base mineral oil and found reductions in wear compared with tests with just mineral oil. There may be some key differences that caused this discrepancy. Bisht et al. did not document their test methods, which makes it difficult to form a sound comparison, the source of jojoba oil can also influence performance and could cause the variation, as discussed in Section 5.1. It is thought that the roughness of the surface was an influence in results here, as discussed in Section 6.2, there is an optimal surface roughness to aid spreading of the lubricants over a surface. This roughness of steel specimens used in these learning experiments was 1 µm, while literature showed that a surface roughness of over 0.5 µm gave a reduction in spreading. The rougher surface also increases the level of abrasion in the contact zone. As Table 8-1 shows, in some cases the lubricant film may not have been adequate and asperity contact will have occurred.

Due to the variation in results, represented by the error bars, it was felt that using blends of oils for further tests would add complexity without any noticeable performance improvements.

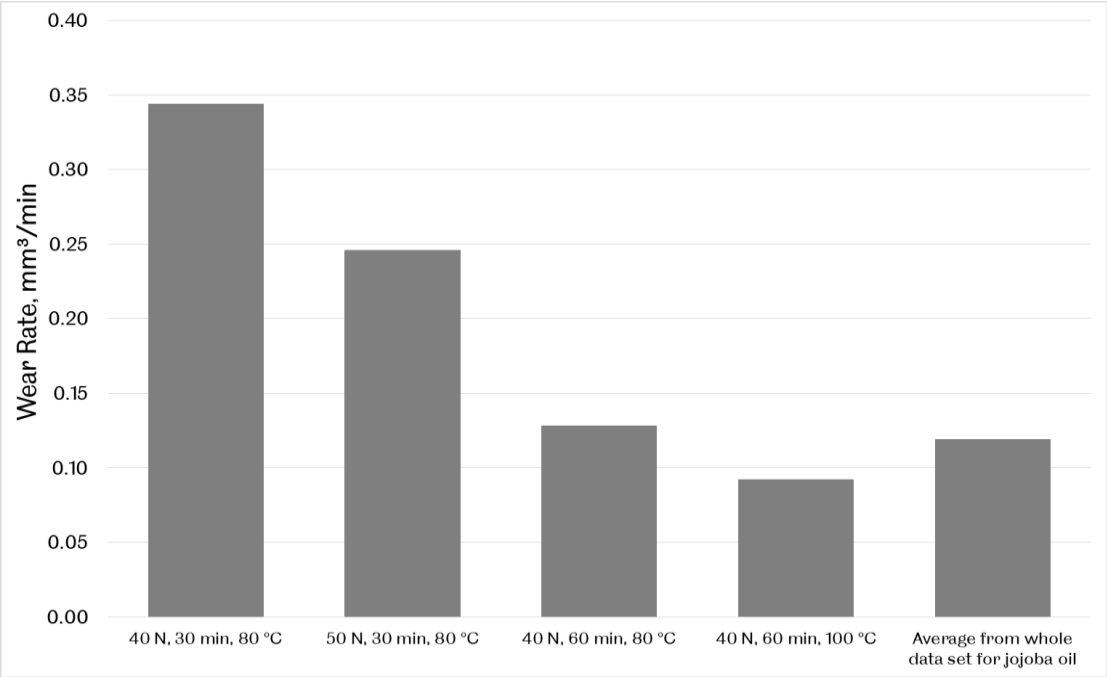

Figure 8-1, Results from Learning Experiments Compared with Average Results from Blended Oil Tests

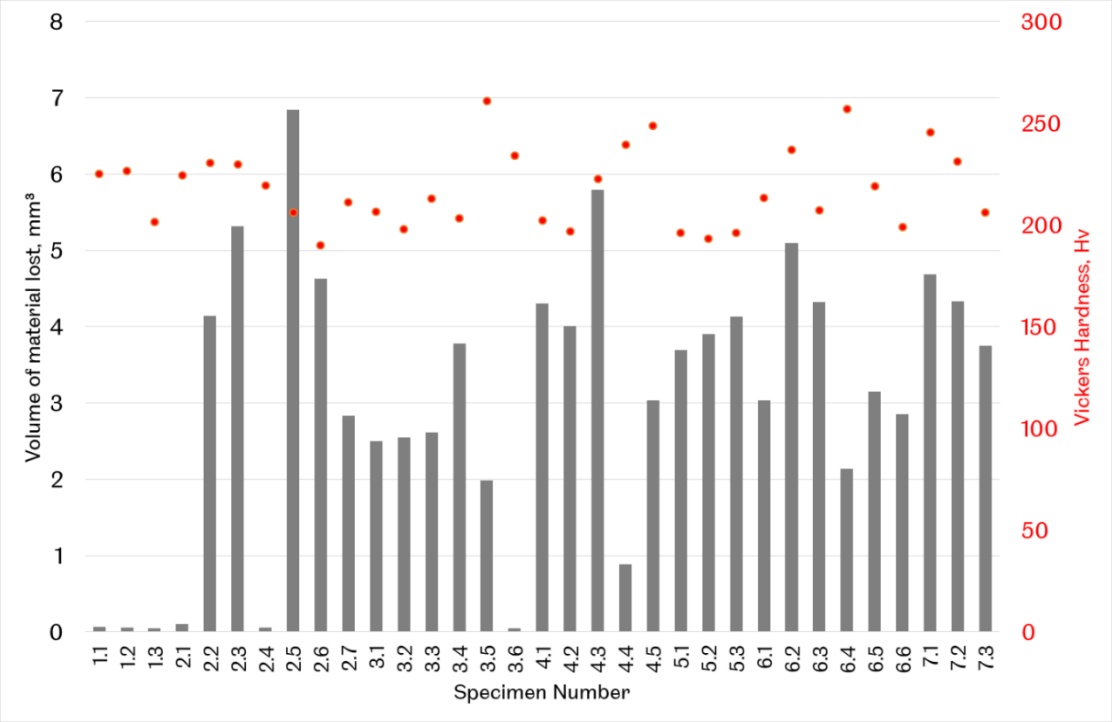

Figure 8-2, Results for Wear Tests Carried Out Using Varying Blends of Jojoba and Mineral Base Oil, Volume Loss is on The Left Hand Axis, Hardness is on The Right Hand Axis

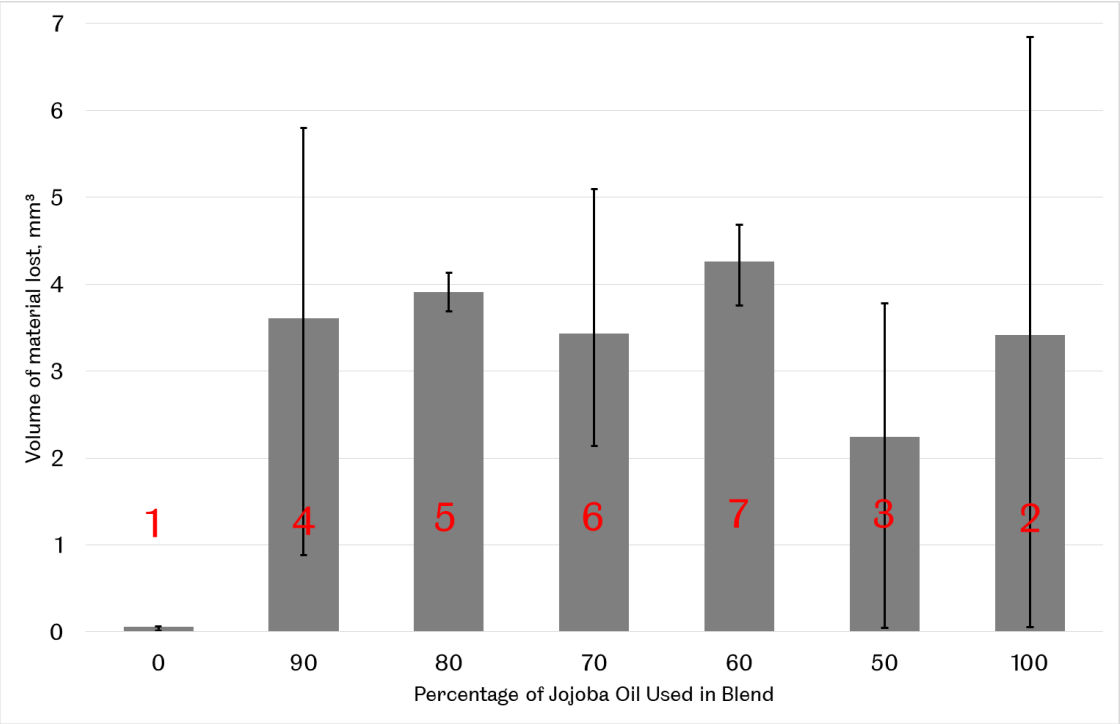

Figure 8-3, Volume Losses from Wear Tests Carried Out with Varying Blends of Jojoba and Mineral Oil

8.1 Conclusions

The results from learning experiments presented in this chapter were used to define the test parameters used to conduct the experiments detailed in Chapter 9. The learning experiments showed that the majority of wear in a reciprocating wear test occurs at the start of the test. Varying the load made little difference to the observed wear and calculated film thickness. A normal load of 40 N was therefore selected to prevent excessive substrate deformation. This load, and the substrate to coating hardness ratio, allows some cracking and spalling of the coating could still occur, meaning coating failure mechanisms could be observed without complete coating breakthrough. The learning experiments did not clarify the source of the inconsistent results, but they did clarify that slight variations in hardness did not result in measurable variations in wear. It is also thought that the surface roughness could have reduced the ability of the lubricant to spread effectively over the surface. Finally, there was no performance benefit to blending jojoba oil with mineral oil, and due to the inconsistent results this would add an extra level of complexity to the further test programme.

9 Wear Tests with Multi-Layer Surface Treatments

The chapter begins with results from scratch tests, which give information on the integrity of the multi-layer coatings.

The performance of multi-layered surface treatments is analysed from experiments with the TE77. Firstly, a generalised view of the performance of the multi-layered surface treatments is covered, comparing varying combinations and looking at ideal layering order. Results are then discussed, with a focus on the performance of the different bio-lubricant base stocks with the multi-layered surface treatments. An assessment of the potential chemical interaction of the base stocks and surface treatments is made. The composition of the base stocks and its effect on performance is considered, as are such parameters as wettability.

Characterising the surface treatments by measuring hardness, surface roughness and adhesion properties are also discussed.

The discussion is separated into two sections; coating performance and lubricant performance, in an attempt to isolate any performance effects that just occur as a result of the surface treatment combination used and performance effects that are mainly a result of the different lubricants used.

Analysis of the fatty acid profile (through gas chromatography) for unused and used bio-lubricant base stocks was carried out by an external laboratory. This was done to observe any change in structure of the oils after being subjected to heat and mechanical stress. The wettability (spreading parameter) of the coatings and lubricants was also considered.

9.1 Adhesion Test Results

Scratch tests were carried out to assess the adhesion properties of the various multi-layer surface treatments and can give an indication of the integrity of the coating. The scratch tests were performed as described in Section 7.4.2.2. The adhesive critical scratch load, L_{C2}, was then calculated using the method described in ASTM C1624-05 (211) and using Equation 9-1.

$$L_{C2} = \left(L_{rate} * \left(L_N / X_{rate}\right)\right) + L_{start}$$

Equation 9-1

Where;

L_{rate} *= rate of application of force, N min^{-1}= 180N min^{-1}*

L_N *= distance from start of scratch to start of damage*

X_{rate} *= rate of horizontal displacement, mm min^{-1} = 40.2 mm min^{-1}*

L_{start} *= pre load at start of test, N = 5 N*

The adhesive critical scratch load was calculated for each scratch and values shown in Figure 9-1. Error bars represent the spread in results. The higher the value for critical scratch load, the better the adhesion of the coating to the substrate.

Specimens 3 and 4 were not tested as these specimens were only shot blasted, with no other surface treatment carried out. The reference specimens, 0 and 18, were also not tested as no surface treatment was applied.

Comparing specimens with the same group of coatings, there is slightly higher adhesion with the DLC coated specimen 2 (SF, DLC), compared with the surface ground DLC coated specimen, 1, as Figure 9-1 shows lower wear with specimen 2. It is unlikely that wear is lower just because adhesion is slightly higher; the surface roughness of the coating will also be a factor.

A similar trend of coating adhesion being dependant on substrate finish was observed for the chemical dip specimens, 6 and 9. Specimen 6 was surface ground, 9 super finished. Specimen 9 had higher adhesion, but contrary to the DLC samples, the super finished chemical dip specimen had higher wear. The validity of using the scratch test method for the chemical dip specimens is, however, questionable. ASTM C1624-05 states that this method is suitable for coating thicknesses in the range of 0.1 – 30 μm. As shown in Section 7.3.2.6, the chemical dip coating layer appears to be less than 0.1 μm, therefore the validity of this method is questionable as the coating layer may be too thin. Scratch tests may indicate resistance to scratching rather than measuring the integrity of the surface treatment.

Comparing multi-layer coatings of chemical dip and DLC, for coatings that had the chemical dip applied before DLC, as with specimen 14, has a similar adhesion to specimens 1 and 2 (just DLC). The substrate of specimen 13 (SF, CD, DLC), which was super finished before coating applied, had a lower coating adhesion than 14, 1 or 2. Applying chemical dip before DLC makes little difference to coating adhesion, as specimens 5 (SF, DLC, CD) and 7 (DLC, CD) show.

For specimen 16 (SB, DLC) and specimen 17 (SF, SB, DLC), there does not appear to be a significant difference in coating adhesion. There is, however, increased wear with specimen 17; this may suggest that the slight reduction in coating adhesion for specimen 17 could be caused by the doping media; the reduced adhesion could also be responsible for increased wear.

The application of chemical dip after shot blasting, for specimen 10 (SB, CD) gave the highest adhesion values, but considering the wear data in

Figure 9-2, wear was also higher than most other coating combinations. Specimen 8 (SF, SB, CD) had lower adhesion values and lower wear. The poor adhesion in this case could contribute to a solid lubricating action, with the treatment layers effectively shearing over one another to reduce wear. A combination of all three surface treatments, specimen 15 gave lower adhesion than the shot blasted, chemical dip specimen 10 and shot blasted DLC specimen 16. Compared with the full set of specimens, the coating adhesion of specimen 15 is reasonable. Using multiple interfacial layers in coatings is known to improve coating performance, as it reduces the stress in each layer. This is discussed in more 5.2.

Overall, results from scratch tests do not provide conclusive evidence of coating performance. There are many influencing factors that must be considered to explain

the wear and friction performance, and lubricant interaction, which are discussed in Section 9.4.

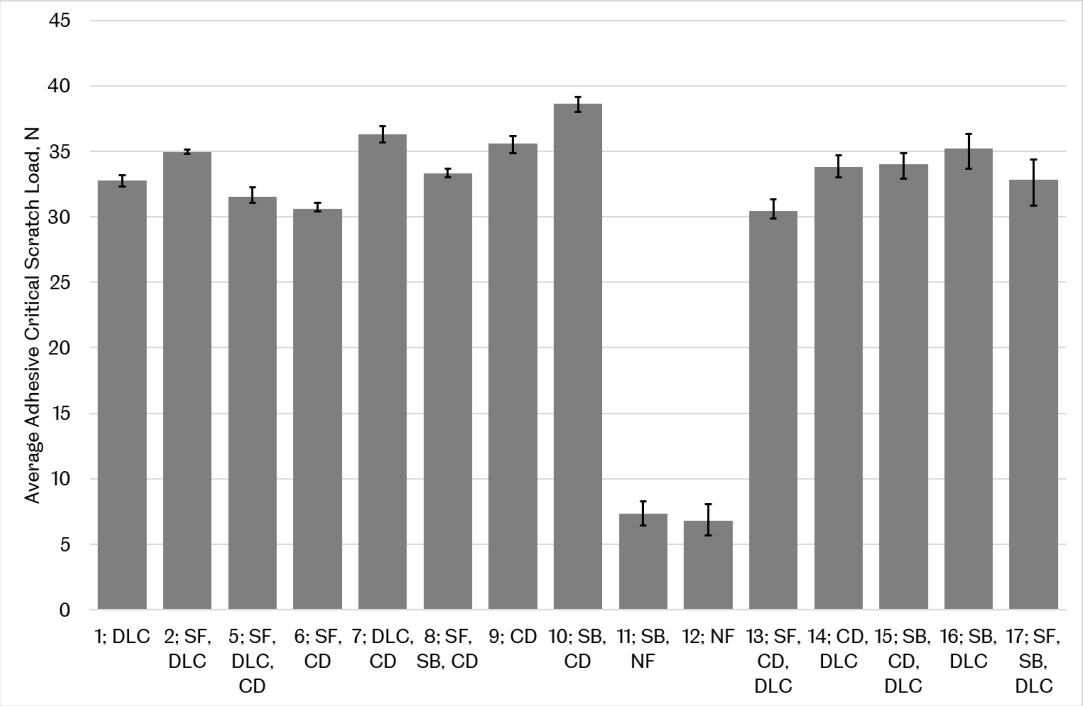

Figure 9-1, Average Critical Scratch Load for Specimens with Multi-Layer Surface Treatments

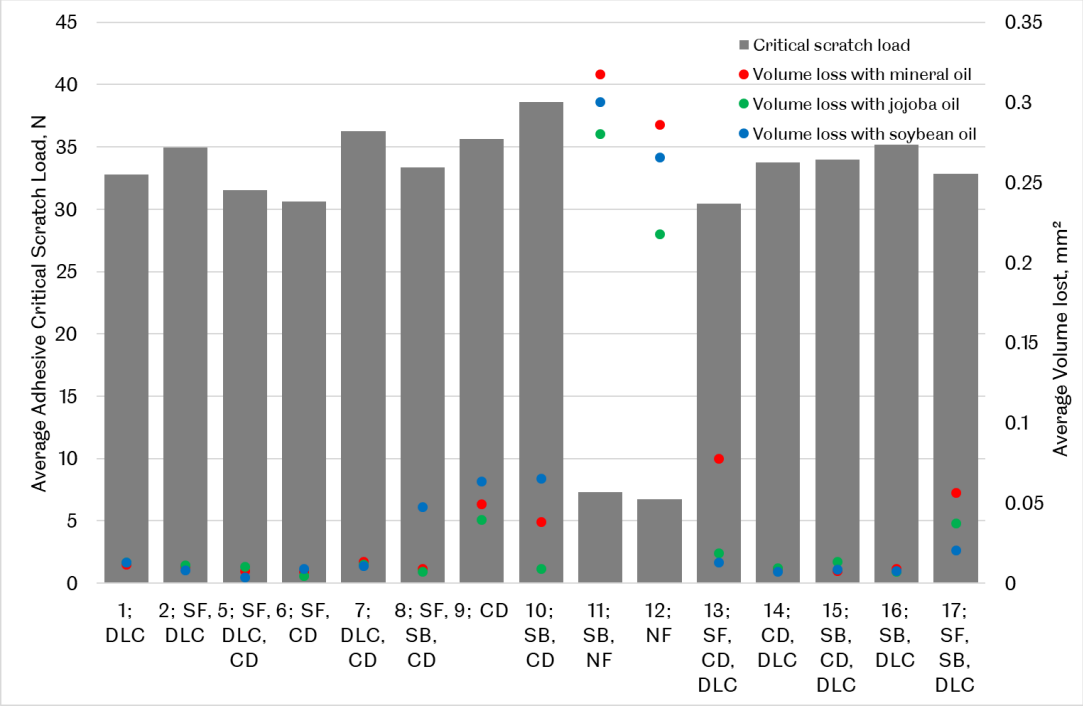

Figure 9-2, Average Adhesive Critical Scratch Load and Volume Loss Data for Specimens with Mult-Llayer Surface Treatments

9.2 Results for Wear Measurements

Figure 9-3 shows the average result from three repeated tests, apart from specimens 0 (SG reference), 1 (DLC), 3 (SB), 9 (CD) and 18 (SF reference), (see Section 7.3.2) which are averaged from two repeats. Values for tests carried out in the first round of testing with 0, 1, 3, and 9 could not be obtained via the optical scanning method of wear scar analysis as these specimens were sent for an initial trial for sectioning in preparation for examining the wear scars and coatings subsurface.

Error bars represent the spread of results. As there are only three measurements per data set, more complex error analysis was not seen as valuable. While the spread in results highlights that wear tests with bio-base stocks can give inconsistent results, this was also seen with wear tests in Chapter 8.

Figure 9-3 shows that for some specimens there is a large variation in results. This may be caused by poor selection of the substrate, in terms of unsuitable ratio of elasticity between the substrate and coating material. SEM images, in Section 9.3, show cracking of the coating. Cracking was followed by delamination and the possibility of hard coating particles getting entrained in the contact causing severe abrasive wear. Lubricant film collapse is another reason for poor wear protection results. This may be caused by the inability of the lubricant to form a protective tribofilm over the coated surfaces, as discussed further in Section 9.4.

Interestingly, all the base stocks tested performed best in tests with specimen 18, the super finished reference sample. Considering tests with the mineral base stock (MO), 0.005 mm^3 of material was lost on average in tests. The best performing surface treatments for mineral base stock was specimen 6 (SF, CD), with an average volume loss of 0.007mm^3. This is a novel and not widely used coating currently, particularly in comparison to DLC. The results with the comparable specimen (super finished substrate) coated in DLC, specimen 2, had volume losses of 0.01 mm^3. The other specimens that performed well with MO also contained the chemical dip, specimens 5 (SF, DLC, CD) and 15 (SB, CD, DLC), both had average volume losses of 0.008 mm^3. MO also performed well with specimen 4, (SF, SB), with the same volume losses. The solid lubricant doping media, MoS_2 appears to have aided wear protection.

The bio-lubricant base stock candidate, Jojoba oil (JO), also had low volume losses with specimen 18, with 0.005 mm^3 of material lost on average. It is well documented that JO can offer wear protection comparable to a MO equivalent (69) (134) (67), although work carried out has been contradictory in literature (57) (128) and results in Chapter 8. There are many factors that can contribute to the varying performance of JO. The way in which the oil crop is grown has a significant influence on the fatty acid profile of the oil, and therefore performance. Factors such as, but not limited to, seed genetics, the growing climate and methods, the point in the plant's life cycle when it is cropped, and the way it is stored all affect the fatty acid profile of the oil (228).

In contrast, the source of mineral oil is reasonably consistent, with slight variations in the composition depending on which continent it originated from (34). The temperature used in tests may also be a contributing factor, as the thermal stability of vegetable oils is not as good as mineral based oils. Similarly to MO tests, JO performed well with specimen 6 (SF, CD) showing good levels of wear protection,

with an average volume loss of 0.005 mm^3. JO performed well with specimen 4 (SF, SB), with the same average volume loss as specimen 6 and 18. Results for specimen 16 (SG, SB, DLC) also produced low volume losses of 0.007 mm^3.

There was a general trend for the soybean bio-lubricant base stock candidate (SO) to offer better wear protection than the other oils tested. For the reference specimen, 18, average volume loss was 0.003 mm^3. The best performing surface treatment specimen was specimen 5 (SF, DLC, CD), with volume losses of 0.004 mm^3. This coating order reversed, in specimen 14 (CD, DLC) also performed well, with volume losses of 0.007 mm^3. This was a slight improvement on the volume losses compared with specimens with just CD (0.009 mm^3) or DLC (0.008 mm^3). Specimen 16 (SB, DLC) produced the same volume losses as 14 at 0.007 mm^3.

9.2.1.1 Archard Wear Coefficient

The Archard's wear coefficient was calculated for only a selected set of coating combinations and the steel reference specimens due to issues obtaining hardness values, as discussed in Section 9.2.4. This was done using the Archard Wear Equation shown in Equation 9-2 (35);

$$V = \frac{kPL}{H}$$

Equation 9-2

Where V is the volume lost, P is the load, L is the sliding distance and H the hardness. Hardness values are given in Section 9.2.4, the hardness of the steel specimens was 297 Hv_{20}. The wear coefficients for the steel reference specimens are as expected (229). The wear coefficients for the DLC coatings is higher than values found in literature. The discrepancy could be due to several factors, the wear coefficient is dependent on the system, loads, contact pressures, counter surfaces, test temperature and duration and type of lubrication will all influence this value. No literature was found for wear coefficients for a-C:H DLC coatings and vegetable oils or the same test conditions, therefore a direct comparison could not be made. Muhmud et al. (230) found a wear coefficient of $9*10^{-7}$ m^3/Nm for a-C:H DLC against steel (no contact pressure given), for a ball on flat, lubricated with SAE40 at 100̊C. Values shown in Figure 9-4 are twice this value. It could be the case that the tests conducted by Muhmud et al. were at a lower contact pressure. Fully formulated oil with anti wear and extreme pressure additives will have improved lubrication compared with neat vegetable oils, which could also explain the difference. Figure 9-4 may indicate more severe wear mechanisms caused by the delamination of the coatings under high contact pressures. Zahid et al. (231) found wear coefficients of around $8*10^{-7}$ m^3/Nm, but this was for ta-C DLC against steel with palm trimethylolpropane ester. Kosarieh et al. (232)and Solis et al. (233) found wear coefficients of $70*10^{-18}$ and $65*10^{-18}$ m^3/Nm respectively for wear tests with H-DLC on steel, interestingly Solis et al. obtained these values from unlubricated testing. These values are considerably smaller then Zahid et al. or Muhmud et al. The discrepancies could also be caused by the variation in composition and quality of the DLC coating.

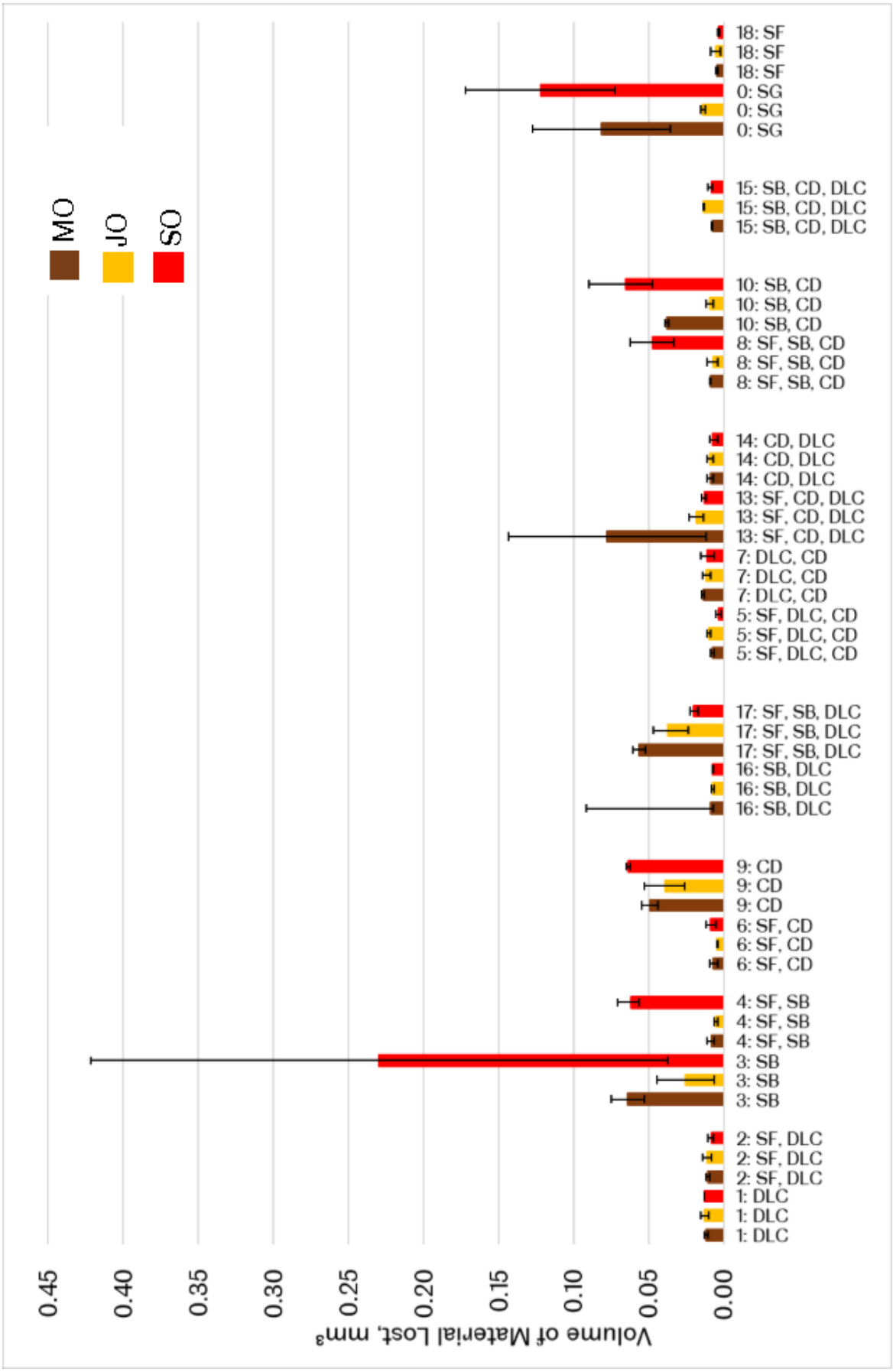

Figure 9-3, Average Volume Loss from Three Rounds of Testing Multi-layer Surface Treatments

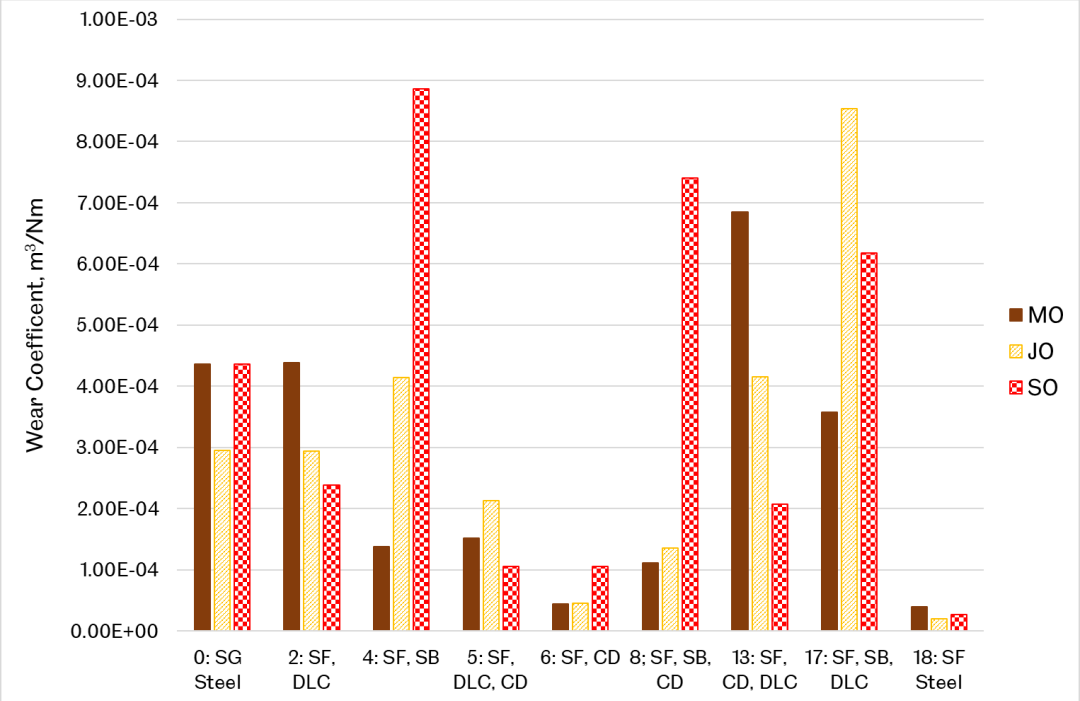

Figure 9-4, Wear Coefficients for a Selection of Multi-Layer Coatings

9.2.1.2 Nano Fullerene Coating Results

Figure 9-5 and Figure 9-6 give justification for not continuing tests with nano fullerene coatings, specimen 11 (shot blasted first) and specimen 12 (surface ground). The volume of material lost was consistently higher than all the other specimens tested, with all base stocks. Specimen 11 (SB, NF) had volume losses of at the lowest 0.2438 mm^3 (for PO) and at the highest, 0.3174 mm^3 (for MO). Specimen 12 (SG, NF) had a range of volume losses of 0.2177 to 0.3036 mm^3. These volume losses are an order of magnitude higher than almost all the other specimens tested. Most of the other coatings had volume losses of under 0.025 mm^3.

9.2.1.3 Results for Tests with Palm Kernel Oil

Figure 9-6 also gives justification for not continuing tests with palm kernel oil. This decision was made prior to specimens being optically analysed (method not available sooner), therefore only the calculated data was considered. When comparing the calculated data for SO and PO, there was a trend for tests with SO to produce lower volume lost values than PO. Eleven results for PO have higher volume losses than SO, which has seven results that are larger than PO. This changes when considering the optical scanning method results, with PO having six results that are higher than SO, while SO has nine results that are higher. If the optical scanned data is considered, then it is less clear which oil performs better, with nine specimens having higher volume losses when tested with SO and PO six.

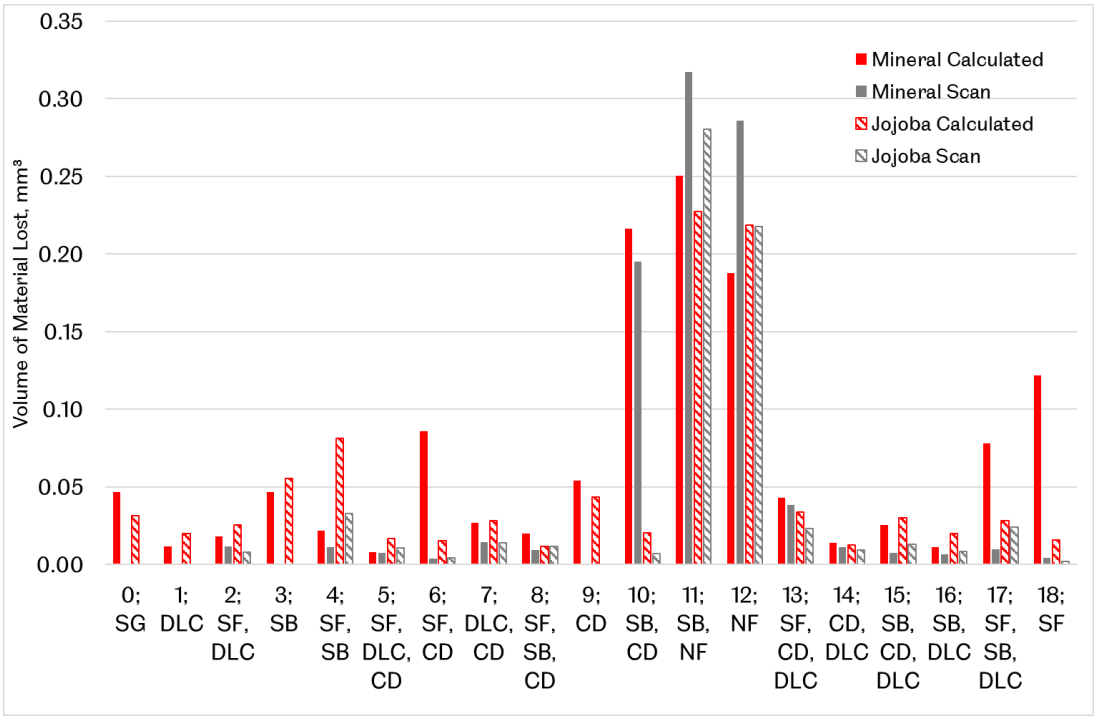

Figure 9-5, Comparison of a Calculated Method for Working Out Volume Lost and Using a 3D Scanner for Mineral and JO

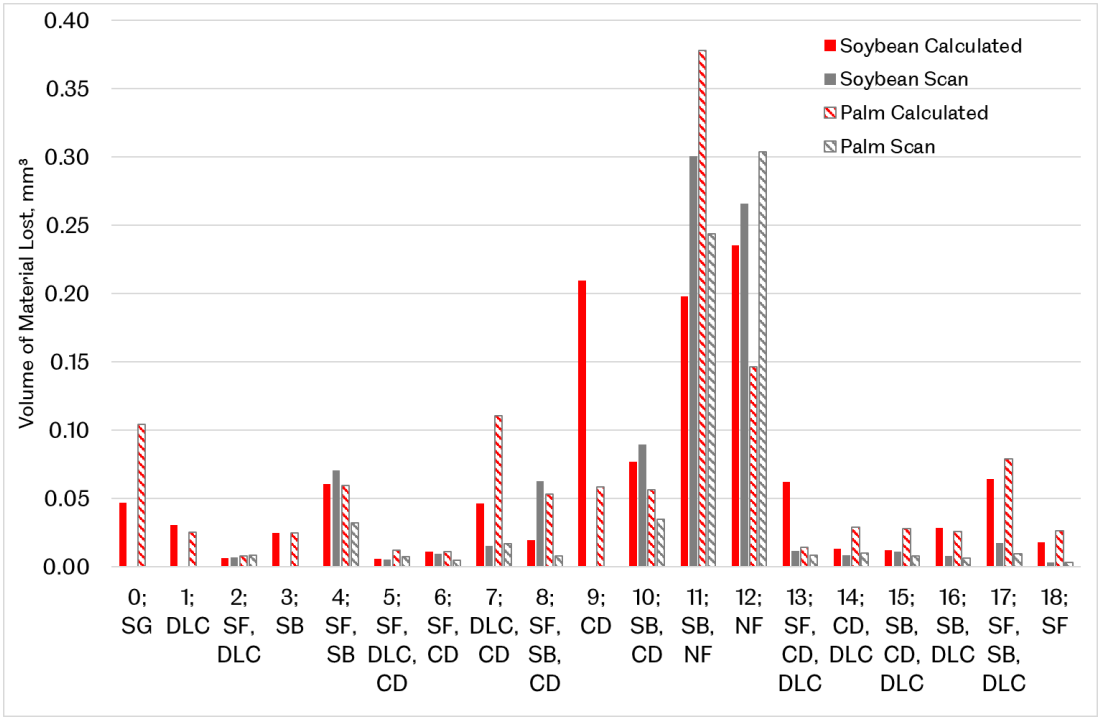

Figure 9-6, Comparison of a Calculated Method for Working Out Volume Lost and Using a 3D Scanner for Soybean and Palm Oil

9.2.2 *Coefficient of Friction Results*

Figure 9-7 shows the averaged CoF results for all specimens tested. The results for PO are from the first round of testing, as are results for specimen 11 and 12 (NF) for all base stocks. Averages for specimen 0 and 18 (surface ground and superfinished reference specimen) used only two values, only two tests were performed per oil. Averages for specimens 5 (SF, DLC, CD), 13 (SF, CD, DLC) and 17 (SF, SB, DLC) for SO, and specimens 4 (SF, SB), 14 (CD, DLC) and 16 (SB, DLC) for mineral oil are only from two sets of data, as data acquisition failed in these tests. The error bars represent the experimental spread of results.

As with results for volume loss, CoF values were generally lowest with the super finished reference specimen, 18. The average CoF for MO was 0.05. The average in this case, however, is not a good representation of the range of values, for test one, CoF was 0.01 and for test two, 0.089. Further testing is required to identify a CoF trend for this oil and specimen combination. A similar issue was present with CoF data for specimen 16, the averaged result was 0.044, but only two values could be used for this result, and these varied considerably, with test one CoF 0.077 and test two CoF 0.01. Overall, however, CoF results for MO showed consistency over the three rounds of testing. CoF values for MO were consistently higher than for the other base stocks tested. It is well documented that, generally, vegetable base lubricants give lower CoF than mineral based lubricants. There has been much work done using vegetable based oils as friction modifiers and to show the friction reduction properties in comparison to mineral based lubricants (16) (68) (70) as discussed in Section 6.1. The mechanisms for this are discussed in more detail in Section 9.4.

CoF results for SO were lower than for tests with MO, in all cases apart from specimen 16 (SB, DLC), where COF was an average of 0.08. Due to the discrepancies with CoF values for MO and specimen 16, this is not considered a significant result. The reference specimen 18 with SO produced an average CoF of 0.058. Values for specimen 6 (SF, CD) came close, with a CoF value of 0.06, volume losses for this specimen when tested with SO were also some of the lowest.

An interesting result for tests with SO is the CoF values for the nano fullerene coated specimen, 11 (SB, NF), the CoF value for this test was 0.061. Significant volumes of material were lost in this test, wear scars showed abrasion, adhesion and plastic deformation. The nano fullerene is more commonly used as a lubricant additive, as discussed in Section 6.4. Under high pressures, the fullerene spheres are thought to exfoliate and unwind to provide lubricity (Figure 6-10 in Section 6.4). Analysis of wear debris could provide further information on this phenomenon. Specimen 11 was shot peened prior to the nano-fullerene coating being applied; the solid lubricant media used in this technique could also be responsible for the lower CoF values. The surface texturing may also have aided the retention of lubricant in the contact, the lubricant film was, however, not thick enough to cover the flaky surface finish and protect the surface from wear. Further discussion on the wear and friction mechanisms of this coating can be found in Section 9.3.

CoF values for specimen 11 and JO was also low, at 0.049. Specimen 12, with just nano fullerene, also produced low CoF value of 0.064. Aside from these specimens, specimen 8 (SF, SB, CD) produced the lowest average CoF value for tests with JO, at 0.063. Specimens 3 and 4 also produced low CoF values of 0.066. It appears that there

may be some favourable interaction between the solid lubricant doping media in the shot peened specimen with JO, as overall results with this treatment and JO performed well. Further discussion on this is given in Section 9.4.7.

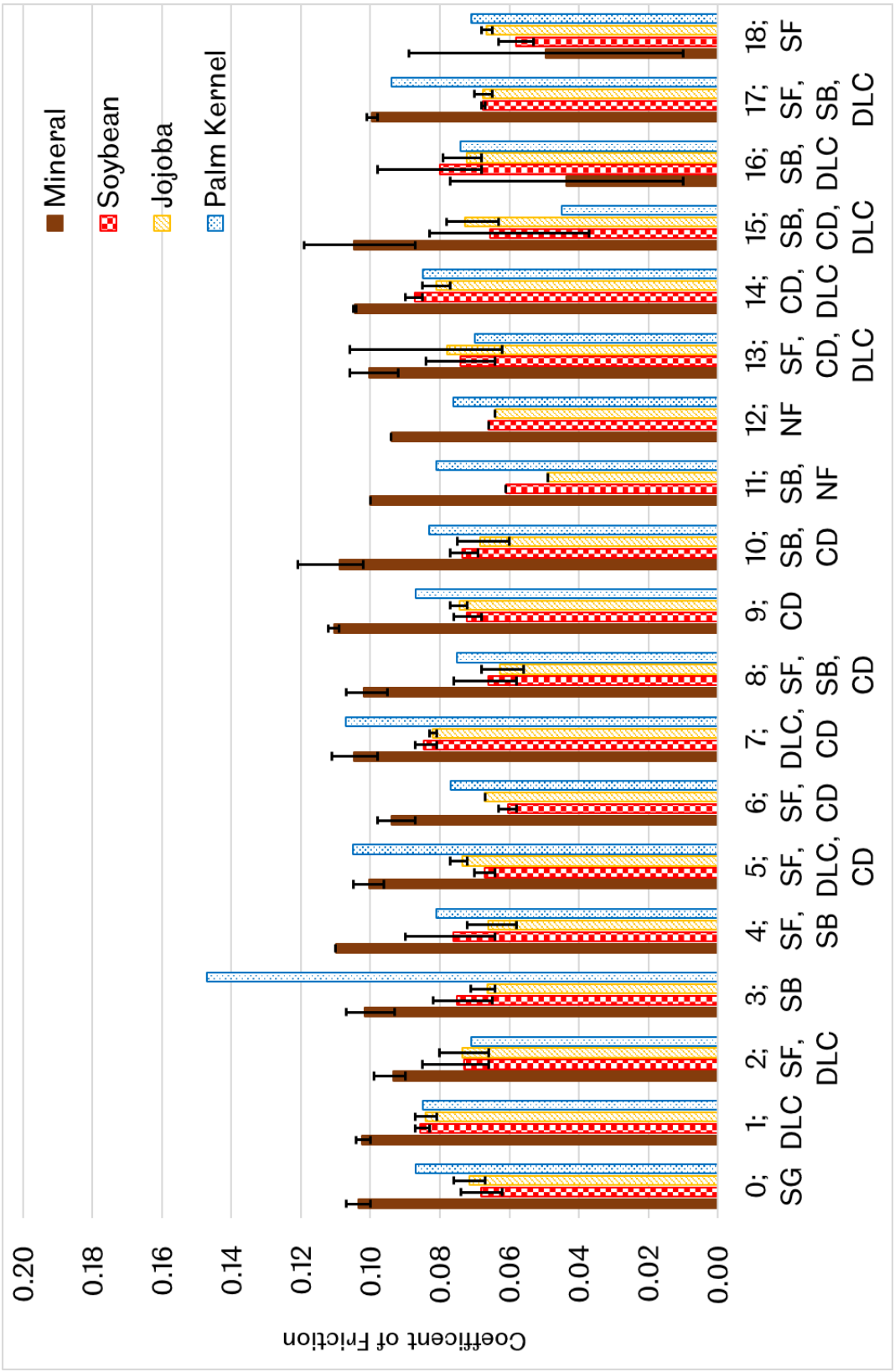

Figure 9-7, Averaged Coefficient of Friction Results for Wear Tests with Multi-layer Surface Treatments

Overall results show no particular trend in wear and CoF, as Figure 9-8 illustrates by presenting CoF data overlaid on volume loss data. This is not unexpected, as wear and friction are independent of one another. It is possible to have shearing at the interface of the contact and still remove or displace material. Sometimes high CoF corresponds to high wear, but other times there is no correlation. For example, results for specimens 13 (SF, CD, DLC) and 17 (SF, SB, DLC) show some correlation between higher CoF values and higher wear. If specimens such as 1 (DLC) and 2 (SF, DLC) are considered though, there is no apparent trend.

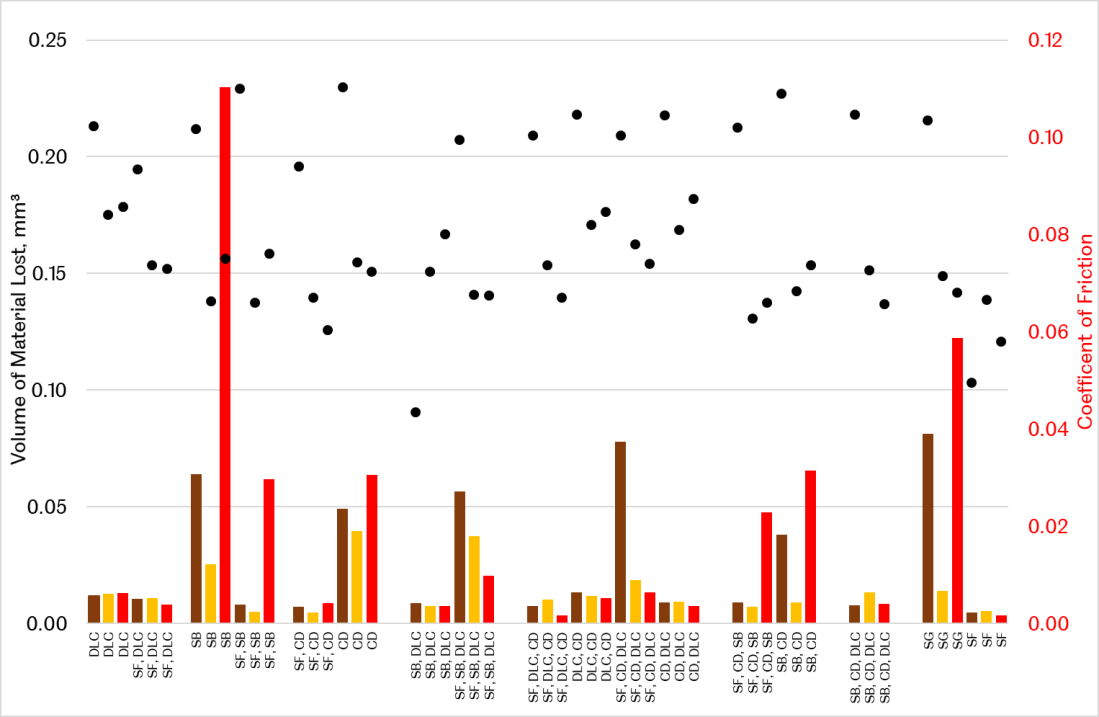

Figure 9-8, Averaged Volume Loss and Coefficient of Friction Results for Mineral, Jojoba and Soybean Oil

From general evaluation of SEM images of the wear scar region and 3D scans of the wear scars, it is clear that some coatings collapsed during testing and higher volumes of material were lost. Further discussion on this point is made in Section 9.3. Specimen 2 tested with JO is a good example of this. In the third round of testing, this test combination produced a volume loss value of 0.024 mm^3, over double the average of 0.011 mm^3, but the average CoF value was the lowest of the three repeats, at 0.066. Figure 9-9 shows SEM and 3D scan images of this wear scar; complete removal of the coating in the wear track is apparent. Figure 9-10 shows a section from the wear scar region of a test with specimen 2 and JO, in the first round of testing. Cracking of the coating is visible, and imperfection under the coating, as highlighted will contribute to the collapse and delamination of this coating. These very hard delaminated coating particles will act as an effective knife to remove further material from the softer interfacial and substrate layers in the contact region. This can result in high wear and low CoF.

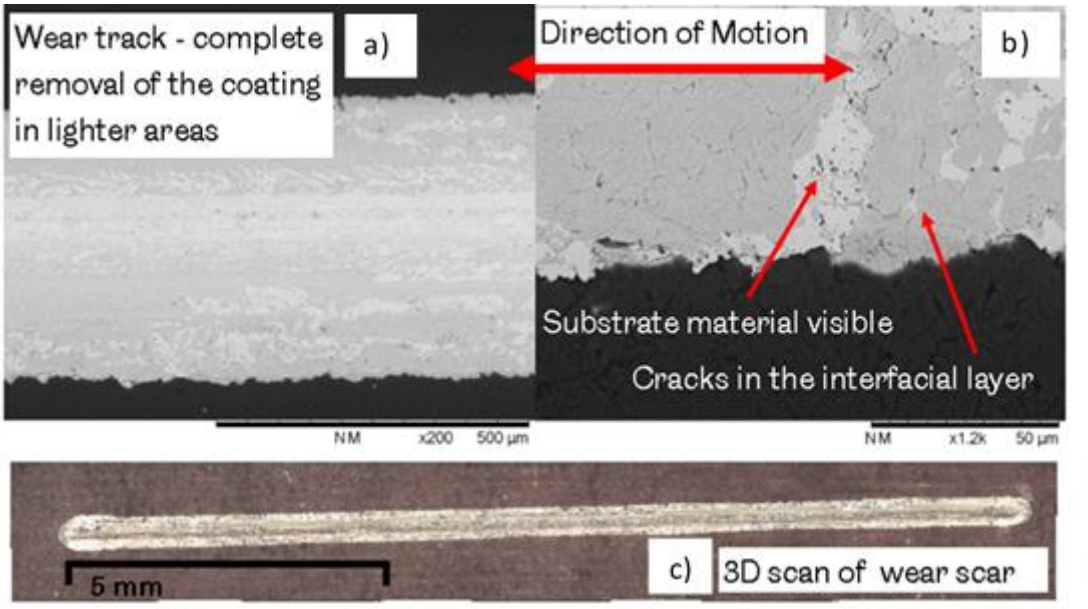

Figure 9-9, Wear Track for Specimen 2 Tested with Jojoba Oil

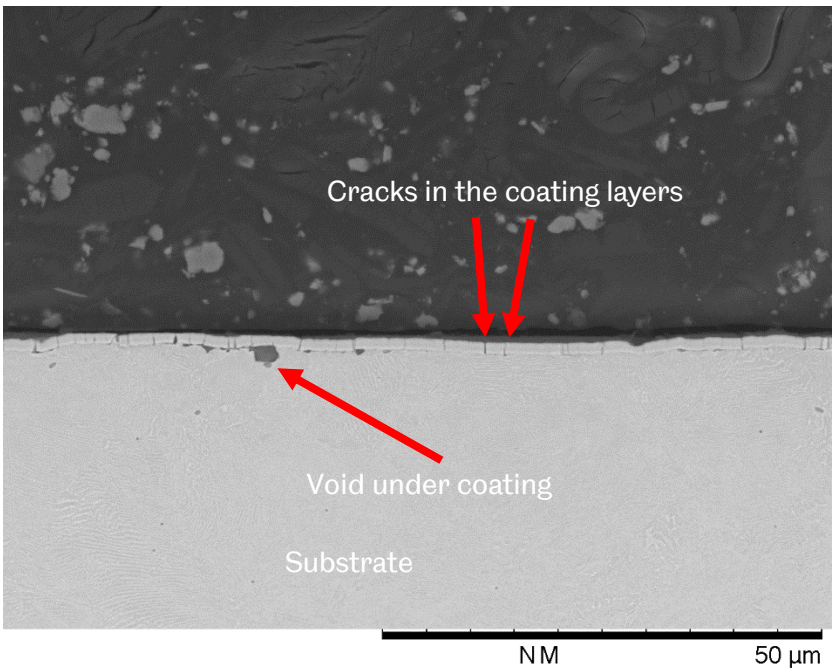

Figure 9-10, Specimen 2, Section of Wear Scar Region for Test with Jojoba Oil (note, not the same test as Figure 9-9)

9.2.3 *Surface Roughness*

The surface roughness was measured using an optical scanner, as described in Section 7.4.1.2. Results are shown in Figure 9-11. The final coating surface roughness is influenced by the substrate finish; surface ground (SG) specimens 0, 1, 3, 7, 9, 10, 14, 15 and 16 had higher surface roughness than specimens with a super finished (SF) substrate, specimens 2, 4, 5, 6, 8, 13, 17, 18. In material pairs 1 & 2, 3 & 4, 6 & 9, 8 & 10 and 0 & 18, the super finished specimens had lower wear. This is expected, rougher surfaces have a lower real contact area, less uniform stress distribution and higher maximum pressures. As rough surfaces have more asperities, this also means there is more opportunity for adhesive junctions to be formed, which can increase friction. Surface roughness also has an impact on a lubricant's ability to 'wet' the surface, as discussed in Section 6.7.

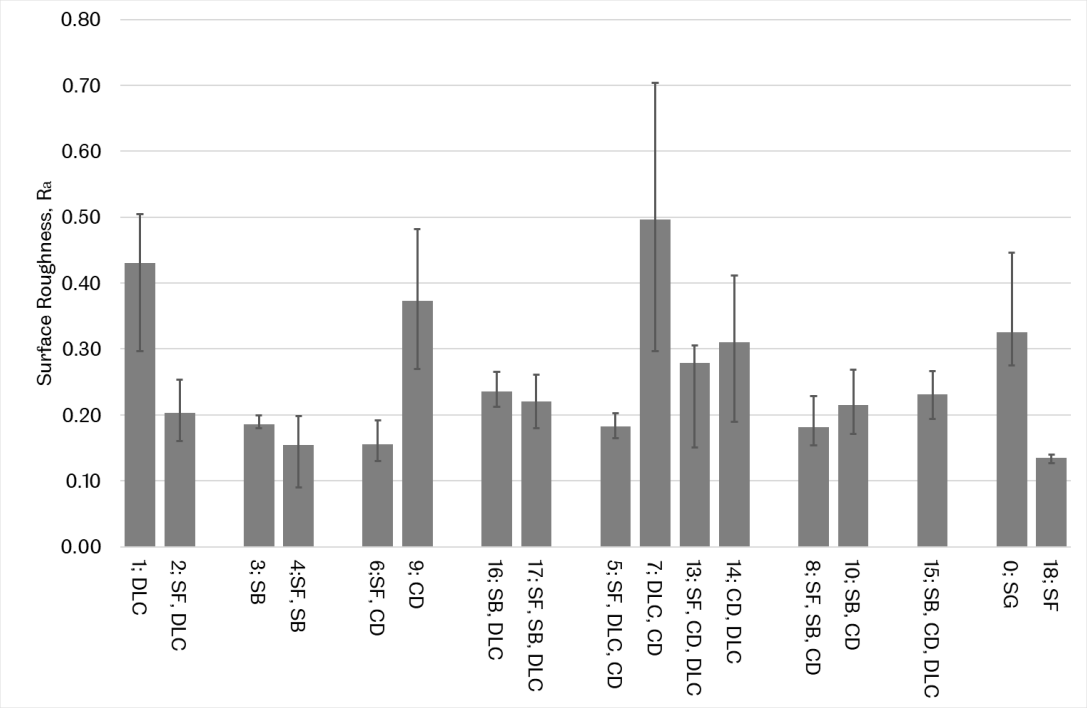

Figure 9-11, Surface Roughness of Multi-Layer Surface Treatment Specimens

9.2.4 *Coating Hardness*

The hardness of groups of multi-layer surface treatments were obtained using a micro hardness tester, with a load of 0.1 kg, as described in Section 7.4.1.3. The hardness measurements for specimen 0 (SG reference specimen) where taken using a different machine and a higher load of 20 kg.

Figure 9-12 shows the results for hardness measurements. Manufacturer reported hardness values for DLC are 1600 Hv (0.05). The difference in readings in this case is attributed to the different load used.

Five measurements were taken for each specimen, apart from specimen 0, where only three readings were taken. The average results for specimens 2 (SF, DLC) and 17 (SF, SB, DLC) only include three of the measurements taken. For specimen 2, the

variation in results was 681 Hv; two numbers were either very large (1600) or very small (919) and did not follow the trend of the other three values, this may be the result. This may be a result of in correct measurement technique. The range of measurements for specimen 17 was also large, at 729 Hv.

Results for specimen 17 show that shot blasting the specimen before applying a DLC coating makes little difference to the hardness. Shot blasting increases the hardness of the steel specimen, as can be seen by comparing specimens 0 and 4 (SF, SB); this is expected and the mechanism for this discussed in Section 5.2.2. Results also show that a layer of DLC under or on top of the chemical dip treatment increases the hardness of specimens compared with a single layer of chemical dip treatment.

Interestingly, applying DLC before the chemical dip resulted in a harder surface than when the application order was reversed; results are however reasonably close together and it does not appear to make a significant difference if the spread of results is considered. The relevance of these results in combination with wear test results are discussed in more detail in Section 9.3.

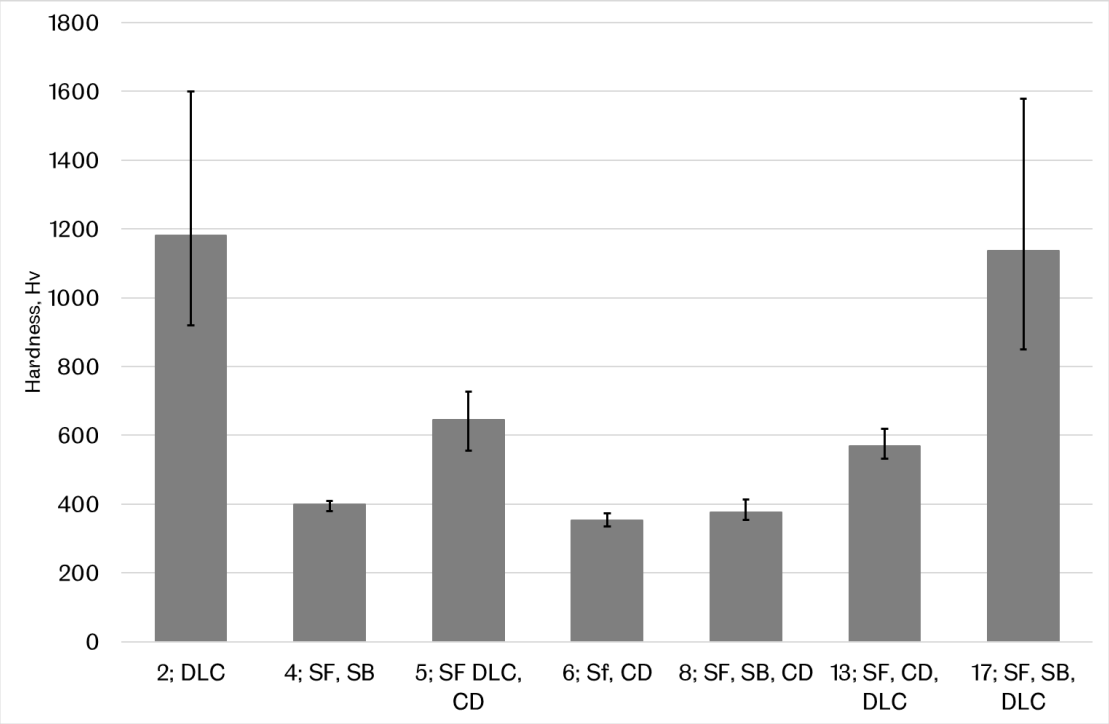

Figure 9-12, Vickers Hardness Values for the Eight Groups of Coatings

9.2.5 *Element Analysis for the Chemical Dip Surface Treatment*

The exact composition of the chemical dip surface treatment is unknown. Elemental analysis was attempted and has proved difficult as the layer effected by the chemical dip is very thin, possibly around 0.1 µm (Figure 7-14). Information provided by the academic partner suggested that this chemical dip is calcium sulphate based. Figure 9-13 shows element analysis before a specimen went through the chemical dip process and Figure 9-14 shows the analysis after. The main difference between the two is the addition of calcium and sulphur detected.

Energy dispersive X-ray spectroscopy (EDS) was used to produce a layered image of detected elements for the surface treatment after testing, as shown in Figure 9-15. This revealed aluminium oxide particles embedded in to the surface of the substrate, with particle sizes ranging from around 1-2 µm. This is an unexpected result, as there is no indication of aluminium oxides in Figure 9-13 and Figure 9-14. The particle sizes appear to be too large to be left over from the polishing process (235), but this cannot be ruled out.

The absence of calcium is the most notable result. This is reasonably easy element to detect using EDS. It is thought that there may have been some interaction between the fatty acids in the bio-base stocks that leads to the decomposition of this coating. This is discussed in more detail in Section 9.4.6. The absence of sulphur is also notable, it may be that EDS was unable to detect this element due to a combination of its low atomic weight and the thin coating layer.

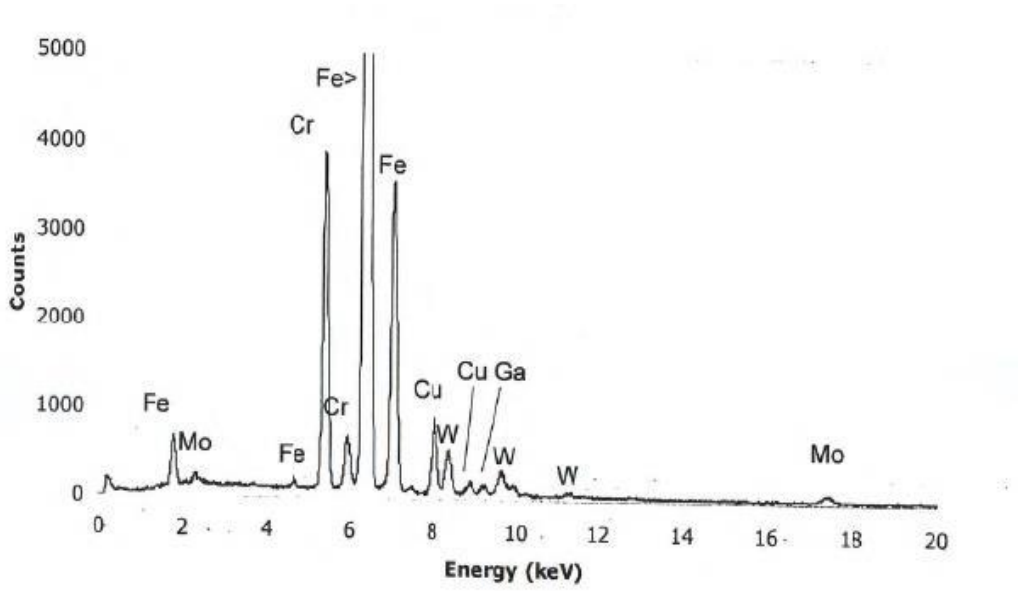

Figure 9-13, Element Analysis Performed on a Specimen Prior to the Chemical Dip Process with no Calcium Present

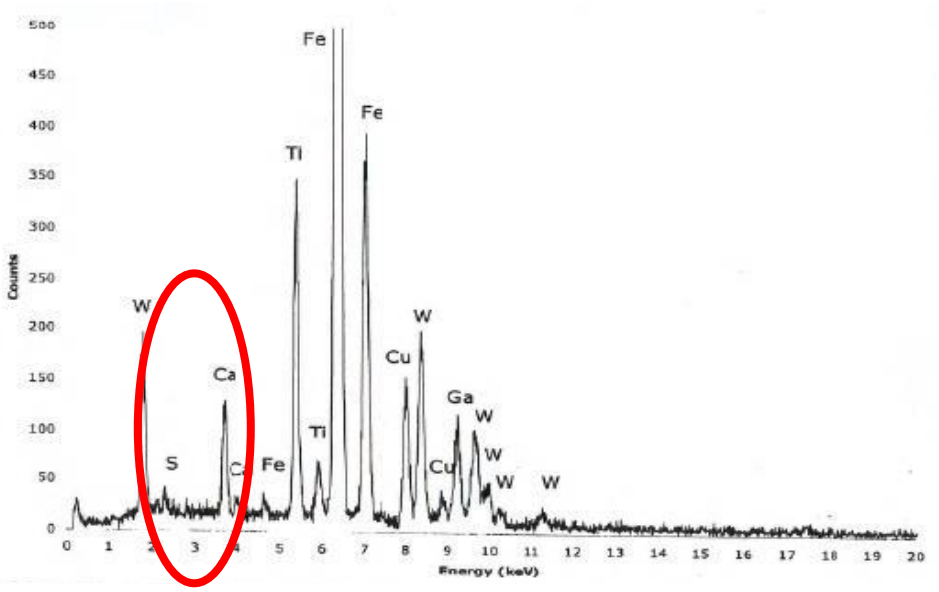

Figure 9-14, Element Analysis of a Specimen After the Chemical Dip Process, Showing Calcium Present

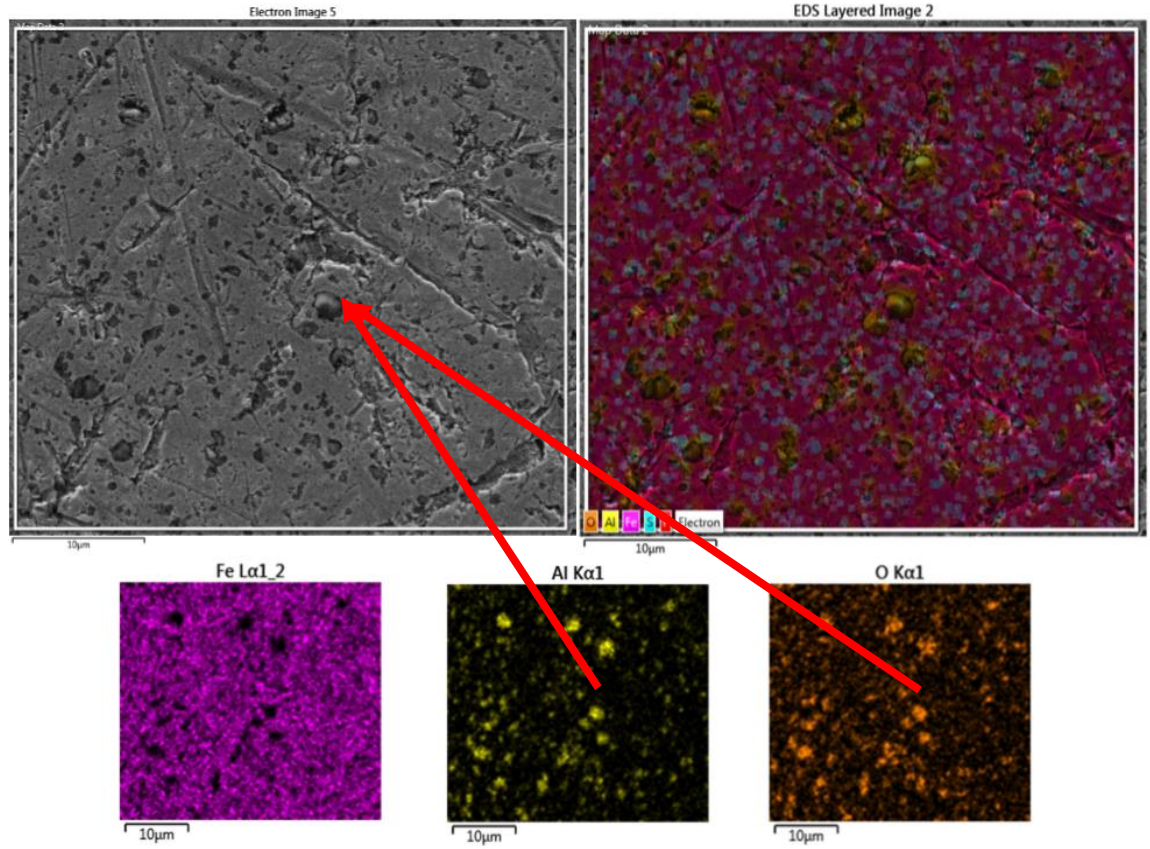

Figure 9-15, Energy Dispersive X-ray Analysis of Specimen 6 (SF, CD)

9.3 Comparing Substrate and Coating Effects

This section discusses the performance and results of tests with multi-layered surface treatments in a generalised way, irrespective of the lubricant used. The performance of specimens containing DLC is discussed first. Treatments applied in varying orders were: super finishing, shot blasting with a doping media and a calcium based chemical dip. Then, multi-layered surface treatments that have a calcium based chemical dip are discussed. Finally, the specimens that were only treated with shot blasting are discussed, to compare performance with multi-layer treatments.

9.3.1 *Diamond-Like-Carbon*

While wear is predominantly a surface effect, and therefore a coating's ability to resist wear is important, the combination of coating and substrate must be optimised for the given load carrying needs. The effects of a hard coating on a soft substrate, and vice versa, is well understood. Reciprocating wear tests were carried out with high contact pressures to accelerate wear. Test conditions have highlighted a weakness in the combination of a very hard DLC coating with a relatively soft substrate. Holmberg and Matthews (64) describe that, in these test conditions, tensile stresses behind the ball and compressive stresses in front of the ball result in material ploughing and increased shear stress, which contribute to frictional forces, as well as wear.

Figure 9-16 shows a cross sectional view of the DLC coatings, not in the wear scar region. Even outside the wear scar region, the beginnings of coating failure are visible, with cracking in the interfacial layer. The images shown in Figure 9-16 are from the underside of the specimen. The voids, seen more in specimen 2, could be caused by poor adhesion during the application. The adhesive critical scratch load for specimens 1 (SG, DLC) and 2 (SF, DLC) was calculated to be 33 and 35 N respectively.

As discussed in Section 9.1 and shown in Figure 9-18, specimen 2 had lower wear and friction values overall compared with specimen 1, and a combination of adhesive strength of the coating and surface roughness was responsible for this. A rougher surface will have more asperities that can be plastically deformed and therefore increase friction. As discussed Section 5.2.1.2. Wang et al. (142) found that the substrate finish influenced the surface finish of the coating. Imperfections in the substrate could be mirrored in the coating, and these contribute to wear and spalling. As discussed in Section 5.2.1.3, links with substrate roughness and the type of crack that forms in the coating were made. With rougher surface having more radial cracks while smoother surfaces had more ring cracks. Therefore the substrate dictates the type of wear and likely failure mechanisms for coatings. For specimen 1, with a SG substrate and rougher coating finish R_a of 0.43 µm, while specimen 2 had a R_a of 0.203 µm. It is proposed that the dominant wear in SG substrate coating combinations is caused by plastic deformation of asperities and adhesion, while for SF substrate coating combination the dominant wear is caused by spalling and delamination caused by ring cracks. Imaging techniques were not detailed enough to observe the types of cracks formed, as shown in Section 5.2.1.3, Figure 5-3.

Overall, specimen 1 saw some adhesion and plastic deformation of the surface grinding marks and some abrasion in the wear track. Some cracks parallel to the surface was visible, but not many. Figure 9-17 shows a typical wear scar for 1 and 2. With specimen 2, however, there was significant cracking visible in the wear track, and distinct layers were visible, showing wear through the interfacial layers and

thinning of the coating. This reinforces the proposed spalling dominant wear mechanism for smoother surfaces, while rougher surfaces suffer plastic deformation of asperities as an initial dominant wear mechanism. Wear mechanisms and figures showing wear in the wear track, related to each base stock tested, are discussed in more detail in Section 9.4.

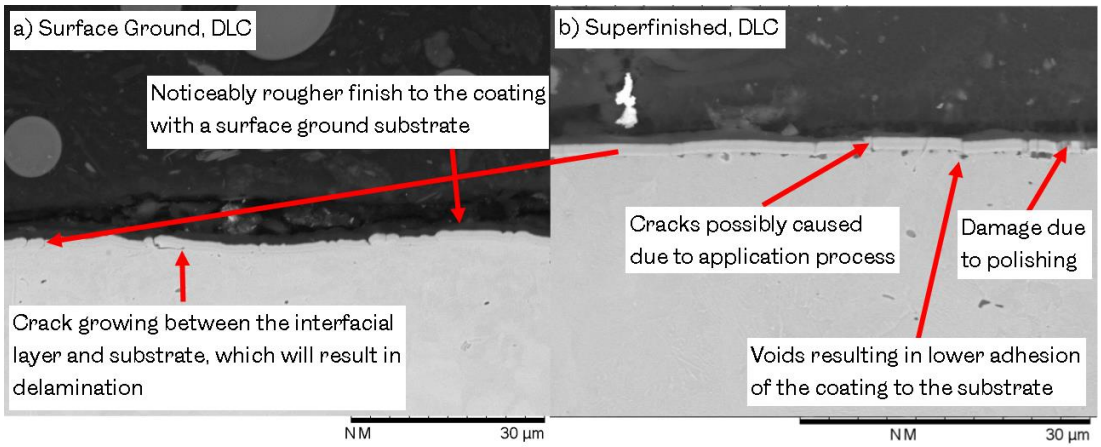

Figure 9-16, A Cross Sectional View of a) the Surface Ground Substrate with DLC and b) Superfinished Substrate with DLC

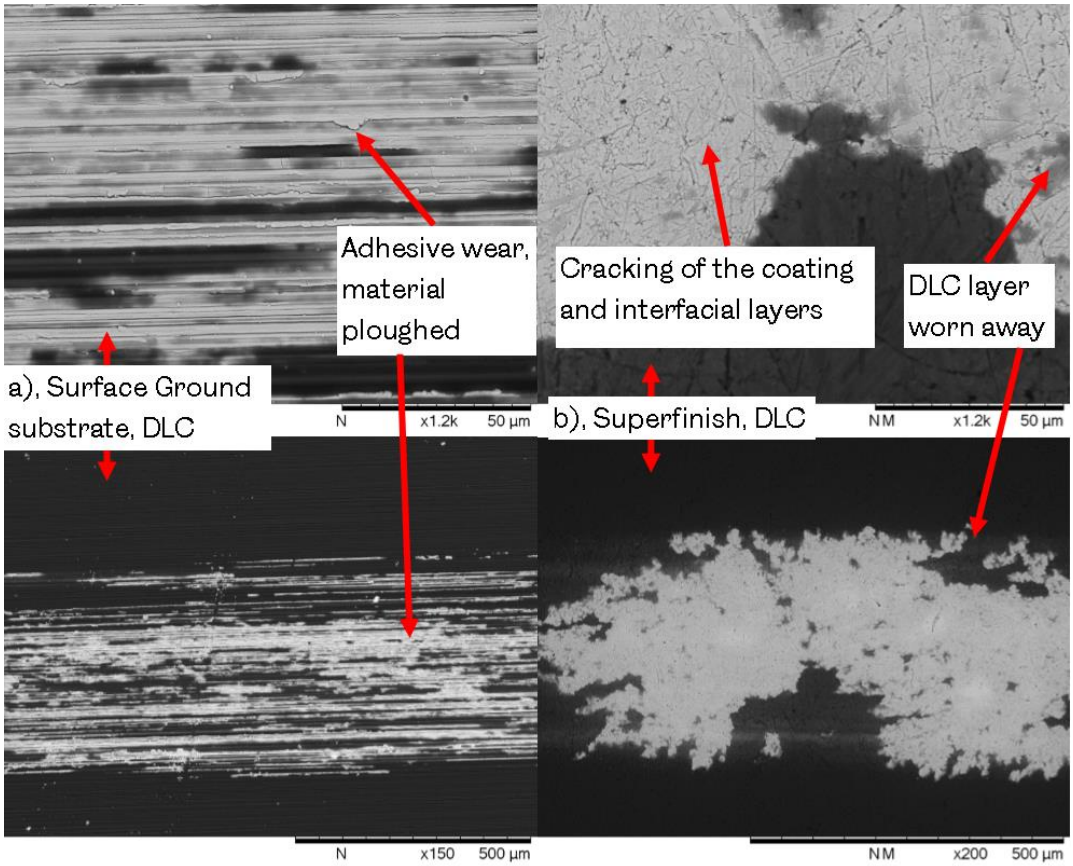

Figure 9-17, Typical Wear Scars Highlighting the Difference Between a) Surface Ground and b) Super Finished

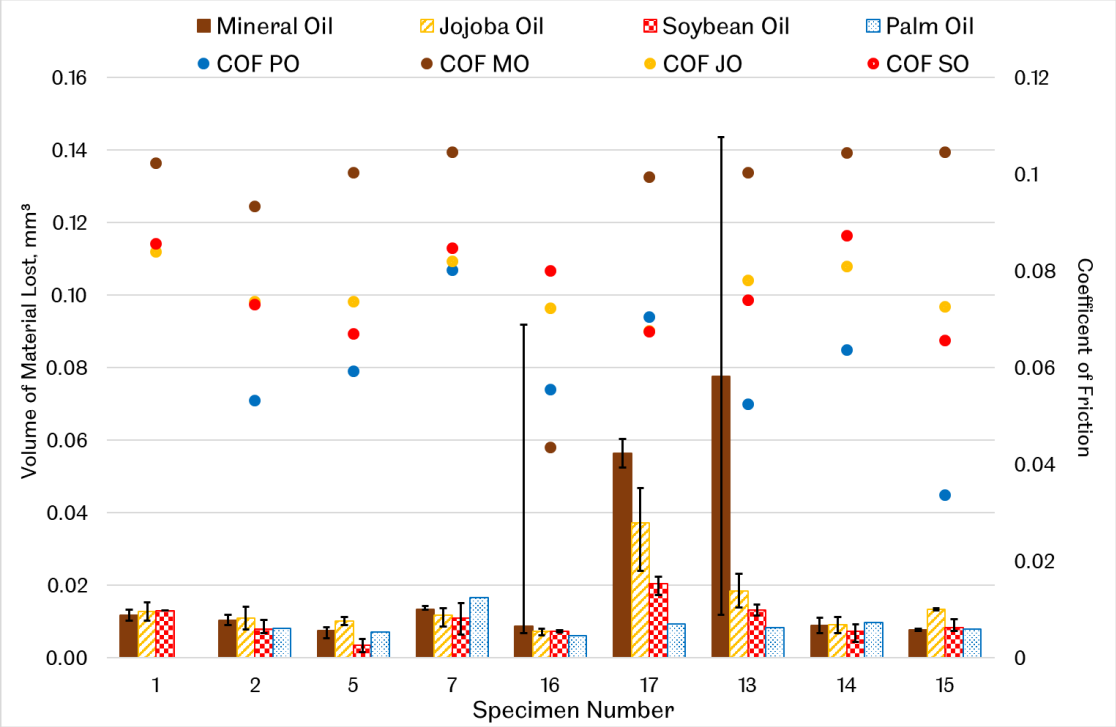

Figure 9-18, Wear and CoF results for Specimens with DLC in the Multi-layered Treatment

9.3.2 *Diamond-Like-Carbon with Ultra-Fine Shot Blasting*

Specimens 16 (SG, SB, DLC) and 17 (SF, SB, DLC) were shot blasted with MoS_2 before DLC was applied. This technique left a random surface texture with an R_a of between 0.15 – 0.19 µm without a coating applied, which is less rough than the surface ground finish, which had an R_a of 0.33 µm. The application of the DLC increased the R_a to 0.24 and 0.22 µm respectively for specimens 16 and 17. For specimens 16 and 17 overall CoF values were lower than for specimens 1 (SG, DLC) and 2 (SF, DLC), and wear was only lower with specimen 16, as seen in Figure 9-18. Specimen 16 had a similar adhesive critical scratch load as specimen 2, of 35.2 N, showing no reduction in the adhesion of DLC by using a solid lubricant doping media on the substrate first. The reduced coating adhesion in super finished specimens compared with the same coating combinations on a surface ground substrate could be due to a reduction in actual surface area for the interfacial layer to adhere to. This trend is seen with all specimens with substrates that have rougher finishes.

These results show that, in a lubricated contact, a certain amount of surface texturing can improve wear and friction performance. This is attributed to the surface texture creating wells in the surface that can act as lubricant reservoirs, as discussed in Section 6.3 and also proposed by Pattersson & Jacobson (143). Figure 9-19 highlights that the surface finish of specimen 16 is more 'wavy' and therefore potentially acting as a lubricant reservoir.

Matsui & Kakishima (148) showed that using an MoS_2 doping media reduced the CoF in shot blasted specimens, as discussed in Section 6.3. There was a reduction in CoF overall with shot blasted DLC specimens compared with just DLC; this result is not

thought to be significant if the experimental spread of results is considered. The DLC covered any MoS_2 left on the surface from this treatment, but the benefit of this is that, if the DLC coating is removed, there is an extra layer of protection. Therefore, the CoF reduction in this case is not due to MoS_2.

The coating layer on both specimens in Figure 9-19 shows substrate surface imperfections, such as cracks; the compressive stresses induced by shot blasting could have acted to terminate crack growth. There are small areas with no coating visible at all in areas of substrate inclusions. The coating may have been removed in these areas during polishing, this would indicate weak adhesion of the coating due to shadowing effects in the PVD application process. The surface finish seen here, with inclusions surface cracks, is seen with all specimens that were subject to shot blasting. Surface ground specimens also possess a similar surface finish to super finished specimens, as seen in Figure 9-19.

The dominant wear mechanism observed with specimen 16 (SG, SB, DLC) was adhesion and plastic deformation, similarly to other surface ground specimens. Some abrasion was present in the wear track, which is likely three-body, as scratch tracks visible were visible. As with specimen 2 (SF, DLC) (discussed in Section 9.3.1) specimen 17 (SF, SB, DLC) predominantly suffered cracking and thinning of the coating; adhesion was also visible (similar to Figure 9-17). Wear mechanisms for the different lubricants tested are discussed in Section 9.4.5.

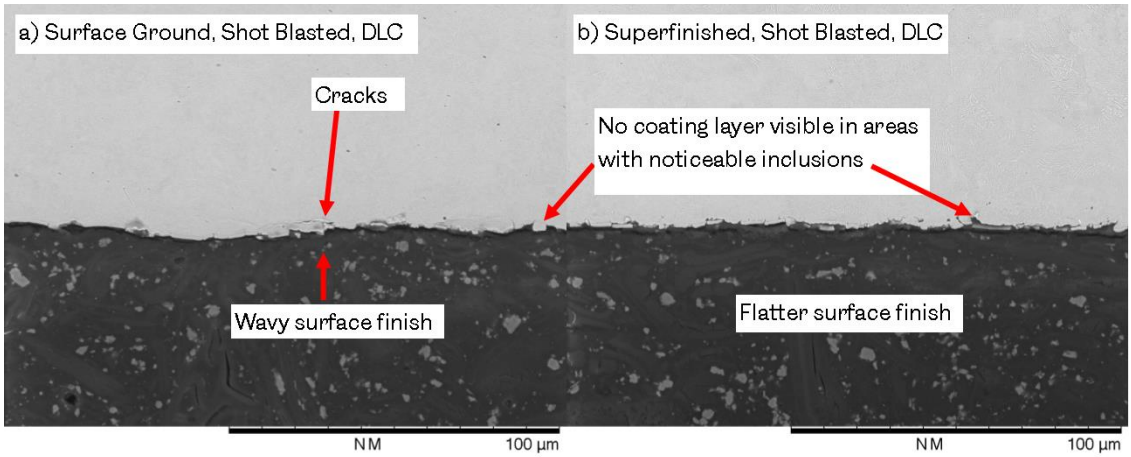

Figure 9-19, Cross Sections from a) Surface Ground, shot blasted, DLC Specimen and b) Superfinished, Shot Blasted DLC Specimen, Not in the Wear Scar Region.

9.3.3 *Diamond-Like-Carbon with a Chemical Dip Interfacial Layer*

Applying a chemical dip (CD) before the DLC coating led to slightly reduced adhesive critical scratch load in specimens, but the reduction was not large. Specimen 13 (SF, CD, DLC) had a load of 30.4 N and specimen 14 (SG, CD, DLC) 33.8 N. As mentioned in 9.1, the DLC on a super finished specimen had a lower adhesive critical scratch load. The hardness of the CD DLC multi-layer surface treatment was significantly reduced compared with a single layer DLC, as well as for SB, DLC combinations. The hardness (results in Section 9.2.4) of this coating combination was significantly lower, at 569 Hv, compared with either just a DLC coating, or shot blasting followed by DLC, with

hardnesses of 1130 Hv and 1137 Hv respectively. This is due to the higher ductility of the surface as a result of the CD treatment.

In general, specimen 14 had lower wear than specimen 13 (Figure 9-18); this can be attributed to lubricant wells in the rougher surface. There was no significant general variation in CoF for these two samples. Figure 9-20 shows similar DLC coating coverage as is seen with shot blasted specimens in Figure 9-19.

As with the single layer DLC specimens discussed in Section 9.3.1, the surface ground specimen 14 predominantly suffered plastic deformation of the grinding marks, with adhesion also visible in the wear track (similar to Figure 9-17). There was no indication of abrasive wear with this specimen. Specimen 13, like its super finished counterpart in Section 9.3.1, suffered thinning of the coating; there were significant cracks and flaking or spalling of coating layers visible, and the varying layers of DLC and Cr/CrC interfacial layers were revealed in the wear track. No abrasive marks were observed.

A review of literature found no work that looked at the performance of DLC with a calcium sulphate CD applied to the substrate first. As already suggested, it is unclear what bonding occurs between DLC and CD. Combinations of specimen 14 (SG, CD, DLC), and specimen 16 (SG, SB, DLC) did not change wear rate compared with just SG or SF DLC. The variation in lubricant performance meant results with specimens 13 and 17 could not be directly compared, this is discussed in 9.4.5. The wear rate of specimen 6 (SF, CD) was comparable to specimens 14, 16, 1 and 2.

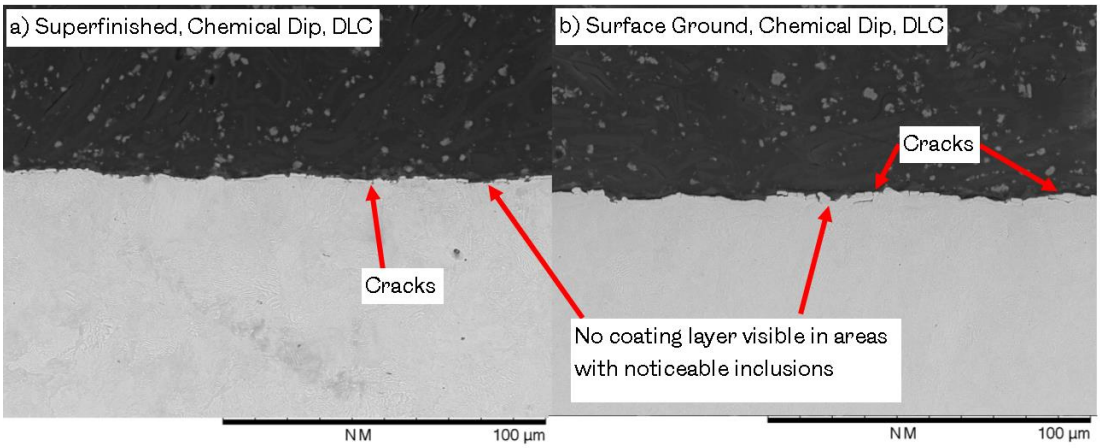

Figure 9-20, A Cross Sectional View of a) Superfinished, Chemical Dip, DLC Specimen and b) Surface Ground, Chemical Dip, DLC Specimen

9.3.4 *Diamond-Like-Carbon with a Chemical Dip Outer Layer*

Specimens 5 (SF, DLC, CD) and 7 (SG, DLC, CD) had a reversed layering order to those discussed in 9.3.3. Figure 9-21 shows a cross section of specimens 5 and 7 compared with 13 (SF, CD, DLC) and 14 (SG, CD, DLC). Some coating damage is thought to be caused by the polishing process in preparing sectioned specimens. When DLC is applied before the CD, the resulting coating layers look very similar to that seen with just a DLC coating in Figure 9-21. More voids are visible with specimen 5 than 13; these voids are also seen in specimen 2 in Figure 9-21. The application of a surface treatment, such as SB or CD, results in fewer voids. These voids may have been created in the application process; an extra interfacial layer using CD may have

reduced the impact of stresses induced in the coating and substrate on cooling. CD applied before the DLC did, however, result in a less even DLC layer with more cracking. The adhesive critical scratch load for specimen 7 was 36.3 N, the highest critical scratch load of all the specimens containing DLC. As can be seen in Figure 9-21, specimen 7 has considerably fewer voids, therefore a greater contact area between the coating and substrate, and higher substrate adhesion.

In terms of tribological performance, specimen 5 offered the best wear protection in comparison with all the specimens shown in Figure 9-21, as well as slightly lower CoF, although CoF values were all very close. The voids seen under the coating in specimen 5 have not affected performance in these short wear tests, but it may be that, with long term cyclic loading, these voids could become sites of crack growth in the interfacial layers and lead to delamination. The hardness of the DLC, CD coating group was measured at 645 Hv, lower than just DLC, but slightly higher than when the layer order is reversed and still within the experimental spread (results in Section 9.2.4).

Specimen 7 had the highest surface roughness of all specimens tested, at 0.5 µm Ra; this did not result in a significant detriment to wear protection, however, as Figure 9-18 shows. This contradicts the literature, where a correlation between surface roughness and wear is reported (94) (96) (97). The reason may be that the use of lubricants meant there were more factors influencing CoF and wear than just surface topography. Rougher coatings may have dominant wear mechanisms, such as abrasion and asperity fatigue, instead of adhesion. In lubricated contacts, and as discussed in Section 6.3, some degree of surface roughness was found to be beneficial, as it caused hydrodynamic lubrication to occur at a wider range of loads and speeds (148) (149) (150) (151). There is an optimal surface roughness, whether from surface grinding, or uniform patterns, and this will be dependent on the system it is applied to. There is evidence that, if the surfaces are too rough, it affects lubricant wetting and increases CoF, and for hard coated surfaces at risk of lubricant starvation, it may cause increased abrasive wear (148) (149).

The same differences in wear mechanisms can be seen with super finished and surface ground specimens 5 and 7, as with those reported in Sections 9.3.1 and 9.3.3, namely specimens 1, 2, 13 and 14.

The addition of a soft layer over DLC acted as a low shear layer to reduce wear and protect the DLC from abrasion and adhesion. SEM analysis of the wear track reveals some thinning of the DLC coating; this is discussed in more detail in Section 9.4.5 in relation to the different base stocks tested.

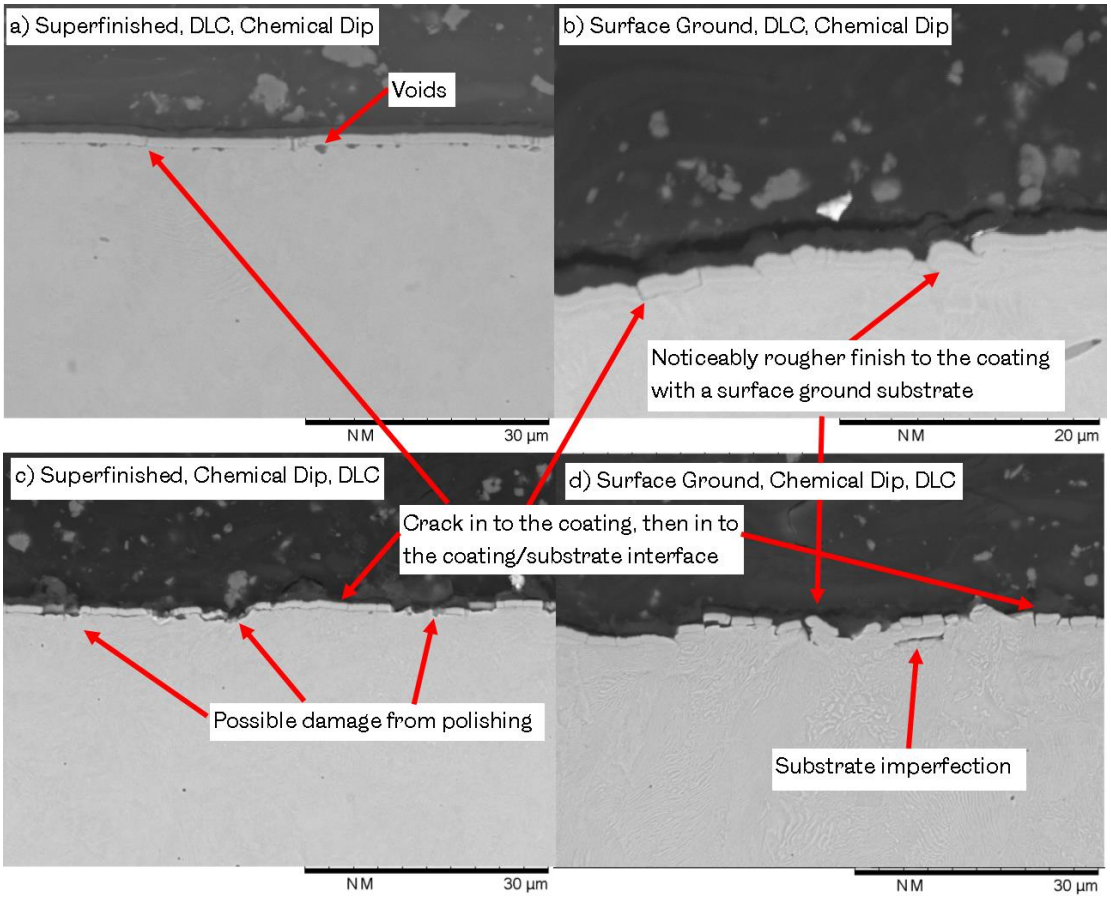

Figure 9-21, Cross Section of a) Superfinished, DLC, Chemical Dip Specimen, b) Surface Ground, DLC, Chemical Dip Specimen c) Superfinished, Chemical Dip, DLC Specimen and d) Surface Ground, Chemical Dip, DLC Specimen

9.3.5 *Diamond-like-Carbon with Shot Blasting and Chemical Dip*

The final specimen tested with DLC was specimen 15 (SB, CD, DLC). Comparing this with the other combinations of DLC, CD and SB, on SG substrates, (specimens 14 and 16), wear performance between these are comparable, as Figure 9-18 shows. Specimen 1, (SG, DLC) had the highest volume of material removed. This specimen also had the highest surface roughness, at 0.43 µm R_a, while specimen 15 had the lowest at 0.23 µm R_a. CoF was generally slightly lower with specimen 15. The coating adhesion was slightly improved compared with SB under DLC (25.2 N), or just DLC alone (34 N). This shows there are marginal tribological performance improvements by applying these three surface treatments, compared with only DLC, or SB or CD before DLC.

Figure 9-22 shows a cross sectional view of specimen 15. Specimens that had CD applied to the substrate have less surface imperfections visible, less cracking and inclusions. It appears that CD acts to smooth the surface of SG specimens, as does SB. This is clear from surface roughness data presented in Section 9.2.3. As with other specimens that have a treatment applied before DLC, there is more cracking and uneven coverage than with specimens just coated in DLC. These areas where there is no coating could propagate delamination of the coating.

The wear mechanism present in specimen 15 overall was thinning of the coating, particularly at the peaks of the surface roughness, induced by shot blasting. Spalling was also observed, as highlighted in Figure 9-23 and some adhesive marks in the direction of motion.

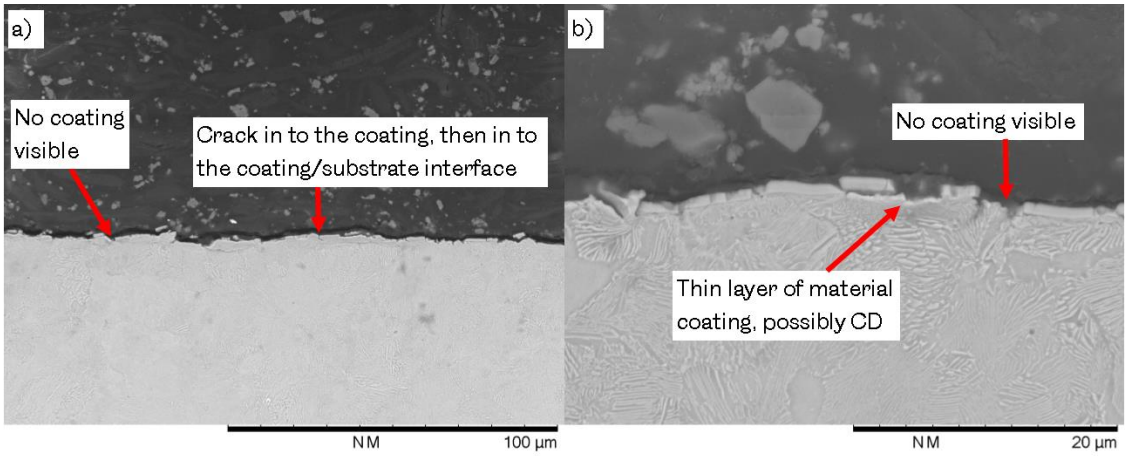

Figure 9-22, A Cross Sectional View of the Surface Ground, Shot Blasted, Chemical Dip, DLC Specimen at Different Scales a) 100µm and b) 20µm

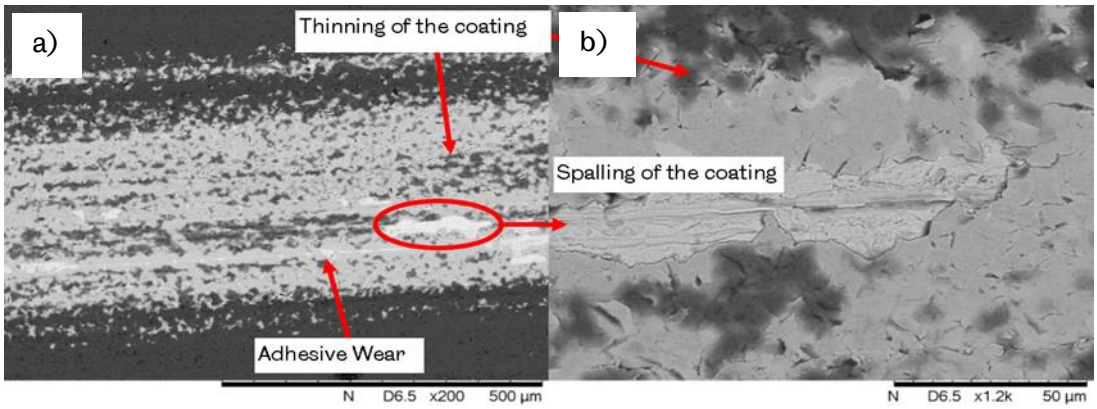

Figure 9-23, An Example of a Wear Scar for the Surface Ground, Shot Blasted, Chemical Dip, DLC Specimen, *Tested with JO, which Exhibited the Highest Wear for this Coating, a) 500 µm and b) 50µm*

9.3.6 *Crack Growth and Cracks in the Diamond-Like-Carbon Layers*

Cracks start because of imperfections such as broken bonds at interfaces, voids and inclusions, as shown in the cross sections of specimens in Sections 9.3.1 to 9.3.5. Surface cracks propagate into coating and interfacial cracks propagate in the interface direction, growing in the opposite direction to load displacement (64). Cracks grow from rough surface features like grinding marks, as well as on large peaks, and result in spalling; this can be seen in specimen 1 in Figure 9-16 as well as in Figure 9-24. The lubricants used may also have contributed to crack growth, due to the hydraulic pressure they applied when the lubricants were pushed into surface cracks under the high contact pressures, thus opening and growing the crack. Crack growth in the surface ground specimens will have removed surface features, which

may have stopped cracks propagating into the adhesion layers, which is seen with super finished, smoother specimens, as shown in Figure 9-25.

Gong and Komvopoulos (236) modelled crack growth in multi-layer media; the most relevant findings from this were that the crack tips of cracks that grow in the outer layer must come very close to the next layer in order to cause plastic deformation. They found that the distance must be equivalent to around an eighth of the thickness of the layer the crack is growing in. CoF is dominant in the accumulation of plastic strain in the second layer. The maximum plastic strain increases rapidly as the crack tip approaches the interface, due to the high stress field at the crack tip, so that maximum plastic strain in the second layer is always right under the crack. As the CD layer is very thin, it is likely that any fatigue induced surface cracks spread to the DLC layer with relative ease. In specimens where CD is next to the substrate, this may help to prevent cracks travelling into the bulk material by deflecting cracks along the interface. Laukkanen et al (237) found that cracks initiate from the coated surface and not the interface between coating and substrate. The residual compressive stresses induced by SB act to stop these types of cracks growing.

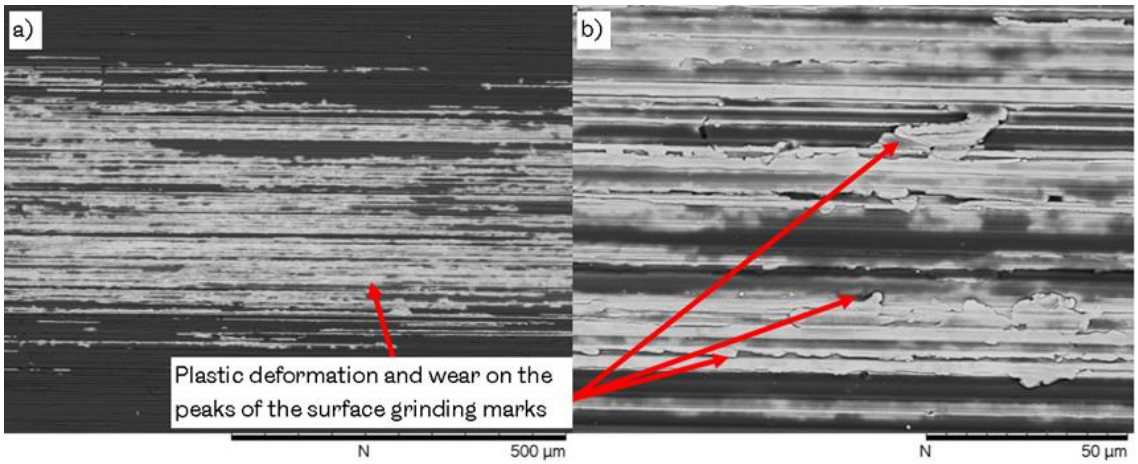

Figure 9-24, An Example of Typical Wear Features for Surface Ground Substrates with Multi-Layer Surface Treatments Including DLC, Showing the Surface Ground, Chemical Dip, DLC Specimen, Tested with JO, a) 500 µm and b) 50µm

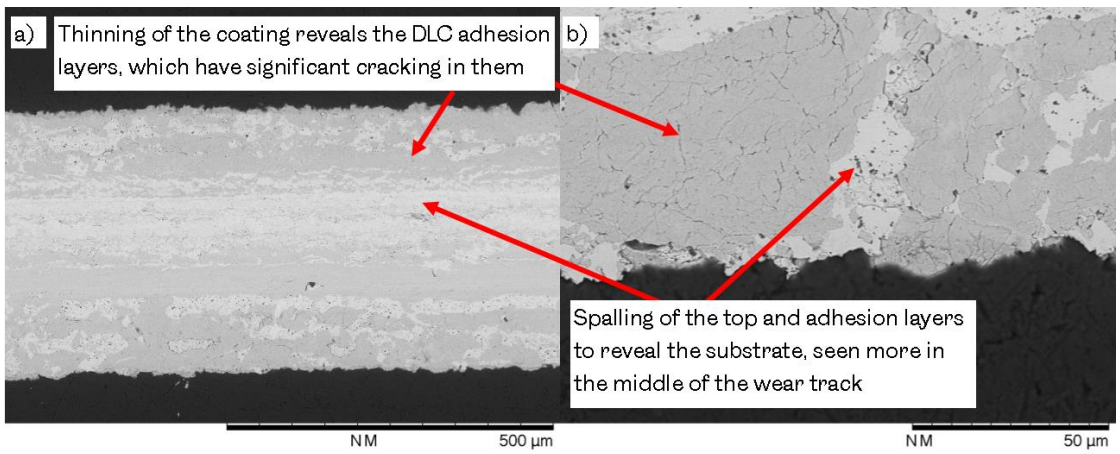

Figure 9-25, An Example of Typical Wear Features for Super Finished Substrates with Multi-Layer Surface Treatments Including DLC, Showing the Superfinished, DLC Specimen, Tested with JO a) 500 µm and b) 50µm

9.3.7 *Summary of DLC in Multi-Layer Surface Treatments*

There is some tribological performance benefit of applying either shot blasting with an MoS_2 doping media or a calcium based chemical dip to the substrate first, if the substrate finish is similar to a surface ground finish. If the substrate has a low surface roughness, such as a super finished specimen, applying layers of surface treatment underneath will have a detrimental effect on wear performance. Overall, no clear differences were observed in CoF for any of the specimens discussed in this section, this would indicate that the bio-base stocks tested are all equally compatible with the multi-layer surface treatments. The difference is CoF for the base stocks tested is discussed in Section 9.4.

The adhesion of DLC is not significantly affected by the application of surface treatment layers underneath, with the critical adhesive scratch load ranging from 30.4 N for specimen 13, to 35.2 N for specimen 16. Adhesion is improved when the coating order is reversed to have DLC as the first layer, with the highest adhesive critical scratch load for specimen 7 at 36.3 N.

The tribological performance of multi-layered surface treatments is improved by reversing the layer order to have DLC first and then CD, compared with CD then DLC, with lower wear and CoF values seen in those tests.

Further assessment of the durability of these coatings is required to fully understand the implications and assess any possible negative performance consequences of using multiple surface treatments. Longer duration wear tests and wear tests in carrying contact geometries would help to improve understanding of the durability of these coatings. Static immersion tests to assess the corrosion performance could provide more detailed understanding of whether the types of surface imperfection found, such as cracks and inclusions, would lead to delamination.

Taking a generalised view of the performance, irrespective of lubricant, these multi-layer coatings reveal that, of all the coating combinations with DLC, specimen 16 ((SG, SB, DLC) had the lowest wear with all the oils tested; it also gave low CoF values and had the highest critical adhesive scratch load. Close in wear performance was specimen 14 (SG, CD, DLC), although CoF values were not particularly low comparatively.

In terms of general wear mechanisms observed in the DLC group of coatings, these could be split into two distinct groups linked to the substrate finish. The surface ground group of coatings had predominantly plastic deformation and adhesion around the grinding marks; an example of this is shown in Figure 9-24 in Section 9.3.6. Some indication of three body abrasion was present with surface ground samples; this is as a result of hard wear particles, from coating failure, becoming entrained in the contact. The amount of wear caused by this mechanism was still found to be small.

It is interesting that the rougher surfaces performed well; the peak contact pressures were distributed over a smaller area, mainly the peaks of the grinding marks. This is obvious from the amount of wear these peaks show. The very hard DLC meant that this reduced area of contact did not have such a negative impact on wear protection. It is also likely that the troughs have acted as lubricant and wear debris reservoirs to aid retention of the lubricant in the contact area. As discussed in Section 6.7, Prabhu et al. (170) found that up to an R_a of 0.5µm lubricants had improved spreading, as the

contact angle of the drops of lubricant on the surface was lower; the R_a for all the specimens tested was below 0.5µm, therefore was within the optimal spreading zone in terms of surface roughness. Longer tests with assessment of coating performance at defined intervals would reveal if after longer testing, the wear mechanism becomes more like the SF specimens. This is needed for a better understanding of how such coating may perform if they were used in internal combustion engines.

The DLC coated specimens that had super finished substrates all showed cracking, thinning of the coating, spalling and delamination. An example of the typical wear features from this set of coatings is shown in Figure 9-25 in Section 9.3.6. These features are due to the level of lubricant retention is poorer for smoother surfaces, as well as the cracking mechanism discussed in Section 9.3.1. There are no 'peaks' such as with surface ground specimens, to plastically deform and protect the bulk of the coating. As discussed in Section 9.3.6, these peaks may have also prevented significant cracking occurring and could be seen as sacrificial surface features.

9.3.8 *The Performance of Calcium Based Chemical Dip*

This coating is of particular interest because it has shown similar performance to the DLC surface coatings. The mechanism behind the tribological performance of this surface treatment is not fully understood; further discussion of this is in Section 9.4.6, as the type of lubricant used is thought to have a significant influence on performance.

Specimens in this group of surface treatments were specimen 9 (SG, CD), 6 (SF, CD), 8 (SF, SB, CD) and 10 (SG, SB, CD). Specimen 6, compared to its SF DLC counterpart, had improved wear protection, while CoF was generally similar. This treatment had the lowest hardness out of all the specimens tested. SB before applying this treatment slightly improved the hardness but, if the experimental spread is considered, there is no real improvement, as can be seen from Figure 9-7 in Section 9.2.2.

When compared with specimens that had only the CD applied (6 & 9), the addition of DLC under CD (5) increased volume losses in wear tests. Section 9.4.5, Figure 9-37 shows SEM images of the wear track for 5. This increased wear could be due to the eventual spalling of the DLC layer, which gave hard wear particles and accelerated wear.

The dominant wear mechanisms for the CD group of coatings were adhesion and plastic deformation. Specimen 6 (SF, CD) is shown in Figure 9-26, with adhesion visible across the wear scar; volume losses were relatively low and so was the severity of adhesion. Figure 9-27 shows a typical wear track for specimens 8 and 9; this shows the level of adhesion is greater and plastic deformation at the edge of the wear track, and the peaks of grinding marks are visible. The plastic deformation observed with these specimens indicated the outer material is ductile.

Specimen 10 had the highest adhesive scratch load, at 38.6 N, of all coating combinations tested. It is, however, unclear whether scratch testing is a valid method for assessing the adhesion properties of the CD treatment, as discussed in Section 9.1. MoS_2 does not bond with Al_2O_3 (238), but there was no loss in adhesion of the coating for specimen 10. This could mean that a scratch test is not a suitable method for assessing the integrity of this coating group. Al_2O_3 may in fact be a contaminant and not present in large enough quantities, it may also have been disrupted by the SB process.

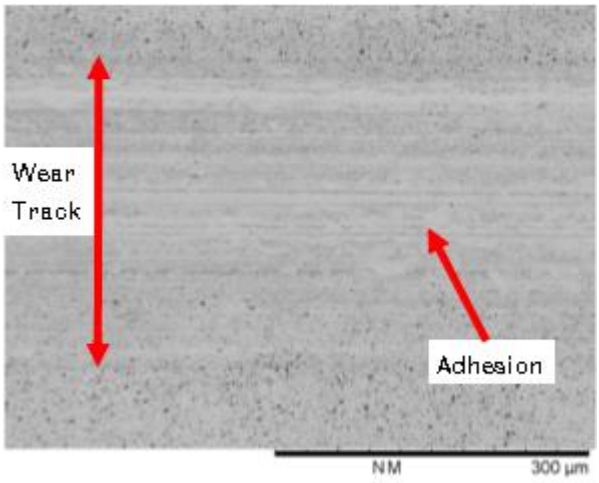

Figure 9-26, An Example of a Typical Wear Track for the Superfinished, Chemical Dip Specimen, Tested with SO

Not enough is known about the CD surface treatment, such as the application process and its bonding potential with other materials. The mechanical properties, such as Young's modulus, toughness, thermal expansion coefficients, are needed to give an absolute explanation for its performance. Softer layers, such as the CD, under DLC may act to dissipate energy and reduce plastic deformation (64). A softer layer above DLC may offer the same protection and prevent voids from propagating cracks, as internal and applied stresses are distributed through the layers (239). The application of CD under DLC might also help with any thermal expansion issues that arise from the DLC application process.

It is also unclear what type of bonding is present between the CD and DLC, whether there is a strong bonding between the layers, or a layer of mixed phase of the two materials is present or a weakly bonded layer. The double bonded oxygen molecules in calcium may form a bond with the dangling hydrogen orbital bonds when CD is applied over DLC. Analysis of the interface would aid understanding of how these multi-layers work in the transition region.

The inner layers next to the substrate need to have good adhesion properties; any other inner layers should also control the hardness and strength of the coating, and the outer layer of the coating needs to be optimised for wear and friction reduction. In the case of lubricated contacts, the outer layer would benefit from the ability to form bonds with lubricants to aid chemisorbed film generation. It appears that CD may interact with the base stocks tested; further discussion on this point is presented in 9.4.6.

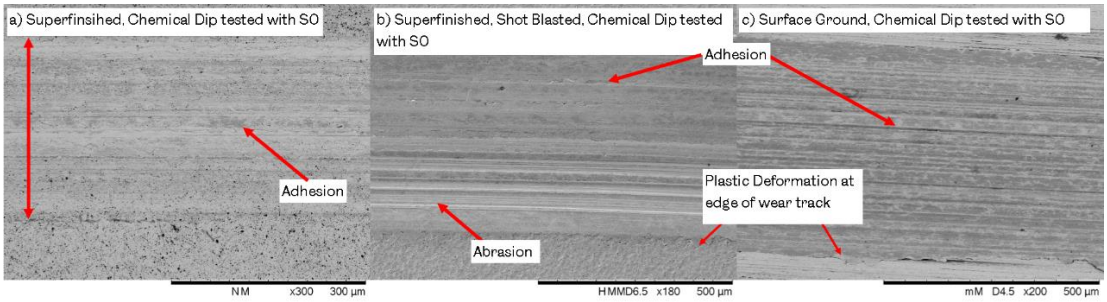

Figure 9-27, An Example of a Typical Wear Track for a) the Superfinished, Chemical Dip Specimen Tested with SO, b) the Superfinished, Shot Blasted, Chemical Dip Specimen Tested with SO and c) the Surface Ground, Chemical Dip Specimen Tested with SO

9.3.9 *Ultra-Fine Shot Blasting*

Two specimens had just a SB surface treatment prior to testing. This treatment had a solid lubricant MoS_2 doping media to aid lubrication. The performance of this surface treatment is discussed in more detail in Section 9.4.7, as the wear protection with this treatment varied considerably based on the lubricant used. There was no real improvement in tribological performance when applying SB before a CD treatment, with higher wear rates seen in specimens that were SB before having CD applied.

Shot blasting before applying DLC only gave tribological performance improvements for specimens that had a SG substrate, as discussed in Sections 7.3.2.5 and 9.3.5. This can be attributed to a better surface finish with shot blasted specimens, with lower surface roughness, as can be seen in Figure 9-11 in Section 9.2.3.

As with other SG specimens tested, some abrasion was visible in specimen 3, with removal or plastic deformation of the peaks of the surface grinding marks, as seen in Figure 9-28. Plastic deformation was observed at the edges of the wear track. With specimen 4, plastic deformation, or polishing of the surface features left by shot blasting, was the main wear mechanism present, as with other SF specimens tested. The plastic deformation observed with these specimens indicated the outer material is ductile.

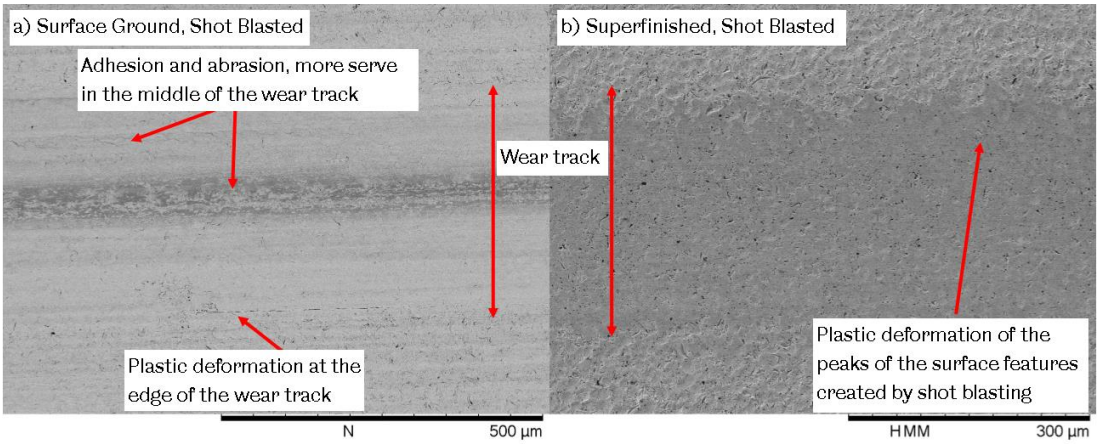

Figure 9-28, An Example of as Typical Wear Track for a) the Surface Ground Shot Blasted Specimen, Compared with b) the Superfinished Shot Blasted Specimen, both Tested with Jojoba Oil.

9.3.10 *Nano Fullerene Coating*

As discussed in Section 7.3.2.7 and 9.2.1.2, the nano fullerene coating did not adhere well to the substrate and did not perform well in wear tests in terms of volume lost, compared with other coatings. It performed poorly as the coating failed to adhere properly to the substrate. A dip method of application was used; this was performed by the external academic partner. Untested specimens had a 'flaky' and patchy finish, as Figure 7-15 shows in Section 7.3.2.7. After testing, in the contact region the coating was completely removed, and the coating surrounding the contact region showed flaking and blistering, as can be seen in Figure 9-29. The high wear for these specimens is attributed to three body abrasive wear, highlighted in Figure 9-29, with abrasive scratches visible in the wear track.

Specimen 11 had SB applied before the fullerene coating. This only produced smaller wear scars for PO compared with specimen 12, while wear increased with the other base stocks. This could be attributed to the thin hard layer on the surface of the substrate, due to SB, producing harder wear debris.

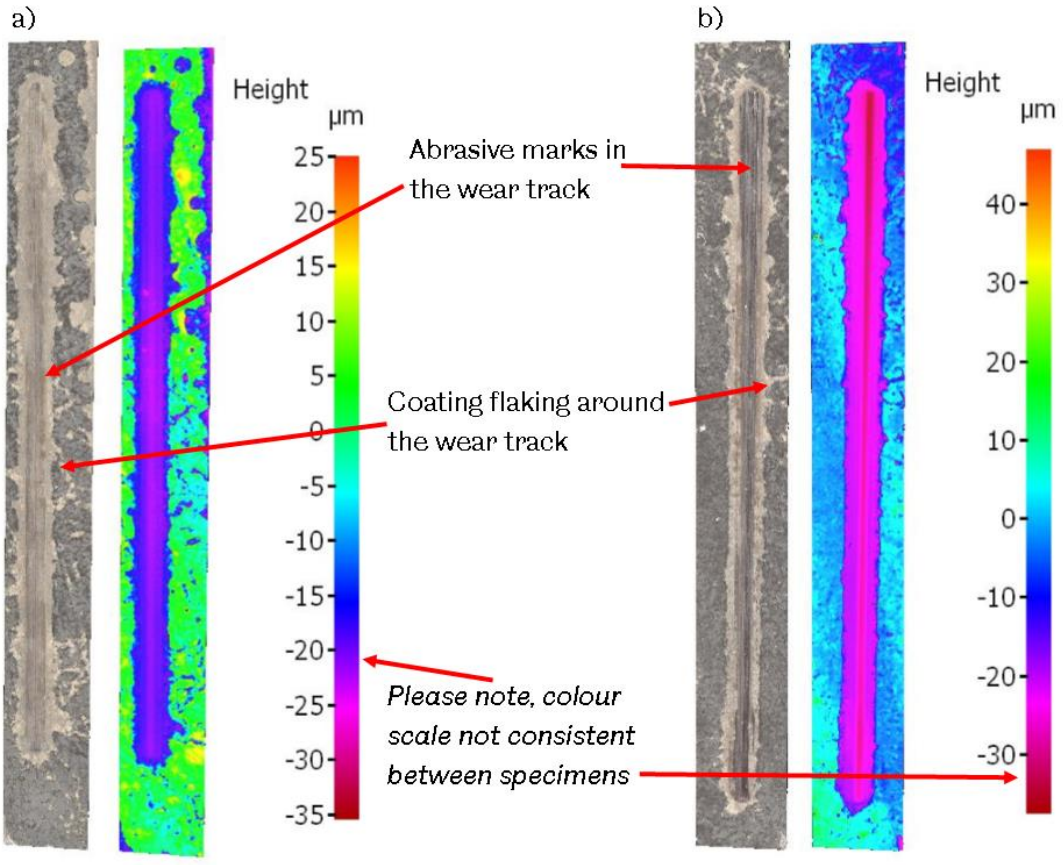

Figure 9-29, a) Wear Track for the Shot Blasted Nano Fullerene Specimen, b) Wear Track for the Nano Fullerene Specimen, both Tested with MO

As discussed in Section 9.2.1.2, while the volume of material lost in wear tests was an order of magnitude higher than with the other coating combinations, the CoF, particularly with JO and SO, were some of the lowest observed. The nano fullerene coating was made up of agglomerations of spherical carbon atoms. From the SEM image shown in Figure 9-30, these spherical arrangements can be seen to be

approximately 0.25 µm, individual fullerenes are in the order of 1 nm (240). There could be up to 250 individual fullerenes in each of the visible spheres in Figure 9-30.

Alberdi et al. (156) described a process of exfoliation and oxidation of the fullerene structure, at high pressures, which provided lubricity. This exfoliation was described on a nanometre scale. This exfoliating mechanism may have occurred in the contact region, Figure 9-29 clearly shows removal of the coating. Due to the poor adhesion of this coating, the exfoliation mechanism is likely to have occurred on a larger scale, with larger agglomerations of fullerene being removed during wear tests. It is hypothesised that, when these agglomerations exfoliated in the contact region, they may have acted as a shearing layer and aided the reduction of CoF. Once the agglomerations, now wear debris, left the contact region, they may have been re-entrained, no longer in the spherical arrangements, and therefore acted as an abrasive to remove any remaining coating and wear away substrate material. These agglomerations were large compared with those Alberdi et al. tested; their impact as wear debris would be considerable compared with exfoliated fullerene structures that are in the order of nanometres.

The CoF for nano fullerene were lowest for SO and JO for both specimens; wear was lower for these base stocks and specimen 12. The agglomerations of exfoliated fullerene could oxidise, they could also react with the highly polar carboxylic function groups. The –C=O bond is a hydrogen acceptor as shown in Figure 9-34. The fullerene could also have bonded at the site of the double bonds in the unsaturated fatty acid chains that make up SO and JO. PO being a saturated oil does not have any double bond sites for the fullerene to react with, neither has the paraffinic base stock used. This could explain the difference in friction performance. An examination of the altered fatty acid structures would be required to confirm whether this mechanism occurred. If this does occur, the fullerene wear debris is soluble in the oil and could act as a lubricant additive. As the agglomerations of fullerene molecules were large, this nano scale lubrication additive mechanism did not work effectively. In order for smaller scale exfoliation to occur, an improved adhesion method would be required, and potentially trying to produce such a coating with smaller agglomerations of fullerenes.

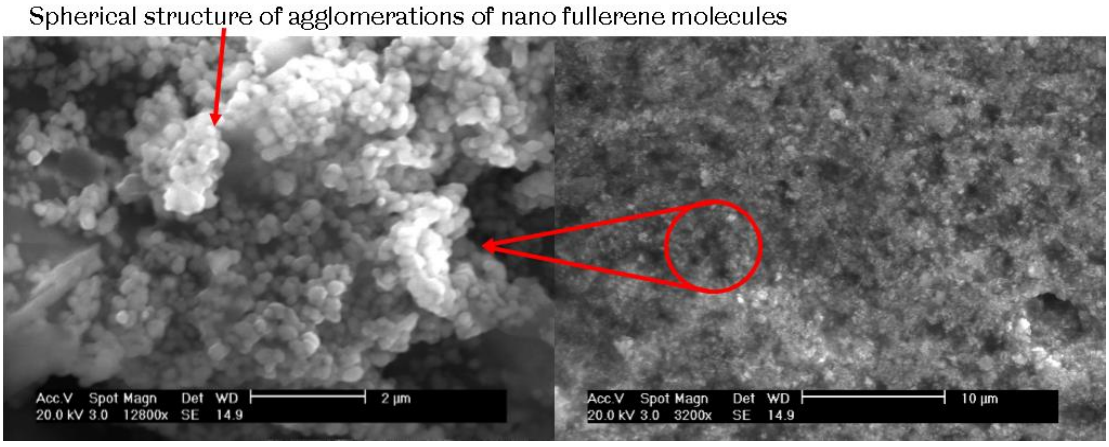

Figure 9-30, SEM Image of Agglomerations of Nano Fullerene Molecules in the Nano Fullerene Coating

9.4 Comparing the Performance of Base Stocks

This section discusses the performance of multi-layer surface treatments in terms of the different base stocks tested. Initially, a general comparison of the best surface treatments for each base stock is made. The performance of base stocks is then broken down into the surface treatments used; the interaction of the bio-base stocks with the steel reference specimens is described first. The discussion is then separated into DLC and calcium based chemical dip (CD), and finally the interaction of the base stocks with the molybdenum disulphate SB doping media is discussed.

9.4.1 *Fatty Acid Profile*

The fatty acid profile of base stocks, PO, JO and SO, were analysed using gas chromatography and performed by an external commercial laboratory (as detiled in Section 7.4.4). Unused samples were tested, as well as samples tested with specimen 18 (SF reference specimen). Oils used with specimen 18 were sent for analysis so that the change in fatty acid profile could be analysed without the complexity of considering any reactions with the coatings or coating wear debris that may have caused the oils' structure to change. The degradation of oils can be catalysed by the presence of metals, which is another justification for using specimen 18, which saw very low levels of wear. The changes in composition are therefore due to heat and the effects of being subject to shear loads. The fatty acid composition of vegetable oils dictated their tribological performance, as discussed Section 3.1.

Table 9-1, Table 9-2 Table 9-3 show the fatty acid profiles for SO, JO and PO. All fatty acids that had a great concentration then 1.5% are listed. Those fatty acids that made up less than 1.5% are included in 'other' unless their change is of significance, in which case they are listed.

Table 9-1 shows that over the course of a one hour test at 100 °C small changes in the fatty acid composition of SO occurred. With slight increase in saturated fatty acids, such as C16:0 and C18:0, as expected. The decomposition of unsaturated acids, such as C18:1 to C18:3, caused the increase in saturated fatty acids, as detailed in the stages of degradation in Section 3.7. The decrease in polyunsaturated fatty acids was caused by the transformation of these to trans fatty acids. Isomerisation (shifting of the double bond position) occurred with the transformation of cis and alpha configuration fatty acids as well as trans.

Soybean Oil		
Fatty Acid	Unused, %	Used, %
C16:0	10.7	11
C18:0	4	4.1
C18:1 (cis)	23.9	24.1
C18:2 (cis)	52.9	52.4
C18:3 (alpha)	5.9	5.8
Other	2.6	2.6
	g/100g	
Saturated Fatty Acids	15.2	15.5
Monounsaturated Fatty Acids	23.4	23.6
Polyunsaturated Fatty Acids	56.3	55.7

Table 9-1, Fatty Acid Profile for SO

Table 9-2 shows the change in fatty acid composition for JO. As with SO, there was a small increase in saturated fatty acids, such as C16:0 and 18:0, with the total saturated fatty acids increasing from 1.7 to 3.1 g per 100g. The decrease in monounsaturated fatty acid is caused by the beginning of polymerisation and increase in saturated fatty acids. The increase in polyunsaturated fatty acids is due to the increase in cis orientated double bonds, such as C18:1 and 18:2. Overall JO is still predominantly a mono unsaturated fatty acid oil.

Jojoba Oil		
Fatty Acid	Unused, %	Used, %
C16:0	1.2	1.9
C18:0	0.1	0.9
C18:1 (cis)	8.4	9
C18:2 (cis)	0.1	0.4
C20:1	72.2	70.2
C22:1	15.3	15
C24:1	1.8	1.8
Other	0.9	0.8
	g/100g	
Saturated Fatty Acids	1.7	3.1
Monounsaturated Fatty Acids	93.5	91.8
Polyunsaturated Fatty Acids	0.3	0.6

Table 9-2, Fatty Acid Profile for JO

The fatty acid composition of PO is shown in Table 9-3, it is predominantly a saturated fatty acid. Very little change in the composition of PO was seen. This is because it has a high proportion of saturated fatty acids. This means PO is in a way protected from first stage of decomposition most vegetable oils go through, in unsaturated fatty acids becoming saturated. The very small increase in monounsaturated fatty acids and reduction of saturated fatty acids may be an early indication of the onset of polymerisation.

Palm Kernel Oil		
Fatty Acid	Unused, %	Used, %
C8:0	1.7	1.7
C10:0	2.3	2.3
C12:0	40.8	39.9
C14:0	15.4	14.4
C16:0	12.4	12.5
C18:0	20.2	20.6
C18:1 (trans)	1.5	1.5
C20:1	0.1	0.3
C22:1	0	0.1
Other	5.6	6.7
	g/100g	
Saturated Fatty Acids	89.3	88.9
Monounsaturated Fatty Acids	4.1	4.5
Polyunsaturated Fatty Acids	0.6	0.7

Table 9-3, Fatty Acid Profile for PO

The decomposition process is defined by thermodynamics but is also dependant on kinetics; therefore the extent of the change in fatty acid profile would be greater if the base stocks were used as an automotive lubricant. All the base stocks followed the process of decomposition outlined in Section 3.7, particularly SO and JO. As the changes were small, they are unlikely to have an impact on performance over the short duration wear tests. SO has alpha linolenic acid (C18:3), unused this was 5.9% and used was 5.8%; this shows that very little oxidation occurred over the test duration. This fatty acid has three double bonds, which causes it to be particularly susceptible to oxidation, particularly as the bonds are all close together (as discussed in Section 7.3.1.1).

SO and JO both saw geometrical or positional isomerisation of unsaturated fatty acids, which is the shifting of the double bond position. The positions of double bonds are known as cis, if the hydrogen atoms in the double bond are on the same side of the carbon chain, and trans if they are on opposite sides. This is of importance, as the location of the hydrogen atoms dictates the shape of the fatty acid. Cis fatty acids have a kink in them, which will result in an increase in friction in tribological tests, as the fatty acid chains would not shear over one another effectively. In contrast, trans fatty acids do not have a kink, therefore a higher proportion of these would be desirable for tribological purposes. SO saw the increase in C18:1 18:2 and 18:3 cis and trans, likely due to the decrease in alpha and potentially the polymerisation of short fatty acid chains.

Isomerisation of double bonds happens at around 200°C, and polymerisation (also a function of time) and cyclisation occur at high temperatures too (232). Therefore it is considered that the test temperature of 100 °C would not have a considerable impact on fatty acid composition change. The temperature of automotive lubricants for most of their journey around the oil circuit would be around 100 °C, but they are exposed to flash temperatures of 200 °C at the piston liner and ring interface. This means that the process of decomposition is going to be thermodynamically dominant, due to the short durations of exposure to high temperatures. This could mean that the degradation of the lubricant is less extreme than if it were held at these high temperatures for long periods of time. This is particularly important for minimising polymerisation.

In Section 6.10, the degradation of vegetable oils was discussed briefly, Dréau et al. (175) found that JO was stable up to 120 °C, but then began to oxidise quickly. This means that an operating temperature of 100 °C may be too high to ensure low oxidation long term. Tenbohlen & Koch (176) found little change to PO and SO over a thermal degradation process, where oils were held at 130°C for 164 hours. When the test duration was increased to 1440 hours, significant polymerisation occurred. It is important to note that it is likely that, if PO, SO and JO had been subject to a longer test duration, or were used in an automotive engine, polymerisation would occur within months, which would lead to lubricant starvation because the oil would be too viscous to flow round the narrow oil ways, and excessive engine wear would occur.

In Summary, the fatty acid analysis shows the beginning of degradation, and it follows the oxidation pathway described in Section 3.7. This is a useful starting point in mapping the degradation due to thermal and oxidation effect. To build on this work, subjecting the base stocks to cyclic temperature changes to represent real engine

conditions would help to identify the effect of cyclic temperature variation and flash temperatures on long term performance of the base stocks.

9.4.2 *Spreading Parameter and Surface Energy*

The performance of a lubricant on a surface can partly be defined by its ability to spread over a surface, as discussed in Section 3.8.2. In order to calculate the spreading parameter, the surface energy of the solid interface and the surface tension of the liquid is required. To obtain values for surface energy and tension, the contact angle between the liquid drop and solid surface must be measured, and then methods such as the Owens–Wendt–Rabel–Kaelble method for calculating values can be used, as discussed by Kalin et al. (172). The total surface energy has some correlation to tribological performance, as Kalin found. Figure 9-31 shows results from correlating CoF with surface tension performed by Kalin, where he found the highest correlation with CoF and the polar component of surface energy. The polar component of the surface energy is important, as optimal wetting occurs when the polar components are identical (200). This is due to the polar interactions forming permanent dipoles, as discussed in Section 3.8.2. These polar forces are up to ten times stronger than dispersive forces, which only form instantaneous dipoles.

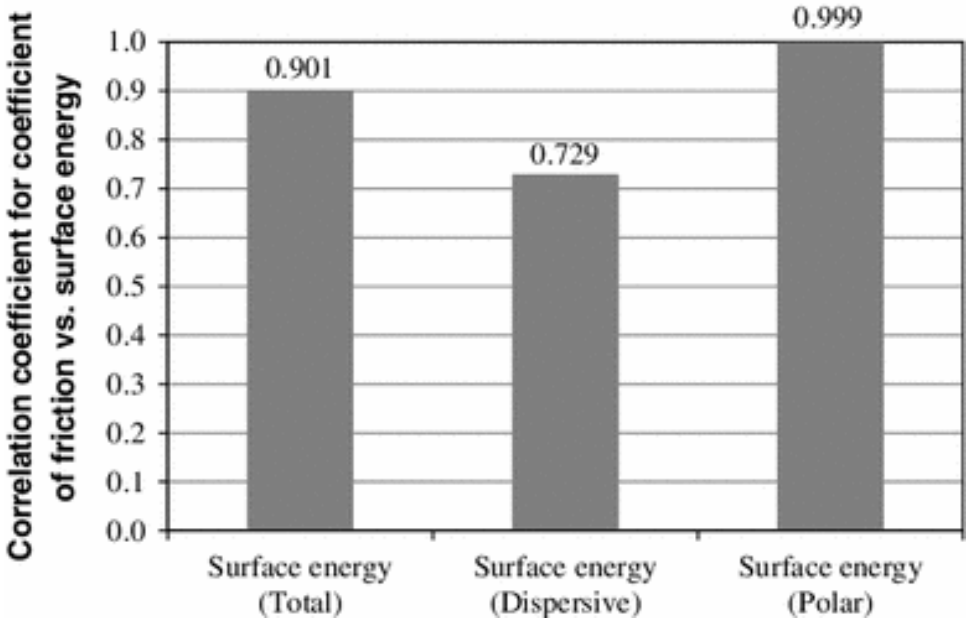

Figure 9-31, Correlation Between Surface Energy and Coefficient of Friction of Various DLCs Based on Total, Dispersive and Polar Surface Energy (65)

The spreading parameter, given in Equation 3-7, Section 3.8.2, requires the separation of the polar and dispersive components. For lower values of the spreading parameter, there is weaker interaction with the surface, this means there is higher slip at the solid/liquid interface and consequently lower friction.

In the absence of experimental data to calculate surface energy and tension values, an attempt was made to calculate the components of surface tension values for the base stocks, with the components of the Hanson Solubility Parameters. Koenhen & Smolders (242) proposed a relation between Hanson Solubility Parameters and surface tension as shown in Equation 9-3 Equation 9-4.

$$\delta_d^2 = A(1/V_m)^{1/3}\gamma_d$$

Equation 9-3

$$\delta_p^2 = A(1/V_m)^{1/3}\gamma_p$$

Equation 9-4

Where;
$\delta_d^2 = Dispersive\ solubility\ parameter$
$\delta_p^2 = Polar\ solubility\ parameter$
$A = Constant, ususally\ \approx 13.5$ (242) *or 1.8*10^{-9} mol$^{1/3}$* (243)
$V_m = Molar\ Volume$
$\gamma_d = Dispersive\ surface\ tension$
$\gamma_p = Polar\ surface\ tension$

Koenhen & Smolders found that this relation did not work for carboxylic acids among others; their reasoning for this was related to values obtained for solubility parameter for compounds with carboxylic acid being 'arbitrarily' chosen. The volume additive method using solubility parameters from individual fatty acids that make up each bio-base stock, as detailed in Section 7.4.5. It is thought that the polar element of HSP may be underestimated using this method, but it has still been shown to work well for determining solubility parameters for vegetable oils, which are predominantly made of fatty acids with carboxylic acids (195) (244).

The uncertainty with the relations in Equation 9-3Equation 9-4 extend to the constant, A, as well. Only two values for this constant could be found in literature, both are significantly different. Koenhen & Smolders state that this value is approximately 13.5, finding a correlation coefficient of 0.99 for 54 substances (242). Equations stated in this paper, linking solubility parameters to surface tension, have the value of the constant between 13.2 to 13.9 (no units). In Barton's review of cohesion parameters (243), he gives the constant as 1.8*10^{-9} mol$^{1/3}$ (units) and states this was obtained by Siow and Patterson (245); however, this paper does not state a value for the constant. It is unclear why this discrepancy has occurred. It is possible that the constant without units was divided by another parameter to make it non-dimensional, but this was not discussed.

Values for total surface tension for the base stocks used are available in literature, and shown Table 9-4, in but the polar and dispersive components for surface tension could only be found for SO. A crude attempt to use Equation 9-3Equation 9-4 to derive dispersive and polar components for the bio-base stocks was performed. A value for A was obtained by trial and error, so that the values for γ_d and γ_p for SO matched the values found in literature. The constants differed for γ_d and γ_p, at 51.85 and 38.1. It is unclear whether the results are valid, no attempt at correlation analyses could be performed unless significantly more values were calculated using this method. Experimental values are needed for verification, which is beyond the scope of this current work. The total surface tension, $\gamma_{T,}$ values obtained in literature are shown in Table 9-4 and the values obtained through the method are detailed here.

In a review of the application of cohesion parameters (243), Barton stated that with Equation 9-3 Equation 9-4;

'Because of the empirical and rather arbitrary way in which the partial cohesion parameters are evaluated, precise correlation with the partial surface free energy terms is not to be expected, but agreement is reasonably good.'

It is therefore thought that the results for surface energies, while perhaps not as accurate as they would be if they were derived from experiments, could be a reasonable estimate.

Base stock or surface	δ_D, $MPa^{1/2}$	δ_p $MPa^{1/2}$	V_m cm^3 mol^{-1}	γ_T, mJ $(m^2)^{-1}$ (lit)	γ_T, mJ $(m^2)^{-1}$	γ_D, mJ $(m^2)^{-1}$	γ_P, mJ $(m^2)^{-1}$
Palm Kernel	15.48	3.5	251.5	31.5*	30.62	28.63	1.99
Jojoba	15.71	2.74	306.2	34*	32.77	31.47	1.3
Soybean	16.11	2.99	276.5	33.5*	33.50	32	1.5
Mineral	17.4	3		31.24 (178)		31.24 (178)	0 (178)
Steel (178)				39		31.2	12.3
a-C:H DLC (178)				36		32	4.3
CaS_2 (243)				356			
Al_2O_3 (244)				638		100	538
MoS_2 (245)				45.9			

Table 9-4, Solubility and Surface Energy Values for the Materials and Base Stocks Tested

Figure 9-32 shows the correlation between the spreading parameter, polar surface tension and CoF for the steel reference specimens 0 and 18. There is some correlation, between these three values for PO, jojoba and SO. The mineral base oil sees correlation between SP and CoF, the polar value for mineral oil is 0 and therefore not included. This proves the theory that lower SP corresponds to lower CoF due to weaker interaction in the solid/liquid interface that means it is able to resist the shearing motion in the contact. This is particularly important for boundary and EHL conditions.

Figure 9-33 shows the correlation between spreading parameter, polar and dispersive surface tension and coefficient of friction for DLC specimens 1 and 2. The correlation between all values is not as clear for DLC specimens as for steel specimens. This may be due to the CoF results being close together; results were within a range of 0.02 for specimen 1 and 0.022 for specimen 2. The SP for mineral base and DLC is the lowest, but CoF is the highest; this may be due to other effects occurring in the contact during testing, such as delamination of the coating. It may also be that with the lower polarity DLC, dispersive interactions are dominant, where more instantaneous dipoles occur. While the highly polar steel is dominated by polar interaction with permanent dipole formed, this also explains the lower CoF seen in steel specimens compared with DLC.

Kalin (65) (172) found that a-C:H DLC had lower CoF than steel and attributed this to the DLC's lower polar component. They also had the link between the hydrogen content of the DLC and polar component of surface energy. The hydrogen content of these specimens is not known, therefore a solid conclusion cannot be drawn.

Podgornik et al. (171) found no clear correlation between surface energy, tension and CoF, as discussed in Section 6.7. They stated that these are not the only factors influencing tribological performance, which is also suspected with the poor correlation with results presented in this section. They did find some correlation, in

that mineral oil plus additive on DLC showed the lowest CoF, surface tension and surface energy.

The calculation of surface tension values using the method proposed by Koenhen & Smolders (242), and then spreading parameters via the method proposed by Kalin & Polajnar (65) (172), has the ability to act as a powerful tool, if it can be validated. It has the potential to be a quick and relatively simple estimation of coating and lubricant interaction without the need to perform lengthy experiments.

This is particularly relevant for bio-lubricants, with such a large group of possible base stocks, ranging from almost any plant based oil to any number of combinations of fatty acids for synthesised lubricants. Initial experiments to characterise the solid surface could be performed, then surface tension values derived using Equation 9-3 and Equation 9-4. Currently, designing new lubricants with fatty acids using computational structural modelling is difficult, due to the conformations of their chain structures and the high molecular weight of vegetable oil in general (163).

Given the uncertainty in calculations, values and literature, the spreading parameter has not been calculated for specimens with more than one surface treatment applied. It is unclear whether multi-layer surface treatments would affect the spreading parameter. Surface energy values would initially need to be obtained experimentally for the solid interface to see if there are any alterations in values due to layering. In order to improve understanding of the validity of this method, a larger data set is needed.

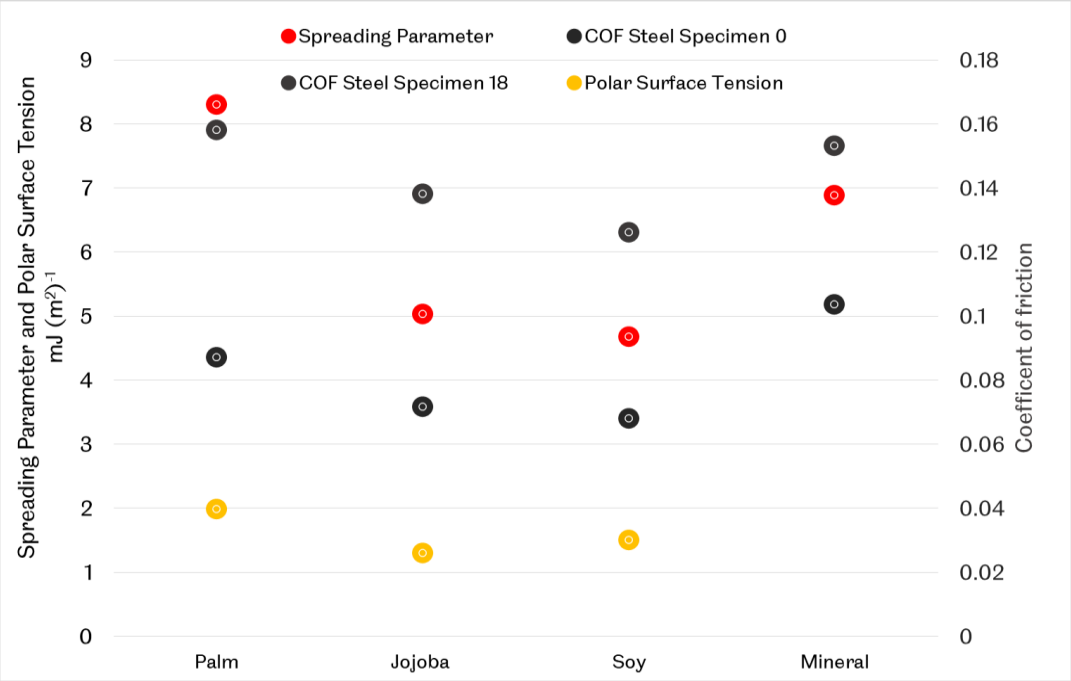

Figure 9-32, Correlation Between Spreading Parameter, Polar Surface Tension and Coefficient of Friction for Steel Specimens

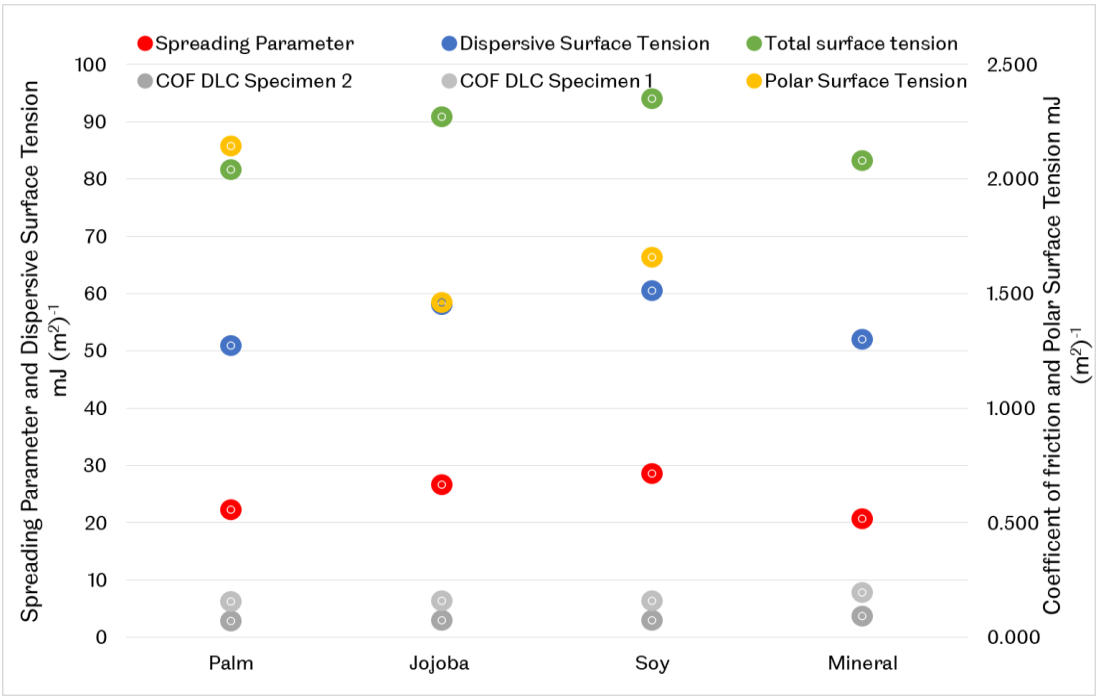

Figure 9-33, Correlation Between Spreading Parameter, Polar and Dispersive Surface Tension and Coefficient of Friction for DLC Specimens

9.4.3 *A Generalised Comparison of the Top Surface Treatments by Base Stock*

Results showed that overall the wear protection which bio-lubricant base stocks could offer differed significantly based on the multi-layer surface treatment used. There were groups of multi-layer surface treatments that performed well overall, as discussed in Section 9.3. Table 9-5 shows the top five performing coatings for each base stock.

Base Stock	Rank	JO	Volume loss, mm^3	SO	Volume loss, mm^3	PO	Volume loss, mm^3	MO	Volume loss, mm^3
Specimen	1	6 SF, CD	0.005	18 SF	0.003	18 SF	0.003	18 SF	0.005
	2	4 SF, SB	0.005	5 SF, DLC, CD	0.004	6 SF, CD	0.005	6 SF, CD	0.007
	3	18 SF	0.005	16 SB, DLC	0.007	16, SB, DLC	0.006	15 SB, CD, DLC	0.008
	4	8 SF, SB, CD	0.007	14, CD, DLC	0.007	5 SF, DLC, CD	0.007	4 SF, SB	0.008
	5	16 SB, DLC	0.007	2 SF, DLC	0.008	8 SF, SB, CD	0.008	5 SF, DLC, CD	0.008

Table 9-5, The Top Five Specimens in Terms of Wear Protection for Each Base Stock Tested

9.4.4 *Steel Reference Specimens*

9.4.4.1 Super Finished Steel Specimens

The reference specimen, 18, a medium carbon steel SF specimen, with a very low surface roughness, R_a of 0.135 µm was the only specimen to be in the top five for all base stocks. This performance is relatively easily explained. In Section 9.4.1, the polarity of the steel surface is given; it is nearly four times higher than the polarity of DLC, at 12 mJ $(m^2)^{-1}$, compared with 4.3 mJ $(m^2)^{-1}$.

Vegetable oils are well known for their high polarity, which originates in the carboxylic function group sited on the end of fatty acid chains. These carboxylic groups are highly polar because they are hydrogen bond acceptors (in the –C=O bond) and donators (in the –OH hydroxyl group), as Figure 9-34 shows. This means that they have a good ability to form chemisorbed films, as discussed in Section 3.8.3, with the steel surface.

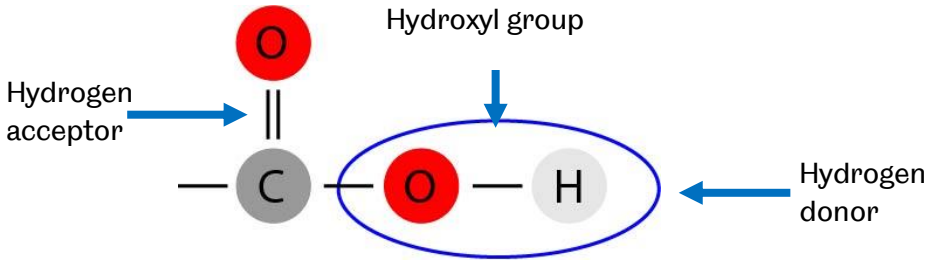

Figure 9-34, Carboxylic Acid with a Hydroxyl Group

The effect of this polarity is also well explained by the spreading parameter in in Section 9.4.1. PO has the highest spreading parameter, highest CoF but lowest wear. PO is made up of medium chained fatty acids and is predominantly saturated, with 89.3 g/100g saturated fatty acids. Saturated fatty acid chains are straight chains, which are able to align with one another more easily than fatty acids with double bonds. These double bonds cause a kink in the chain, making it harder for the chains to conform. This should mean that PO has a lower CoF than JO and SO, which have considerably lower levels of saturation at 1.7 and 15.2 g/100g respectively. The spreading parameter for PO is higher than the other oils tested, as is the polar component for the surface tension. This means that PO forms a stronger chemisorbed film on the steel surface, justified by the very low volume of material removed during wear tests. These high cohesive forces between POs fatty acid chains cause high viscous friction and slip conditions as discussed in Section 6.7.1.

The mechanism for protecting the surface with SO is different to PO. SO has the lowest spreading parameter, low CoF, with only MO having a lower CoF. This indicates the ability of fatty acid chains to shear over one another more effectively than PO, meaning that the wear protection SO offers is due to its ability to shear effectively at the interface. SO is primarily made up of linolenic (52.9% and two double bonds), oleic (23.9% one double bond) and palmitic (10.7% and saturated) acids. The more double bonds in a fatty acid chain, the more bent the fatty acid chain is. This has been

considered to be an influencing factor in the viscous friction of fatty acids. The surface tension and spreading parameter results show that cohesive forces have more influence on viscous friction than kinks in fatty acid chains. MO had a high spreading parameter, CoF and higher wear, in terms of surface tension, MO does not have a polar component, and therefore is not effective at forming chemisorbed films on steel surfaces without the aid of additives, therefore increasing CoF. MO has higher intermolecular dispersive forces, which may contribute to viscous friction.

JO had the same level of wear as MO but lower CoF. Compared with SO and PO, JO has the lowest polar component for surface tension, therefore may not generate such an effective chemisorbed film. Cohesive energy increases with increasing chain length; the lower polarity may be offset by the increase in cohesive energy due to being made up of mainly long chain fatty acids, (gadolenic acid, C20:1). This means that JO has more dispersive forces aiding the generation of a physisorbed film, and less polar forces to generate a chemisorbed film. Gadolenic acid has a carboxylic function group with a hydroxyl group contained in it, so will form a chemisorbed film to some degree. More resistance to mechanical shear, due to these chemical interactions, may also aid the retention of the lubricant in the contact region.

A review of literature found that JO was more effective at wear protection than MO, and had lower CoF (67) (249). The results show that CoF is lower for JO than MO, as is wear generally. Literature revealed that JO and MO often gave very similar results for tribological performance. Literature for PO and SO do not provide consistent enough results to be able to compare the performance of these oils with results.

9.4.4.2 Surface Ground Steel Specimens

While the SF specimen performed very well in wear tests, the SG specimen did not. The relatively rougher surface (R_a 0.33 µm) meant that the actual contact area was reduced, with the peaks of the surface grinding marks supporting the load in the contact. This resulted in considerable plastic deformation in the wear track, as seen in Figure 9-35. The wear track has been polished, with all grinding marks removed. Adhesion and abrasion are visible as well. The effect of a reduced contact area and increased maximum pressure meant that retention of the lubricant in the contact area was reduced. The higher contact pressure meant that the chemisorbed films that vegetable oils can generate are more likely to be disrupted.

JO offered the highest wear protection out of the base stocks tested. This is attributed to its being made up of longer fatty acid chains (C_{20}) in comparison to SO and PO. The increased chain length gives increased cohesive forces, needed to protect the surface. While having higher overall cohesive forces, JO had the lowest calculated polar surface tension value, at 1.3 mJ $(m^2)^{-1}$. As already discussed in detail in Section 9.4.4, this results in higher levels of slip at the interface. While shearing at the interface will not always result in less wear, in this case it aided wear reduction.

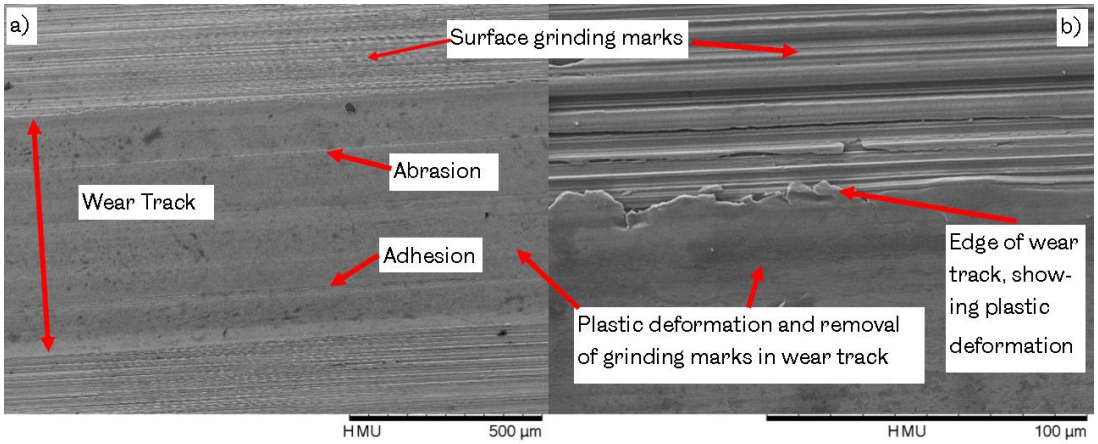

Figure 9-35, An Example of the Wear Track for Tests Reference Specimen, Surface Ground Steel, Tested with PO, at a) 500 µm and b) 100 µm

9.4.5 *Diamond-Like-Carbon-Lubricant Interactions*

While DLC is considered chemically inert, the surface is electrochemically reactive. The tetrahedral bonding structure of the a-C:H DLC has a vacant carbon electron at the surface, known as a dangling bond orbital. This bond allows for weak van der Waals bonding at the surface, which aids shearing at the interface. The type of oil used with DLC is said not to be important in friction reduction, as there are no vacancies for the additional hydrogen to bond with (64) (103). This is not the case for the bio-base stocks JO, SO and PO, however. As Figure 9-34 shows, the carboxylic acids situated on the end of fatty acid chains have the potential to form weak bonds with the surface, as they are hydrogen acceptors and donors. The results in Figure 9-18 in Section 9.3.1 show that in almost every case for tests with various DLC containing multi-layer surface treatments, the CoF is lower for the bio-base stocks compared with the mineral base stock. The CoF was only lower for the mineral base stock for specimen 16; the variation in results for CoF for this base stock coating combination, however, means that the averaged value shown in Figure 9-18 is not a particularly representative value.

While a review of literature did not find any work with PO, SO and JO in wear and friction tests with DLC, there was limited research with sunflower oil (103), a PAO ester (80) and palmitic acid (104) (SO contains 10.7% and PO 12.4%). While it was still proposed that the coating is more important than the lubricant used (103), friction reductions were observed in all cases compared with conventional lubricants. The researchers all proposed the formation of physisorbed films, as described in Section 3.8.3.

Simic & Kalin (104) also proposed that there was chemisorption due to a reduction in wear and that, when the surface is disrupted during graphitisation (as discussed in Section 6.2). There is more bonding potential between the carboxylic acids and surface. The results from Figure 9-18 do not give a clear relationship between the type of base stock used and wear, which may suggest that the type of base stock used is irrelevant. It is hypothesised that this is not the case, but that different mechanisms of lubrication are dominant.

The inert lubricity of the mineral base stock offers a shear interface, but with a low spreading parameter and therefore low resistance to shear. There is no interaction

with the surface, but wear is relatively low due to the base stock's ability to provide this low shear interface. The polarity of the bio-base stocks seems to have some influence, PO has the highest polarity, while JO has the lowest, as shown in Section 9.4.1. As only one set of tests was performed with PO, it is difficult to compare results with SO and JO, but for five specimens in Figure 9-18, results for volume loss were lowest for PO. For the other four results shown in Figure 9-18, SO had the lowest wear. This would indicate some form of adsorption of the base stocks onto the DLC surface.

There is some correlation between polarity and wear for specimens containing DLC. There is less of a trend with viscosity and friction. Increasing friction may occur with increasing viscosity due to viscous friction. The lack of correlation with friction data for specimens containing DLC can be attributed to increased friction due to ploughing effects caused by the delaminated coating wear debris.

The wear mechanisms observed are independent of the lubricant, but the severity of the wear mechanisms is dependent on the lubricant. Figure 9-36 shows this for specimen 2 (SF, DLC), from around three tests. In this case, the more polar JO did not offer better wear protection than MO. The coating delamination in this case resulted in the removal of layers of the coating, with 0.024 mm^3 of material removed. This was also high compared with rounds one and two testing, that saw 0.008 and 0.014 mm^3 material removed. The coating delamination mechanism was particularly effective in this case. This could have been due to flaws in the coating at the interfacial layer; it could also have been propagated by a large piece of wear debris. MO has less delamination and more coating thinning or removal of the top layer of the coating. SO wear track is not quite as wide and also has less delamination and removal of the top layer of the coating.

Interestingly, the addition of CD over DLC, in specimen 5 (SF, DLC, CD), reduces the severity of wear for all base stocks, as seen in Figure 9-37. The volume loss reduced by 10, 20 and 50 percent for JO, MO and SO respectively by applying CD over DLC instead of DLC over CD. The addition of a layer of CD has not prevented the delamination of the DLC layer, but it has slowed it. Figure 9-37 shows delamination of the coating for tests with JO, with some of the coating embedded in the substrate due to high contact pressures. SEM examination of the MO wear track reveals cracking that would result in delamination of the coating long term. The SO wear track for specimen 5 shows little coating damage compared with the other base stocks tested. This coating gave the lowest wear for SO, leading to the suggestion that the CD layer acts as a sacrificial layer to protect the DLC. There may be some interaction between the bio-base stocks and the CaS_2 and aluminium oxide, particularly with SO, which has a high polar surface tension. This is discussed in more detail in Section 9.4.6.

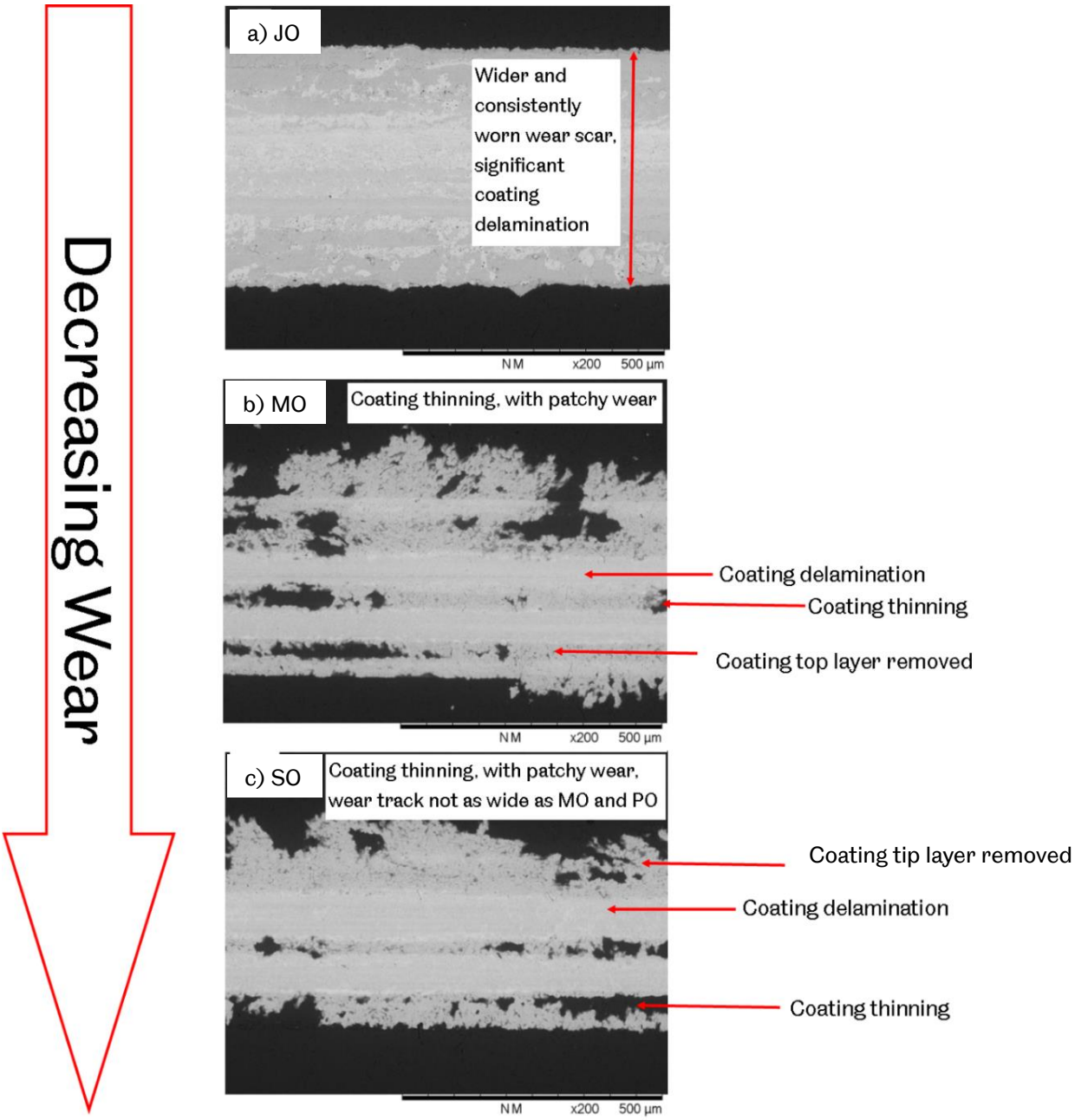

Figure 9-36, Wear Scars for the Superfinished, DLC Specimen, Tested with a) JO, b) MO and c) SO, Showing that the Severity of Wear is Dependent on the Lubricant Used

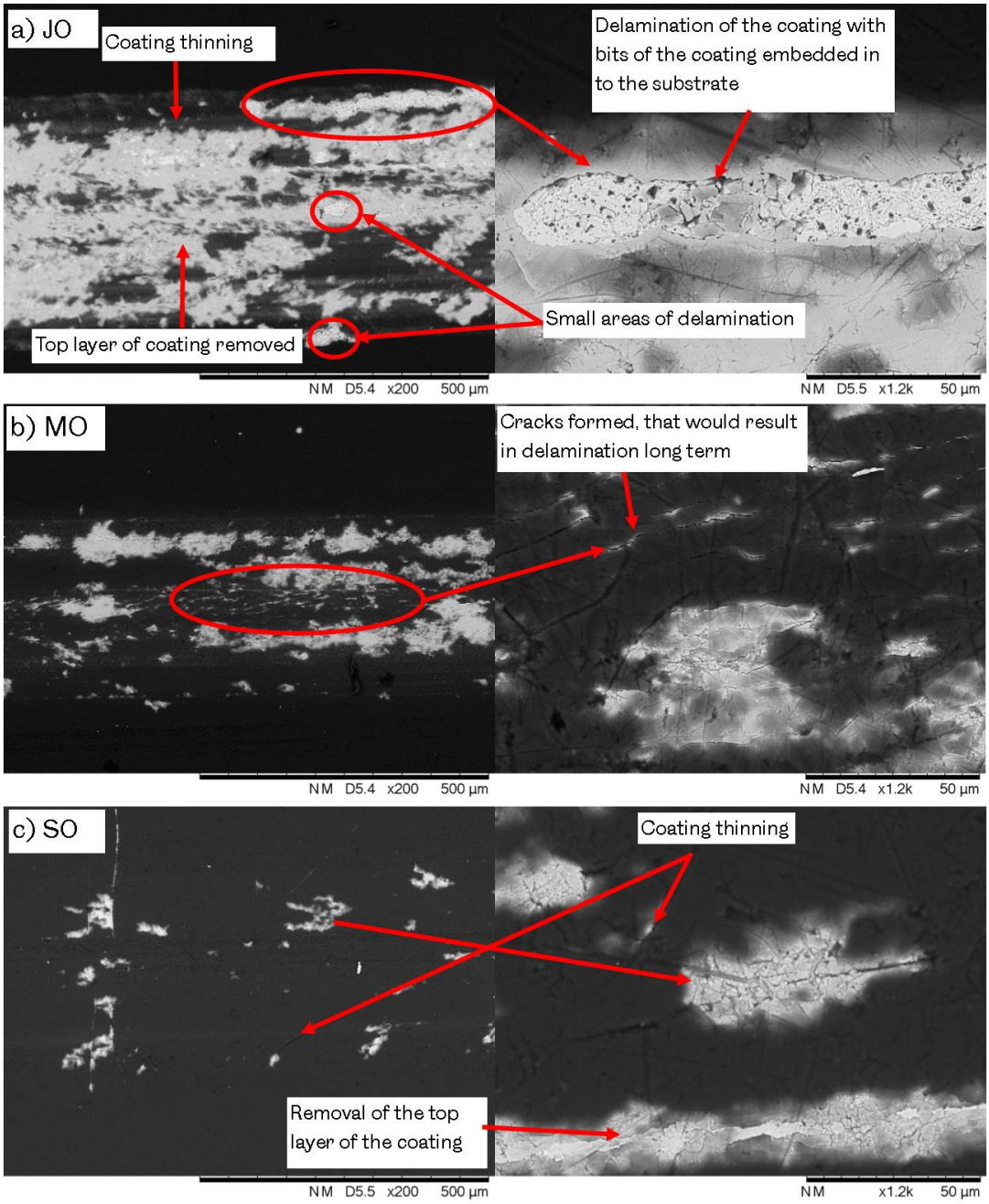

Figure 9-37, Severity of Wear with the Superfinished, DLC, Chemical Dip Specimen, Tested with a) JO, b) MO and c) SO (decreasing wear)

9.4.6 *Chemical Dip Lubricant Interactions*

Specimens subject to CD surface treatment produced some significant results, as discussed in Section 9.3.8, with wear protection as good as, if not better in some cases than DLC. The CoF was also slightly lower for CD specimens compared with DLC specimens. The mechanism for this surface treatment's tribological performance is not well understood. There is no published data on this specific CD surface treatment, but there is some information on components of this coating.

The surface treatment was found to have particles of Al_2O_3, as shown in Section 0, which is a well understood solid lubricant, with oxide layers offering a low shear interface. The interaction with Al_2O_3 and the base stock is less well understood. Al_2O_3 is capable of hydrogen bonding, as the Al^{+3} ion in Al_2O_3 is strongly attracted to OH^- ions (250). The hydroxyl group in carboxylic acid is a hydrogen donor (or OH^- ion) as shown in Figure 9-34. The oxygen ions are negatively charged and can react with acids, as well as steel surfaces (251). This would indicate that it is possible for fatty acids to form tribofilms with Al_2O_3 and offer wear protection to a surface. There is a strong bond energy between Al and O (238), therefore this part of the surface treatment is unlikely to decompose in its reactions with the fatty acids in the bio-base stocks.

The surface treatment is also made up of calcium sulphate ($CaSO_4$). As discussed in Section 6.5, there is some evidence that $CaSO_4$ can reduce friction (114), and sulphide layers alone have also been shown to do this (113). When wear debris is formed from sulphate base coatings, the sulphate has been shown to be carried in the lubricant and act as a lubricant additive (252). Sulphur is also a well-known anti wear additive, as discussed in Section 3.4.

Calcium has been found to react with C16:1 fatty acid to form a plate shaped lamellar crystalline powder with varying particle sizes from 2 µm to 10's of µm. Yamamoto et al. (253) found that this calcium fatty acid structure offers lubricity better than the lubricity the fatty acid can offer on its own. This was also the case for palmitic (C16:0) and oleic acid (C18:1) when reacted with calcium. Calcium has also been found to react with steric acid (254) to form calcium stearate. This leads to the possibility that the surface treatment decomposed by the mechanism of the fatty acids reacting with the calcium. The sulphur has the bonding potential to react with Fe. Al_2O_3 would not be likely to react with sulphur due to the higher bonding energy between the aluminium and oxygen (238). This could explain the lack of calcium when a used specimen was analysed using EDS. It is clear that these reactions are thermodynamically possible, but how quickly these reactions occur, whether they only occur in the contact area or across the entire specimen, and how temperature affects these reactions is unclear. It is also unclear whether the $CaSO_4$ decomposes completely during testing. If it does decompose, it may be more beneficial to use calcium as a lubricant additive rather than a surface treatment, as the benefits of $CaSO_4$ decomposing would only be seen in the initial life of an engine component with this surface treatment applied and lubricated with some form of bio-lubricant.

The results from wear tests reinforce this hypothesis, in that enhanced lubricity occurred with the fatty acid containing bio-base stocks. The CoF values for all bio-base stocks were lower than for MO. Figure 9-39 shows that CoF values were between 0.094 – 0.11 for MO, while for JO, SO and PO they were 0.063 – 0.082, 0.06 – 0.085 and

0.075 – 0.107 respectively. The reduction in CoF is particularly helpful for the bio-base stocks, as reduced frictional heating effects could reduce thermal degradation.

JO and SO are made up of long chain fatty acids (predominantly C20:0 and C18:2 respectively), while PO is made up of medium chain fatty acids (predominantly C14:0). This may explain the higher CoF for PO. As discussed in Section 3.8.2, the longer chains have a higher cohesive energy, therefore are better at aligning with one another to offer a more stable shearing interface. JO had the lowest wear for four out of the six CD specimens, which reinforces this theory.

While there was a clear trend with base stock, CoF and the CD surface treatment, a trend was less apparent with volume loss and base stock. In general, with specimens 6, 9, 5 and 7, there was not a significant difference in volume of material lost, if the range of results is considered. Figure 9-38 shows an example of wear scars produced during testing of SO, MO and JO, with the varying degree of wear highlighted. Interestingly, for all specimens containing CD and tested with MO, the wear track and region around the wear track appeared distinctly different to the bio-base stocks tested. As highlighted in the magnified view of the wear tracks in Figure 9-38, the MO wear track has plate like smears visible, which could be an indication of $CaSO_4$ still on the surface. The $CaSO_4$ may be have been decomposed in the wear track region for SO and JO. For both MO and SO the wear scars are around 6 and 5.5 µm deep, this means that they have worn in to the substrate. The plate like smears seen with MO in Figure 9-38 could be the result of adhered $CaSO_4$ or iron sulphate wear debris, which is not present in SO wear scars as the Ca has dispersed in to the base stock. The tribofilm formed by JO meant that wear scar depths were around 1 µm.

Results for specimens 8 and 10 show that SO with SB does not produce good wear protection; the potential reasons for this are discussed in more detail in Section 9.4.7, but the polar SO may decompose the MoS_2 in the SB specimens, while JO is less polar and therefore might not cause this. It is difficult to say whether there is any interaction with MoS_2 and PO, as only one test was performed.

To summarise, the proposed mechanism for bio-base stocks with the chemical dip surface treatment is that there is decomposition of the surface treatment to some degree acts as a solid lubricant. Calcium reacts with the fatty acids to enhance the lubricity of the base stock. The iron in the steel surface reacts with the sulphur from $CaSO_4$ to offer wear protection on the surface. The addition of Al_2O_3 particles may act as a back-up wear protection and friction reduction mechanism if the other mechanisms fail. The performance of this surface treatment is of particular interest as it has shown equal, and in some cases improved, wear protection and friction reduction compared with DLC. This surface treatment is not a hard coating like DLC, therefore may not have the same cracking and substrate miss match issues that can occur with DLC.

Further work to establish what initiates these mechanisms and to what extend they occur is needed. Larger data sets are required, and more detailed element analysis of specimens after set intervals of wear tests would begin to give a better understanding of the mechanisms dominating this surface treatment.

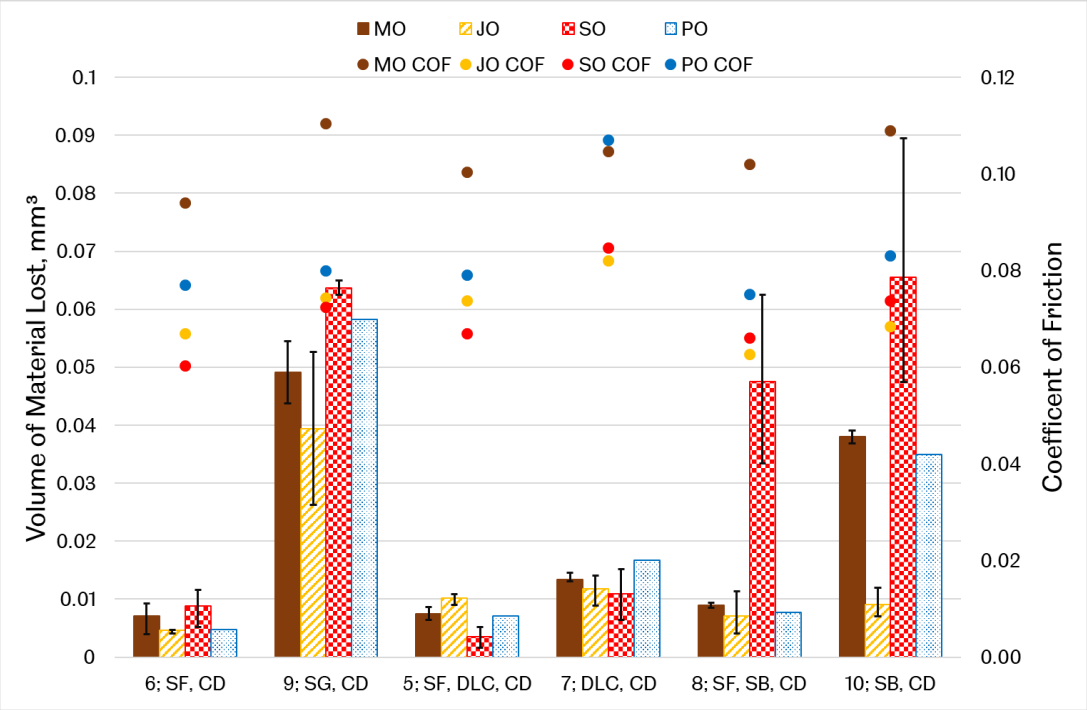

Figure 9-39, Volume Loss and Coefficient of Friction for Specimens with Chemical Dip

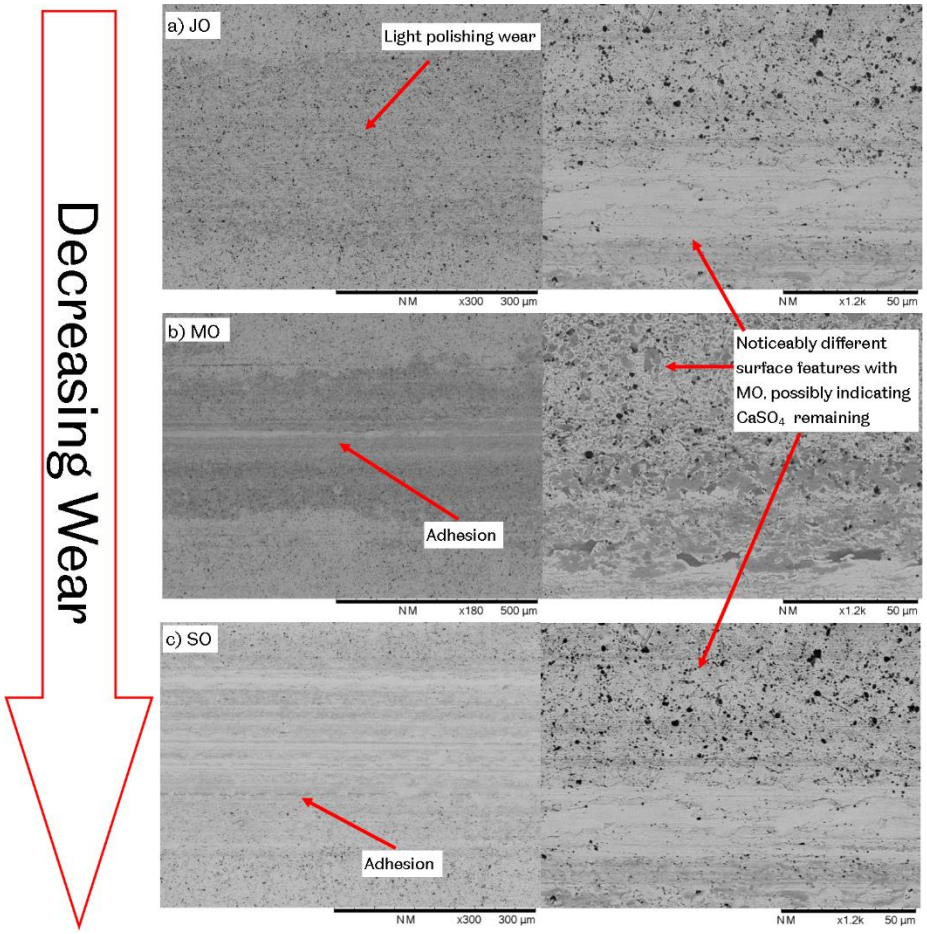

Figure 9-38, Levels of Wear for the Superfinished, Chemical Dip Specimen with a Magnified View of the Wear Track for a) JO, b) MO and c) SO

9.4.7 *Molybdenum Disulphide Lubricant Interactions*

Molybdenum disulphide (MoS_2) was used as a doping media for specimens subjected to SB. Figure 9-40 shows the averaged results for wear and friction tests. The results show that MO and JO performed comparably in terms of wear, with low volumes of material removed. The super finished specimen 4 was better for wear protection due to the smoother surface finish reducing the asperity interaction to cause adhesion and abrasion.

Results for SO were consistently higher compared with MO and JO. Results with specimen 3 for SO were inconsistent. In round one, only calculated values for volume loss were available, which are not considered as accurate as the optical scanning method (as discussed in Section 0) Round one results were, however, more consistent with round two results, volume losses for round one were 0.025 mm^3 and for two were 0.038 mm^3, while the value for round three was 0.422 mm^3. This accounts for the large experimental spread values seen in Figure 9-40. If the result from round three is discounted, then the average is close to that of JO. The cause of the increased volume loss with SO and specimen three is three body abrasion, where wear debris became entrained in the contact and caused long scratches in the direction of wear. This is also the case for tests with specimen 4 and SO. Figure 9-41 shows the variation in wear tracks for each base stock tested.

Literature that discusses liquid lubricant interaction with the solid lubricant MoS_2 could not be found. It is known that MoS_2 can oxidise at relatively low temperatures (85˚C), as discussed in Section 6.2, and can also react with steel. MoS_2 has a certain degree of polarity (111), therefore it is proposed that there is some lubricant interaction with MoS_2, particularly with the more polar SO, that disrupts its function as a solid lubricant.

The double bond oxygen molecule in the carboxylic acid group (shown in Figure 9-34) could act as an oxidant and bond with either Mo or S. There may also be competing action of attempting to form a physi- or chemisorbed film on the steel ball and any exposed steel on the specimen, which results in both SO and MoS_2 failing to form a stable protective layer. The transfer film of MoS_2 in unlubricated contacts has been shown to reduce friction and aid shearing (238).

As discussed in in Section 6.2, MoS_2 wear debris can agglomerate in the contact zone to enhance wear protection. The use of SO along with the fact that there may be lower levels of MoS_2 wear debris (as it was only a doping media) means it is unlikely that this wear mechanism occurred.

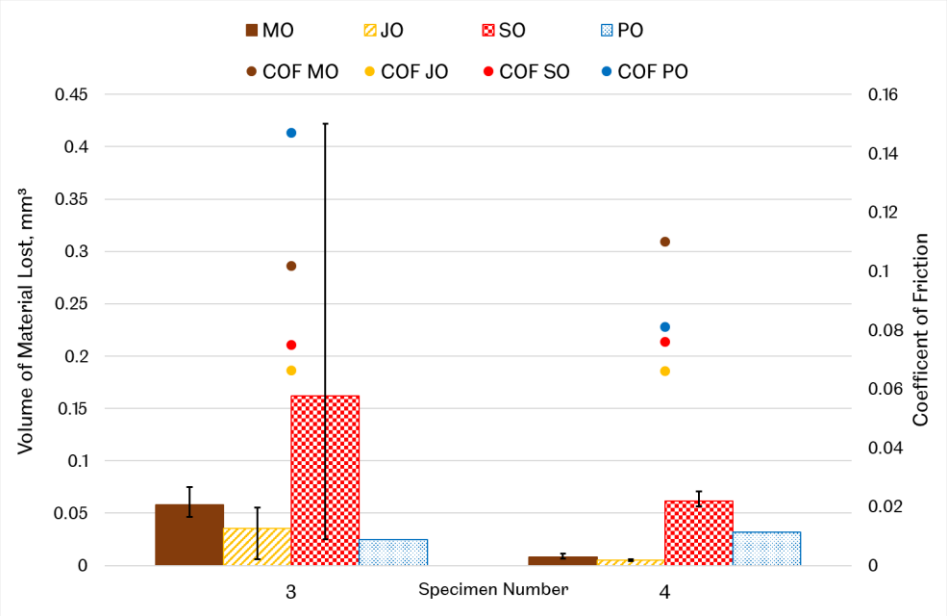

Figure 9-40, Results from Wear and Friction Tests With Shot Blasted Specimens 3 & 4

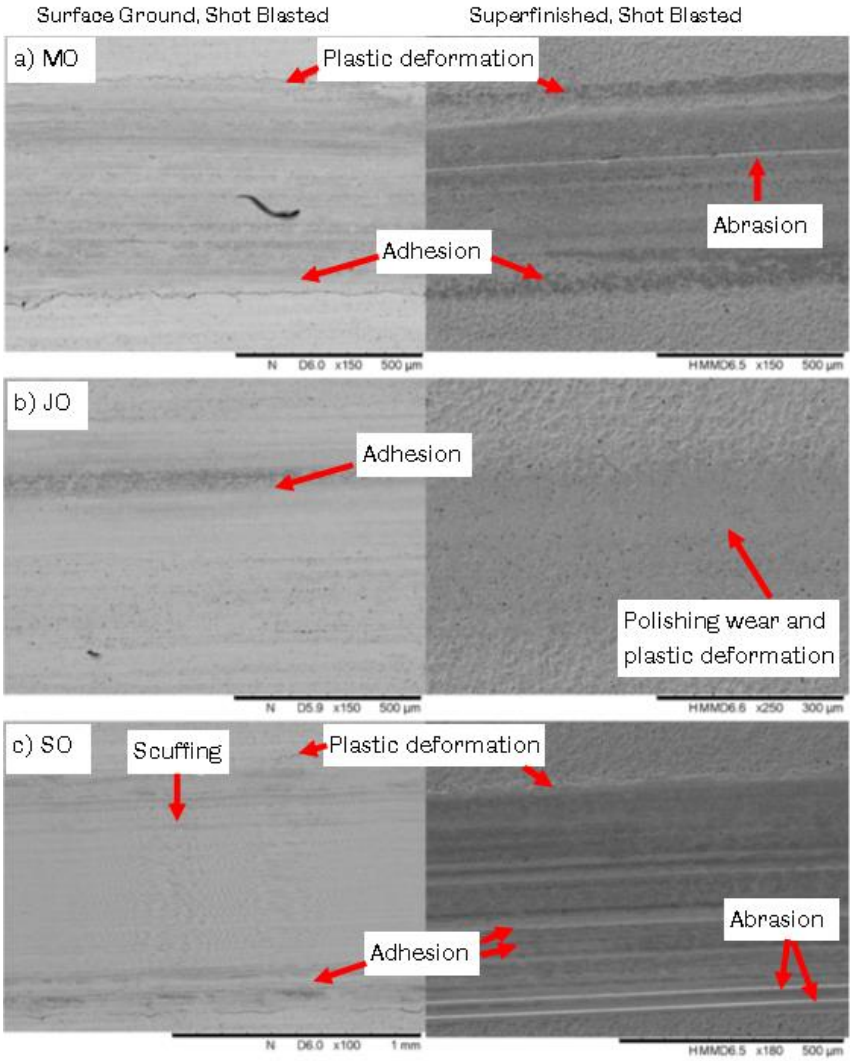

Figure 9-41, Variation in Wear for Surface Ground, Shot Blasted Specimens on the LHS and Superfinished, Shot Blasted Specimens on the RHS for a) MO, b) JO and c) SO

9.5 Conclusion of Interactions Between Base Stocks and Surface Treatments

The interaction of steel and bio-base stocks is dominated by chemisorbed films formed by the carboxylic acids groups. This is a very effective wear and friction reduction mechanism for smooth surfaces.

The interaction of bio-base stocks is dominated by physi- and chemisorbed films generated between the dangling bond orbital on the DLC coating and the carboxylic acids groups. This lubricant mechanism is not as effective as that of steel and bio-base stocks.

The interaction of bio-base stocks and CD is proposed to be through decomposition of CD. Calcium bonds with the fatty acids to enhance lubricity. Sulphur forms bonds with the steel surface. Physisorbed films are generated between aluminium oxide and fatty acids. This in general provides a better lubrication mechanism to protect against wear and reduce friction than the DLC or SB lubricant mechanism.

The mechanism of lubrication present with SB specimens is that the carboxylic acid group could act as an oxidant and bonds with Mo or S to form a physisorbed film. This mechanism is not as effective as the DLC or CD mechanisms.

The results to assess the tribological performance of the bio-lubricant base stock candidates and mineral base stock reference have been presented. Overall results show the potential for bio-lubricant base stocks to give improved tribological performance, with comparable and better wear protection with many of the multi-layer surface treatments. Coefficient of friction values were consistently lower for bio-lubricant base stocks, particularly compared with the mineral base stock.

10 The Compatibility of Elastomers with Bio-Base Stocks

In this chapter, the results of stress relaxation tests with elastomers and base stocks are discussed, separated into each elastomer tested: EPDM, FKM and nitrile rubber (NBR). This is followed by a comparison with the results obtained computationally using HSPiP software to predict elastomer and base stock interaction. To finish the chapter, the uses and limitations of HSP in determining elastomer compatibility are discussed.

10.1 Experimental Results for Stress Relaxation Tests

A comprehensive set of consistent results was obtained from testing with the Elastocon Relaxation Tester, as described in 7.4.8. Force readings were normalised by dividing the force readings by the initial force reading; this removes any slight variation in force readings that might be caused through error induced in measuring the initial thickness of the seal, which would carry an error through to the amount the seal is compressed by. It is difficult to quantify the value of this error, as measuring the thickness of the seal using other mechanical methods could result in slight compression of the seal. It is thought that that this error could extend to giving thickness readings of 0.07 mm less than the actual thickness. It is unlikely that the measurement would overestimate the seal thickness, as it would be apparent that the seal was not secure in the compression plates when moving the compression rig. The cyclic fluctuations that occur over some results are caused by variation in ambient temperature, as mentioned in Section 7.2.2.

Figure 10-1 to Figure 10-3 show averaged results from EPDM, nitrile rubber and FKM O-ring tests. An increase in normalised force values represents swelling in the O-rings, and a reduction represents shrinkage. A control test (green line in Figure 10-1 to Figure 10-3) was carried out with each elastomer material in air for the 168 hour test duration to take into account any stress relaxation induced by compression that causes the elastomer molecules to move.

The results are not as expected. It was anticipated that the bio-base stocks would react with (swell or shrink) with the elastomers considerably more. The results show that for EPDM O-rings, shown in Figure 10-1, MO and JO cause the O-rings to swell, while PO and SO caused minor shrinkage. The shrinkage may not be caused by the oils, as the control test followed a very similar trend, thus indicating that the shrinkage may be caused by the compression of the elastomer molecules (stress relaxation).

Figure 10-2 shows the variation in normalised force readings for tests carried out with FKM O-rings. Only slight shrinkage was observed for all base stocks tested, with less shrinkage for PO and SO compared with MO and JO. Similarly, Figure 10-3 shows results for tests with nitrile rubber O-rings. All the base stocks tested showed similar results, with considerable shrinkage. This is attributed to the removal of plasticisers, which are commonly used in nitrile rubber for low temperature stability.

Finally, Figure 10-4 shows the average percentage mass change of the three elastomer samples when tested in the base stocks. These results prove that stress relaxation data is a valid method for assessing the shrinkage or swell of O-rings.

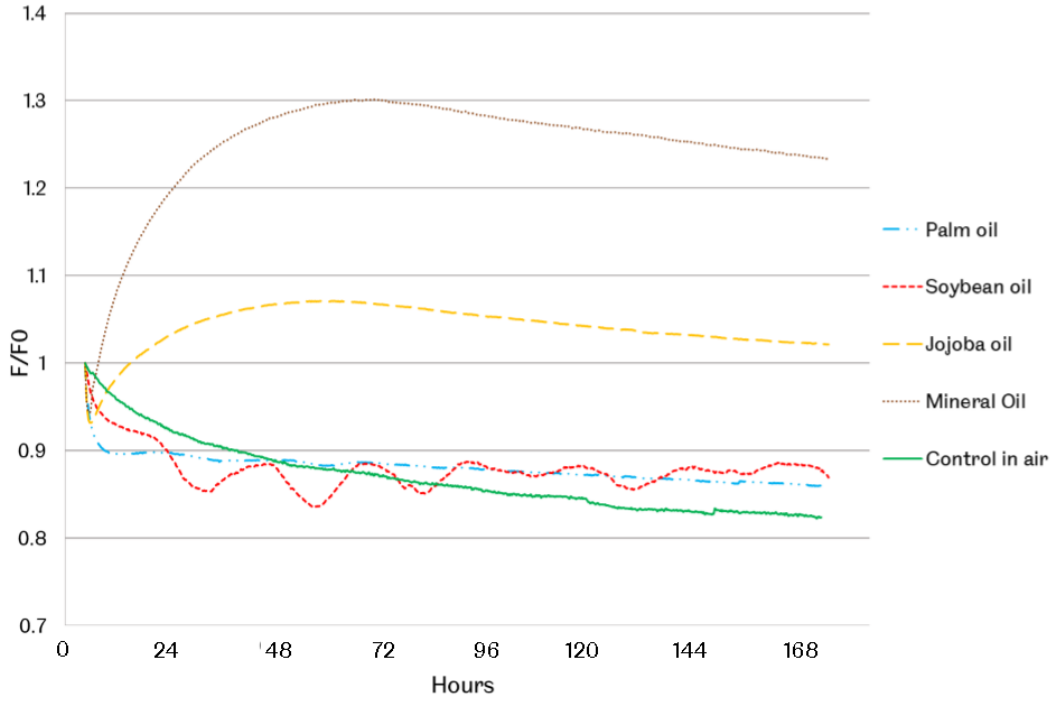

Figure 10-1, , Results from Stress Relaxation Tests with EPDM O-rings

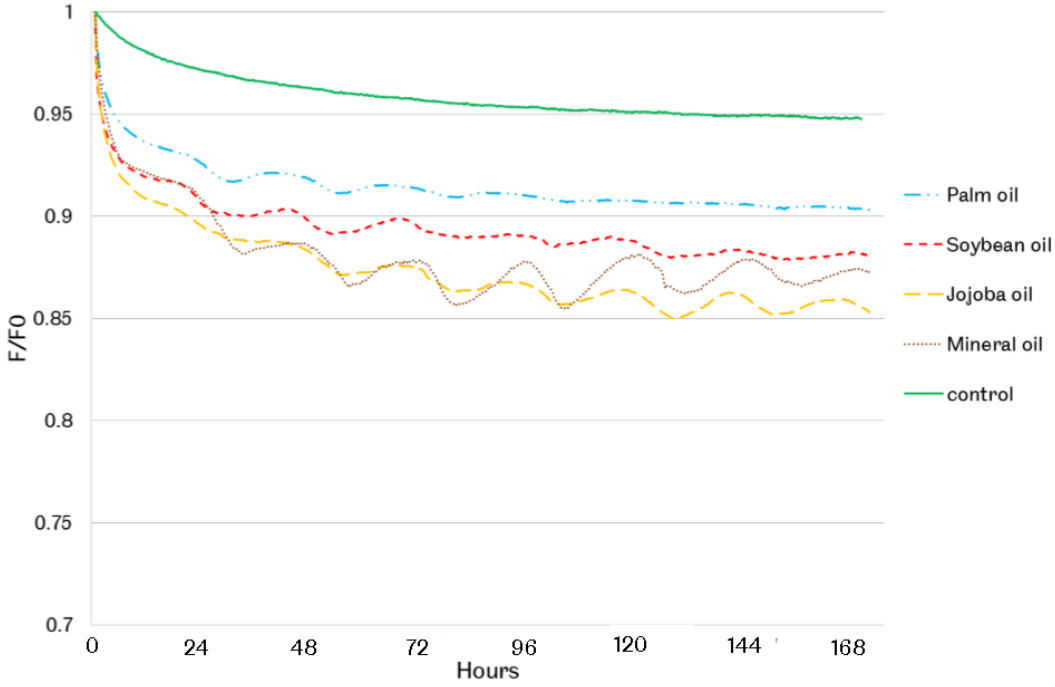

Figure 10-2, Results from Stress Relaxation Tests with FKM O-rings

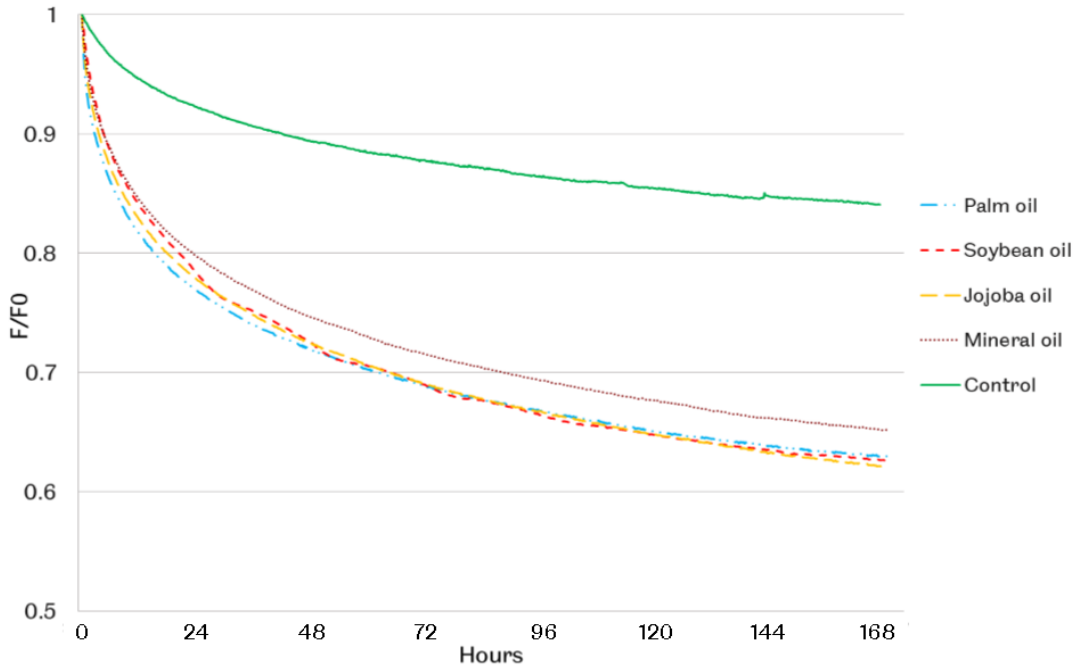

Figure 10-3, Results from Stress Relaxation Tests with Nitrile Rubber O-Rings

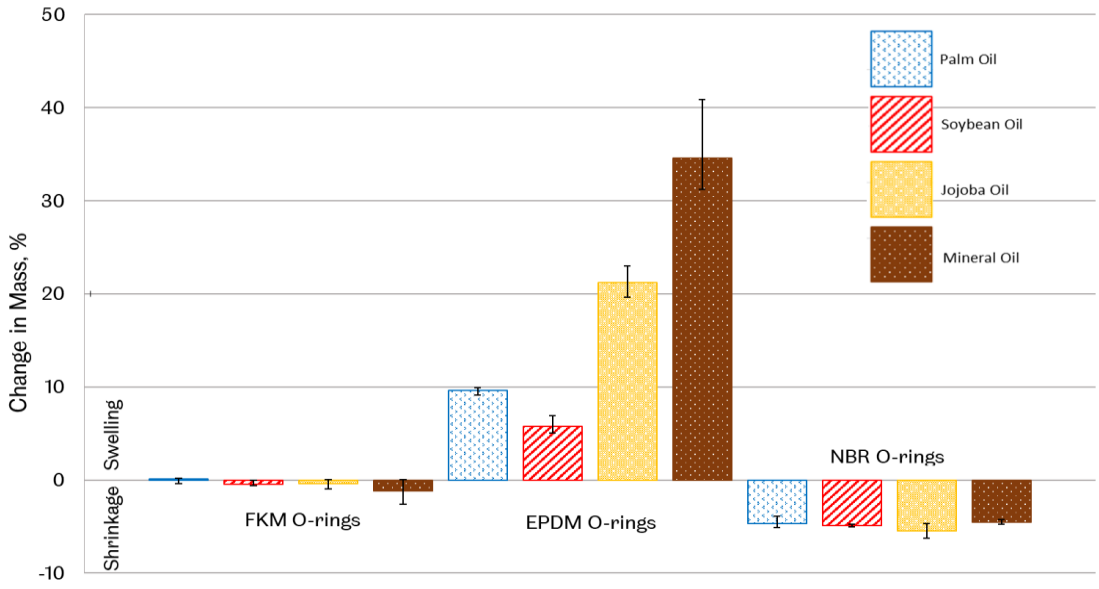

Figure 10-4, Mass Change for Each Group of Elastomers with Base Stocks

10.1.1 *Hanson Solubility Parameter*

This section details the results from using the HSPiP software as described in Section 7.4.5 and compares it with experimental results for stress relaxation tests detailed in Section 10.1.

10.1.2 *Relation Between Experimental and Computational Data*

Figure 10-5 highlights the link between the change in mass of the elastomer O-rings after testing and the Relative Energy Difference (RED), obtained from HSP software. Some correlation can be seen between mass change and RED for tests with EPDM, but no correlation for nitrile rubber (NBR) or FKM.

MO with FKM had a RED of 1.07 and very similar results for stress relaxation data and percentage mass loss as PO, which had a RED of 0.97. Both JO and SO had a RED of 1.02 with FKM and also very similar results to PO and MO. The lack of trend was also noted by Nielson (201), who compared RED and swelling of FKM. Volume change is proportional to mass loss through the relation with density. This lack of correlation is due to the fact that fluorocarbon based elastomers are co-polymers; each polymer will have its own HSP values, which could vary considerably.

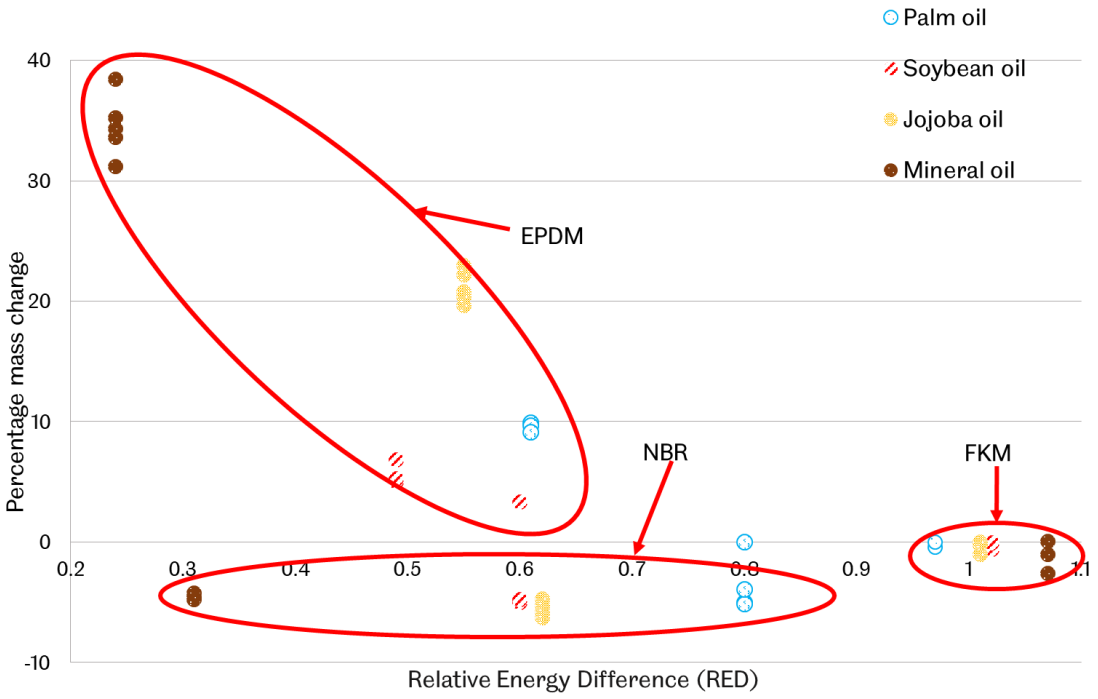

Figure 10-5, Relationship Between Mass Change and Relative Energy Difference for the Elastomers and O-Rings Tested

The HSP values used to obtain RED values are shown in Table 10-1. Some values found in literature for SO and PO are included, these are methyl ester versions of the oils though, HSP values for unprocessed SO, PO or JO could not be found. Limited work has been carried with HSP and vegetable oils, thus far it has been confined to biofuels. Through transesterification, biofuels have an altered structure compared with vegetable oils, reducing polarity, and that is clear from the difference in HSP values.

These values were derived using volume additive rules using HSP values for the fatty acids that make up the vegetable oils, as described in Section 7.4.5. Table 10-2 gives values for each fatty acid and its composition. All HSP values were found in the HSPiP database apart from stearic acid. The DIY HSP function in the Y-MB solver in HSPiP was used to obtain these values based on the international chemical identifier (InChI) for stearic acid. As discussed in 9.4.1, the volume additive method for obtaining HSP values has been shown to work well, although may underestimate the polar element.

Base Stock	Dispersive forces, δ_D, $MPa^{1/2}$	Polar Forces, δ_P, $MPa^{1/2}$	Hydrogen Bonding, δ_H, $MPa^{1/2}$	Mvol, cm^3 mol^{-1}	Methyl Esters* δ_D, $MPa^{1/2}$	Methyl Esters* δ_P, $MPa^{1/2}$	Methyl Esters* δ_H, $MPa^{1/2}$
MO	17.4	3	5.3	Not available			
JO	15.71	2.74	5.15	306.15	Not tested		
SO	16.11	2.99	6.01	276.47	15.9	1.4	3.2
PO	15.48	3.5	6.38	251.5	16	1.6	3.6

Table 10-1, Hanson Solubility Parameters Calculated Using HSPiP and Values Found in Literature (204)

Fatty Acid	Chain Length	Proportion in composition	δ_D, $MPa^{1/2}$	δ_p, $MPa^{1/2}$	δ_H, $MPa^{1/2}$	Mvol, cm^3 mol^{-1}
PO						
Lauric	C12:0	0.408	16.2	4.1	7.5	224.5
Myristic	c14:0	0.154	16.3	3.4	6.6	257.4
Palmitic	C16:0	0.124	16.3	3.4	6	290.6
Stearic	C18:0	0.202	16.3	3.3	5.5	336.5
Decanoic	C10:0	0.023	16.2	4.2	8.3	191.6
Oleic	C18:1	0.042	16	2.8	6.2	282
TOTAL		0.953	15.48	3.5	6.38	251.49
SO						
Palmitic	C16:0	0.107	16.3	3.4	6	290.6
Stearic	C18:0	0.04	16.3	3.3	5.5	336.5
Oleic	C18:1	0.239	16	2.8	6.2	282
Linoleic	C18:2	0.529	16.8	3.1	6.2	280
Linolenic	C18:3	0.059	17	3.2	6.5	278
TOTAL		0.974	16.11	2.99	6.01	276.47
JO						
Erucic	C22:1	0.153	16.5	2.7	4.8	383.3
Gadoleic	C20:1	0.722	16.4	2.9	5.4	310
Oleic	C18:1	0.084	16	2.8	6.2	282
TOTAL		0.959	15.71	2.74	5.15	306.15

Table 10-2, HSP Values for Fatty Acids, Used to Derive Final HSP Values

10.2 Ethylene Propylene Diene Monomer

10.2.1 *Stress Relaxation Tests*

Figure 10-6 shows results from all stress relaxation tests with EPDM, with bio-base stock candidates JO, represented by the yellow lines, PO, represented by the blue lines, and SO, represented by the red lines, as well as MO, represented by the brown lines. A control test was performed in air, which is represented by the green lines. The base stocks represented in all figures in this section follow the same colour coding.

The stress relaxation for the control test carried out in air follows a similar trend to results obtained with PO and SO. This would suggest that PO and SO have little interaction with EPDM. EPDM and MO, on the other hand, demonstrated swelling behaviour, apparent early on in the test with F/F_o greater than 1; stress relaxation occurs after initial swelling occurs.

These results contradict industry defined chemical resistance data (255). These rate the interaction of EPDM with SO, 'vegetable' and MOs all as '3', which is defined as moderate to severe swell (10-20%), only suitable for static applications. The experimental data in Figure 10-6 clearly show that EPDM does not act similarly with SO, PO, JO and MO. While volume measurements were not taken, changes in mass were, and are proportional to change in swell. Mass increase of EPDM samples tested in MO was in the range of 31-38.5%, JO in a narrower range of 20-23%, while EPDM samples in PO and SO were in the range of 9-10% and 5-7.5% respectively.

Furthermore, to highlight the extent of the discrepancy, the industry standard tests are performed at room temperature; as the tests in this work were carried out at 80˚C, this should have accelerated aging. Industry defined chemical resistance is based on volume swell, compression set and aging resistance. Stress relaxation tests are felt to offer a good insight into material interaction, as they have the ability to dynamically measure samples under compression, giving an indication of the level of swell and in service behaviour. As well as this, the results show that a near equilibrium state is reached early on in the test period. This could give an indication of behaviour during normal service life, but not necessarily towards end of life, where a rapid drop off in material properties may be expected, therefore not necessarily giving a full view of aging behaviour.

Nonetheless, it is felt that chemical resistance data, in this instance, are giving a particularly cautious overview in terms of JO, PO and SO. These discrepancies can also be linked to that fact that no specific data is offered for PO and SO. While they come under the class of vegetable oil, vegetable oils have a wide range of chemical structures, which will cause varying results on contact with elastomers. Figure 10-6 also shows that the rate of absorption of oil into the elastomer is faster than the rate of desorption of elastomer into oil. This can be seen by observing the relatively quick rate of swell in the MO and JO tests, within the 24 hours of testing. The rate of shrinkage is much slower, over 48-72 hours.

As discussed Section 6.11, Fafan-Cabrera et al. (187) found high levels of swell in static emersion tests with EPDM and mineral based engine oil and low levels for jatropha oil. The molecular weight of jatropha oil 866 kg/kmol (208)z, this is close to the molecular weight of PO, at 846 kg/kmol (213), so they should possess a similar diffusion quality (as discussed in Section 5.3.4). Jatropha oil is also made up of similar

fatty acids to SO (oleic and linoleic), so they should possess similar solubility parameters. Therefore a fair estimate would be that EPDM would exhibit a similar stress relaxation profile to these oils. This also agrees with the theory that compression reduces the levels of swell (as discussed in Section 5.3.3).

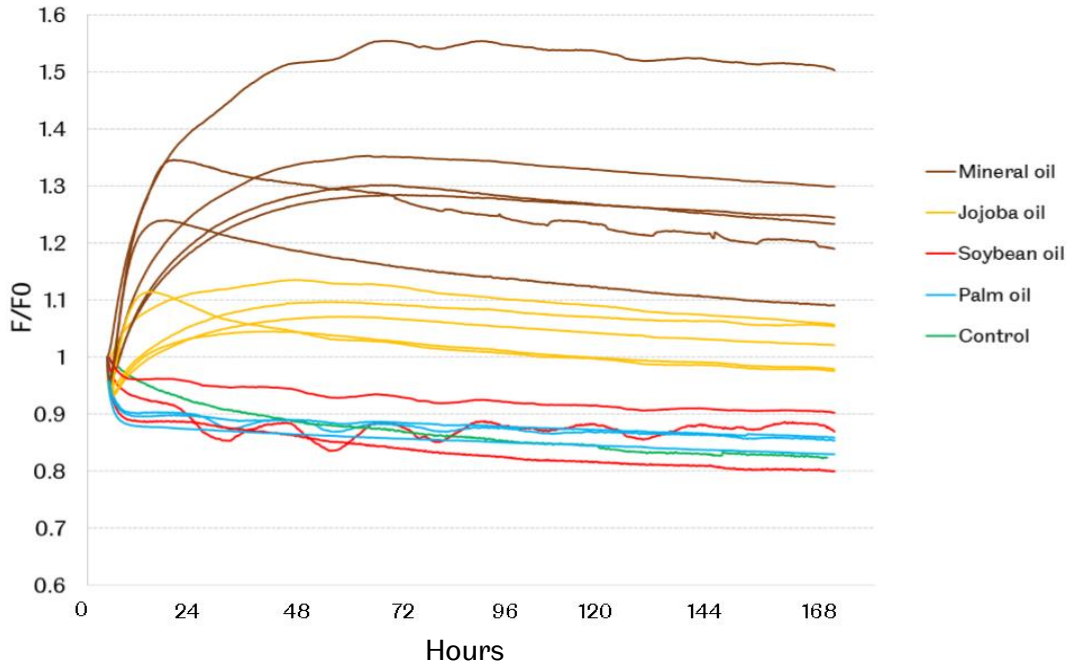

Figure 10-6, Results from Stress Relaxation Tests with EPDM and Base Stocks, Each Line Represents one 168 Hour Test Cycle, the Green Line Represents a Control Test Done in Air

10.2.2 *HSP results*

Figure 10-7 shows stress relaxation data correlated with relative energy difference; an RED of 0 would mean that 2 materials have a strong interaction, an RED greater than 1 would mean materials are less likely to interact, as described in detail in Section 5.3.5. Simply put, RED is a measure of similarity. This shows that it is possible to relate the experimental data with the theoretical data to some extent.

If RED between two substances is less than one, the two substances are likely to dissolve in one another. If RED is greater than one, it is likely there will be little effect, as discussed in Section 5.3.5. The RED data demonstrates that MO interacting with EPDM results in an RED of 0.24, the lowest RED of the oils tested, and shows the most variation in mass and applied force, while PO, with an RED of 0.61, the highest of the oils tested, showed the least variation in mass change and applied force. The problem in reaching a definite correlation lies with the data for JO and SO. SO with EPDM has an RED of 0.49 and JO with EPDM has an RED of 0.55. JO and EPDM had considerably more variation with mass change than SO. This should mean that JO has a lower RED than SO, but it is not the case.

The anomaly in the results is potentially attributable to an error that occurs when HSP values are derived through volume additive rules, rather than experimentally

determining them. Graham et. al. (194) hypothesised that this method underestimates the polar element of HSP. Graham noticed a link between increased δ_P and increasing levels of swell, Nielson et. al. (201) also found this link. Therefore, if the polar element is misrepresented, the RED value will be less accurate.

It is also quite likely that the molecular weight of the oils is a factor here. HSP does not take this into account and, while the HSP values for JO and SO are very similar, the molecular weights are not, at 610 (207) and 920 kg/kmol (256) respectively. This would account for the fact that considerably less mass change is observed in tests with SO, due to the molecules not being able to diffuse into the polymer matrix, as they are too large. PO has a slightly lower molecular weight of 846 kg/kmol (213), but also behaves similarly to SO in stress relaxation tests.

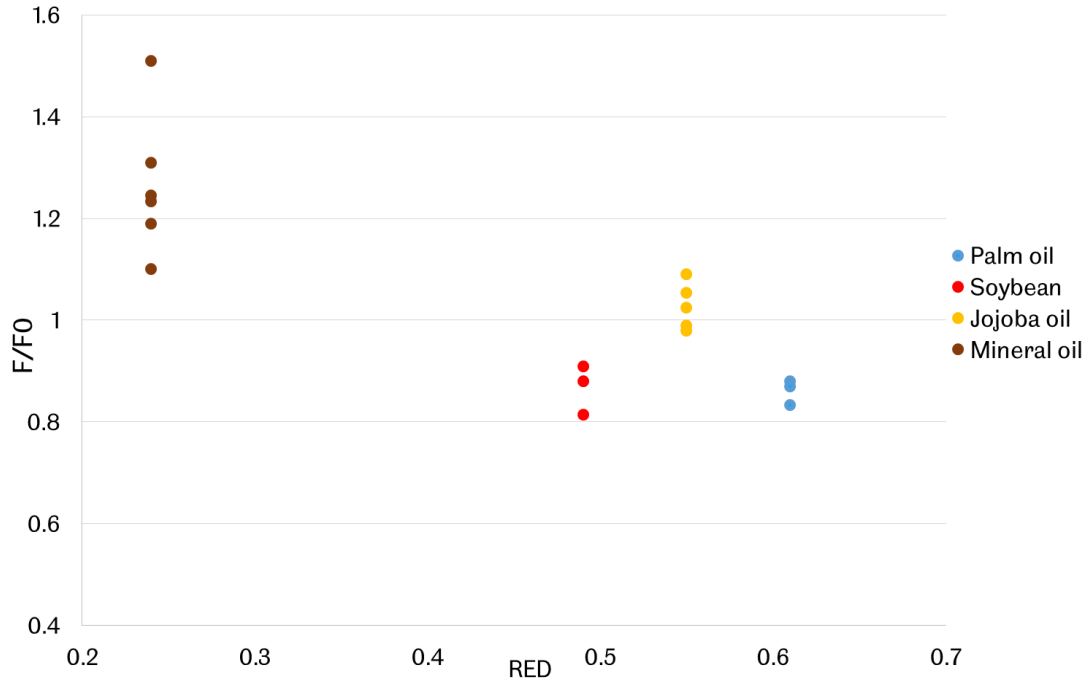

Figure 10-7, Stress Relaxation Test Data Correlated with Relative Energy Difference from Tests with EPDM

10.3 Fluorocarbon elastomer

10.3.1 *Stress Relaxation Tests*

FKM is known for its superior performance in comparison to other types of elastomer. It has better heat resistance and is more resistant to chemical degradation, particularly from fuels and lubricants, partly due to its extremely low permeability to a range of fluids (188). The industry chemical resistance data validate this, reporting it as a '1', which is defined as minor degradation with little swelling, between 0-5%, for all the fluids tested here.

Experimental data for stress relaxation agrees with the industry chemical resistance data, as well as literature (187), as shown in Figure 10-8. There is little difference between the results for all the bio-base stocks, as well as MO. The control test showed a gradual and small reduction in the force required to maintain the distance between

plates, with results for normalised force going to 0.95 and seeming to reach an equilibrium state. The majority of the other results fall in the range of 0.81-0.9 for normalised force data. This shows only slightly more degradation of the elastomer in the base stocks than air, which could be attributed to the removal of plasticizers and fillers; this is discussed in more detail in 10.4.

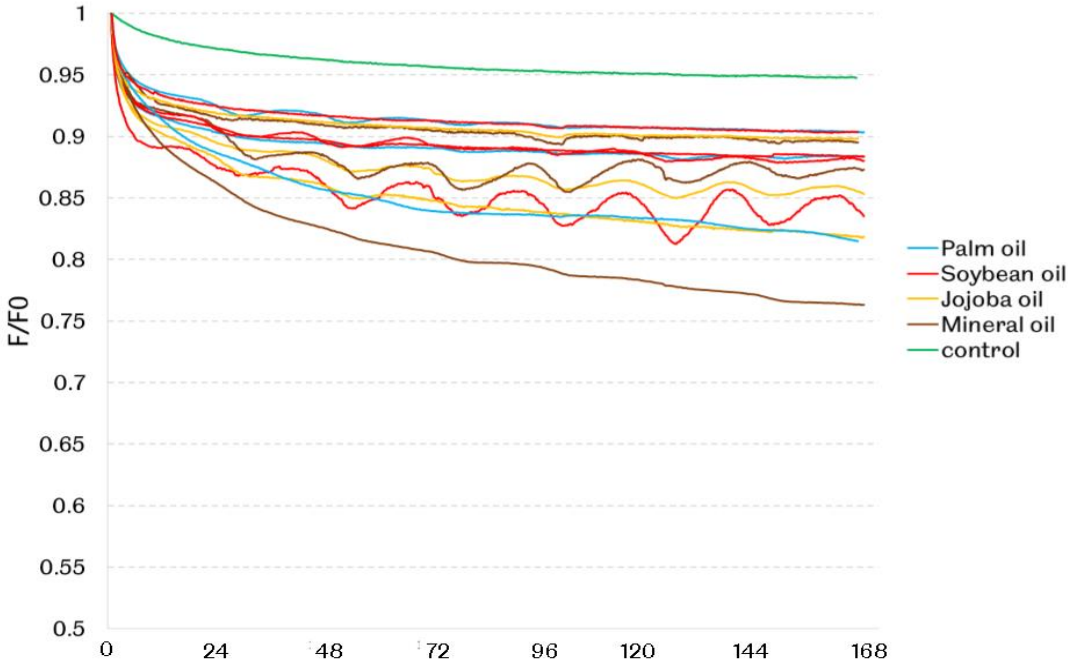

Figure 10-8, Stress Relaxation Data for Tests with FKM and Base Stocks

10.3.2 *HSP Results*

Figure 10-9 shows that there is no apparent correlation between RED and experimental data with FKM. MO has an RED of 1.07 and has very similar results for F/F_0 and percentage mass loss as PO with an RED of 0.97; both JO and SO have similar RED values of 1.01 and 1.02 and also very similar results to PO and MO. This lack of trend was also noted by Nielson (201), who compared RED and swelling of FKM. This lack of correlation is due to the fact that FKM is a co-polymer; each polymer will have its own HSP values and these could be very different. The proportion of each polymer would be required in order to derive more accurate HSP values. The underestimation of the polar component of HSP, as discussed in HSP results, is not thought to be an issue in this case as the interaction of FKM with the base stocks is overall less sensitive to polar effects.

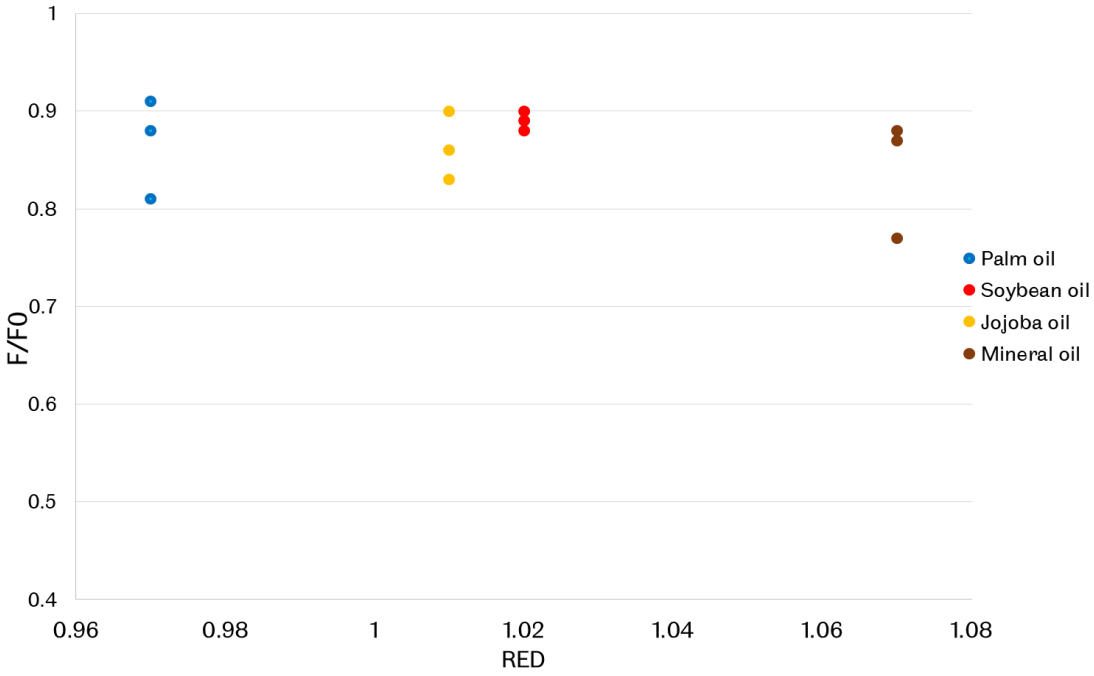

Figure 10-9, Stress Relaxation Test Data Correlated with Relative Energy Difference from Tests with FKM

10.4 Nitrile Rubber

10.4.1 *Stress Relaxation Results*

Similarly to FKM, there is little variation in stress relaxation results between the base stock candidates, as seen in Figure 10-10. This shows that the bio-base stocks are consistent with mineral base stocks in terms of compatibility performance. All tests showed a considerable drop off in the force required to maintain the distance between plates in the first 48 hours of testing, demonstrating shrinkage in the seal material. This is attributed mainly to the loss of plasticisers that leach out (196); these plasticisers are needed for low temperature flexibility and performance but are relatively easily extracted at elevated temperatures, as they leach into polar and nonpolar liquids. The rate of this leaching is a function of temperature and plasticiser concentration. The plasticisers are found in the amorphous parts of the polymer and can be attached to the polymer chains or free among the polymer network (117); either way they can still be extracted. Figure 10-11 shows plasticisers positioned in-between polymer chains.

Conventional plasticisers have been found to be carcinogenic, disrupt hormone production and pose an environmental risk. For these reasons, novel plasticisers have been developed, which can be made from fatty acids. If polymers with these types of plasticisers come into contact with bio-base stocks, it is more likely they will be extracted, in line with the principles of 'like dissolves like', which HSP is based on

.

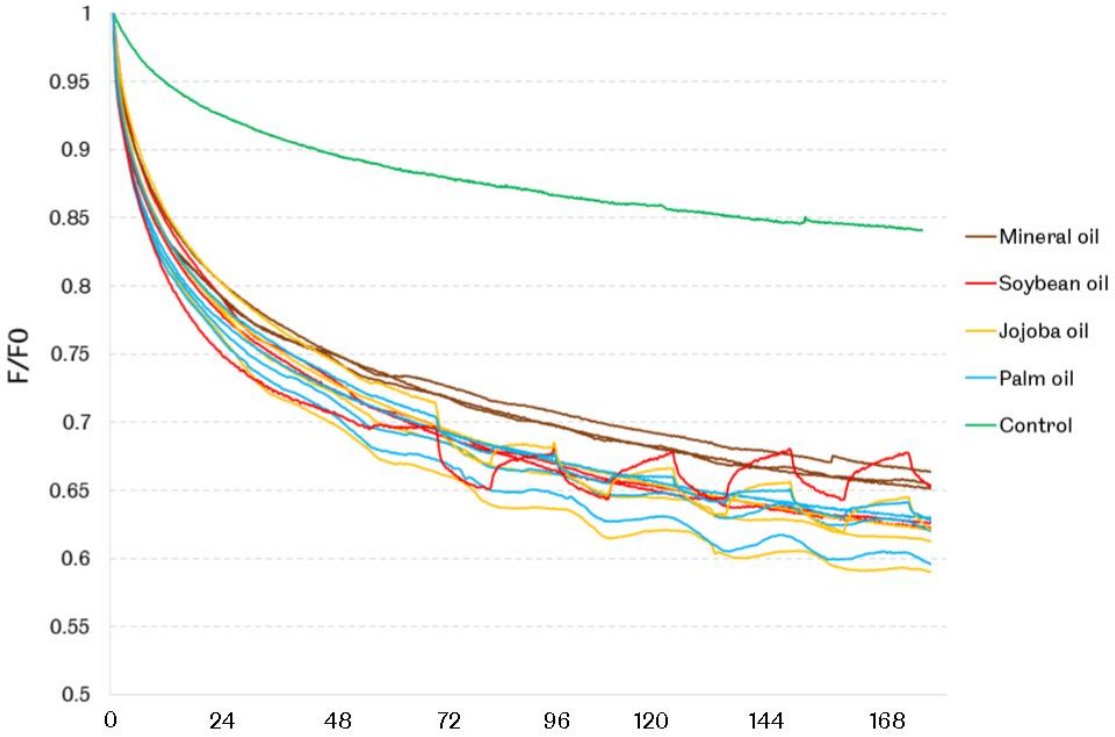

Figure 10-10, Stress Relaxation Data for Tests with NBR and Base Stocks

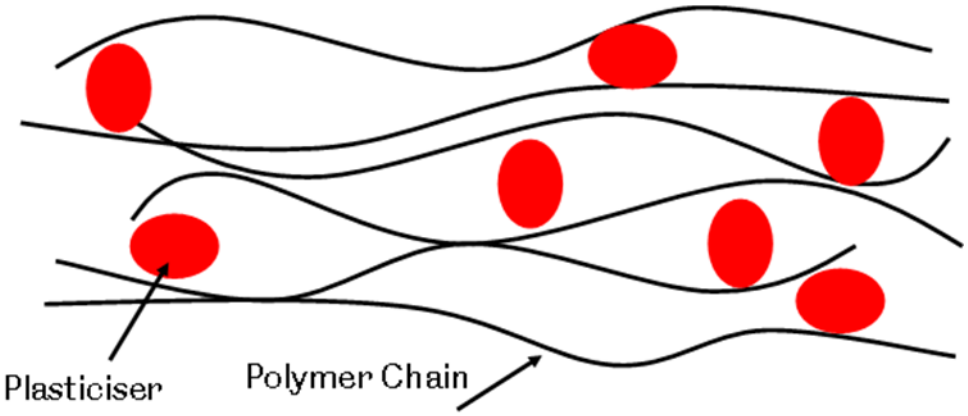

Figure 10-11, Representation of Plasticisers among Polymer Chains

As with the tests carried out with EPDM, results do not agree with those provided in industrial chemical resistance data; there are no specific data on JO and PO, but 'vegetable', SO and MO are all rated '1' for minor degradation. This is clearly not the case when looking at stress relaxation data. The data is also not similar to those with FKM tests, which also have a '1' rating for all base stocks. As previously mentioned, chemical resistance data are obtained from tests carried out at room temperature, and the extraction of plasticisers, which is the most likely cause of the considerable shrinkage in the seal, is temperature driven, therefore results would differ at room temperature and 80°C. NBR has more plasticisers than other common elastomer

materials (196), which also accounts for the fact that there is considerable shrinkage in NBR and not FKM and EPDM. Heitzig et. al. (193) also attributed the degradation of NBR elastomers tested to the extraction of plasticisers.

The degradation in the NBR seal sample during the control test was considerably less than when the seal is tested in the base stocks. The rate of diffusion of plasticisers into air is slower, as they are not as chemically compatible. The main driver of degradation in the control test was the application of heat, giving the plasticiser molecules increased kinetic energy.

Methods for assessing elastomeric compatibility (ISO 3384-1:2011, ASTM D4054) assess 'new' material properties, rather than the material properties an elastomer would have in service. Artificially aging the seals before testing would mean that compatibility could be assessed for the bulk of the sealing material, rather than assessing how quickly the base stocks extract the plasticisers. A method was developed, in conjunction with another project, for conditioning has been developed with NBR in mind. It would involve subjecting O-rings to standard stress relaxation test conditions, but at a lower temperature (30 °C) for 150 hours. Another proposed method for conditioning and aging has been developed to compare methods, this involves subjecting O-rings to standard stress relaxation test conditions at higher temperatures (85 °C) for 300 hours. For both methods the test fluid must be monitored to ensure no significant thermal degradation. This could be monitored based on the change in fatty acid structure for the vegetable oils. Once O-rings are conditioned and/or aged, the stress relaxation test can be performed.

10.4.2 *HSP Results*

It is difficult to see a correlation between stress relaxation data and RED values with NBR data in Figure 10-12, even less between RED and mass change in Figure 10-5 in Section 10.1.2. As discussed in Section 6.11, Heitzig et. al. (193) also found a lack of correlation between HSP data and experimental data, citing the fact the NBR is a copolymer as the reason, as previously mentioned. On the other hand, Liu (257) found a correlation between F/F_0 and RED with stress relaxation data obtained when testing NBR and various alternative potential jet fuels. It is unclear why there is a discrepancy here; it is possible that tests discussed here did not present a wide enough and varied range of RED numbers for a correlation to become apparent. Liu drew a correlation from 25 different blends of potential jet fuel that all had different RED values. Further experimental data would need to be obtained in order to explore this further.

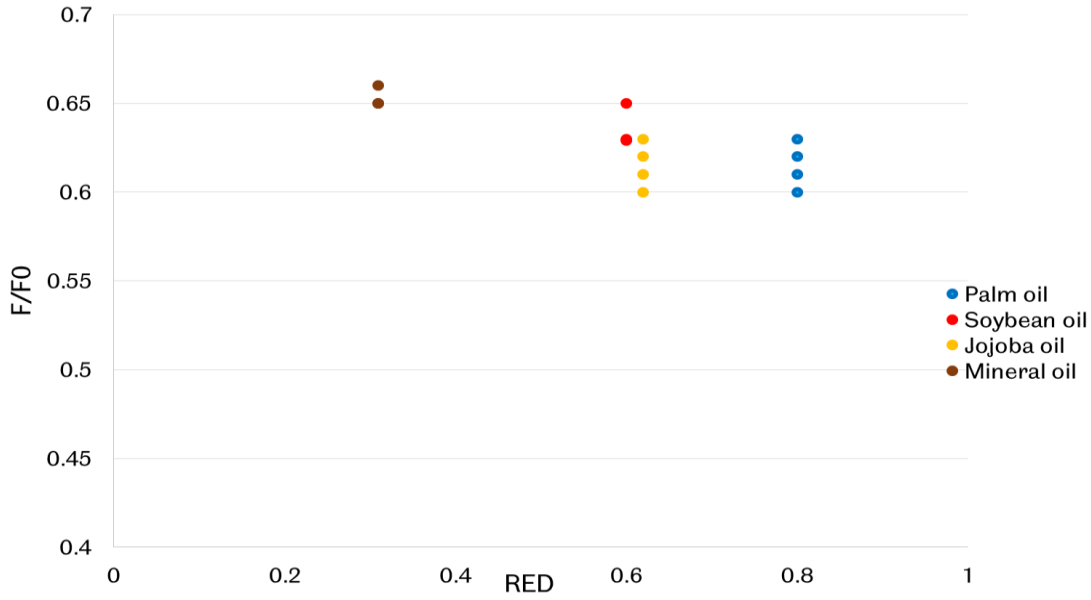

Figure 10-12, Stress relaxation test data correlated with Relative Energy Difference from tests with NBR

10.5 The Uses and Limitations of Hanson Solubility Parameters in Predicting Material Compatibility

The use of Hanson Solubility Parameters and HSPiP software to predict material compatibility has potential for use in assessing the compatibility of elastomer with base stock candidates. The software translates some complex molecular interaction theory into simple to understand visual representations. The HSPiP software is simple to use and gives quick results for estimates of compatibility, provided information on solubility parameters for the elastomers and fluids is available. HSPiP could be a useful tool for large engineering organisations, such as automotive and aviation manufacturers. The aviation industry, for example, has rigorous and lengthy approval processes for elastomers, fuels and lubricants, and similarly the automotive and industrial fluids industries, albeit to a lesser extent. HSPiP could act as a tool to reduce the amount of compatibility testing required by acting as a filtering tool to narrow the selection of new elastomers, fuels and lubricants, leaving fewer options for compatibility testing. Within HSPiP's current limitations it has the potential to filter out materials that are clearly compatible or not compatible. It's limitation lies in predicting compatibility of materials whose interactions are more subtle.

The software is currently orientated to the chemical industry, rather than the lubricant or fuel industry. This means the data base does not include many of the important fluids used in these industries, or the correct elastomer specifications commonly used. The DIY HSP function in the Y-MB solver can be used to predict solubility parameters (as discussed in Section 7.4.5), but must be used with caution, and some understanding of the chemical behaviour of the fluid is still required to ensure it is accurate (221). Therefore, in order to improve the functionality of the software, the data base needs expanding for more lubricant based chemicals.

The software's main limitation is that it cannot accurately model co-polymers or complex fluids. This could be improved by experimentally determining solubility

parameters for some of the more common co-polymer elastomers. Alternatively, working with elastomer manufacturers to accurately model the co-polymers based on the 'recipes' used would also improve the database.

HSPiP may also have a use in the assessment of surface energy and the interaction of lubricants with surfaces, as the work in Section 9.4.2 covers. Solubility parameters can be linked with surface energy values. As with elastomer compatibility predictions, HSPiP could be used as a filtering tool in the process of optimising lubricants and surface treatments, acting to reduce the amount of testing required to find the ideal lubricant for a given surface.

10.6 Conclusions

The bio-lubricant base stock candidates presented varied results in terms of compatibility with different elastomer seal materials. All base stock candidates were found to be compatible with FKM seals, and it is likely that none would cause failure of this seal material. Very little mass loss was observed, most mass change was seen with FKM samples tested in MO, with 2.5% reduction in mass. No significant stress relaxation occurred during the length of testing.

Compatibility of the base oil candidates with EDPM is more difficult to define. EPDM used with mineral base oil could cause seal failure due to degradation of the seal material and levels of swell, leading to increased strain in the contact. EDPM used with SO and PO is likely to be compatible. An average increase in mass of 5.7% was measured with EPDM tested in SO, while this figure was 9.6% for PO. Both exhibited small amounts of stress relaxation, but this was equivalent to the amount of stress relaxation observed with control tests. EPDM compatibility with JO is, again, more difficult to define; average increase in mass was 21%, while a small increase in stress was observed during testing. This could be advantageous in aiding seal performance, but it is unclear whether the increase in mass would have a detrimental impact on the material performance long term.

The use of the base oil candidates with NBR is not advised; the extraction of the plasticisers used in this particular seal caused significant stress relaxation due to shrinkage in the seal. JO caused the largest reduction of mass, 5.8%. This would cause seal failure if used in application.

These results for compatibility tests with EPDM and NBR contradict industry defined chemical resistance data. It is thought that, while the methods used elastomer compatibility provide important knowledge for material interaction for certain applications, such as low temperatures, they may not provide an accurate view for automotive lubricants and elastomeric interactions. The discrepancy in results is related to the test methods employed. It is felt that stress relaxation tests may provide relevant data that provides more realistic predictions for compatibility.

Further work is required to improve the accuracy of modelling elastomer compatibility using HSPiP software. The expansion of the database for both lubricants and elastomers, particularly improving the accuracy of co-polymer elastomers, is required. It is, however, thought that the software can act as a useful tool in filtering out materials that are not compatible. There is potential to expand the software's function to assessing the interaction of lubricants and surface treatments. The software could be used as a tool, using HSP and surface energy values to explain the spreading parameter of a solid and liquid interfaces.

11 Conclusion

This chapter begins with a justification of the research theme, by revisiting the objectives and drawing together the main findings from literature, theoretical knowledge and experiments. To follow, recommendations for future work are given.

11.1 Justification of Research Theme

A review of the legislative environment and future lubricant performance demands concluded that legislation is in place, or in the process of being implemented, which should act as a driver in the move towards bio-lubricants (as well as other environmentally friendly fluids). The European Union's Registration, Evaluation, Authorisation and Restriction of Chemicals (REACH), along with similar standards in other parts of the world, and programmes such as eco-labels and passenger car lubricant standards like GF-6, should set the environmental and tribological performance requirements for bio-lubricants. As the bio-lubricants market is predicted to grow in the near future, research is still required to ensure the effective delivery of a bio-lubricant product that meets the ever increasing performance needs of users and industry. There is therefore an opportunity to utilise the legislative restrictions of bio-fuels to switch production to bio-lubricants and reduce the issue for using land that can grow food crops for industrial purposes. The research presented here goes some way towards supporting that opportunity, and the research gaps identified in existing bio-lubricants work (chiefly; material compatibility, wear and friction performance) demonstrate the validity of performing the work presented in this thesis.

11.2 Conclusion of work

The aim of this thesis was to investigate the feasibility of bio-lubricants for use in four stroke internal combustion engines. To achieve this the tribological properties of bio-lubricants were assessed using experimental methods. Objectives were set in Section 1.3, following a review of the legislative environment, current knowledge on bio-lubricants, and future lubricant performance demands. Following this review, the theme of the 'journey around the oil circuit' was adopted with a focus of the compatibility of bio-lubricants with novel surface treatments and elastomers.

Overall the work has shown that while there is a growing body of research on the topic of bio-lubricants, there are several areas where knowledge is lacking. This thesis, as well as a review of literature, has demonstrated that data on bio-lubricants is inconsistent and lacking. More work is required to bring the understanding of the performance of bio-lubricants to the same level as mineral based lubricants, particularly how mechanical and chemical degradation impacts this performance. This is a key area of improvement required before bio-lubricants are feasible in four stroke internal combustion engines.

The main conclusions from this work are as follows;

1. There is no performance benefit, in terms of wear and friction reduction, to blending jojoba and mineral oil, as seen from results of the learning experiments. It was therefore decided that using blends would add complexity to the test programme with potentially no performance benefit. The learning experiments also revealed that there was not significant sensitivity to the parameters varied (temperature, normal load and test duration). Therefore

other considerations were used to help define test parameters, these were parameters used in literature, to help compare the performance of bio-lubricants and knowledge of coating failure zones, such as the scratch test failure map (Section 5.2.1).

2. Results showed that there are performance advantages to using bio-lubricants with diamond-like-carbon (DLC) coatings, with lower wear and friction observed in comparison to the mineral base stock tested. There are some clear wear protection and friction reducing performance gains to be made through using multi-layer surface treatments with bio-base stocks.

3. The substrate finish is an important factor for the type of wear that occurs. Rougher substrates resulted in plastic deformation and adhesive wear being dominant in the DLC coating, while smoother substrates caused cracking and spalling in the DLC coating. Overall a smoother substrate resulted in lower levels of wear. There were exceptions, such as the surface treatment combination of shot blasting and DLC, the surface ground substrate specimen produced lower wear then its super finished counterpart. This may be due to the rough surface offering lubricant wells, which aided lubricant retention.

4. There is evidence in literature that carboxylic acid groups in bio-base stocks are able to form physi- and chemisorbed films by bonding with dangling bond orbitals on the surface of DLC. Results reinforce this theory as there is a clear performance difference between the bio-base stocks and mineral base stocks. The difference in performance between bio-base stocks is less clear, indicating that all are compatible with DLC. DLC is a common automotive coating, therefore this is an encouraging result in the assessment of the feasibility of bio-lubricants for use in automotive applications.

5. The calcium based chemical dip (CD) has proved to be as effective in terms of wear protection as DLC, while potentially offering an improved benefit over DLC with less issue with substrate miss matching, adhesion issues and cracks in the coating layers. It is proposed that the bio-base stocks interact with this surface treatment through decomposition of CD, in that the calcium bonds with the fatty acids to enhance lubricity. Sulphur forms bonds with the steel surface to offer wear protection. This surface treatment is most suited to jojoba oil. This coating is currently used in the motorsport sector, but could have potential for passenger cars if the lubricant interactions and wear life of it are better understood.

6. The carboxylic acid groups in the bio-base stocks could act as an oxidant and bonds with Mo or S to form a physisorbed film and aid lubrication. This mechanism appears to have been particularly effective with jojoba oil. This mechanism is not as effective as the mechanisms described for DLC or the calcium based chemical dip. The interaction of steel and bio-base stocks is dominated by chemisorbed films formed by the carboxylic acids groups. This is a very effective wear and friction reduction mechanism for smooth surfaces.

7. Experiments to assess the compatibility of elastomers with bio-lubricant base stocks found that, contrary to industry defined chemical resistance data, bio-base stocks are at least as compatible with elastomers as mineral base stocks. The contradiction between results presented in this thesis and industry

defined results is noticeable with EPDM and NBR elastomers. The test methods used to produce the industry chemical resistance data is thought to be the cause of this discrepancy. This results in a cautious overview of compatibility of bio-base stocks and elastomers. It is felt that stress relaxation tests are a more effective measure of sealing performance and lubricant compatibility. These tests are a better representation of in service conditions in comparison to static immersion tests. The ability to continually measure changes in sealing force give a better understanding of the rates of adsorption of base stock in to the elastomer and the rate of desorption of components of the elastomer in to the base stock.

8. The use of solubility parameters may provide a useful tool in simplifying the selection process for assessing compatibility of materials with lubricants, and not just limited to bio-lubricants. The current power of the HSPiP software detailed in this thesis is beneficial for an initial assessment of compatibility, but must be used with understanding of its limitations. The limitations are that it does not consider molar volume, which is an important factor in diffusion theory. It is difficult to theoretically predict solubility parameters for complex materials and fluids. Although group contribution and volume additive methods have been showed to give a fair estimation of these parameters.

11.3 Novelty Statement

The novelty in this work is linked to the multi-layer surface treatments tested with bio-lubricants. Little or no research has been conducted with the materials used in this thesis and bio-lubricants. No work has assessed the compatibility of nitrile rubber, EPDM and fluorocarbon elastomers with bio-lubricants using a stress relaxation test method. The link between experimental data and Hanson Solubility Parameter for bio-lubricants is also novel.

11.4 Reflection and Future Work

The results of the work presented in this thesis provide the foundations for developing a suitable bio-lubricant for four stroke internal combustion engines. While the results have shown that bio-base stocks can match the performance of mineral base stocks, further work is required to map the complete tribological performance of these bio-base stocks.

There are several limitations to this work that need further consideration:

1. The lack of certainty in solubility parameter values is a limitation of this work. Estimation had to be made for solubility and surface tension values. Increasing the certainty of these values would improve the ability to predict bio-lubricant behaviour in the boundary lubrication regime through the spreading parameter. This has a dual use of being able to assess the link between surface tension values and solubility parameters.
2. The mechanism of interaction between the bio-lubricant base stocks and the calcium based chemical dip was hypothesised. While there is evidence in literature to reinforce this hypothesis, further element analysis of specimens before and after testing would confirm this.

3. A review of literature revealed inconsistent data for the pressure viscosity coefficient value required to calculate EHL film thicknesses.
4. The accuracy of film thickness measurements presented in this thesis is not certain.

A programme of further work is proposed to develop some key ideas generated in this thesis that may make characterising bio-lubricants simpler.

11.4.1 *Solubility Parameters*

The theory of linking spreading and solubility parameters needs experimental validation. To do this contact angle measurement for a variety of bio-base stocks must be made so that the components of surface tension can be more accurately calculated. This would mean that spreading parameter values could be calculated. The solubility parameters may offer a dual use in the characterisation of lubricants with novel surface treatments, such as the calcium based chemical dip. This could take the form of an add-on to the HSPiP software to give spreading parameter predictions. This would require further work to confirm the relationship between surface tension and solubility parameters for carboxylic containing fluids particularly. The experiments to determine contact angles would give the information to begin this process. A large and varied data set would be required to develop an empirical relationship that could be used to predict values for untested lubricants and surfaces.

If a clear link between the solubility parameters and potential friction performance for lubricant base stocks it would give the potential to speed up selection and classification of automotive lubricants. This is particularly relevant for bio-lubricants as there is such a wide variety of potential feedstocks for lubricants, this method could be used as a filtering tool to speed up the development of these lubricants.

11.4.2 *Calcium-based Chemical Dip*

Leading on from this, further wear testing with the calcium based chemical dip could be carried out, to confirm the type of interaction between this surface treatment and bio-base stocks. It is proposed to conduct further wear and friction tests with the addition of more comprehensive elemental analysis techniques. This is required to assess if there is the proposed interaction mechanism between calcium and fatty acids. Clarification on whether this surface treatment could withstand internal combustion engines conditions is required. Performing some component based wear testing, such as using a piston ring and liner attachment for the Plint TE77 could form the beginning of this assessment.

Alongside this, developing an additive package suited to bio-base stocks utilising the lubricity enhancing ability of calcium and fatty acids would determine the best use of calcium with bio-lubricants. If an additive package can be developed to improve the negative aspects of bio-lubricant performance, such as oxidative stability, and enhance the positive performance aspects, such as wear protection and friction reduction, laboratory scale tests could be conducted to assess the use of bio-lubricants in engines designed for mineral based lubricants. Along with using a calcium-based additive in the lubricant, an antioxidant needs to be selected as a minimum requirement. Initial characterisation with reciprocating wear tests is needed to develop an optimal additive package.

As there is an ever increasing demand on automotive engines to be more fuel efficient, one current method for achieving this is by using lower viscosity lubricants. This means that automotive engine components are increasingly operating in boundary lubrication. To protect these components, the use of surface treatments is becoming more common. In order for bio-lubricants to become feasible automotive lubricants, surface treatments that are compatible must be developed. Results from this work have shown that the calcium based chemical dip has the potential to be a suitable surface treatment and is already being used in motorsport. There is no literature on the performance of this type of coating. Therefore, much work is required to ascertain its suitability in passenger cars.

11.4.3 *Pressure-Viscosity Coefficients*

A review of literature found discrepancies in values for pressure viscosity coefficient for vegetable oils. An experimental programme is proposed to calculate values for pressure viscosity coefficient for vegetable oils. This would improve understanding of bio-lubricants and enable accurate predictions for film thicknesses in all boundary and elasto-hydrodynamic lubrication regimes. This could be performed using ultrasonic measurement techniques during tribological tests of the Plint TE77 used for wear and friction measurements in this thesis. If this can be better characterised, an assessment of the lubrication ability for bio-lubricants and contacts in internal combustion engine can be made.

As discussed in this thesis, internal combustion engines have lubricated contacts under the full range of lubrication regimes. An improved understanding of how a lubricant behaves under high pressures will mean that particularly engine components that operate in the elasto-hydrodynamic regime (see 4.2 for more details), can be designed to ensure safe operation. Surface roughness finishes and materials could be better selected if more accurate film thicknesses can be calculated. Meaning components are less likely to fail with the use of bio-lubricants.

11.4.4 *Elastomer Compatibility*

Finally, further work to improve the prediction of elastomer compatibility using solubility parameters needs to be carried out. As mentioned in further work for developing spreading and solubility parameters, working with solubility parameters could have a dual use in material compatibility assessments. Therefore further elastomer testing to improve the data set for solubility parameters is required. Solubility parameters can be measured experimentally, this requires mixing fluids or elastomers with fluids with known solubility parameter, to calculate the new solubility parameters. Aging seals, as discussed in Section 10.4.1, could also be performed to further improve the in-service replication of stress relaxation tests.

A more accurate picture of the compatibility of elastomers and bio-lubricants will ensure that seal failure does not occur if bio-lubricants are used in automotive engines. From the work carried out so far, further data on elastomer compatibility will also act to remove a barrier to the implementation of bio-lubricants in automotive (and other) applications, as current industry standard recommendations are not an accurate reflection of the compatibility of vegetable oil based bio-lubricants and are unnecessarily cautious.

11.5 Publications Arising

11.5.1 *Peer Reviewed Journal Paper - In Print*

Carrell, J., Slatter, T., Little, U., Lewis, R. (2017) "*Combining DLC, Shot blasting, chemical dip and nano fullerene surface treatments to reduce wear and friction when used with bio-lubricants in automotive contacts.*" SAE Technical Papers. 2017-01-0878. ISSN 0148-7191 (Presented at SAE World Congress, Detroit, USA, April 2017).

12 References

1. Grand View Research. *Biolubricants Market Analysis By Raw Material, By Application, Industrial, by end-use, Segmet Forecasts To 2024.* 2016.

2. Hirsch, R. L., Bezdek, R. H. and Wendling, R. M. *Peaking Oil Production: Sooner Rather Than Later?,* 2005, Issues in Science and Technology, Vol. 21, pp. 22-30.

3. Owen, N. A., Inderwildi, O. R. and King, D. A., *The Status of Conventional World Oil Reserves - Hype or Casue for Concern?* 2010, Energy Policy, Vol. 38, p. 4743.

4. Cohen, G., Joutz, F. and Loungani, P., *Measuring energy security: Trends in the diversification of oil and natural gas supplies,* 2011, Energy Policy, Vol. 39, pp. 4860-4869.

5. Mcglade, C. and Ekins, P., *The Geographical Distribution of Fossil Fuels Unused when Limiting Global Warming to 2oC*, 2015, Nature , Vol. 517, pp. 187-190.

6. United Nations Framework Convention on Climate Change. *The Paris Agreement.* 2015.

7. Joyner, C. C. and Kirkhope, J. T., *The Persian Gulf Was Oil Spill: Reassessing the Law of Environmental Protection and the Law of Armed Conflict*, 1992, Case Western Reserve Journal of International Law, Vol. 24.

8. Lindén, O, Jernelöv, A and Egerup, J. *The Environmental Impacts of the Gulf War 1991.* International Institute for Applied Systems Analysis. 2004.

9. Schneider, M. P., *Plant-oil-based Lubricants and hydraulic Fluids,* 2006, Journal of the Science of Food and Agriculture, Vol. 86.

10. Biosynthetic Technologies. Environmental and Social Benefits . [Online] http://biosynthetic.com/environmental.

11. Mananhire, I. and Mbohwa, C., Lubricant Additive Impacts on Human Health and the Environment. *Mitigating Environmental Impact of Petroleum Lubricants.* 2016.

12. European Chemicals Agency, *Report on the Operation of REACH and CLP 2016.* 2016.

13. Lube-Tech, *REACH and its Impact on Base Oils and Lubricants Markets.* 2010, Vol. 96, pp. 1-5.

14. ATIEL REACH:Introduction. [Online] 2017. https://atiel.org/reach/introduction.

15. Environmental Protection Agency . *The Frank R. Lautenberg Chemical Safety for the 21st Century Act. EPA.gov.* [Online] 2017. https://www.epa.gov/assessing-and-managing-chemicals-under-tsca/frank-r-lautenberg-chemical-safety-21st-century-act.

16. Bart, J. C. J., Gucciardi, E. and Cavallaro, S. *Biolubricants Science and Technology.* 2013. ISBN 13: 9780081016084

17. European Chemical Agency. *Support Document for Identification of Trixylyl Phosphate as a Substance of Very High Concern Because of its CMR Properties.*

18. Agency, European Chemical. *Support Document For Identification Of 1,2-Benzenedicarboxylic Acid, DI-C6-10-Alykyl Esters; 1,2-Benzenedicarboxylic Acid, Mixed Decyl And Hexyl And Octyldiesters With ≥ 0.3% Of Dihexyl Phthalate (EC NO. 201-559-5) As Substances Of Very High Concern.* 2015.

19. European Chemical Agency. *Support Document For Identification Of Alkanes, C10-13, Chloro as a Substance of Very High Concern.* 2008.

20. Intersessional working group on Short-Chain Chlorinated Paraffins under the POPs Review Committee of the Stockholm Convention. *Short-Chain Clorinated Paraffins (SCCPs) Additional Infomation .* 2016.

21. nova-Institut GmbH (nova), Netherlands Standardization Institute (NEN), Agricultural University of Athens (AUA). *Knowledge Based Bio-based Products' Pre-Standardization, Deliverable N° 5.3:Market entry barriers.* 2015.

22. Theissen, H. *The German Market Introduction Program for Biobased Lubricants.* 2010, Tribology Online, Society of Japanese Tribologists, Vol. 5, pp. 225-229.

23. USDA, Washington DC. *Food, Conservation and Energy Actof 2008.* 2008.

24. Holmberg, K., Andersson, P. and Erdemir, A. *Global Energy Consumption Due to Friction in Passenger Cars.* 2012, Tribology International, Vol. 47, pp. 221-234.

25. National Highway Traffic Safety Administrasion, Fedral Register. *2017 and Later Model Year Light-Duty Vehicle Greenhouse Gas Emissions and Corporate*

Fuel Economy Standards. Department of Transportation . 2012. Volume 77, No. 199.

26. The European Parliament. *Setting Emission Performance Standards for New Passenger Cars as Part of the Community's Integrated Approach to Reduce CO2 Emissions from Light-Duty Vehicles.* 2009, amended 2014. B Regulation (EC) No 443/2009.

27. International Lubricant Specification Advisory Committee. *ILSAC GF-6A Recommendations for Passenger Car Engine Oils - Draft .* 2014.

28. Rathmann, R., Szklo, A. and Schaffer, R., *Land Use competition for Production of Food and Liquid Biofuels: An Analysis of the Arguments in the Current Debate.* 2010, Renewable Energy , Vol. 35, pp. 14-22.

29. BP. *BP Statistical Review of World Energy, Bio-Fuels Production by Region.* 2017.

30. Transparency Market Research . *Lubricants Market (By Product- Mineral oil, Synthetic and Bio-based) - Global Industry Analysis, Size, Share, Growth, Trends, and Forecast, 2014 - 2020 .* 2015.

31. United States Environmental Protection Agency . *Environmentally Acceptable Lubricants .* Office of Wastewater Management. 2011. EPA 800-R-11-002.

32. *Cold Rolling Mill Lubricant . US Patent 4891161* USA, 1990.

33. Motavalli, J. Oil Goes 'Green', With the Help of Some Cows. *The New York Times.* 2009.

34. Mortier, R. M., Fox, M. F. and Orszulik, S. T. *Chemistry and Technology of Lubricants.* 2010. ISBN 978-1-4020-8661-8.

35. Williams, J. *Engineering Tribology.* 2005. ISBN 978-0-521-60988-3.

36. Rudnick, L R and Bartz, W J. Comparison of Synthetic, Mineral Oil and Bio-Based Lubricant Fluids. [book auth.] L R Rudnick. *Synthetics, Mineral Oils and Bio-Based Lubricants.* 2013, pp. 347-365. ISBN 9781439855379

37. Coordinating European Council. *OECD Guidelines for Testing of Chemicals .*

38. Luna, F. M., Cavalcante, J. B., Silva, O. N., Cavalcante Jr, C. L., *Studies on biodegradability of bio-based lubricants.* 2015, Tribology International, Vol. 92, pp. 301-306.

39. Cecutti, C. and Agius, D., *Ecotoxicity and Biodegradability in Soil and Aqueous Media of Lubricants Used in Forestry Applications.* 2008, Bioresource Technology , Vol. 99, pp. 8492-8496.

40. OECD, *OECD Guidelines for the Testing of Chemicals 201, Freshwater Alga and Cyanobacteria, Growth Inhibition Test.* 2011.

41. OECD, *OECD Guideline for Testing of Chemicals 202, Daphnia sp. Acute Immobilisation Test.* 2004.

42.OECD, *OECD 203 Guidelines for Testing Chemicals 203 Fish Accuate Toxicity.* 1992.

43. ASTM International *ASTM D6046 Standard Classification of Hydraulic Fluids for Environmental Impact.* 2012.

44. Tamada, I. S., Montagnolli, R. N., Lopes, P. R. M., Bidoia, E. D., *Toxicological Evaluation of Vegetable Oils and Biodiesel in Soil During the Biodegradation Process.* 2012, Brazilian Journal of Microbiology, Vol. 43, pp. 1576-1581.

45. ASTM International. *Standard Guide for Conducting Laboratory Soil Toxicity or Bioaccumulation Tests with the Lumbricid Earthworm Eisenia Fetida and the Enchytraeid Potworm Enchytraeus Albidus.* 2004. E1676.

46. Lopes, P. R. M., Montagnolli, R. N., de Fatima Domingues, R., Bidoia, E. D., *Toxicity and Biodegradation in Sandy Soil Contaminated by Lubricant Oils.* 2010, The Bulletin of Environmental Contamination and Toxicology , Vol. 84, pp. 454-458.

47. Honary, L. *Biobased Automotive Lubricants, ASTM International.* 2012.

48. Erhan, S. Z. and Perez, J. M. *Bio-based Industrical Fluids and Lubricants.* 2002 : AOCS Press. ISBN 1-893997-30-8.

49. Echavarri Otero, J, Lafont Morgado, P, Chacon Tanarro, E, de la Guerra Ochoa, E, Diaz Lantada, A., Munoz-Guijosa, J. M., Munoz Sanz, J. L., *Analytical Model for Predicting the Friction Coefficient in Point Contacts with Thermal Elastohydrodynamic Lubrication.* 2011, Journal of Engineering Tribology, Vol. 225, pp. 181-191.

50. Why Measure Viscosity. *Brookfield Engineering.* [Online] http://www.brookfieldengineering.com/education/viscosity_whymeasure.asp #nonNewton.

51. Lu, X. and Khonsari, M., *On the Lift-Off Speed in Journal Bearings.*, 2005, Tribology Letters, Vol. 20, pp. 299-305.

52. Bishop, J., Nedungadi, J., Ostrowski, G., Surampudi, B., *An Engine Start/Stop System for Improved Fuel Economy.* 2007, SAE Technical Paper . 2007-01-1777.

53. G.W. Stachowiak, A.W. Batchelor. *Engineering Tribology, Third Edition.* 2005. ISBN 13: 978-0-7506-7836-0.

54. Fryza, J., Sperka, P., Kaneta, M., Krupka, I., Hartl, M., *Effects of Lubricant Rheology and Impact Speed on EHL Film Thickness at Pure Squeeze Action.* 2017, Tribolgy International, Vol. 106, pp. 1-9.

55. Van Leeuwen, H., *The Determination of the Pressure–Viscosity Coefficient of a Lubricant Through an Accurate Film Thickness Formula and Accurate Film Thickness Measurements.* 2009, Proc. IMechE Part J, Engineering Tribology , Vol. 223.

56. . Blaine, S., and Savage, P. E., *Reaction Pathways in Lubricant Degradation. 1. Analytical Characeterisation of n-hexadecane Autooxidation Products*, 1991, Industrial and Engineering Chemistry Research, Vol. 30, pp. 792-798.

57. Carrell, J., *Bio-derived Lubricants.* University of Sheffield. 2013.

58. Fazal, M. A.., Haseeb, A. S. M. A., and Masjuki, H. H., *Comparative Corrosive Characteristics of Petroleum Diesel and Palm Biodiesel for Automotive Materials.* 2010, Fuel Processing Technology, Vol. 91, pp. 1308-1315.

59. Natarajan, S., Olson, W. W., Abraham, M. A., Matarajan, S., *Reaction Pathways and Kinetics in the Degradation of Forging Lubricants.* 2000, Industrial and Engineering Chemical Research, Vol. 39, pp. 2837-2842.

60. . Fox, N. J., and Stachowiak, G. W., *Vegetable Oil Based Lubricants - A Review of Oxidation,* 2007, Tribology International, Vol. 40, pp. 1035-1046.

61. Maduako, A. U. O., Ofunne, G C and Ojinnaka, C. M., *The Role of Metals in the Oxidative Degradation of Automotive Crankcase Oils.* 1996, Tribology International, Vol. 29, pp. 153-160.

62. Diaby, M., Sablier, M., Le Negrate, A., El Fassi, M., Bocquet, J., *Understanding Carbonaceous Deposit Formation Resulting from Engine Oil Degradation.* 2009, Carbon, Vol. 47, pp. 355-366.

63. Gouveia de Souza, A.., Oliveira Santos, J. C., Conceição, M. M., Dantas Silva, M. C., Prasad, S *A Thermoanalytic and Kinetic Study of Sunflower Oil.* 2004, Brazilian Journal of Chemical Engineering, Vol. 21, pp. 265-273.

64. Holmberg, K., and Matthews, A., *Coatings Tribology, Properties, Mechanisms, Techniques and Applications in Surface Engineering.* 1994. ISBN 9780444527509

65. Kalin, M., and Polajnar, M., *The Effect of Wetting and Surface Energy on the Friction and Slip in Oil-Lubricated Contacts.* 2013, Tribology Letters, Vol. 52, pp. 185-194.

66. Lugscheider, E., and Bobzin, K.., *Wettability of PVD Compound Materials by Lubricants.* 2003, Surface and Coatings Technology, Vol. 165, pp. 51-57.

67. Bisht, R.. P. S., Sivasankaran, G. A., and Bhatia, V. K., *Additive Properties of Jojoba Oil for Lubricating Oil Formulations*. 1992, Wear, Vol. 161, pp. 193-197.

68. Biresaw, G., Adhvaryu, A.., Erhan, S. Z.., Carriere, C. J., *Friction and Adsorption Properies of Normal and High-Oleic Soybean Oils.* 2002, Journal of American Oil Chemists , Vol. 79.

69. Sivansakaran, G. A., Bisht, R. P. S., Jain, V. K., Gupta, A., Sethuramiah, A., Bhatia, V. K., *Jojoba Oil Based Two Stroke Gasoline Engine Lubricant.*, Pages 327–333, 1988, Tribology International, Vol. 21.

70. Adhvaryu, A., Erhan, S. Z., and Perez, J. M., *Tribological Studies of Thermally and Chemically Modified Vegetable Oils for Use as Environmentally Friendly Lubricants.* 2004, Wear, Vol. 257.

71. Totten, G. E., *Fuels and Lubricants Handbook: Technology, Properties, Performance, and Testing, ASTM.* 2003.

72. Anderson, K.. J. *A., History of Lubricants.* 1991, MRSBullentin, Vol. 16, p. 69.

73. Kerley, R. V., *A History of Aircraft Piston Engine Lubricants.* 1981, SAE International .

74. Castrol. Histroy. [Online] http://www.castrol.com/en_in/india/about-us/history.html.

75. Sharma, B. K. and Erhan, S. Z., Modified Vegetable Oils for Environmentally Friendly Lubricant Applications. [book auth.] L R Rudnick. *Synthetic, Mineral Oils and Bio-based Lubricants.* 2013. ISBN 9781439855379

76. FUCHS Lubricants PLC. PLANTO. [Online] 2017. https://www.fuchs.com/uk/en/brands/l-r/planto/.

77. John Deere. *Bio HyHARD Brochure .* 2017.

78. Jayadas, N. H., Prabhakaran Nair, K., Ajithkumar, G., *Tribological Evaluation of Coconut Oil as an Environment-Friendly Lubricant. pp.* 350-354, 2005, Tribology International, Vol. 40.

79. Lee, P. M. and Priest, M., *Influence of Gasoline Engine Lubricant on Tribological Performance, Fuel Economy and Emissions*. 2007 p. 235-246, Leeds, Vols. Internal Combustion Engines : Performance Fuel Economy and Emissions, IMechE. ISBN 1843344513.

80. Kano, M., *Super Low Friction of DLC Applied to Engine Cam Follower Lubricated with Ester Containing Oil.* 2006, Tribology International , Vol. 39, pp. 1682-1685.

81. Association, European Aluminium. Applications – Power train – Engine blocks. 2011.

82. Online, ABC Science. New Light-Weight Engine Block. *ABC Science.* [Online] 10 2002. http://www.abc.net.au/science/articles/2002/10/18/704154.htm.

83. Funatani, K., Kurosawa, K., Fabiyi, P. A., Puz, M. F., *Improved Engine Performance Via Use of Nickel Ceramic Composite Coatings (NCC Coat), SAE Technical Paper Series.* 1994. 940852.

84. Bhushan, B. *Introduction to Tribology.* 2013. ISBN 978-1-119-94453-9

85. Mobarak, H M., Masjuki, H. H., Niza Mohamad, E., Ashrafur Rahman, S. M., Mahmud, K. A. H., Habibullah, M., Salauddin, S., *Effect of DLC Coating on Tribological Behavior of Cylinder Liner-piston Ring Material Combination When Lubricated with Jatropha Oil.* 2014, Procedia Engineering , Vol. 90, pp. 733-739.

86. Gangopadhyay, A., *A Review of Automotive Engine Friction Reduction Opportunities Through Technologies Related to Tribology.* 2017, Transaction of the Indian Institute of Metals , Vol. 70, pp. 527 - 535.

87. Around and Around - Where the Oil Goes in Your Engine. *Machinerylubrication.com .* [Online] 2017.

88. Fontana, M. G. *Corrosion Engineering.* 1987. ISBN 0-07-100360-0.

89. Glaeser, W. A. and Shaffer, S. J., Contact Fatigue. *ASM Handbook, Volume 19: Fatigue and Fracture.* 1996.

90. Wood, R. J. K., Understanding Surface Wear in Engineering Materials. [book auth.] B G Mellor. *Surface Coatings for Protection Against Wear.* 2006.

91. Cartier, M., *Handbook of Surface Treatments and Coatings.* 2003. ISBN 978-1-860-58375-9

92. Robertson, J., *Diamond-Like Amorphous Carbon.* 2002, Materials Science and Engineering R: A Review Journal, Vol. 37, pp. 129-281.

93. Holmberg, K and Matthews, A., *Coatings Tribology Properties, Mechanisms, Techniques and Applications in Surface Engineering.* 2009.

94. Jiang, J. and Arnell, R. D., *The Effect of Substrate Surface Roughness on the Wear of DLC Coatings.* 2000, Wear, Vol. 239, pp. 1-9.

95. Singh, R. K., Xie, Z. H., Bendavid, A., Martin, P. J., Munroe, P., *Effect of Substrate Roughness on the Contact Damage of DLC Coatings.* 2008, Diamond and Related Materials, Vol. 17, pp. 975-979.

96. Podgornik, B., Hogmark, S. and Sandberg, O., *Influence of Surface Roughness and Coating Type on the Galling Properties of Coated Forming Tool Steel.* 2004, Surface Coatings Technology , Vol. 184, pp. 338-348.

97. Svahn, F., Kassman-Rudolph , A., and Wallen, E., *The Influence of Surface Roughness on Friction and Wear of Machine Element Coatings*. 2003, Wear, Vol. 254, pp. 1092-1098.

98. John, H. A., *Improvement of the Corrosion Resistance of PVD Hard Coating–Substrate Systems.* 2000, Surface and Coatings Technology, Vol. 125, pp. 212-217.

99. Haque, T., Morina, A., Neville, A., Kapadia, R., Arrowsmith, S., *Effect of Oil on the Durability of Hydrogenated DLC Coating Under Boundary Lubrication Conditions.* 2009, Wear, Vol. 266, pp. 147-157.

100. Holmberg, K., Laukkanen, A., Ronkainen, H., Wallin, K., Varjus, S., Koskinen, J., *Tribological Contact Analysis of a Rigid Ball Sliding on a Hard Coated Surface: Part I: Modelling Stresses and Strains.* 12-13, 2006, Surface and Coatings Technology, Vol. 200, pp. 3793-3809.

101. Holmberg, K., Laukkanen, A., Ronkainen, H., Wallin, K., Varjus, S., Koskinen, J., *Tribological Contact Analysis of a Rigid Ball Sliding on a Hard Coated Surface: Part II: Material Deformations, Influence of Coating Thickness and Young's Modulus.* 2006, Surface and Coatings Technology, Vol. 200, pp. 3810-3823.

102. Ho, L K., *The Effect of Coating to Substrate Hardness Ratio on the Behaviour of Coating Failure Caused by Single Pass Scratch Test.* 2006, City University Hong Kong.

103.Vercammen, K., Van Acker, K., Vanhulsel, A., Barriga, J., Arnsek, A., Kalin, M., Meneve, J., *Tribological Behaviour of DLC Coatings in Combination with Biodegradable Lubricants.* 2004, Tribology International , Vol. 37, pp. 983-989.

104. Simic˘, R. and Kalin, M. *Adsorption Mechanisms for Fatty Acids on DLC and Steel Studied by AFM and Tribological Experiments.* 2013, Applied Surface Science , Vol. 283, pp. 460-470.

105. Mannan, A., Sabri, M. F. M., Kalam, A., Masjuki, H. H., *Tribological Properties of Steel/Steel, Steel/DLC and CLD/DLC Contacts in the Presence of Biodegradable Oil.* 2019, Journal of the Japan Petroleum Institute , Vol. 62, pp. 11-18.

106. Meccanica, *Review of Boundary Lubrication Mechanisms of DLC Coatings Used In Mechanical Applications.* 2008, Vol. 43, pp. 623-637.

107. Kosarieh, S., Morina, A., Flemming, J., Laine, E., Neville, A., *Wear Mechanisms of Hydrogenated DLC in Oils Containing MoDTC.* 2016, Tribology Letters, Vol. 64.

108. Podgornik, B. and Vizintin, J., *Tribological Activated Surface Layers in Lubricated DLC Contacts .* 2008, Surface and Interface Analysis, Vol. 40, pp. 867-870.

109. He, B. Y., Katsamenis, O. L. and Reed, P. A. S., *3-D Analysis of Fatigue Crack Behaviour in a Shot Peened Steam Turbine Blade Material.* 2015, Materials Science and Engineering: A, Vol. 642, pp. 91-103.

110. Jack Champaigne Electronics Inc. *Shot Peening, An Overview.* 2001.

111. Farr, J. P. G., *Molybdenum Disulphide in Lubrication. A Review.* 1975, Wear , Vol. 35, pp. 1 - 22 .

112. Essa, F. A., Zhang, Q. and Huang, X., *Investigation of the Effects of Mixtures of WS2 and ZnO Solid Lubricants on the Sliding Friction and Wear of M50 Steel Against Silicon Nitride at Elevated Temperatures.* 2017, Wear, Vols. 374-375, pp. 128-141.

113. Liu, Y., Wang, C., Yuan, J., Liu, J., *Investigation on Anti-Wear Properties of Sulfide Layer on Bearing Steel Lubricated by Oil-Containing FeS Particles.* 2010, Surface and Coatings Technology, Vol. 205, pp. 470-474.

114. John, P. J., Prasad, S.V., Voevodin, A.A., Zabinski, J.S., *Calcium sulfate as a high temperautre solid lubricant.* 1998, Wear, Vol. 219, pp. 155-161.

115. Costa , M Y. P, Venditti, M L. R., Cioffi, M O. H., Voorwald, H J. C., Guimarães, V A., Ruas, R., *Fatigue Behavior of PVD Coated Ti–6Al–4V Alloy.* 2011, International Journal of Fatigue, Vol. 33, pp. 759 - 765.

116. Treloar, L. R. G., *The Physics of Rubber Elasticity.* Third. 1975. ISBN 0 19 851355 0.

117. . Rahman, M., and Brazel, C. S., *The Placticizer Market: An Assessment of Traditional Plasticizers and Research Trends to Meet New Challenges.*, 2004, Progress in Polymer Science, Vol. 29, pp. 1223-1248.

118. Oil Seal Materials and Specifications . *epm.com.* [Online] 2014. http://www.epm.com/oil_material.htm.

119. Brown, M., *Seals and Sealing Handbook.* 1995.

120. Parker Hannifin GmbH. *O-ring Handbook.* 2015.

121. James Walker. *Elastomer Engineering Guide.* James Walker Sealing Products and Services Ltd. 2012.

122. Keller, R. W., *Effects of Lubricants on Seal Elastomers.* SAE International, 1987. International Off-Highway & Powerplant Congress & Exposition. 871626.

123. Hertz, D. L., *Elastomers in Automotive Fuels, Oils & Fluids at High Temperatures.* Detroit, 1993. Interational Congress and Exposition, SAE International. 930993.

124. Flory, P. J., *Principles of Polymer Chemistry.* 1953. ISBN 13 978-0-8014-0134-3

125. Huggins, M. L., *Thermodynamic Properties of Solutions of Long-Chain Compounds.* 1942, Annals of the New York Academy of Sciences , Vol. 43, pp. 1-32.

126. Hanson, C. M., *The Three Dimentional Solubility Parameter - Key to Paint Component Affinities 1 Solvents, Plasticizers, Polumers and Resins.* 1967, Journal of Paint Technology, Vol. 39, pp. 104-117.

127. Hanson, C. M. and Hanson, K. M., *Solubility Parameter Prediction of the Barrier Properties of Chemical Protective Clothing.* 1988. Performance of Protective Clothing: Second Symposium. pp. 197-208. ASTM STP 989.

128. Cheenkachorn, K. and Fungtammasan, B., *Development of Engine Oil Using Palm Oil as a Base Stock for Four Stroke Engines.* 2010, Energy, Vol. 35, pp. 2552-2556.

129. Masjuki, H. H., Maleque, M. A., Kubo, A., Nonaka, T., *Palm Oil and Mineral Oil Based Lubricants - Their Tribological and Emission Performance.* 1999, Tribology International , pp. 305-314.

130. Reeves, C. J., Menezes, P. L., Jen, T., Lovell, M. R., *The Influance of Fatty Acids on Tribological and Thermal Properties of Natural Oils as Sustainable Biolubricants.* 2015, Tribology International, Vol. 90, pp. 123-134.

131. Quinchia, L. A., Delgdo, M. A., Reddyhoff, T., Gallegos, C., Spikes, H. A., *Tribological Studies of Potential Vegetable Oil-Based Lubricants Containing Environmentally Friendly Viscosity Modifiers.* 2013, Tribology International , Vol. 69, pp. 110-117.

132. Alves, S. M., Barros, B. S., Trajano, M. F., Ribeiro, K. S. B., Moura, E., *Tribological Behavior of Vegetable Oil-Based Lubricants with Nanoparticles of Oxides in Boundary Lubrication Conditions.* 2013, Tribology International , Vol. 65, pp. 28-36.

133. Syahrullail, S., Zubil, B. M., Azwadi, C. S. N., Ridzuan, M. J. M., *Experimental Evaluation of Palm Oil as Lubricant in Cold Forward Extrusion Process.* 2011, International Journal of Mechanical Sciences, Vol. 53, pp. 549-555.

134. Gupta, M., Pandey, N K., Singhal, S., Mishra, G. C., *Development and Performance Aspects of Jojoba Based Lubricant Formulations for 2 Stroke Gasoline Engines.* 1993, SAE.

135. Carrell, J. *Bio-derived Lubricants.* University of Sheffield. White Rose, 2013.

136. Kalhapure, A. S., Mhaske, V. M. and Bajaj, D. S., *Tribological Evaluation of Vegetable oils as a Multi-cylinder Engine lubricant.* 2016, International Advanced Research Journal in Science, Engineering and Technology, Vol. 3, pp. 68-72.

137. Bahari, A., Lewis, R. and Slatter, T., *Friction and Wear Response of Vegetable Oils and their Blends with Mineral Engine Oil in a Reciprocating Sliding Contact at Severe Contact Conditions.* 2017, Part J.

138. Dearnaley, G. and Arps, J. H., *Biomedical Aapplications of Diamond-like Carbon (DLC) Coatings: A Review.* Science Direct, 2005, Surface and Coating Technology , Vol. 200, pp. 2518-2524.

139. Hainsworth, S.V. and Uhure, N.J., *Diamond-Like Carbon Caotings for Tribology: Production Techniques, Characterization Methods and Applications.* International Materials Reviews.

140. Bobzin, k., Bagcivan, N., Goebbels, N., Yilmaz, K., Hoehn, B. R., Michaelis, K., Hochmann, M., *Lubricated PVD CrA1N and WC/C Coatings for Automotive Applications.* 2009, Surface and Coating Technology, Vol. 204.

141. de Barros Bouchet, M. I., Martin, J M., Le-Mogne, T., Vacher, B., *Boundary Lubrication Mechanisms of Carbon Coatings by MoDTC and ZDDP Additives.* 2005, Tribology International , Vol. 38, pp. 257-264.

142. Wang, R., Mercer, C., Evans, A G., Cooper, C V., Yoon, H. K., *Delamination and Spalling of Diamond-like Carbon Tribological Surfaces.* 2002, Diamond and Related Materials, Vol. 11, pp. 1797-1803.

143. Kalin, M., Vizintin, J., Vercammen, K., Barriga, J., Arnsek, A., *The lubrication of DLC Coatings with Mineral and Biodegradable Oils having Different Polar and Saturation Characteristics.* 2005, Surface and Coating Technology , Vol. 200, pp. 4515-4522.

144. Mobarak, H. M. and Chowdhury, M., *Tribological Performance of Hydrogenated Amorphous Carbon DLC Coating When Lubricated With Biodegradable Vegetal Canola Oil.* 2014, Tribology in Industy, Vol. 36, pp. 163-171.

145. Vizintin, J., Kalin, M. and Vizintin, J., *A Comparison of the Tribological Behaviour of Steel/Steel, Steel/DLC and DLC/DLC Contacts When Lubricated with Mineral and Biodegradable Oils.* 2006, Wear, Vol. 261.

146. Al Mahmud, K. A. H., Kalam, M. A., Masjuki, H. H., Abdollah, M. F. B., *Tribological Study of a Tetrahedral Diamond-Like Carbon Coating under Vegetable Oil–Based Lubricated Condition.* 2015, Tribology Transactions , Vol. 58, pp. 907-913.

147. Pettersson, U. and Jacbson, S., *Influence of Surface Texture on Boundary Lubricated Sliding Contacts.* 2003, Tribology Interational , Vol. 36, pp. 857-864.

148. Yan-qing, W., Gao-feng, W., Qing-gong, H., Liang, F., Shi-rong, G., *Tribological Properties of Surface Dimple-textured by Pellet-Pressing.* 2009, Procedia Earth and Planetary Science, Vol. 1, pp. 1513-1518.

149. Kovalchenko, A., Ajayi, O., Erdemir, A., Fenske, G., Etsion, I., *The Effect of Laser Surface Texturing on Transitions in Lubrication Regimes During Unidirectional Sliding Contact.* 2005, Tribology International , Vol. 38, pp. 219-225.

150. Ryk, G., Lligerman, Y. and Etsion, I., *Experimental Investigation of Laser Surface Texturing for Reciprocating Automotive Components.* 2002, Tribology Transactions, Vol. 45, pp. 444-449.

151. Ramesh, A., Akram, W., Mishra, S P., Cannon, A. H., Polycarpou, A A., King , W. P., *Friction Characteristics of Microtextured Surfaces Under Mixed and Hydrodynamic Lubrication.* 2013, Tribology International , Vol. 57, pp. 170-176.

152. Matsui, M. and Kakishima, H., *Improvement of Tribological Performance of Steel by Solid Lubricant Shot-peening in Dry Rolling/Sliding Contact Wear Tests.* 2006, Wear, Vol. 260, pp. 667-673.

153. Wang, L. and Li, D. Y., *Mechanical, Electrochemical and Tribological Properties of Nanocrystalline Surface of Brass Produced by Sandblasting and Annealing.* 2003, Surface And Coating Technology, Vol. 167, pp. 188-196.

154. Jiang, X. P., Wang, X Y., Li, J X., Man, C. S., Shepard, M J., Zhai, T., *Enhancement of Fatigue and Corrosion Properties of Pure Ti by Sandblasting.* 2006, Mateials science and engineering, Vol. 429, pp. 30-35.

155. Liu, B. and Li, H., *Alkylated Fullerene as Lubricant Additive in Paraffin Oil for Steel/Steel Contacts.* 2016, Fullerenes, Nanotubes and Carbon Nanostructures, Vol. 24, pp. 712-719.

156. Alberdi, A., Hatto, P., Diaz, B., Csillang, S., *Tribological Behaviour of Nanocomposite Coatings Based on Fullerene-like Structures.* 2011, Vacuum, Vol. 85, pp. 1087-1092.

157. Piazzoni, C., Buttery, M., Hampson, M R., Roberts , E W., Ducati, C., Lenardi, C., Cavaliere, F., Piseri, P., Milani, P., *Tribological Coatings for Complex Mechanical Elements Produced by Supersonic Cluster Beam Deposition of Metal Dichalcogenide Nanoparticles.* 2015, Journal of Physics D: Applied Physics, Vol. 48.

158. Wu, K., Qiang, L., Gong, Z., Zhao, G., Gao, K., Zhang, B., Zhang, J., *The Tribological Perforrmance of Fullerene-like Hydrogenated Carbon Films Under Ionic Liquid Lubrication.* 2015, Surface and Interface Analysis, Vol. 47, pp. 903-910.

159. John, P. J., Prasad, S. V., Voevodin, A. A., Zabinski, J. S., *Calcium sulfate as a high temperature solid lubricant.* 1998, Wear, Vol. 219, pp. 155-161.

160. Wang, H., Mu, B., Ren., Jian, L., Zhang, J., Yang, S., *Mechanical and Tribological Behaviors of PA66/PVDFBlends Filled With Calcium Sulphate Whiskers.* 2009, Polymer Composites, Vol. 30, pp. 1327-1332.

161. Liu, D., Zhang, M., Zhao, G., Wang, X., *Tribological Behavior of Amorphous and Crystalline Overbased Calcium Sulfonate as Additives in Lithium Complex Grease.* 2012, Tribology Letters, Vol. 45, pp. 265-273.

162. Hao, L., Li, J., Xu, X., Ren, T., *Preparation and Tribological Properties of a Kind of Lubricant Containing Calcium Borate Nanoparticles.* 2012, Industrial Lubrication and Tribology, Vol. 64, pp. 16-22.

163. Yamamoto, Y., Kawamura, Y., Yamazaki, Y., Kijima, T., Morikawa, T., Nonomura, Y. P., *almitoleic Acid Calcium Salt: A Lubricant and Bactericidal Powder from Natural Lipids.* 2015, Journal of Oleo Science, Vol. 64, pp. 283-288.

164. Liu, B., Huang, S., Van Humbeeck, J., Vleugels, J., *A comparative study of spark plasma sintered TiCx-Ni3Ti/Ni cermets.* 2018, International Journal of Refractory Metals and Hard Materials, Vol. 72, pp. 110-116.

165. . Anwar, S., Answar, S. and Nayak, P., *Multilayer Composite Ceramic-Metal Thin Film: Structural and Mechancial Properties.* 2018, Surfaces and Interfaces, Vol. 10, pp. 110-116.

166. Holleck, H., *Material Selection for Hard Coatings.* 1986, Journal of Vacuum Science and Technology A: Vacuum, Surfaces and Films, Vol. 4, pp. 2661 - 2669.

167. Yang, J., Jiang, Y., Hardell, J., Prakash, B., Fang, Q., *Influence of Service Temperature on Tribological Characteristics of Self-Lubricant Coatings: A Review.* 2013, Frontiers of Material Science, Vol. 7, pp. 28-39.

168. Sliney, H., *The Role of Silver in Self-Lubricating Coatings for Use at Extreme Temperatures.* 1985. Annual Meeting of the American Society of Lubrication Engineers.

169. Pauleau, Y., Juliet, P. and Gras, R., *Tribological Properties of Calcium Fluoride-Based Solid Lubricant Coatings at High Temepratures.* 1998, Thin Solid Films, Vol. 317, pp. 481-485.

170. Prabhu, K. N., Fernades, P. and Kumar, G., *Effect of Substrate Surface Roughness on Wetting Behaviour of Vegetable Oils.* 2009, Materials and Design, Vol. 30, pp. 297-305.

171. Podgornik, B., Zajec, B., Strnad, S., Stana-Kleinschek, K., *Influence of Surface Energy on the Interactions Between Hard Coatings and Lubricants.* 2007, Wear, Vol. 262, pp. 1199-1204.

172. Kalin, M. and Polajnar, M., *The Correlation Between the Surface Energy, the Contact Angle and the Spreading Parameter, and their Relevance for the Wetting Behaviour of DLC with Lubricating Oils.* 2013, Tribology International , Vol. 66, pp. 225-233.

173. Esteban, B., Riba, J-R., Baquero, G., Puig, R., Rius, A., *Characterization of the Surface Tension of Vegetable Oils to be Used as Fuel in Diesel Engines.* 2012, Fuel, Vol. 102, pp. 231-238.

174. Melo-Espinosa, E. A., Sánchez-Borroto, Y., Errasti, M., Piloto-Rodríguez, R., Sierens, R., Roger-Riba, J., Christopher-Hansen, A., *Surface Tension Prediction*

of Vegetable Oils Using Artificial Neural Networks and Multiple Linear Regression. 2014, Energy Procedia, Vol. 57, pp. 886-895.

175. Durak, E., Cetinkaya, M., Yenigun, B., Karaosmanog, F., *Effects of Sunflower Oil Added to Base Oil on the Friction Coefficient of Statically Loaded Journal Bearings.* 2004, Journal of Synthetic Lubrication, Vol. 21, pp. 208-222.

176. Biresaw, G. and Bantchev, G. B., *Elastohydrodynamic (EHD) Traction Properites of Seed Oils.* 2010, Tribology Transactions, Vol. 53.

177. Biresaw, G. and Bantchev, G. B., *Pressure Viscosity Coefficient of Vegetable Oils.* 2013, Tribolgy Letters, Vol. 49, pp. 501-512.

178. Lockwood, F. E., Benchaita, M. T. and Friberg, S. E., *Study of Lyotropic Liquid Crystals in Viscometric Flow and Elastohydrodynamic Contact.* 1986, Tribolgy transaction, Vol. 30, pp. 539-548.

179. Bantchev, G. B., Biresaw, G. and Cermak, S. C., *Elastohydrodynamic Study of Blends of Bio-Based Esters with Polyalpaolefin in the Low Film Thickness Regime.* 2012, Journal of American Chemists , Vol. 89, pp. 1091-1099.

180. Bantchv, G. and Biresaw, G., *Elastohydrodynamic Study of Vegetable Oil - Polyalphaolefin Blends.* 2008, Lubrication Science, Vol. 20, pp. 283-297.

181. G. Biresaw, G.B. Bantchev., *Pressure Viscosity Coefficent of Vegetable Oils .* pp. 501-512, Tribolgy Letters, 2013, Vol. 49.

182. Hamrock, B. J. and Dowson, D., *Minimum Film Thickness in Eliptical Contacts for Different Regimes of Fluid Film Lubrication.* 1978, NASA Technical paper 1342.

183. Ethan, S. Z., Sharma, B. K. and Oerez, J. M., *Oxidation and Low Temperature Stability of Vegetable Oil-based Lubricants.* 2006, Industrial Crops and Products, Vol. 24, pp. 292-299.

184. Le Dréau, Y., Dupuy, N., Gaydou, V., Joachim, J., Kister, J., *Study of Jojoba Oil Aging by FTIR.* 2009, Analytica Chimica Acta, Vol. 642, pp. 163-170.

185. Tenbohlen, S. and Koch, M., *Aging Performance and Moisture Solubility of Vegetable Oils for Power Transformers.* 2010, IEEE Transactions on Power Delivery, Vol. 25, pp. 825-830.

186. Besser, C., Schneidhofer, C., Dorr, N., Novotny-Farkas, F., Allmaier, G., *Investigation of Long-Term Engine Oil Performance Using Lab-Based Artificial Aging Illustrated by the Impact of Ethanol as a Fuel Componant.* 2012, Tribology International, Vol. 46, pp. 174-182.

187. Farfan-Cabrera, L. I., Galardo-Hernandez, E. A. and Perez-Gonzalez, J., *Compatibility Study of Common Sealing Elastomers with a Bio-Lubricant (Jatropha Oil).* 2017, Tribology International, Vol. 116, pp. 1-8.

188. DuPont. *DuPont Viton Selection Guide, Technial Infomation.* 2010.

189. Alves, S. M., Mello, V. S. and Medeiros, J. S., *Palm and Soybean Biodiesel Compatibility with Fuel System Elastomers.* 2013, Tribology Interantional, Vol. 65, pp. 74-80.

190. Chai, A. B., Andriyana, A., Verron, E., Johan, M. R., Haseeb, A. S. M. A., *Development of a Compression Test Device for Investigating Interaction Between Diffusion of Biodiesel and Large Deformation in Rubber.* 2011, Polymer Testing, Vol. 30, pp. 867-875.

191. Ch'ng, S. Y., Andriyana, A., Verron, E., Kahbas, O., Ahmad, R., *Development of a Novel Experimental Device to Investigate Swelling of Elastomers in Biodiesel Undergoing Multiaxial Large Deformation.* 2013, Experimental Mechanics, Vol. 53, pp. 1323-1332.

192. Barnes, L. D., *Evaluation of Elastomeric Compounds in 'Fresh' and 'Used' CG-4 Engine Oils.* 1996. International Spring Fuels & Lubricants Meeting . 961226.

193. Heitzug, S., Weinebeck, A. and Murrebhoff, H., *Testing and Prediction of Material Compatibility of Biofuel Candidates with Elastomeric Materials.* 2015, SAE Int. J. Fuels Lubr., Vol. 8.

194. Graham, J. L., Striebich, R. C., Myers, K. J., Minus, D. K., Harrison III, W. E., *Swelling of Nitrile Rubber by Selected Aromatics Blended in a Synthetic Jet Fuel.* 2006, Energy and Fuels , Vol. 20, pp. 759-765.

195. Zhu, L., Cheung, C. S., Zhang, W. G., Huang, Z., *Compatibility of Different Biodiesel Composition with Acrylonitrile Butadiene Rubber (NBR).* 2015, Fuel, Vol. 158, pp. 288-292.

196. Trelleborg. Internal Momorandum. 9 12 2015.

197. Hanson, C. M. and Just, L., *Prediction of Environmental Stress Cracking in Plastics with Hansen Solubility Parameters.* 2001, Industrial & Engineering Chemistry Research , Vol. 40, pp. 21-25.

198. Fried, J. R., *Polymer Science and Technology.* 2nd edition . 2003.

199. Guo, C. J. and Kee, D. D. E., *Effect of Molecular Size and Free Volume on Diffusion in Liquids.* 1991, Chemical Engineering Science , Vol. 46, pp. 2133-2141.

200. Barton, A F. M., *Handbook of Solubility Parameters and Other Cohesion Parameters.* 1983.

201. . Nielsen, T. B. and Hanson, C. M., *Elastomer Swelling and Hansen Solubility Parameters*2005, Polymer Testing , Vol. 24, pp. 1054-1061.

202. Seehra, M. S., Yalamanchi, M. and Singh, V., *Structural Characteristics and Swelling Mechanism of Two Commercial Nitrile-Butadiene Elastomers in Various Fluids.* 2012, Polymer Testing , Vol. 31, pp. 564-571.

203. Krauskopf, L. G., *Prediction of Plasticizer Solvency Using Hansen Solubility Parameter.* 1999, Journal of Vinyl & Additive Technology, Vol. 5.

204. ASTM International. *Standard Test Method for Linearly Reciprocating Ball-on-Flat Sliding Wear.* 2016. G133-05.

205. ASTM International. *Standard Test Method for Conducting Friction Tests of Piston Ring and Cylinder Liner Materials Under Lubricated Conditions.* 2017. G181.

206. International Organisation for Standardisation. *Rubber, vulcanized or thermoplastic – Determination of Stress Relaxation in Compression – Part 1: Testing at Constant Temperature'.* 2011. ISO 3384-1:2011.

207. Baldwin, A. R., *Eventh International Conference on Jojoba and Its Uses: Proceedings.* American Oil Chemists Society.

208. Patzek, T. W., *A First Law Thermodynamic Analysis of Biodiesel Production From Soybean.* Department of Petroleum and Geosystems Engineering, The University of Texas at Austin. 2009.

209. Baldwin, A. R., *Specifications, Physical Properties and Methods ofAnalysis for Jojoba Oil.* 1988. American Oil Chemists Society.

210. Mihail, I. and Zoran, P. S., Polymerization of Soybean Oil with Superacids. [book auth.] Tzi-Bun Ng. *Soybean - Applications and Technology.* 2011, pp. 365 - 387.

211. Basiron, Y., *Palm Oil Production Through Sustainable Plantations.* 2007, European Journal of Lipid Science and Technology , Vol. 109, pp. 289–295.

212. Malaysian Palm Oil Council. *The Oil.* 2012, Journal of Oil Palm Environment and Health .

213. Narváez, P. C., Rincón, S. M., Castañeda, L. Z., Sánchez, F. J., *Determination of Some Physical and Transport Properties of Palm Oil and of its Methyl Esters.* 2008, Latin American Applied Research, Vol. 38, pp. 1-6.

214. Dymon-iC™ Coatings. *Teer Coatings UK.* [Online] http://www.teercoatings.co.uk/?page=44.

215. Ogihara, H. and Ishiwata, M., *Metallic Sliding Member, Piston for Internal Combustion Engine, Method of Surface-Treating These, and Apparatus Therefor. 7399733* Japan, 2008. Grant.

216. ASTM International . *Standard Classification System for Rubber Products in Automotive Applications.* 2017. ASTM D2000 - 12.

217.International Institute of Synthetic Rubber Producers, INC. *10 EPDM, Ethylene-Propylene Rubbers & Elastomers*2012.

218. International Institute of Synthetic Rubber Producers, INC. *07 NBR, Acrylonitrile-Butadiene Rubber.* 2012.

219. International Institute of Synthetic Rubber Producers, INC. *06 FKM, Fluoroelastomers.* 2012.

220. ASTM International . *Standard Test Method for Ahdesion Strength and Mechanical Failure Modes of Ceramic Coatings by Quantitive Single Point Scratch Testing.* 2015. C1624-05.

221. Abbott, S., Hanson, C., Yamamoto, H., Valpey, R., *Hansen Solubility Parameters in Practice.* 4th. 2008.

222. Royal Society of Chemistry. Stearic Acid. *ChemSpider.* [Online] http://www.chemspider.com/Chemical-Structure.5091.html?rid=d933a4c5-d978-4720-9523-5069370cc501.

223. Sharma, S., Sangal, S. and Mondal, K., *On the Optical Microscope Method for the Determination of Ball-on-Flat Surface Linearly Reciprocating Wliding Wear Volume.* 2013, Wear, Vol. 300.

224. . Bahari, A., Slatter, T. and Lewis, R., *Friction and Wear Phenomena of Vegetable Oil–Based Lubricants with Additives at Severe Sliding Wear Conditions.* 2016, Tribology Transactions .

225. ASTM International . *Standard Guide for Measuring and Reporting Coefficient of Friction Data.* 2013. G115-10 .

226. Morina, A., Neville, A., Priest, M., Green, J. H., *ZDDP and MoDTC Interactions and Their Effect on Tribological Performance – Tribofilm Characteristics and its Evolution.* 2006, Tribology Letters , Vol. 24.

227. Fam, H., Kontopoulou, M. and Brynt, J. T., *Method for Friction Estimation in Reciprocating Wear Tests.* 2011, Wear , Vol. 271, pp. 999-1003.

228. Balbino, S., Vegetable Oil Yield and Composition Influanced by Environmental Stress Factors. [book auth.] P. Ahmad. *Oilseed Crops: Yield and Adaptations under Environmental Stress.* 2017, 5.

229. Rabinowicz, E., *The Wear Coefficient - Magnitude, Scatter, Uses.* 1981, Journal of Lubrication Technology - Transactions of the ASME, Vol. 103, pp. 188-194.

230. Mahmud, K.A.H, Varman, M., Kalam, M. A., Masjuki, H. H., Mobarak, H. M., Zulkifli, N. W. M., *Tribological characteristics of amorphous hydrogenated (a-C:H) and tetrahedral (ta-C) diamond-like carbon coating at different test temperatures in the presence of commercial lubricating oil.* 2014, Surface and Coatings Technology, Vol. 245, pp. 133-147.

231. Zahid, R, Mufti, R. A., Gulzar, M., Hassan, M.B.H., Alabdulkarem, A., Varman, M., Kalam, M. A., Zulkifi, N.W.B.M., Yunus, R., *Tribological compatibility analysis of conventional lubricant additives with palm trimethylolpropane ester (TMP) and tetrahedral amorphous diamond-like carbon coating (ta-C).* 2018, Vol. 232, pp. 999-1013.

232. Kosarieh, S., Morina, A., Laine, E., Flemming, J., Neville, A., *Tribological performance and tribochemical processes in a DLC/steel system when*

lubricated in a fully formulated oil and base oil. 2013, Surface and Coating Technology , Vol. 217, pp. 1-12.

233. Solis, J, Zhao, H; Wang, C; Verduzco, J A; Bueno, A S; Neville, A., T*ribological performance of an H-DLC coating prepared by PECVD.* 2016, Applied Surface Science, Vol. 383, pp. 222-232.

234. . Green, D. A., Lewis, R and Dwyer-Joyce, R. S., *Wear Effects and Mechanisms of Soot-Contaminated Automotive Lubricants.* 2006, Proceedings of the Institution of Mechanical Engineers, Part J: Journal of Engineering Tribology, Vol. 220.

235.Hazan, Y., Reuter, T; Werner, D; Clasen, R; Graule, T., *Interactions and Dispersion Stability of Aluminum Oxide Colloidal Particles in Electroless Nickel Solutions in the Presence of Comb Polyelectrolytes.* 2008, Journal of Colloid and Interface Science, Vol. 323, pp. 293-300.

236. Gong, Z. and Komvopoulos, K., *Surface Cracking in Elastic-Plastic Multi-Layered Media Due to Repeated Sliding Contact.* 2004, Journal of Tribology, Vol. 126, pp. 655-663.

237. Laukkanen, A., Holmberg, K; Koskinen, J; Ronkainen, H; Wallin, K; Varjus, S., *Tribological Contact Analysis of a Rigid Ball Sliding on a Hard Coated Surface, Part III: Fracture Toughness Calculation and Influence of Residual Stresses.* 2006, Surface Coating and Technology, Vol. 200, pp. 3824-3844.

238. Tannous, J., Dassenoy, F; Lahouij, I; Le Mogne, T; Vache, B; Bruhács, A; Tremel, W., *Understanding the Tribochemical Mechanisms of IF-MoS2 Nanoparticles Under Boundary Lubrication.* 2011, Tribology Letters, Vol. 41, pp. 55-64.

239. Holleck, H. and Schier, V., *Multilayer PVD Coatings for Wear Protection.* 1995, Surface and Coating Technology , Vols. 76-77, pp. 328 - 336.

240. Noh, S. H., Kwon, C; Hwang, J; Ohsaka, T; Kim, B; Kim, T; Yoon, Y; Chen, Z; Sea, M H; Han, B., *Self-Assembled Nitrogen-Doped Fullerenes and their Catalysis for Fuel Cell and Rechargeable Metal–Air Battery Applications.* 2017, Nanoscale, Vol. 9, pp. 7373-7379.

241. Cihelkova, K., Zárubová, M; Hrádková, I; Filip, V; Šmidrkal, J., *Changes of Sunflower Oil Polyenoic Fatty Acids under High Temperatures.* 2009, Czech Journal of Food Science , Vol. 27, pp. 13-16.

242. Koenhen, D. M. and Smolders, C. A., *The Determination of Solubility Parameters of Solvents and Ploymers by Means of Correlations with Other Physical Quantites.* 1975, Journal of Applied Polymer Science, Vol. 19, pp. 1163-1179.

243. Barton, A. F., *Application of Cohesion Parameters to Weeting and Adhesion, A Review.* 1982, Journal of Adhesion , Vol. 14, pp. 33-62.

244. De La Peña-Gil, A, Toro-Vazquez, J T and Rogers, M A., *Simplifying Hansen Solubility Parameters for Complex Edible Fats and Oils.* 2016, Food Biophysics, Vol. 11, pp. 283–291.

245. Siow, L. S. and Patterson, D., *The Prediction of Surface Tensions of Liquid Polymers.* 1971, Macromolecules, Vol. 4, pp. 26–30.

246. Dundon, M L and Mack, E., *The Solubility and Surface Energy of Calcium Sulfate .* 1923, The Journal of American Chemical Society, Vol. 45, pp. 2479-2485.

247. Kim, G. and Ajersch, F., *Surface Energy and Chemical Characteristics of Interfaces of Adhesively Bonded Aluminium Joints.* 1994, Journal of Materials Science, Vol. 29, pp. 676-681.

248. Saha, B., Dirckx, M; Hardt, D. E; Tor , S. B; Liu, E; Chun, J. H., *Effect of Sputtering Power on Friction Coefficient and Surface Energy of Co-Sputtered Titanium and Molybdenum Disulfide Coatings and its Performance in Micro Hot-Embossing.* 2014, Microsystem Technology , Vol. 20, pp. 1069-1078.

249. Sivansankaran, G. A., Bisht, R. P. S; Jain, V. K; Gypta, M; Sethuramiah, A; Bhatia, V. K., *Jojoba oil based two stroke gasoline engine lubricant.* 1988, Tribology International, Vol. 21, pp. 327–333.

250. Gordon, L., Abu-Farsakh, H; Janotti, A; Van de Walle, C. G., *Hydrogen Bonds in Al2O3 as Dissipative Two-Level Systems in Superconducting Qubits.* 2014, Scientific Reports, Nature, Vol. 4.

251. Goodwin, V., Yoosuk, B; Ratana, T; Tungkamani, S., *Hydrotreating of Free Fatty Acid and Bio-Oil Model Compounds: Effect of Catalyst Support.* 2015, Energy Procedia, Vol. 79, pp. 486-491.

252. Timma, C., Lostak, T; Jansssen, S; Flock, J; Mayer, C., S*urface Investigation and Tribological Mechanism of a Sulfate-Based Lubricant Deposited on Zinc-Coated Steel Sheets.* 2016, Applied Surface Science, Vol. 390, pp. 784-794.

253. Yamamoto, Kawamura, Y; Yamazaki, Y; Kijima, T; Morikawa, T; Nonomura, Y., *Palmitoleic Acid Calcium Salt: A Lubricant and Bactericidal Powder from Natural Lipids.* 2015, Journal of Oleo Science, Vol. 64, pp. 283-288.

254. *On the Coating of Precipitated Calcium Carbonate with Stearic Acid in Aqueous Medium.* Shi, X., Rosa, R. and Lazzeri, A., 2010, Langmuir, Vol. 26, pp. 8474-8482.

255. The Los Angeles Rubber Group Inc. *TLARGI Chemical Resistance Chart .*

256. Patzek, Tad W., *A First Law Thermodynamic Analysis of Biodiesel Production From Soybean.* 2009, Bulletin of Science, Technology & Society , Vol. 29, pp. 194-204.

257. Liy, Y.. *Investigation on Elastomer Compatibility with Alternative Aviation Fuels.* University of Sheffield . 2013. Thesis .

258. Spetz, G., *Stress Relaxation, Tests methods, instruments and lifetime estimation.* Elastocon AB. 2015.

259. Haque, T, Morina, A.; Neville, A.; Kapadia, R.; Arrowsmith, S., *Effect of oil on the durability of hydrogenated DLC coating under boundary lubrication conditions.* 2009, Wear, Vol. 266, pp. 147-157.